e - ISSN 2586-9396

Current Applied Science and Technology

Vol. 20 No. 3

September - December 2020

KING MONGKUT'S INSTITUTE OF TECHNOLOGY LADKRABANG

Advisory Board

Current Applied Science and Technology or CAST, formerly KMITL Science and Technology Journal, has been established since its inception as KMITL Science Journal published by King Mongkut's Institute of Technology Ladkrabang (KMITL) in 2001. The journal has been dedicated to publishing advanced and applied knowledge in the form of high-quality research and review articles covering the main areas of Biotechnology, Environmental Science, Agricultural Technology, Food Science and other fields related to Applied Science and Technology. Special issues devoted to important topics in advanced science and technology will occasionally be published.

The journal is an open access peer-reviewed and double blinded journal using Online Journal System (OJS) publishing online academic research and review articles. Previously, articles were published in print on a regular basis (two issues per year) since 2001 and since 2010 onward the articles have been published both in print and electronic forms starting from volume 10. In 2017, the journal title has been changed from *KMITL Science and Technology Journal* to *Current Applied Science and Technology* (CAST) (e-ISSN 2586-9396) to be more identifiable to the international scientific community according to the suggestion of Thai-Journal Citation Index Centre. The journal has been published online only since volume 17(2) (July-December, 2017). In addition, the journal has attracted researchers from other countries more than 22% according to the data. Because of more demands on publication in CAST, the editorial board has decided to publish online original academic research and review articles three issues per year (April, August and December) from 2018 onward.

Furthermore, the advisory board and editorial board comprises honorable and well-known members from around the world in which 50% of editorial board members are from various countries like U.K., Norway, Japan, India, China, Canada, Estonia and Egypt. Only 25% of Thai editorial board members are from the publisher organization and 25% from other publisher organizations. Most of advisory and editorial board members have high H-index according to SCOPUS.

The journal is also committed to maintaining the high level of integrity in the content published and has a Conflict of Interest policy in place. The journal uses plagiarism detection software to screen the submissions. The journal has been working closely with Thai-Journal Citation Index Centre to ensure that the journal complies with international standard of SCOPUS.

Current Applied Science and Technology (CAST)

(formerly KMITL Science and Technology Journal)

Editor

Dusanee Thanaboripat
King Mongkut's Institute of Technology Ladkrabang, Thailand

Editorial Board

CONTENTS

Page

Research Articles:

Effects of Gel Rooting Medium Containing *Methylobacterium radiotolerans* Ed5-9 and *Streptomyces* TM32 Fermentation Broth on Cutting Propagation of *Gymnema inodorum* (Lour.) Decne. **343**

Siripun Sarin, Nareeluk Nakaew and Aphitchat Chidburee

Detection of Pathogenic Bacteria in the Air by Culture Techniques in Combination with Multiplex Polymerase Chain Reaction **354**

Wimon Chanchaem and Somchai Awakairt

Expression of Recombinant *Alcohol Dehydrogenase* in *Escherichia coli* Strain BL21 (DE3) and *In Planta Agrobacterium* Transformation of Tomato Seeds **363**

Mastura Sani and Hairul Azman Roslan

Phytochemical Screening and GC-MS Analysis of Bioactive Constituents in the Methanolic Extract of *Caulerpa racemosa* (Forssk.) J. Agardh and *Padina boergesenii* Allender & Kraft **380**

Cholaraj Ragunath, Yohannan Aron Santhosh Kumar, Iwar Kanivalan and Sruthi Radhakrishnan

A Simple and Green Approach for Colorimetric Ammonia Determination by Combining Pervaporation with Paper Impregnated Anthocyanins Extracted from Red Cabbage **394**

Jurairat Jongprakobkit, Wannakan Wisaichon and Wiboon Praditweangkum

Assessment of Some Biochemical Parameters and Dielectric Relaxations in *β*-Thalassemic Children **408**

Yasser Khedr, Metwally Kotb, Samir Abd El-Kareem and Omar El-Bayady

The Use of Ozone for Controlling European House Dust Mite, *Dermatophagoides pteronyssinus* (Trouessart) **420**

Jarongsak Pumnuan, Ammorn Insung and Teerapong Wangapai

Genetic Diversity of Commercial Field Corn Hybrids in Thailand as Verified by SSR Markers and Their Inbreeding Depression **429**

Terdsak Suwanatape, Sansern Jampatong and Choosak Jompuk

Studying the Safety of Instant Noodles Sold in Egyptian Hypermarkets **440**

Eman Trabia, Hanaa Ismail and Samar Aborhyem

The Relationships Between Extreme Precipitation and Rice and Maize Yields Using Machine Learning in Sichuan Province, China **453**

Jun Fan, Attachai Jintrawet and Chanchai Sangchyoswat

Micropropagation of *Koelreuteria bipinnata* Using Juvenile and Mature Explants **470**

Azza A. Tawfik, Omer H. Ibrahim and Mona A. Taha

Identification and Plant Growth-Promoting Activities of Proteobacteria Isolated from Root Nodules and Rhizospheric Soils **479**

Kingchan Malisorn, Supunnee Chanchampa, Pawina Kanchanasin and Somboon Tanasupawat

Oil Removal from Produced Water Using *Imperata cylindrica* as Low-Cost Adsorbent **494**

Hind J. Hadi, Khalid M. Mousa Al-zobai and Mohammed Jaafar Ali Alatabe

Semi-field Application of a New Formulation Based on *Spodoptera litura* Nuclear Polyhedrosis Virus and *Bacillus thuringiensis* subsp. *mexicanensis* Against Cotton Leaf Worm, *Spodoptera littoralis* and Root Knot Nematode, *Meloidogyne incognita* in Egypt **512**

Hanan Alfy, Rehab Y. Ghareeb and Wesam Z. Aziz

Effect of Different Application Methods for Pendimethalin Herbicide on Growth and Productivity of Green Pea Plant (*Pisumsativum* L.) **528**

Nahla Salim Hammok and Fathi Abdullah Al-mandeel

Instructions for Authors **I**

Effects of Gel Rooting Medium Containing *Methylobacterium radiotolerans* Ed5-9 and *Streptomyces* TM32 Fermentation Broth on Cutting Propagation of *Gymnema inodorum* (Lour.) Decne.

Siripun Sarin[1], Nareeluk Nakaew[1] and Aphitchat Chidburee[2]*

[1]Department of Microbiology and Parasitology, Faculty of Medical Science, Naresuan University, Phitsanulok, Thailand
[2]Agricultural Technology Research Institute, Rajamangala University of Technology Lanna, Lampang, Thailand

Received: 5 October 2019, Revised: 5 December 2019, Accepted: 8 April 2020

Abstract

As plant cuttings have no roots, they are easily damaged and dehydrate when planted in growth medium. Better ways of protecting plants against environmental stress and increasing the sustainability of crop production after cutting propagation are needed. The aim of this study was to investigate the effects of alginate beads that contained *Methylobacterium radiotolerans* ED5-9 and *Streptomyces* TM32 fermentation broth as the growing medium on the cutting propagation of a Thai herbs, Chaing da, *Gymnema inodorum*. After 4 weeks of cultivation, the plant cuttings tested with alginate bead supplemented with both bacterial fermentations gave a higher percentage of survival than did those treated without bead (T10). The T1, 2.60 ml/l of *Streptomyces* TM32 and 0.25 mg/l of *M. radiotolerans* ED5-9 fermentation broths blended with 3% alginate treatment, presented the highest percentage of survival (90.48±6.56%), rooting (50.00±22.40%) and number of leaves per plant (5.17±0.54). These promising results were obtained when compared with the non-alginate and the synthetic IAA treatments. Therefore, using a gelling biocompatibility technique with bacterial fermentation broth was able to improve organic cutting propagation that was vulnerable to dehydration and infection by pathogens.

Keywords: *Methylobacterium radiotolerans*, *Streptomyces*, fermentation broth, *Gymnema inodorum*, gel rooting medium, cutting propagation
DOI 10.14456/cast.2020.21

*Corresponding author: Tel.: 086-183-7244
E-mail: chidburee@rmutl.ac.th

1. Introduction

Plant cutting, a simple cloning method which allows commercial growers to clone a certain plant to ensure consistency throughout their crops and can be effective depending on various factors such as type of cutting, plant species, cutting time and environment. Plant cuttings have no root systems, therefore, they are likely to die from dehydration if the conditions are not appropriate [1]. There are ways of improving the growth of cutting propagations. For example, a number of moist media are used, including but not limited to soil, perlite, vermiculite, coir, rock wool, expanded clay pellets, compost [2], and even water given the right conditions. Moreover, the roots of the cutting will usually follow the wound after dipping the cutting into accelerating hormone or anti-fungal agents. The rooting hormones, indole-3-acetic acid (IAA), indole-3-butyric acid (IBA) and 1-naphthaleneacetic acid (NAA), which are also known as auxins, can be applied to the stems of root cuttings to increase the number of adventitious roots [1]. However, in organic production, the synthetic forms of auxins such as IAA, IBA and NAA are often not permitted, and thus alternative hormones/stimulators or techniques are employed to improve rooting success rate and quality. There are natural and organic sources that can successfully provide a rooting boost to freshly taken cuttings such as honey [3], coconut water [4], willow extract [5] and even bacterial phytohormone [6].

Among the plant growth-promoting bacteria (PGPB), bacterial endophytes can be isolated from various plants that have the capacity to synthesize antibiotics and substances like plant hormones. Bacterial hormones, such as indole-3-acetic acid (IAA), cytokinins (CKs) and gibberellins (Gas), can affect not only growth and development of plant [6] but also stimulate the plant defense system [7]. Pink pigmented facultative methylotrophs (PPFMs) from the genus *Methylobacterium* were found to be plant growth-promoting bacterial endophytes that had great potential to synthesize and release IAA as a secondary metabolite [8, 9]. From our previous study, PPFMs isolate with the ability to produce phytohormone, IAA, was isolated from *Murdannia loriformis* (Hassk.) R. Rao & Kammathy leaves and the most effective isolate ED5-9 was identified later by partial 16S rDNA gene sequencing as a strain of *Methylobacterium radiotolerans* JCM 2831(T) [10]. Further work using *M. radiotolerans* ED5-9 has been done *in vitro* conditions for growth promotion in some plants, such as *Rauvolfia serpentina* [11], *Murdannia loriformis* and *Gymnema inodorum* [12], by addition of its fermentation broth into the growing plant media. Furthermore, the phytohormone synthesizing actinobacteria isolate *Streptomyces* TM32, which was related to *Streptomyces sioyaensis* discovered by Nakaew *et al*. [13], exhibited antagonistic activity against the fungus, *Rigidoporus* sp., which is known to cause white root rot disease of rubber trees, with an effective dose (ED_{50}) of fermentation broth at 2.60 ml/l. There is also a promising result examined by Sarin *et al.* [14] on the application of the isolate *M. radiotolerans* ED5-9 fermentation broth in combination with crude antimicrobial agents extracted from fermentation broth of the isolate *Streptomyces* TM32 on tissue culture of *Gymnema inodorum* (Lour.) Decne., Asclepiadaceae, known as Chiang Da (Thai name). This plant is one of the reputed medicinal plants that can decrease blood glucose [15, 16] and is widely used in Northern Thai cuisine as a local vegetable and in commercial herb tea. Therefore, an efficient method of asexual propagation via cuttings of vegetative Chiang Da is needed for the production in large quantity.

Rooting hormone, in gel form, has become the popular form of rooting hormones, because there is no preparation needed and it can be applied right to the plants, with no extra step involved [17]. It easily adheres and covers the cut surface completely, and it is the least likely to get washed away when the plants are watered. Gel IBA, a commercial hormone, has been favorable for rooting native olive cutting [18]. In particular, alginate hydrogels, which are naturally occurring anionic polymers typically obtained from brown seaweed, have been attractive to numerous applications due to their biocompatibility, low toxicity, relatively low cost, and mild gelation by addition of divalent cations such as Ca^{2+} [19]. These gels provide a physiologically moist microenvironment.

All molecules, from small to macromolecules, can also be released from alginate gels being used as growing medium, depending on the cross-linker types and cross-linking methods, which can also be specifically designed to support plant growth and supply roots with necessities such as hormones, water, air, and nutrients. Therefore, the aim of this study was to investigate the effects of fermentation broth of *M. radiotolerans* ED5-9 and *Streptomyces* TM32 blended in alginate as growing medium on the cutting propagation of *Gymnema inodorum* as a means to protect plants against environmental stress and to increase the sustainability of crop production.

2. Materials and Methods

2.1 Preparation of cell-free fermentation broth of the isolate *Methylobacterium radiotolerans* ED5-9

Methylobacterium radiotolerans ED5-9 was cultured in 100 ml liquid nutrient medium (LNM) containing 2 g/l KH_2PO_4, 2g/l $(NH_4)_2SO_4$, 0.125 g/l $MgSO_4.7H_2O$, 0.5 g/l NaCl, 0.002 g/l $FeSO_4.7H_2O$, 0.1 g/l yeast extract and filtered sterile 1% methanol (v/v) in a 250 ml Erlenmeyer flask, and the media was adjusted to pH 5.5. After incubation under the shaking conditions of 150 rpm at 30°C for 60 h, the culture was centrifuged at 10,000 g at 4°C for 15 min. In order to increase the IAA concentration, the supernatant was then evaporated at 40°C, 50 rpm, 7.2 kPa until reaching a half scale of the starting volume in a rotary evaporator (Rotavapor® R-205, Büchi Labortechnik AG) and filtered in order to preserve sterility through a filter paper (0.45 µm). The supernatant was stored at 4°C prior to use. The bacterial IAA concentration in the supernatant of *M. radiotolerans* Ed5-9 (MIAA) was quantified by colorimetric method [20]. A mixture containing 1 ml of the supernatant and 2 ml of Salkowski's reagent was incubated in the dark at ambient temperature for 30 min before its absorbance at 530 nm was measured. The calculated concentration of each sample was achieved from a standard plot of synthetic IAA (Sigma) concentrations ranging from 0.0-30.0 mg/l.

2.2 Preparation of fermentation broth of the isolate *Streptomyces* TM32

Streptomyces TM32 was cultured on Hickey-Tresner (HT) agar [21] at 30°C for 7 days. Its colonies on HT agar were then cut with cork-borers of 0.8 cm diameter, and 5 pieces of its active growth agar were inoculated in 200 ml of International *Streptomyces* Project 2 (ISP2) medium [21]. The culture was incubated at ambient temperature (~25°C) with shaking reciprocally at 120 rpm for 7 days and was later centrifuged at 10,000 g at 4°C for 15 min. *Streptomyces* TM32 supernatant was sterilized by autoclaving and kept at 4°C prior to study and was used at the ED_{50} volume of 2.60 ml/l against fungus, *Rigidoporus* sp., discovered by Nakaew *et al*. [13] to prevent fungal disease infection on the cutting stem. The actinobacterial IAA concentration was also estimated as described before.

2.3 Evaluation of growth promoting activity in plant cuttings

2.3.1 Preparation of plant cuttings

As the production of uniform, vigorous and adequate stem tip cutting stages for rooting were required for testing experiments, a clean culture was prepared by tissue culture technique. Field grown plants of *Gymnema inodorum* cultivar code 4 collected from the Agricultural Technology Research Institute, Rajamangala University of Technology Lanna (RMUTL), Thailand, were used as a source of the explants. The shoot tip explants were first soaked in a solution of 15% Clorox for

10 min and washed three times with sterile distilled water for 5 min. They were then incubated in the modified semi-solid Murashige and Skoog (MS) medium [22] containing 6-benzyl amino purine (BAP) 4 mg/l. The cultures were kept under a light intensity of 42 mol/m^2/s at 25±2°C with a 16-h-light photoperiod and 8-h-dark period for 4 weeks in order to induce plant regeneration. After proper initiation, they were cut and placed onto the new MS media containing BAP 2 mg/l and naphthalene acetic acid (NAA) 0.5 mg/l and used later as the clean culture for the stem tip cutting trials after growing for 4 weeks.

2.3.2 Preparation of alginate rooting medium

Sodium alginate (Sigma) gel (3%) fortified with various concentrations of bacterial fermentation broth or synthetic IAA according to experimental treatment design (Table 1) was prepared in sterile distilled water and was then gently added, drop by drop, through a sterile cut tip syringe into 100 mM $CaCl_2$ solution to make a bead of about 1 cm in size. The resulting alginate beads were allowed to stand for 12 h for hardening and were then autoclaved and kept in the dark at room temperature (25±2 ºC).

Table 1. Treatment design for *G. inodorum* cutting trials

Treatment	*Streptomyces* TM32 fermentation broth* (ml/l)	MIAA (mg/l)	Synthetic IAA (mg/l)
T1	2.60	0.25	-
T2	2.60	0.50	-
T3	2.60	1.00	-
T4	2.60	2.00	-
T5	2.60	-	0.50
T6	-	0.50	-
T7	2.60	-	-
T8	-	-	0.50
T9	-	-	-
T10 (without alginate bead)	-	-	-

*The volume of ED_{50} against *Rigidoporus* sp. discovered by Nakaew *et al*. [13], which contained 0.01 mg/l of IAA.

2.3.3 Experimental trials

A stem tip cutting (2 cm in length) of the *G. inodorum* clean culture was stabbed and placed into the alginate at a depth of about 3-5 mm, and the bead was then planted in a small pot (3.5 cm in diameter and 5 cm. in height) containing moist sterile peat moss. Fifteen replicates per treatment with one stem tip cutting per pot as described in Table 1 were performed. All treatments were left in a dish that was filled with the water under the light intensity of 42 mol/m^2/s for photosynthetic active radiation at 25±2°C with a 16-h-light photoperiod and 8-h-dark period for 4 weeks. Survival rates, stem tip height, leaf numbers and alginate bead morphology were observed and recorded weekly. The four-week-old harvestable fresh plants were measured for the leaf greenness values (SPAD unit) by a chlorophyll meter (Minolta SPAD -502, Japan).

2.4 Statistical analyses

Randomized Complete Block Design (RCBD) was applied for the experimental design. Mean values and the standard error of mean were calculated. Results of the measurements were subjected to analysis of variance (ANOVA) and significance at the p value < 0.05 was tested by Fisher's Least Significant Difference (LSD) by using a Minitab version 17 program.

3. Results and Discussion

After 4 weeks of cultivation, most treatments of plant cuttings with alginate beads gave a higher survival percentage than those treated without beads (T10), except for the T7, which contained only the *Streptomyces* TM32 fermentation broth. The T1, T2 and T4 presented the highest percentages of 90.48% as shown in Figure 1. However, all treatments including T1 to T4 treatments, which contained the fermentation broth of both bacteria, with the exception of T7 were not significantly different from T10.

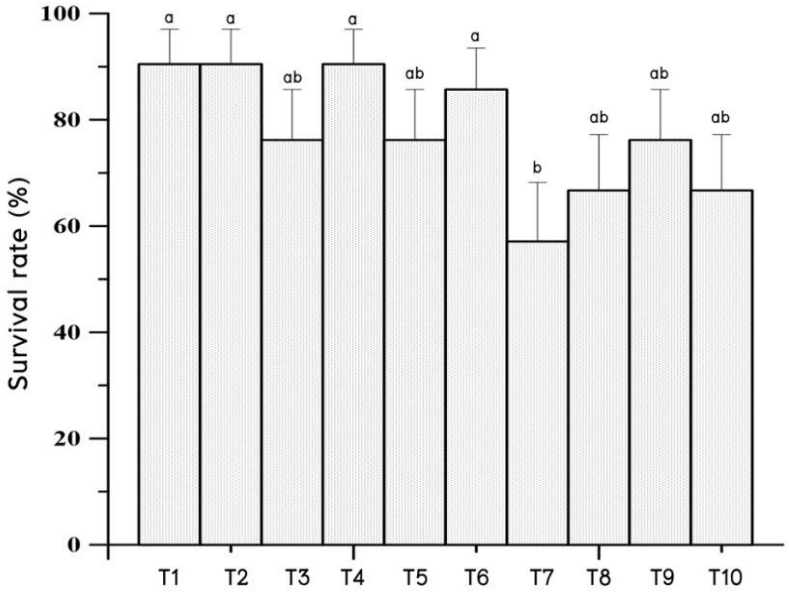

Figure 1. Effect of different concentrations of fermentation broth of *M. radiotolerans* Ed5-9 (MIAA) on survival rate of *G. inodorum*. Means followed by the same letter on the bar chart are not significantly different at p <0.05, n = 15, based on Fisher's Least Significant (LSD).

The highest rooting (50.00±22.40%), number of roots per plant and root length were obtained from the T1 test (Table 2). Although the plant cuttings tested in the T2, T7, T8 and T9 survived, no obvious roots had formed. There were only very small knobs appearing at the end of stems (Figure 2). However, cuttings still have both water and carbon stored, which are available for their growth. This detached part of the plant remains physiologically active, allowing mitotic activity and new rooting. Generally, rooting occurs within 3 to 4 weeks, but some plants take longer. The cuttings that were encouraged to form new roots may have done so due to IAA in the alginate beads;

they then grew by absorbing the minerals and nutrients contained in fermentation broth within alginate medium. Although the tested T1 showed the highest number of leaves per plant, the result was not significantly different from T2, T3, T4, T7, T8, and T10 (Table 2). On the other hand, the height of stem tip of T1was shorter (2.88±0.28 cm) after planting for 4 weeks (Table 3). The T4 and T5 gave the stem tip heights of 3.15±0.16 and 3.16±0.10 cm, respectively, which were higher than other treatments, however, there was no significant difference in stem tip height among the treatments. The alginate bead treatments that contained both bacterial fermentation broths (T1-T4) might have provided minerals and nutrients for the cuttings via their new roots, resulting in better growth of the cuttings than the growth of those treated without bacterial fermentation broth (T10). In line with this observation, the better growth of tested treatments with alginate bead (T1-T4) also showed higher chlorophyll content than the tested treatment without alginate bead of the T10 (Figure 3) and especially T2 and T4 were significantly different from T8 and T10. The alginate beads gradually degraded over the 4 weeks (Figure 4), and the cutting plants continued to grow in the peat moss. There was also no fungal contamination in the treatments.

Table 2. Effect of different concentrations of fermentation broth of *M. radiotolerans* Ed5-9 (MIAA) on rooting percentage, number of roots, root length and number of leaves of *G. inodorum* cuttings (Mean±SE ; n = 15)

Treatment	Rooting (%)	No. of root per plant	Root length (cm)	No. of leaves per plant
T1	50.00±22.40^{ns}	2.67±1.20^{ns}	1.47±0.73^{ns}	5.17±0.54^{a}
T2	nr	nr	Nr	3.83±0.65^{ab}
T3	16.70±16.70^{ns}	1.00±0.00^{ns}	0.41±0.00^{ns}	4.25±1.31^{ab}
T4	33.30±21.10^{ns}	2.50±1.50^{ns}	0.55±0.38^{ns}	3.50±0.5^{ab}
T5	16.70±16.70^{ns}	1.00±0.00^{ns}	0.24±0.00^{ns}	3.00±0.52^{b}
T6	16.70±16.70^{ns}	2.00±0.00^{ns}	0.34±0.00^{ns}	2.67±0.67^{b}
T7	nr	nr	nr	3.33±0.33^{ab}
T8	nr	nr	nr	3.25±1.11^{ab}
T9	nr	nr	nr	2.67±0.67^{b}
T10	16.70±16.70^{ns}	2.00±0.00^{ns}	2.23±0.00^{ns}	4.25±1.03^{ab}

nr = no obvious root

ns = not significantly different between treatments. Means followed by the same letter are not significantly different at p <0.05, based on Fisher's Least Significant (LSD).

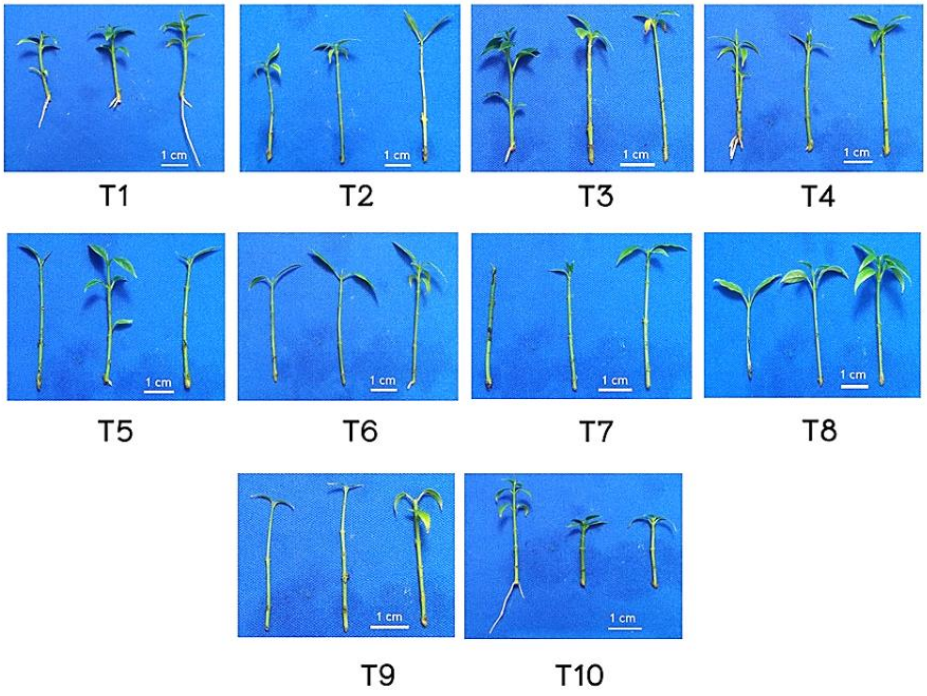

Figure 2. Morphology of *G. inodorum* cuttings after growing in different treatments for 4 weeks

Table 3. Stem tip height of *G. inodorum* cuttings measured at weekly intervals after planting in various treatments (Mean±SE ; n=15)

Treatments	Stem tip height (cm)			
	1st weeks	2nd weeks	3rd weeks	4th weeks
T1	2.74±0.20	2.76±0.21	2.82±0.28	2.88±0.28
T2	2.64±0.27	2.64±0.27	2.64±0.27	2.64±0.27
T3	2.46±0.19	2.46±0.19	2.46±0.19	2.48±0.16
T4	3.06±0.12	3.06±0.12	3.10±0.12	3.15±0.16
T5	3.04±0.08	3.04±0.08	3.04±0.08	3.16±0.09
T6	3.00±0.07	3.00±0.07	3.00±0.07	3.02±0.08
T7	2.82±0.16	2.82±0.16	2.82±0.16	2.82±0.16
T8	2.48±0.16	2.48±0.16	2.48±0.16	2.48±0.16
T9	2.62±0.22	2.62±0.22	2.62±0.22	2.62±0.22
T10	2.78±0.10	2.80±0.11	2.82±0.12	2.86±0.16

There is no significantly difference between treatments at p <0.05

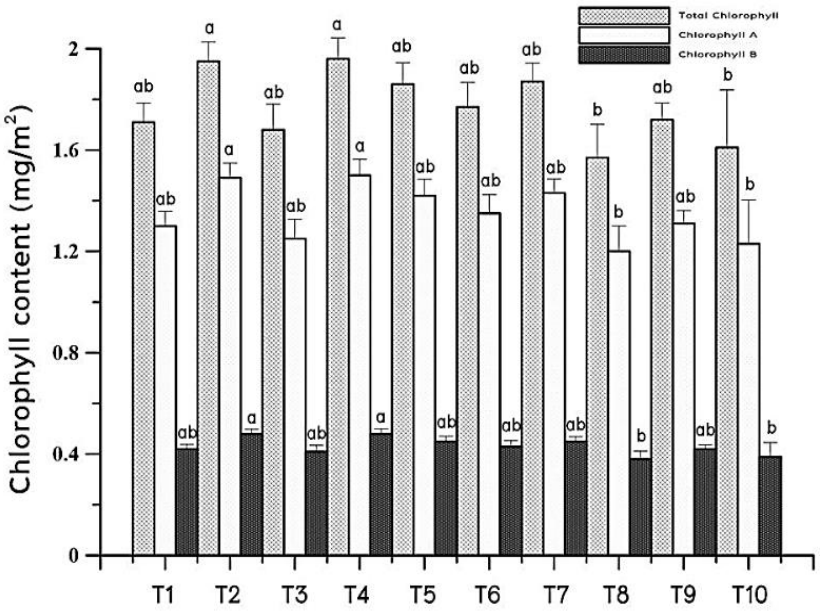

Figure 3. Leaf chlorophyll content of *G. inodorum* stem tip cuttings after planting at various treatments for 4 weeks

Figure 4. Weekly observation of alginate beads

Nowadays, alginate is known to be linear copolymers containing blocks of (1,4)-linked β-D-mannuronate (M) and α-L-guluronate (G) residues. The G-blocks of alginate are believed to participate in intermolecular cross-linking with divalent cations such as Ca^{2+}, used in this study to form hydrogels [23, 24]. Therefore, the rate of IAA hormone and other useful substance release from the fermentation broth gel depends on the physical properties and the stability of the gel.

The proper percentage of alginate in hydrogel affects the diffusion of water and nutrient from alginate bead to plant. Better diffusion in the gel medium and availability of water result in the better growth and plant survival. It has been suggested that gel bead obtained by using 3% of alginate

developed in 100 mM $CaCl_2$ solution was able to improve *in vitro* growth of pomegranate (*Punica granatum* L.) nodal segments [25] and *Cucumis sativus* L. shoot tips [26]. Since Thimann and Koepfli [27] found that synthetic preparations of IAA had root-forming properties, they also demonstrated that it could be used in stimulating root formation on cuttings. The influence of IAA on rooting had been reported by Shibaoka [28], who showed that an increased number of roots in cuttings of adzuki bean [*Vigna angularis* (Willd.) Ohwi & H. Ohashi var. *angularis* (syn. *Azukia angularis* (Willd.) Ohwi) seedlings was obtained when IAA at a high concentration was applied during the first 24 h. However, in this research, the lowest concentration of the natural IAA from *M. radiotolerans* ED5-9 (0.25 mg/l), in cooperation with the fermentation broth from *Streptomyces* TM32 (2.60 ml/l) (T1), was able to enhance rooting percentage better than other treatments. The *M. radiotolerans* ED5-9 used in this study has also been reported to produce cytokinins in an amount of 0.54 μg/ml of culture media after incubation for 5 days [29]. Application of alginate beads for the encapsulation of *Mentha arvensis* nodal segments gave the highest rate of shoot formation (80%) when observed in MS medium containing 2.0 mg/l cytokinins (BAP) and 0.2 mg/l auxin (NAA) [30]. The result showed that the percentage of rooting was reduced when the concentration of MIAA was increased in medium in which the high concentrations of IAA might cause osmotic stress [31]. Moreover, the tested *Streptomyces* TM32 could also produce an IAA concentration of 4.26 mg/l in culture media after incubation for 7 days. The existing growth of root meristem and shoot tip of plants can be stimulated at a low concentration of auxin (0.0001-0.01 mg/l), and auxin concentrations higher than 0.01 mg/l are often inhibitory due to an increase in production of ethylene [32]. The effectiveness of this application in promoting rooting on the stem cuttings may also depend on adequate absorption by plant tissue and depth of treatment where the absorption of supplement substance solution can run down the epidermis and be absorbed through the cut part [33]. Furthermore, this experiment was designed for different concentrations of microbial fermentation study as a means to create a variation of chemical substances attained in the culture medium. The growth of cuttings in this study could be thus affected by nutrient constitution of culture medium. Most of the results related with alginate bead treatments in this preliminary experiment that were not significantly different from the treatment without alginate bead may have been due to all the factors described above. Therefore, further study of the optimum size of alginate bead and some conditions needs to be done.

4. Conclusions

A blended fermentation broth of M. *radiotolerans* Ed5-9 (MIAA) 0.25 mg/l with the fermentation broth of *Streptomyces* TM32 2.60 ml/l could be used to promote rooting and growth of the *G. inodorum* cuttings. Since the aim of this research was to grow *G. inodorum* cuttings in alginate blended with bacterial fermentation broth containing phytohormones such as IAA, antibiotics and some nutrients in order to promote rooting medium and then let them continue growing in peat moss in order to insure root compatibility from the beginning, it can be concluded that promising results were obtained when compared with the non-alginate and synthetic IAA treatments. Thus, the utilization of bacterial fermentation broth with gelling biocompatibility technique can improve organic cutting propagations that are susceptible to fungal pathogens and are vulnerable to dehydration.

5. Acknowledgements

This work was supported by Naresuan University research grants in the year 2018. The authors would like to acknowledge the support of Department of Microbiology and Parasitology, Faculty of Medical Science, Naresuan University and the Agricultural Technology Research Institute, Rajamangala University of Technology Lanna.

References

[1] Hartmann, H.T., Kester, D.E., Davies, F.T. and Geneve, R.L., 2002. *Plant Propagation: Principles and Practices*. 7th ed. New Jersey: Prentice-Hall.

[2] Soundy, P., Mpati, K.W. and Du Toit, E.S., 2008. Influence of cutting position, medium, hormone and season on rooting of fever tea (*Lippia javanica* l.) stem cuttings. *Medicinal and Aromatic Plant Science and Biotechnology*, 2 (2), 114-116.

[3] Nikki, T., 2019. *Honey As A root Hormone; How To Root Cuttings With Honey*. [online] Available at http://www.gardeningknowhow.com

[4] Dunsin, O., Ajiboye, G. and Adeyemo, T., 2016. Effect of alternative hormones on the rootability of *Parkia biglobosa*. *Scientia Agriculturae*, 13(2), 113-118.

[5] Rehman, A., Khan, M.S., Zakaria, S.A., Malik, A.A. and Shahid, M., 2018. To study the effect of willow extract on apple cuttings for different time duration. *Journal of Biology, Agriculture and Healthcare*, 8(13), 21-24.

[6] Saleh-Lakha, S. and Glick, B.R., 2006. Plant growth-promoting bacteria. In: J.D. van Elsas, J.K. Jansson and J.T. Trevors, eds. *Modern Soil Microbiology*. Boca Raton: CRC/Thomson Publishing, pp. 503-520.

[7] Navarro, L., Dunoyer, P., Jay, F., Arnold, B., Dharmasiri, N., Estelle, M., Voinnet, O. and Jones, J.D.G., 2006. A plant miRNA contributes to antibacterial resistance by repressing auxin signaling. *Science*, 312, 436-439.

[8] Ivanova, E.G., Doronina, N.V. and Trotsenko, Yu.A., 2001. Aerobic methylobacteria are capable of synthesizing auxins. *Microbiology*, 70, 392-397.

[9] Omer, Z.S., Tombolini, R., Broberg, A. and Gerhardson, B., 2004. Indole-3-acetic acid production by pink-pigmented facultative methylotrophic bacteria. *Plant Growth Regulation*, 43(1), 93-96.

[10] Sarin, S., Prombunchachai, T., Nakaew, N. and Chidburee, A., 2013. Isolation of indole acetic acid producing pink pigmented facultative methylotrophs (PPFMs) from *Murdannia loriformis* (Hassk.) R. Rao & Kammathy. *Naresuan University Journal*, 21, 14-24. (in Thai)

[11] Bauthet, S., Nakaew, N., Chidburee, A. and Sarin, S., 2014. Effect of plant growth promoting substances produced by pink pigmented facultative methylotrophs on tissue culture of *Rauvolfia serpentina* (L.) Benth. ex Kurz. *Proceeding of 10th National Naresuan University Research Conference*, Phitsanulok, Thailand, 22-23 July, 2014, 150-157. (in Thai)

[12] Chidburee, A., Putawanchai, P. and Sarin, S., 2015. Effect of IAA concentration from fermentation broth with culture condition on growth and development of Chiang-da *in vitro*. *King Mongkut's Agricultural Journal*, Suppl 1, S42-46. (in Thai)

[13] Nakaew, N., Rangjaroen, C. and Sungthong, R., 2015. Utilization of rhizospheric *Streptomyces* for biological control of *Rigidoporus* sp. causing white root disease in rubber tree. *European Journal of Plant Pathology*, 142, 93-105.

[14] Sarin, S., Nareeluk Nakaew, N. and Chidburee, A., 2017. Effects of growth regulators produced by *Methylobacterium radiotolerans* Ed5-9 and crude antimicrobial agents extracted

from *Streptomyces* TM32 on tissue culture of *Gymnema inodorum* (Lour.) Decne. *Naresuan University Journal: Science and Technology*, 26(3), 52-62.

[15] Shimizu, K., Ozeki, M., Tanaka, K., Itoh, K., Nakajyo, S., Urkawa, N. and Atsuchi, M., 1997. Suppression of glucose absorption by extracts from the leaves of *Gymnema inodorum*. *The Journal of Veterinary Medical Science*, 59, 753-757.

[16] Shimizu, K., Ozeki, M., lino, A., Nakajyo, S., Urkawa, N. and Atsuchi, M., 2001. Structure activity relationship of triterpenoid derivatives extracted from *Gymnema inodorum* leaves on glucose absorption. *The Japanese Journal of Pharmacology*, 86, 223-229.

[17] Hartmann, H., Davies, F., and Geneve, R., 2002. Hartmann and Kester's plant propagation: Principles and practices. 7th ed. New Jersey: Prentice Hall.

[18] Ismaili, H., 2016. Study of some forms of IBA in the rooting process of the olive. *International Journal of Current Microbiology and Applied Sciences*, 5 (3), 239-246.

[19] Lee, K.Y. and Mooney, D.J. 2012. Alginate: properties and biomedical applications. *Progress in Polymer Science*, 37(1), 106-126.

[20] Glickmann, E. and Dessaux, Y., 1995. A critical examination of the specificity of the salkowski reagent for indolic compounds produced by phytopathogenic bacteria. *Applied and Environmental Microbiology*, 61, 793-796.

[21] Atlas, R.M., 1996. *Handbook of Microbiological Media*. 2nd ed. Florida: CRC Press.

[22] Murashige, T. and Skoog. F., 1962. A revised medium for rapid growth and bioassays with tobacco tissue culture. *Physiologia Plantarum*, 15, 473-497.

[23] Fischer, F.G., Dörfel, H., 1995. Die polyuronsauren der braunalgen-(kohlenhydrate der algen-I). *Hoppe-Seyler's Zeitschrift fur Physiologische Chemie*, 302, 186-203.

[24] George, M. and Abraham, T.E., 2006. Polyionic hydrocolloids for the intestinal delivery of protein drugs. *Journal of Controlled Release*, 114, 1-14.

[25] Naik, S.K. and Chand, P.K., 2006. Nutrient-alginate encapsulation of *in vitro* nodal segments of pomegranate (*Punica granatum* L.) for germplasm distribution and exchange. *Scientia Horticulturae*, 108, 247-252.

[26] Adhikaria, S., Bandyopadhyay, T.K. and Ghosha, P., 2014. Assessment of genetic stability of *Cucumis sativus* L. regenerated from encapsulated shoot tips. *Scientia Horticulturae*, 170, 115-122.

[27] Thimann, K.V. and Koepfli, J.B., 1935. Identity of the growth promoting and root-forming substances of plants. *Nature*, 135, 101-102.

[28] Shibaoka, H., 1971. Effects of indoleacetic, *p* chlorophenoxyisobutyric and 2,4,6-trichlorophenoxyacetic acids on three phases of rooting in *Azukia* cuttings. *Plant Cell Physiology*, 12, 193-200.

[29] Prombunchachai, T., 2015. *Potential of Pink-Pigmented Facultative Methylotrophs (PPFMs) to Enhance Growth of Murdannia loriformis (Hassk.) R. Rao & Kammathy in Tissue Culture*. Ph.D. Naresuan University, Thailand.

[30] Islam, M.S. and Bari, M.A., 2012. *In vitro* regeneration protocol for artificial seed production in an important medicinal plant *Mentha arvensis* L. *Journal of Bio-Science*, 20, 99-108.

[31] Naser, V. and Shani, E., 2016. Auxin response under osmotic stress. *Plant Molecular Biology*, 91, 661-672.

[32] George, E.F., 2008. Plant growth regulators I: Introduction; auxins, their analogues and inhibitors. In: E.F. George, M.A. Hall and J. Deklerk, eds. *Plant Propagation by Tissue Culture*. 3rded. Dordrecht: Springer.

[33] Blythe, E.K., Sibley, J.L., Tilt, K.M. and Ruter, J.M., 2007. Methods of auxin application in cutting propagation: A review of 70 years of scientific discovery and commercial practice. *Journal of Environmental Horticulture*, 25(3), 166-185.

Current Applied Science and Technology Vol. 20 No. 3 (September-December 2020)

Detection of Pathogenic Bacteria in the Air by Culture Techniques in Combination with Multiplex Polymerase Chain Reaction

Wimon Chanchaem* and Somchai Awakairt

Department of Biology, Faculty of Science, Ramkhamhaeng University, Bangkok, Thailand

Received: 9 November 2019, Revised: 15 March 2020, Accepted: 18 April 2020

Abstract

Respiratory infections are among important infections in human. The causative agents are diverse group of bacteria, virus, fungi and parasites. This research focuses on the detection of microbial contaminants and respiratory pathogens in indoor air of university environment by application of a molecular method. Seven pathogens including *Streptococcus pneumoniae*, *Streptococcus pyogenes*, *Staphylococcus aureus*, *Haemophilus influenzae*, *Klebsiella pneumoniae*, *Pseudomonas aeruginosa* and *Legionella pneumophila* were screened. Twenty-eight air samples were analyzed by conventional culture method and the multiplex polymerase chain reaction (mPCR) that detected those seven pathogens simultaneously within three reactions. The conventional culture method showed the average total count of large lecture rooms at 3.4 CFU plate^{-1} h^{-1}, small lecture rooms at 5.2 CFU plate^{-1} h^{-1}, meeting rooms at 4.3 CFU plate^{-1} h^{-1}, office rooms at 3.0 CFU plate^{-1} h^{-1}, canteen rooms at 31.5 CFU plate^{-1} h^{-1} and service vans at 5.5 CFU plate^{-1} h^{-1}. Contaminants comprised Gram-positive bacteria, Gram-negative bacteria and molds. The genus compositions were *Staphylococcus* spp. (62.50%), *Micrococcus* spp. and *Kytococcus* spp. (58.33%), *Bacillus* spp. (41.64%), *Moraxella* spp. (29.17%), *Corynebacterium* spp. (25.00%) and *Pseudomonas* spp. (20.83%). MultiplexPCR was able to detect *Staphylococcus aureus* and *Streptococcus pyogenes* at 16.67% and 4.17% of air samples, respectively, whereas conventional method did not. These two bacteria are important pathogens of human and are common cause of wide range of infections. The results suggested that mPCR was a useful supplement to the conventional method to monitor indoor air microbiological quality and should be introduced in guidelines of indoor air quality monitoring.

Keywords: Airborne bacteria, respiratory infections, multiplex polymerase chain reaction
DOI 10.14456/cast.2020.22

*Corresponding author: Tel.: (+66) 81-8432-899 Fax: (+66) 2-3108-418
E-mail: chanchaemw@yahoo.com

1. Introduction

Respiratory infections are among most important infections of the world population. Large budgets have been spent by many countries to deal with these diseases. However, they tend to be more severe and widely spread, hence efficient and urgent controls are needed. Starting from understanding the sources and important factors concerning human respiratory infections is agreed to be a reasonable approach [1, 2].There are large variety of respiratory infectious diseases which may be acute or chronic, and examples include influenza, pneumonia, tuberculosis, bronchitis, and the common cold. The causative agents can be bacteria, virus and fungi with a big diverse group and pathogenicity level. These microbes can be transmitted by aerosols from infected human oral and respiratory fluid, causing widely spread of diseases [3-5]. Exposure to contaminated air is a kind of threat for human health because even generally nonpathogenic microbes can cause infection in hosts that are compromised. The reservoirs of pathogens, such as the antibiotic-resistant *Staphylococcus aureus*, are known to be not limited only to hospitals, but are also found in the indoor environments of normal residential buildings [6, 7]. Understanding of aerosols and particles in the indoor environment tends to be closely concerned with infection control of respiratory diseases [2, 3]. Interestingly, it has been expressed that characterization of airborne bacteria is important for understanding disease transmission from person to person.There were also reports that some bacteria isolated from indoor air can be tracked back to human origin [8, 9].

Human occupants are one of the most important factors concerning respiratory infection from indoor air. The efficient prevention and control of the diseases to provide safety to people who spend most of the time indoors should start from learning about the aerosols and materials from human occupants that may disperse in environmental areas. However, the microbial contents in indoor environment of most universities have not been investigated and the essential information for good management is still needed. The conventional method to determine the microbial content is culture and identification which is the gold standard method. However, some fastidious organisms may not be detected when they are present at low amount. Molecular techniques such as Polymerase chain reaction (PCR) have been accepted to be very helpful for microbial detection in various samples according to their sensitivity, specificity and rapidity [10-13].

The multiplex polymerase chain reaction (mPCR) is a type of PCR technique that has become widespread and very popular for amplification of more than one target sequence in a reaction mixture using multiple primer pairs. This technique is time saving since many species of microorganisms can be detected at the same time [14-16]. Therefore, in this study we aimed to investigate indoor air of a university for the concentration and diversity of microbial contaminants including the seven important pathogens by using culture technique in combination with mPCR. The results show the concentration and composition of microbes including some pathogenic species that may exist. This will be a very useful information for universities to prevent and control the respiratory infections for their students.

2. Materials and Methods

2.1 Sampling environment

Total of twenty eight air samples were collected from six groups of locations in a university including large lecture rooms, small lecture rooms, meeting rooms, office rooms, canteen rooms and service vans.

2.2 Cultivation method

Indoor air samples were collected by using settle plate method with the 1/1/1 (1 h, 1 m from the floor, at least 1 m away from walls) schedule [17]. Various culture media in a 10 cm diameter Petri-dish were used according to the investigated microbes, including Plate count agar (PCA), Blood agar (BA), Sabouraud dextrose agar (SDA), Potato dextrose agar (PDA), Chocolate agar for *Haemophilus influenzae* and Legionella BCYE agar for *Legionella pneumophila*. Plate count agar and Blood agar were incubated at 37ºC, Sabouraud dextrose agar and Potato dextrose agar were incubated at 25ºC, Chocolate agar were incubated at 37ºC in candle jar and Legionella BCYE agar were incubated at 37ºC. All plates were incubated for 24-48 h followed by colony examination and identification by conventional method [18]. Levels of contamination were recorded as colony forming unit per plate per hour (CFU plate^{-1} h^{-1}).

2.3 Molecular method

Samples for DNA detection of contaminants were collected by using impactor sampler, Reuter Centrifugal Air Sampler, loading with a 9 cm filter, according to the instruction.The samples were prepared for DNA extraction by cutting each filter into small pieces and suspended in 5 ml buffer peptone water (pH 7.2, 1 l comprising 10 g of peptone, 5 g of sodium chloride, 3.5 g of disodium phosphate and 1.5 g of potassium dihydrogen phosphate). After vortexing for 2 min followed by centrifugation at 12,000 rpm for 5 min, the supernatant was collected for DNA extraction steps. Bacterial DNA from the collected supernatant was extracted using InstaGene^{TM}Matrix according to the manufacturer's instruction and the clear supernatant was collected and stored at -20ºC for using as DNA sample in further steps.

PCR detection of bacterial contaminants in all samples was performed by using primers specific for each of seven important bacterial species including *Streptococcus pneumonia*e (Ply F, Ply R), *Streptococcus pyogenes* (LytA F, LytA R), *Staphylococcus aureus* (sa442 F, sa442 R), *Haemophilus influenzae* (Hae F, Hae R), *Klebsiella pneumoniae* (Pf, Pr2), *Pseudomonas aeruginosa* (PA1, PA2) and *Legionella pneumophila* (Mip F, Mip R), as shown in Table 1.

Table 1. PCR primers, target genes and product sizes from DNA amplification of studied pathogens

Bacterial Species	Target genes	Primers	Primer sequences	Product (bp)/Ref
Haemophilus influenzae	16S rDNA	Hae F	ttg aca tcc taa gaa gag ctc	167/ [19]
		HaeR	tct cct ttg agt tcc cga ccg	
Streptococus pneumoniae	*ply*	Ply F	gaa ttc cct gtc ttt tca aag tc	348/ [20]
		Ply R	att tct gta aca gct acc aac ga	
Klebsiella pneumoniae	16s-23s ITS	Pf	att tga aga ggt tgc aaa cga t	260/ [21]
		Pr2	ccg aag atg ttt cac ttc tga tt	
Pseudomonas aeruginosa	Antigen H	PA1	tcc aaa caa tcg tcg aaa gc	181/ [22]
	16s-23s ITS	PA2	ccg aaa att cgc gct tga ac	
Streptococcus pyogenes	*lytA*	LytA F	gag aga cta acg cat gtt agt a	317/ [19]
		LytA R	tag tta ccg tca ctt ggt gg	
Staphyococcus aureus	*sa442*	sa442 F	tcg gta cac gat att ctt cac	179/ [20]
		sa442 R	act ctc gta tga cca gct tc	
Legionella pneumophila	*mip*	Mip F	acc gaa cag caa atg aaa ga	144/ [19]
		Mip R	aac gcc tgg ctt gtt ttt gt	

The PCR reaction mixture of 50 µl contained 1XPCR buffer, 2.5 mM of $MgCl_2$,1 µM of each primer, 250 µM of dNTPs, 1.25 U *Taq* DNA polymerase and 100 ng of DNA template.Two

amplification profiles of multiplex reactions were used.The first profile for primers Hae F/Hae R, LytA F/LytA R, sa442 F/sa442 R and Mip F/Mip R began with initial denaturation at 95ºC for 30s followed by 40 cycles of denaturation at 94ºC for 15s, annealing at 50ºC for 30s and extension at 75ºC for 30s and then final extension at 72ºC for 10 min. Another profile for the other set of primers including Ply F/Ply R, Pf/Pr2, PA1/PA2 was initial denatured at 94ºC for 10 min followed by 35 cycles of denaturation at 94ºC for 30s, annealing at 57ºC for 20s and extension at 72ºC for 20s before final extension at 72ºC for 10 min. The PCR products were examined by agarose gel electrophoresis and ethidium bromide staining.

3. Results and Discussion

3.1 Microbial diversity and density

From twenty eight air samples of six groups of sampling locations, all were positive for microbial contamination at different levels. The investigation was performed both for total microbial contamination and for seven specified pathogens. Evaluation of total contamination by using conventional culture method showed the average total count on blood agar of large lecture rooms at 3.4 CFU plate^{-1} h^{-1}, small lecture rooms at 5.2 CFU plate^{-1} h^{-1}, meeting rooms at 4.3 CFU plate^{-1} h^{-1}, office rooms at 3.0 CFU plate^{-1} h^{-1}, canteen rooms at 31.5 CFU plate^{-1} h^{-1} and service vans at 5.5 CFU plate^{-1} h^{-1}. The comparison of total aerobic microbial count of those six location groups was shown in Figure 1 and the level of microbiological air quality according to the Standard Index of Microbial Air Contamination (IMA) classes was shown in Table 2. Figure 1 showed the variation of total aerobic microbial count both among location groups and within the same group. The results showed that canteen areas were more contaminated than others, this may depend on many factors such as the number of occupants, their activities, physical factors, sources of contaminants and cleaning practice. It was also found that more contamination was observed in more crowded locations of canteens. So this will be useful data for further improvements. Characterization of microbes demonstrated both Gram-positive and Gram-negative bacteria including some molds. In total of twenty eight samples sites the rates of finding of bacterial genera frequently isolated were *Staphylococcus* spp. (62.50%), *Micrococcus* spp. and *Kytococcus* spp. (58.33%), *Bacillus* spp. (41.64%), *Moraxella* spp. (29.17%), C*orynebacterium* spp. (25.00%) and *Pseudomonas* spp. (20.83%). Figure 2 showed the prevalence rate of each bacterial group in all air samples. These bacteria are generally found in human body and environment. Two of the most prevalent bacteria were *Staphylococcus* spp. and *Bacillus* spp. This corresponded to the fact that *Staphylococcus* spp. naturally lives on skin and surfaces of human and animals whereas *Bacillus* spp. is commonly found in environment such as in air, soil and water and can also be found in human and animals.Thus, it corresponds to the mention that general human activities and shedding of skin can be very large sources of bioaerosols, airborne particles and microbes [2, 9, 23-27]. Investigation of microbiological contamination of indoor air will reflect the quality of indoor air upon utilization by occupants.

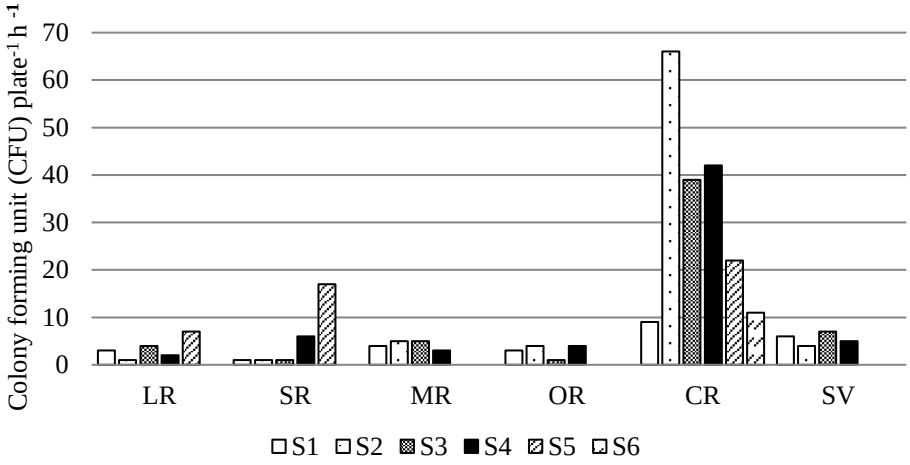

Figure 1. Total aerobic microbial load of indoor air samples from different location groups: Large lecture rooms (LR), Small lecture rooms (SR), Meeting rooms (MR), Office rooms (OR), Canteen rooms (CR) and Service vans (SV). S1-S6 represent contamination level of sampling location 1, sampling location 2, sampling location 3, sampling location 4, sampling location 5, and sampling location 6 within the group

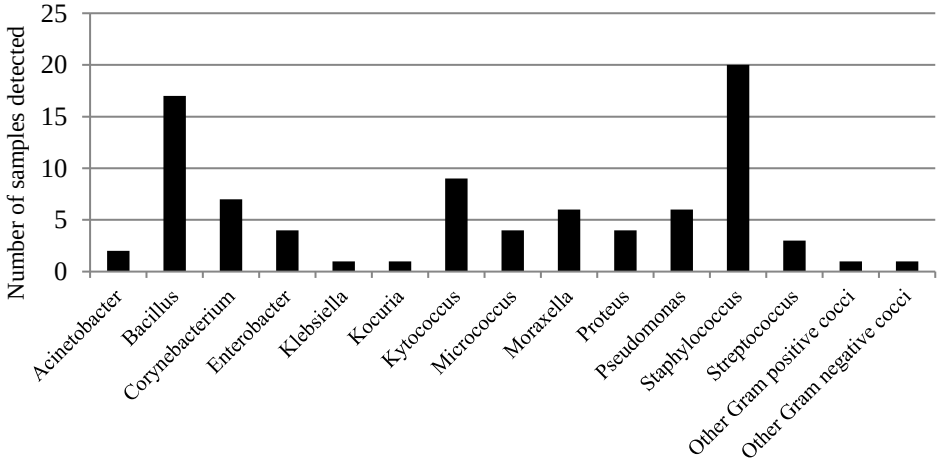

Figure 2. Prevalence rate of aerobic bacterial species in twenty eight air samples of six different sampling locations

Table 2. Microbiological air quality of the six sampling locations according to the Standard Index of Microbial Air Contamination (IMA) classes [17]

Sampling locations	Microbial count (CFU/dm^2/h)	Air quality level (IMA classes)
Large lecture rooms	5.86	Very good (0-9 CFU/dm^2/h)
Small lecture rooms	8.96	Very good (0-9 CFU/dm^2/h)
Meeting rooms	7.33	Very good (0-9 CFU/dm^2/h)
Office rooms	5.17	Very good (0-9 CFU/dm^2/h)
Canteen rooms	54.31	Fair (10-84 CFU/dm^2/h)
Service vans	9.48	Good (10-39 CFU/dm^2/h)

3.2 Detection of specific pathogens by multiplex polymerase chain reaction

Multiplex polymerase chain reaction (mPCR), which is a molecular method, was used to supplement the conventional methods used to evaluate indoor air microbiological quality. As shown in Table 1, seven primers pairs were used to detect seven important pathogens in three PCR reactions with proper optimization for good product at expected length.

Figure 3 showed the electrophoresis result of PCR amplification after proper optimization of DNA from *Haemophilus influenzae* using Hae F/Hae R primers (Panel A), *Streptococcus pneumoniae*, *Klebsiella pneumoniae* and *Pseudomonas aeruginosa* using Ply F/Ply R, Pf/Pr2 and PA1/PA2 primers as multiplex PCR (Panel B) and *Streptococcus pyogenes*, *Staphylococcus aureus* and *Legionella pneumophila* using LytA F/LytA R, sa442 F/sa442 R and Mip F/Mip R as multiplex PCR (Panel C). The length of amplified products specific to each organism was indicated in the illustrations.

By using the mPCR method, *Staphylococcus aureus* and *Streptococcus pyogenes* were detected at 16.67% and 4.17% respectively, of total air samples. The locations of these positive samples were in one small lecture room, one meeting room, two office rooms and one canteen room whereas the conventional method did not detect these pathogens in the same air samples. This corresponded to the fact that the culture method which is known as gold standard method for microbial detection still has some limitations, for example in case of fastidious organisms, viable but nonculturable state and non viable state of microorganisms [28]. *Staphylococcus aureus* and *S. pyogenes* were not observed in the culture process so they were not included in the rate of detection using culture method. This suggested that mPCR could be a helpful tool for detection and monitoring of contaminants since the present of DNA will reflect the presence of that microbe in the area investigated.

Staphylococcus spp. was also reported to be commonly isolated from the air in residential and commercial building [29-33]. It was mentioned that characterization of airborne bacteria can be helpful to determine the source of contaminants and to understand the transmission of microbes from person to person [32-35]. This makes the determination of indoor air contaminants be very important for contamination control.

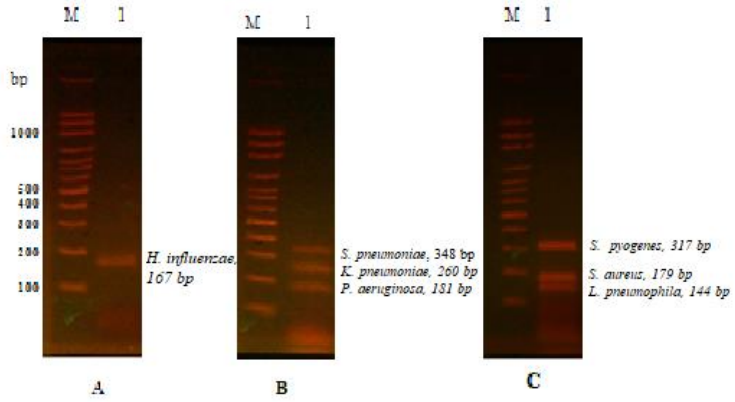

Figure 3. Optimization of mPCR for detection of seven bacterial pathogens as shown by 2% agarose gel electrophoresis of amplification products. (A) *Haemophilus influenzae*, Hae F/Hae R primers, (B) *Streptococcus pneumoniae*, *Klebsiella pneumoniae* and *Pseudomonas aeruginosa*, Ply F/Ply R, Pf/Pr2 and PA1/PA2 primers, (C) *Streptococcus pyogenes*, *Staphylococcus aureus* and *Legionella pneumophila*, LytA F/LytA R, sa442 F/sa442 R and Mip F/Mip R primers. M: Molecular size marker, lane 1 in each panel was from PCR amplification

4. Conclusions

The results demonstrated that despite the conventional culture method for determination of microbial contaminations of indoor air, the using of mPCR method can provide early detection of some important pathogens and will lead to early actions to prevent occupants from infections. The mPCR technique was a useful supplement to conventional methods to determine indoor air microbiological quality and should be introduced to indoor air quality monitoring.

References

[1] Gupta, A.K., Lyon, D.C. and Rosen, T., 2015. New and emerging concepts in managing and preventing community-associated methicillin-resistant *Staphylococcus aureus* infections. *International Journal of Dermatology*, 54, 1226-1232.

[2] Hospodsky, D., Qian, J., Nazaroff, W.W., Yamamoto, N., Bibby, K., Rismani-Yazdi, H. and Peccia, J., 2012. Human occupancy as a source of indoor airborne bacteria. *PLOS One*, 7(4), c34867, https://doi.org/10.1371/journal.pone.0034867

[3] Obbard, J.P. and Fang, L.S., 2003. Airborne concentration of bacteria in a hospital environment in Singapore. *Water, Air, and Soil Pollution*, 144, 333-341.

[4] van Belkum, A., Verkaik, N.J., de Vogel, C.P., Boelens, H.A., Verveer, J., Nouwen, J.L., Verbrugh, H.A. and Wertheim, H.F., 2009. Reclassification of *Staphylococcus aureus* nasal carriage types. *Journal of Infectious Diseases*, 199, 1820-1826.

[5] Yagoub, S.O. and El Agbash, A., 2010. Isolation of potential pathogenic bacteria from the air of hospital-delivery and nursing room. *Journal of Applied Sciences*, 10(11), 1011-1014.

[6] Gandara, A., Mota, L.C., Flores, C., Perez, H.R., Green, C.F. and Gibbs, S.R., 2006. Isolation of *Staphylococcus aureus* and antibiotic-resistant *Staphylococcus aureus* from residential indoor bioaersols. *Environmental Health Perspectives*, 114, 1859-1864.

[7] Lin, J., Lin, D., Xu, P., Zhang, T., Ou, Q., Bai, C. and Yao, Z., 2016. Non hospital environment contamination with *Staphylococcus aureus* and methicillin-resistant *Staphylococcus aureus*: proportion meta-analysis and futures of antibiotic resistant and molecular genetics. *Environmental Research*, 150, 528-540.

[8] Fox, A., Harley, W., Feigley, C., Salzberg, D., Toole, C., Sebastian, A. and Lennard, L., 2005. Large particles are responsible for elevated bacterial marker levels in school air upon occupation. *Journal of Environmental Monitoring*, 7, 450-456.

[9] Fox, K., Fox, A., Elbner, T., Elssner, T., Feigley, C. and Salzberg, D., 2010. MALDI-TOF mass spectrometry speciation of Staphylococci and their discrimination from micrococci isolated from indoor air of school rooms. *Journal of Environmental Monitoring*, 12, 917-923.

[10] Aslam, M., Hogan, J. and Smith K.L., 2003. Development of a PCR-based assay to detect Shiga toxin-producing *Escherichia coli*, *Listeria monocytogenes* and *Salmonella* in milk. *Food Microbiology*, 20, 345-350.

[11] Clalos, M.G. and Ana, R.Q., 2000. PCR as specific, sensitive and simple method suitable for diagnostics. *Biochemistry and Molecular Biology Education*, 28, 223-226.

[12] Martineau, F., Picard, F.J., Menard, C., Roy, P.H., Quellette, M. and Bergeron, M.G., 2000. Development of rapid PCR assay specific for *Staphylococcus saprophyticus* and application to direct detection from urine samples. *Journal of Clinical Microbiology*, 38(9), 3280-3284.

[13] Riffon, R., Sayasith, K., Khalil, H., Dubreuil, P., Drolet, M. and Lagace, J., 2001. Development of a rapid and sensitive test for identification of major pathogens in bovine mastitis by PCR. *Journal of Clinical Microbiology*, 39(7), 2584-2589.

[14] Alka, M. and Utpal, K.M., 2007. Novel multiplex PCR approaches for the simultaneous detection of human pathogens: *Escherichia coli* O157: H7 and *Listeria monocytogenes*. *Journal of Microbiological Methods*, 68(1),193-200.

[15] Elnifro, E.M., Ashshi, A.M., Cooper, R.J. and Klapper, P.E., 2000. Multiple PCR: optimization and application in diagnostic Virology. *Clinical Microbiological Reviews*, 13, 559-570.

[16] Jofre, A., Martin, B., Garriga, M., Hugas, M., Pla, M. and Rodriguez-Lazaro, D. and Aymerich, T., 2005. Simultaneous detection of *Listeria monocytogenes* and Salmonella by multiplex PCR in cooked ham. *Food Microbiology*, 22, 109-115.

[17] Pasquarella, C., Pitzurra, O. and Savino, A., 2000. The index of microbial air contamination. *Journal of Hospital Infection*, 46, 241-256.

[18] Tille, P.M., 2014, *Bailey & Scott's, Dignostic Microiology*, 13th eds, Missouri: Elsevier.

[19] Morozumi, M., Nakayama, E., Iwata, S., Aoki, Y., Hasegawa, K., Kobayashi, R., Chiba, N., Tajima, T. and Ubukata, K., 2006. Simultaneous detection of pathogens in clinical samples from patients with community-acquired pneumonia by real-time PCR with pathogen-specific molecular beacon probes. *Journal of Clinical Microbiology*, 44(4), 1440-1446.

[20] Anbazhagan, D., Mui, W.S., Mansor, M., Yan, G.S.O., Yusof, M.Y. and Sekaran, S.D., 2011. Development of conventional and real-time multiplex PCR assays for the detection of nosocomial pathogens. *Brazillian Journal of Microbiology*, 42, 448-458.

[21] Liu, Y., Liu, C., Zheng, W., Zhang, X., Yu, J., Gao, Q., Hou, Y. and Huang, X., 2008. PCR detection of *Klebsiella pneumoniae* in infant formula based on 16S-23S internal transcribed spacer. *International Journal of Food Microbiology*, 125, 230-235.

[22] Tyler, S.D., Strathdee, A., Rozee, K.R. and Johnson, W.M., 1995. Oligonucleotide primers designed to differentiate pathogenic Pseudomonads on the basis of the sequening of genes coding for 16S-23SrRNA internal transcribed spacers. *Clinical and Diagnostic Laboratory Immunology*, 2(4), 448-453.

[23] Kolly, C.A., Arbogast, J.W. and Macing, D.R., 2006. Bacterial shedding and desquamation from the hands of healthcare workers correlates with skin condition. *American Journal of Infection Control*, 34(5), E85-E86.
[24] Qian, I., Hospodsky, D., Yamamoto, N., Nazarolf, W.W. and Piccia I., 2012. Size-resolved emission rate of airborne bacteria and fungi in an occupied classroom. *Indoor Air*, 22(4), 339-351.
[25] Ferro, A.R., Kopperud, R.J. and Hildemann, L.M., 2004. Source strengths for indoor human activities that resuspend particulate matter. *Environmental Science & Technology*. 38, 1759-1764.
[26] Koistinen, K.J., Edwards, R.D., Mathys, P., Ruuskanen, J., Künzli, N. and Jantunen, M.J., 2004. Sources of fine particulate matter in personal exposures and residential indoor, residential outdoor and workplace microenvironments in the Helsinki phase of the EXPOLIS study. *Scandinavian Journal of Work, Environment & Health*, 30, 36-46.
[27] Koperrud, R.J., Ferro, A.R. and Hildemann, L.M., 2004. Outdoor versus indoor contributions to indoor particulate matter (PM) determined by mass balance methods. *Journal of Air & Waste Management Association*, 54, 1188-1196.
[28] Oliver, J.D., 2010. Recent findings on the viable but nonculturable state in pathogenic bacteria. *FEMS Microbiological Reviews*, 34(4), 415-425.
[29] Gaska-Jedruch, U. and Dudzinska, M.R., 2009. Microbiological pollution in indoor air. In: J. Ozonek and M. Pawlowska, eds. *Polish Environmental Engineering Five Years After the UE Accession*. Lublin: Polish Academy of Sciences.
[30] Rintala, H., Pitkaranta, M., Toivola, M., Paulin, L. and Nevalainen, A., 2008. Diversity and seasonal dynamics of bacterial community in indoor environment. *BMC Microbiology*, 8(56), https://doi.org/10.1186/1471-2180-8-56
[31] Bonetta, S.A., Bonetta, S.T., Mosso, S. and Sampo, S., 2010. Assessment of microbiological indoor air quality in an Italian office building equipped with an HVAC system. *Environmental Monitoring Assessment*, 161(1-4), 473-483.
[32] Seino, K., Takano, T., Nakamura, K. and Watanabe, M., 2005. An evidential example of airborne bacteria in a crowded underground public concourse in Tokyo. *Atmospheric Environment*, 39(2), 337-341.
[33] Hayleeyesus, S.F. and Manaye, A.M., 2014. Microbiological quality of indoor air in university libraries. *Asian Pacific Journal of Tropical Biomedicine*, 4, S312-S317.
[34] Kooken, I.M., Fox, K.F. and Fox, A., 2012. Characterization of Micrococcus strains isolated from indoor air. *Molecular and Cellular Probes, 2*6(1), 1-5.
[35] Madsen, A.M., Jenabian, S.M., Islam, M.Z., Frankel, M., Spilak, M. and Federiksen, M.W., 2018. Concentrations of *Staphylococcus* species in indoor air as associated with other bacteria, season, relative humidity, air change rate, and *S. aureus*-positive occupants. *Environmental Research*, 160, 282-291.

Expression of Recombinant *Alcohol Dehydrogenase* in *Escherichia coli* Strain BL21 (DE3) and *In Planta Agrobacterium* Transformation of Tomato Seeds

Mastura Sani[1]* and Hairul Azman Roslan[2]

[1]Food Technology, School of Engineering and Technology, University College of Technology Sarawak, Sarawak, Malaysia
[2]Faculty of Resource Science and Technology, Universiti Malaysia Sarawak, Sarawak, Malaysia

Received: 26 December 2019, Revised: 13 March 2020, Accepted: 24 April 2020

Abstract

Alcohol dehydrogenase is an enzyme that is involved in various roles in plant such as plant development, growth and plant responses to abiotic and biotic stresses. A recombinant *alcohol dehydrogenase 1* (*Adh1*) cDNA (r-*msAdh1*) from *Metroxylon sagu* has been previously isolated, and it contained 20 nucleotides derived from *Elaeis guineensis* at the 5'-end and had a molecular weight of 1.14 kb. The objective of this study is to determine the function of r-ms*Adh1* via analyses in prokaryotic and eukaryotic hosts. For expression in prokaryotic system, pET-41a(+) with a 8x His tag at the C terminal was used for r-msAdh1 protein purification, and expression was achieved using IPTG for 4-6 h in *Escherichia coli* strain BL21 (DE3) incubated at low temperature. The induced BL21 strain produced a small amount of soluble r-msAdh1 protein while a large amount was present as insoluble aggregates. Subsequently, the r-*msAdh1* cDNA was transformed into tomato seeds (*Solanum lycopersicum* cv. MT1) via *Agrobacterium*-mediated *in planta* transformation. The integration of r-*msAdh1* cDNA and the selectable marker were detected in transformed seedlings, T_0, using polymerase chain reaction technique. The transformation efficiency was determined to be 33% for r-*msAdh1* cDNA and 46% for the selectable marker. For stability analysis of the transgene, eleven T_1 generation randomly selected seedlings from the transgenic T_0 were analyzed for the presence of the cDNA, and all seedlings were found to contain the full length of r-*msAdh1* cDNA. However, out of the eleven T_1 transgenic lines produced, only four seedlings were used for expression analysis using the reverse transcriptase PCR (RT-PCR). Two transgenic lines, $T_1$9 and $T_1$11, were determined to contain r-*msAdh1* cDNA and this was verified by nucleotide sequencing. Although only a small number of T_1 transgenic seedlings was obtained, this study shows that tomato seeds could be used as a target tissue for *Agrobacterium*-mediated *in planta* transformation primarily because the protocol is easy, rapid and cheaper compared to tissue culture-based methods.

Keywords: *Alcohol dehydrogenase*, *Metroxylon sagu*, BL21 (DE3), *Agrobacterium tumefaciens*, tomato seeds
DOI 10.14456/cast.2020.23

*Corresponding author: Tel.: +60 84 36 75 50, Fax: +60 84 36 73 01
Email: masturasani88@gmail.com

1. Introduction

Alcohol dehydrogenase (ADH) is an enzyme that is actively expressed when plants are exposed to environmental stresses, e.g., anoxic or hypoxic conditions, osmotic stress, wound, dehydration and low-oxygen stress in water-logged roots [1- 4]. Apart from this, ADH is also involved in all stages of plant growth [5]. To better understand the role of ADH, expression studies have been conducted to produce soluble, bioactive ADH in various expression hosts [6-10]. While heterologous expression has been reported in many microorganisms, most of the research work has utilized the *E. coli* system because of the ease of genetic manipulation, and because of the availability of optimized expression vectors and host strains for the expression of eukaryotic proteins [11-13]. However, high levels of protein expression in *E. coli* often cause incorrect protein folding due to the bacteria's inability to carry out post-translational modifications, which results in aggregation of insoluble inclusion bodies (IBs) [14, 15]. For that reason, some *E. coli* strains, such as Rosetta (DE3), Rosetta-gami 2 (DE3) and *E. coli* strain BL21 (DE3), have been designed to enhance the expression of eukaryotic protein, and importantly these strains have been shown to successfully express soluble eukaryotic ADH [8-11]. To overcome the insolubility of proteins, induction at low temperature has been shown to alleviate the problem [9-10]. It works because the hydrophobic interactions that causes IBs to form are temperature dependent [16].

The expression in the eukaryotic host system provides several advantages such as easy genetic manipulation, high expression level, glycosylation ability and other eukaryotic post-translational modifications [17] compared to prokaryotic systems. Tomato (*Solanum lycopersicum* cv. MT1) is a member of *Solanaceace* family and abundant in genetic and genomic resources compared to other cultivated species [18]. It has also been used for development of new tools and plant models for genetic and genomic analyses [19]. Tomatoes have been used to study various aspects including herbicide tolerance [20], disease and insect resistance [21, 22], improvement in fruit quality [23], control in fruit ripening [24], improving yield [25], production of foreign protein [26] and food security [27]. Meanwhile, the *in planta Agrobacterium*-mediated transformation of tomato has been used to target various tissue sources such as mature and immature fruits [28, 29], shoot apical meristems [30], floral buds [28, 31] and flowers [28, 29]. However, the study of *in planta* transformation using tomato seeds has not been reported.

The activity of ADH enzyme in sago palm tissues has been previously identified with the highest expression detected in young leaves [1]. A full length r-*msAdh1* cDNA (MN196247) has also been isolated using the rapid amplification cDNA ends (RACE) technique [32]. Here, we report on the expression analysis of r-*msAdh1* cDNA in bacteria and the transformation into tomato plants via *in planta Agrobacterium*-mediated transformation of tomato seeds. The r-*msAdh1* cDNA was firstly cloned into a bacterial expression vector, pET-41a(+), fused to a histidine tag and was expressed in *E. coli* BL21 (DE3). The r-*msAdh1* cDNA was then cloned into a binary vector, pGSA1131, and transformed into tomato seeds.

2. Materials and Methods

2.1 Cloning of recombinant *Adh1* (r-*msAdh1*) *cDNA* into pET41a(+) and expression in *E. coli* strain BL21 (DE3)

2.1.1 Directional cloning of r-*msAdh1* cDNA into pET-41a(+)

The open reading frame of r-*msAdh1* was obtained through PCR by using the following primers: 5'NdeI_adaptor (5'-GGAATTCCATATGGCAAGCACTGTTGG-3') and 3_r-msAdh1_XhoI (5'-

GCTAACTCGAGACCATCCATGTGAATGATGCAC-3'). A 1X PCR mixture was prepared to include 2.5 µl 10x High Fidelity buffer with 15 mM $MgCl_2$, 2.5 µl dNTP (2.5 mM), 0.5 µl high fidelity DNA polymerase enzyme (0.625 U/µl) (Thermo Fisher Scientific, USA), 1 µl forward primer (10 µM), 1 µl reverse primer (10 µM), 17 µl nuclease-free water and 0.5 µl template (10 pmol). The template used in the PCR was pET-41a(+) that contained r-*msAdh1* cDNA with seven stop codons before the His-tag sequence. The PCR was conducted according to the program that includes hotstart at 94°C for 3 min; 35 cycles of 94°C for 30 s, 62°C for 1 min, 72°C for 2 min and a final extension of 72°C for 10 min. The amplified r-*msAdh1* fragment and pET-41a(+) (Novagen, USA) were then subjected to double restriction enzyme digests of *Nde*I and *Xho*I (Thermo Fisher Scientific, USA). The restricted r-*msAdh1* and pET-41a(+) fragments were then ligated using T4 Ligase (Thermo Fisher Scientific, USA) to produce the construct pET-41a(+)/r-*msAdh1*, and transformed into *E. coli* strain XL-1 Blue via heat shock method. Positive colonies were screened on the Luria agar (LA) supplemented with 100 µg/ml kanamycin. The XL-1 blue culture harboring the recombinant plasmid was extracted and the nucleotide sequence was verified via sequencing (Apical Scientific, Malaysia) and restriction enzyme analysis.

2.1.2 Induction and expression of pET-41a(+)/r-*msAdh1* in BL21 (DE3)

For expression in *E. coli*, the pET-41a(+)/r-*msAdh1* was transformed into BL21 (DE3) competent cells via heat shocked method. A single colony of BL21 (DE3) harboring pET-41a(+)/r-*msAdh1* was selected and used to inoculate 6 ml Luria broth (LB) supplemented with 100 µg/ml kanamycin. The culture was grown to OD_{600} of 0.6-1.0 at 37°C and kept at 4°C for overnight. Two milliliters of the overnight culture was pipetted out and centrifuged for 30 s at 3500 rpm. The supernatant was discarded and pellet was re-suspended with 1 ml fresh LB media. The suspension was added with 49 ml LB media supplemented with 100 µg/ml kanamycin and transferred into 250 ml Erlenmeyer flask. The culture was brought to OD_{600} of 0.5-0.6 at 37°C. Once the culture reached the desired OD, 1.5 ml culture was aliquoted to serve as non-induced control. Ten milliliters of the culture was then pipetted into flasks; A, B, C and D, and induced with IPTG with a final concentration of 0.4 mM. Flasks A and B were incubated for 4 h (T4) and 6 h (T6) respectively, at 15°C. Meanwhile, flasks C and D were incubated for 4 h (T4) and 6 h (T6) respectively, at 27°C. At the end of incubation, OD_{600} of all cultures was measured. Next, 1.5 ml of each culture was aliquoted and centrifuged at 13,200 rpm for 4 min. The pellet was stored at -20°C until use. The procedure for bacterial expression was carried out as recommended by the QIAexpressionist™ Kit (Qiagen, Germany) with minor modifications.

2.1.3 Determination of protein solubility, purification under native condition and enzymatic assay of ADH

To determine the solubility of r-msAdh1 protein, the cell pellet was lysed using NP10 lysis buffer (50 mM NaH_2PO_4, 300 mM NaCl and 10 mM imidazole). The volume of lysis buffer used was in accordance with cell culture density (OD_{600} = 0.1, 12.5 µl of NP10 lysis buffer, OD_{600} = 0.6, 75 µl of NP10 lysis), and the total protein concentration was standardized. The crude lysate was centrifuged, soluble and insoluble fractions were analyzed on 12% SDS polyacrylamide gel electrophoresis (PAGE) (Bio-Rad, USA). Meanwhile, for protein purification, 20 ml culture of BL21 (DE3) with r-*msAdh1* expression was used. The purification was done by using Ni-NTA Spin Kit (Qiagen, Germany). The result was analyzed on 12% SDS-PAGE. The catalyzing activity of r-msAdh1 was analyzed spectrophotometrically at OD_{340} [33]. The increase in absorbance was recorded at every one min for the first 15 min as NAD^+ was reduced to NADH. The reaction buffer consisted of 1 ml Tris-HCl 100 mM pH 8.3, 80 µl ethanol and 2 mM NAD^+ and incubated at 25°C. The reaction was initiated by adding 20 µl of r-msAdh1 lysate [33].

2.2 Cloning of r-*msAdh1* cDNA into pGSA1131 and *in planta Agrobacterium* transformation of tomato seeds

2.2.1 Directional cloning of r-*msAdh1* cDNA into pGSA1131

The open reading frame of r-*msAdh1* cDNA was obtained through PCR amplification by using the following primers: 5_NcoI_msAdh1 (5'-GGAATTCCATGGCAAGCAGTGTTGGTCAA-3') and 3_BamHI_msAdh1 (5'-ACCAAGGATCCTTAGTGGTGGTGGTG-3'). A 1X PCR mixture was prepared to include 2.5 µl 10x High Fidelity buffer with 15 mM $MgCl_2$, 2.5 µl dNTP (2.5 mM), 1 µl high fidelity DNA Polymerase enzyme (0.625 U/µl) (Thermo Fisher Scientific, USA), 1 µl forward primer (10 µM), 1 µl reversed primer (10 µM), 0.5 µl template (pET-41a(+)_r-*msAdh1*) (10 pmol) and 16 µl nuclease-free water. The PCR was conducted according to the program that includes hotstart at 94°C for 3 min; 35 cycles of 94°C for 30 s, 64°C for 1 min, 72°C for 1 min and 30 s and 1 cycle of 72°C for 10 min. The amplified r-*msAdh1* fragment and pGSA1131 were then subjected to double restriction enzyme digests of *Bam*HI and *Nco*I (Thermo Fisher Scientific, USA). The restricted pGSA1131 fragment (approximately 9 kb) was recovered from the agarose gel using Gel DNA Extraction Kit (Vivantis, Malaysia) and subsequently ligated with r-*msAdh1* using T4 DNA Ligase (Thermo Fisher Scientific, USA). The ligated mixture was then transformed into *E. coli* strain XL1 Blue via heat shock method. Putative transformants were selected on the Luria agar (LA) supplemented with 30 µg/ml chloramphenicol. Clones harbouring pGSA1131/r-*msAdh1* were isolated and analyzed via nucleotides sequencing (Apical Scientific, Malaysia) and restriction enzyme digestion analysis.

2.2.2 Preparation of *A. tumefaciens* culture, infiltration and post-infiltration broth

Agrobacterium tumefaciens strain LBA4404 was kindly provided by Evra Raunie Ibrahim from Craun Research Sdn. Bhd. (Malaysia). The transformation of pGSA1131/r-*msAdh1* into *A. tumefaciens* using Bio-Rad Gene Pulser Xcell Electroporation Systems (Bio-Rad, USA) was according to method described by manufacturer. Positive colony obtained from electroporation was cultured in LB for 2 days. Six hundred microliters was then added into a 30 ml fresh LB supplemented with 100 µg/ml rifampicin and 30 µg/ml chloramphenicol. The culture was brought to OD_{600} of 0.5-0.6 and centrifuged at 3500 rpm for 5 min. The cell pellet was then re-suspended in an infiltration media (0.5X MS; 3% sucrose; 0.5 g/l MES). Prior to co-cultivation with tomato seeds, the infiltration media was added with Silwet L-77 (0.003%, PhytoTechnology Laboratories, USA) and 200 µM acetosyringone (PhytoTechnology Laboratories, USA).

The tomato (*Solanum lycopersicum*) cultivar MT1 was purchased from Malaysia Research Institute, MARDI (Malaysia). Fifty seeds were incubated in sterilized distilled water for overnight at 4°C. The following day, the seeds were sonicated for 10 min prior to addition of the infiltration media containing Silwet L-77 and acetosyringone. The seed co-cultivation was agitated for 3 h at 180 rpm. After 3 h, the infiltration media was removed and the seeds were rinsed with distilled water several times. The seeds were then treated with 500 µg/ml carbenicillin for an hour to remove any remaining *A. tumefaciens*. The seeds were sown on soil and germinated after 3-5 days.

2.2.3 Analysis of r-*msAdh1* integration in T_0 and T_1 generations using PCR

To analyze the r-*msAdh1* integration in T_0 and T_1 generations, young leaf of putative transgenic seedlings of approximately 0.5 cm^2 was used for genomic DNA extraction. The leaves were surface-sterilized for 2 min in 75% ethanol and 10% Clorox® bleach, and then followed by three

washes using sterilized distilled water. Genomic DNA was extracted using GF-1 Plant DNA Extraction Kit (Vivantis, Malaysia) according to instructions provided by manufacturer. The quantity and purity of the extracted genomic DNA (gDNA) was measured using Ultrospec 1100 Pro UV/Vis Spectrometer (Amersham Pharmacia Biotech, USA). The integration of r-*msAdh1* in putative transformed T_0 seedlings (1-15), and transgenic T_1 seedlings (1-11), were screened by PCR using r-*msAdh1* specific primers: 5_Comseq_Adh (5'-ATGGCAAGCAGTGTTGGTCAAGTGATC-3') and 3_Comseq_Adh (5'- ACCATCCATGTGAATGATGCACCTAAGGC-3'). A 1X PCR mixture was prepared to include 7.5 µl of 2X Green GoTaq master mix (Promega, USA), 1 µl forward primer (10 µM), 1 µl reverse primer (10 µM), 1 µl genomic DNA (0.5 µg/µl) and 4.5 µl nuclease-free water. The PCR was conducted according to the program that includes hotstart at 94°C for 3 min; 35 cycles of 94°C for 30 s, 57°C for 45 s, 72°C for 1 min and 30 s and 1 cycle of 72°C for 10 min.

2.2.4 Analysis of *bar* gene integration in T_0 generation using PCR

The integration of *bar* gene in putative transformed seedlings (T_0 generation) was analyzed using gradient PCR at annealing temperature ranging from 55°C-68°C. The *bar* gene specific primers were used, namely the Bar3_F (5'-ATGAGCCCAGAACGACGCC-3') and Bar3_R (5'-ATCTCGGTGACGGGCAGG-3'). The composition of 1X PCR mixture to detect the presence of *bar* gene was 2.5 µl 10x High Fidelity buffer with 15mM $MgCl_2$, 2.5 µl dNTP (2.5 mM), 1 µl high fidelity DNA Polymerase enzyme (0.625 U/µl) (Thermo Fisher Scientific, USA), 1 µl forward primer (10 µM), 1 µl reverse primer (10 µM), 1 µl genomic DNA (0.5 µg/µl), and 16 µl nuclease free water. The PCR was conducted according to the program that includes hotstart at 94°C for 3 min; 35 cycles of 94°C for 30 s, 55-68°C for 45 s, 72°C for 30 s and 1 cycle of 72°C for 10 min.

2.2.5 Analysis of r-*msAdh1* expression by using reverse-transcription PCR

To analyze r-*msAdh1* expression in tomato putative transformants, only $T_0$2 and $T_1$8, $T_1$9, $T_1$11 lines survived and used in subsequent analysis. Transformed seedling at the 4-5 leaves stage was used for analysis. Young leaf with size approximately of $1cm^2$ was surfaced sterilized and ground to a fine powder with liquid nitrogen in a pre-cooled mortar. Total RNA extraction was performed using Total RNA Mini Kit Plant (Geneaid, Taiwan) according to instructions provided by manufacturer and treated with *DNAse1* (Promega, USA) via standard protocol. The quantity and purity of the total RNA obtained was measured using Ultrospec 1100 Pro UV/Vis Spectrometer (Amersham Pharmacia Biotech, USA). Meanwhile, total RNA integrity was accessed on 1.5% of agarose gel. First strand cDNA synthesis of r-*msAdh1* was carried using RevertAid First Strand cDNA Synthesis Kit (Thermo Fisher Scientific, USA) according to manufacturer recommendation. Three primers were used for the first strand DNA synthesis: 3_Comseq_Adh (5'-ACCATCCATGTGAATGATGCACCTAAGGC-3'), 3_BamHI_msAdh1 (5'-ACCAAGGATCCTTAGTGGTGGTGGTG-3') and 5_msAdh1_R (5'-AACACAGCCAAC ATGGACAA-3') (Figure 1). The presence of r-*msAdh1* expression was determined by RT-PCR using combination of r-*msAdh1* cDNA specific forward and reverse primers: 5_Comseq_Adh (5'-ATGGCAAGCAGTGTTGGTCAAGTGATC-3') and 5'_msAdh1_R (5'-AACACAGCCAAC ATGGACAA-3'). The reaction mixture for amplification includes 12.5 µl 2X Dream-Taq Green PCR Master Mix (Promega, USA), 1 µl forward primer (10 µM), 1 µl reverse primer (10 µM), 2 µl cDNA, 9.5 µl nuclease-free water. The PCR was conducted according to the program that includes hotstart at 94°C for 3 min; 35 cycles of 94°C for 30 s, 55°C for 30 s, 72°C for 45 s and 1 cycle of 72°C for 5 min.

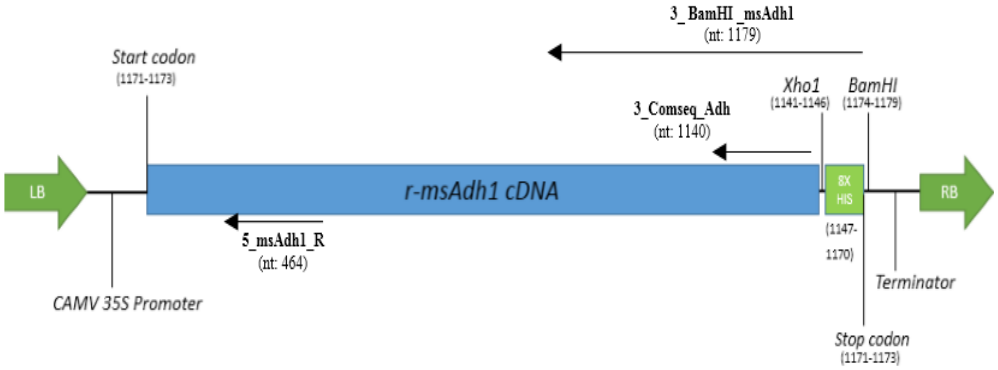

Figure 1. The orientation and position of primers used for first strand cDNA synthesis reaction

3. Results and Discussion

3.1 Determination of protein solubility, purification under native condition and enzymatic assay of ADH

The use of primers combination; 3'XhoI_r-msAdh1 and 5'NdeI_adaptor in PCR to amplify r-*msAdh1* cDNA resulted in amplification of approximately 1.1 kb fragment (Figure 2). Sequence analysis showed that r-*msAdh1* cDNA has been successfully cloned into pET-41a(+) with length of 1.14 kb corresponding to 380 amino acids with C-terminal His-tag fusion. Meanwhile Figure 3 is a PAGE analysis that shows presence of small amount of soluble r-msAdh1 (Lane 2-5, 42.55kD) and a large amount of r-msAdh1 expressed as insoluble fraction (Lanes 6-9, 42.55 kD). The intensity of the bands increased after induction temperature was increased to 27°C for a period of 6 h. Over-expression of heterologous protein causes *in vivo* equilibrium to favor the formation of inclusion bodies (IBs) rather than solubilized protein due to the translation rate exceeding the rate of protein folding [34, 35]. The formation of IBs is hard to predict even with *in silico* analysis of amino acid sequence [36] because they are complex and the aggregates are only formed within similar type of protein or highly similar protein [35, 15]. Analysis using the software GenScript Rare Codon Analysis (https://www.genscript.com/tools/rare-codon-analysis) showed that r-*msAdh1* cDNA has codon adaptation index (CAI) of 0.62 which is below the ideal value (0.8-1.0) to obtain good expression. The strain BL21 (DE3) used in this study was not designed to enhance the expression of eukaryotic gene that has rarely used codons in *E. coli.* In contrast, a large amount of soluble tag protein (GST, 8xHis and S-tag; nucleotides: 1095-150) with molecular weight of 33.71 kD was expressed as seen in Lanes 10-13.

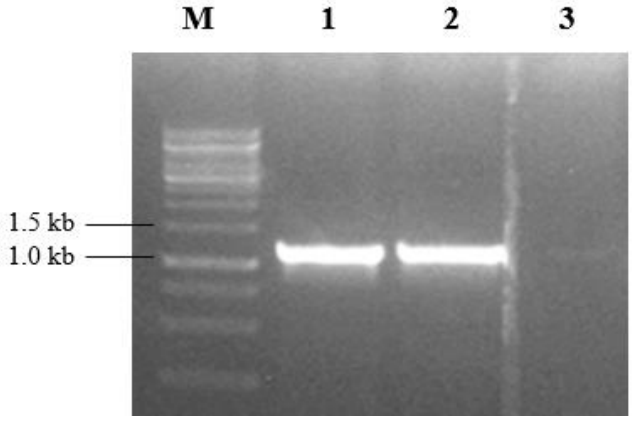

Figure 2. Gel electrophoresis of PCR product visualized on 1% agarose gel stained with EtBr. The PCR product is the full length of r-*msAdh1* cDNA fragment that amplified using the 5'NdeI_adaptor and 3'XhoI_r-msAdh1 primers combination. M: GeneRuler™ 1 kb DNA Ladder (Thermo Fisher Scientific, USA), 1 and 2: PCR products, 3: Negative control (PCR without template)

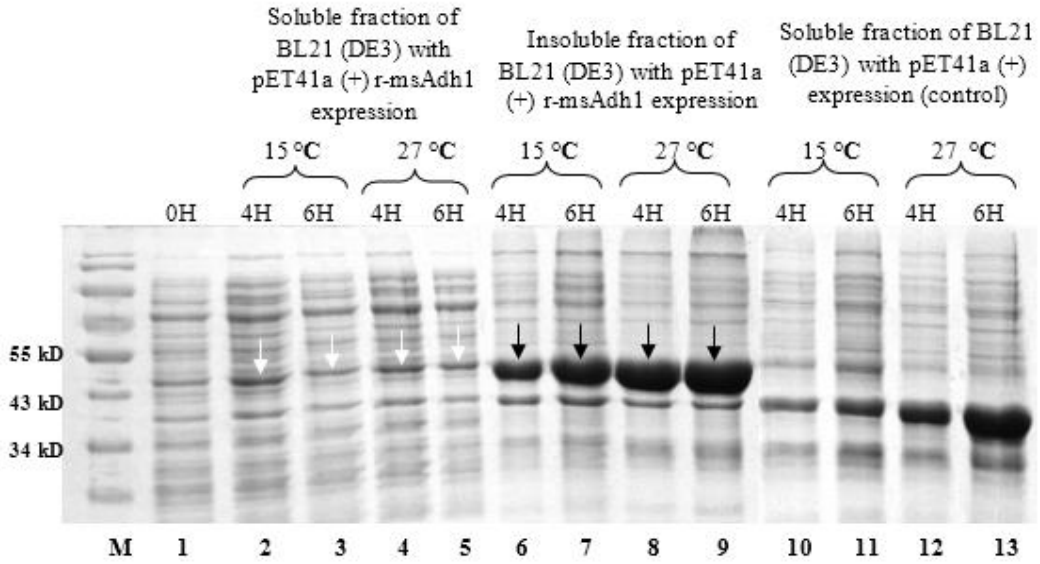

Figure 3. Crude protein analyzed on 12% SDS-PAGE stained with Coomassie Brilliant Blue 1: Soluble fraction of non-induced culture of BL21 (DE3) with r-*msAdh1* expression (0 h). 2-5: Soluble fraction of BL21 (DE3) with r-*msAdh1* expression at 15°C and 27°C for 4 h and 6 h, respectively. 6-9: Insoluble fraction of BL21 (DE3) with r-*msAdh1* expression at 15°C and 27°C for 4 h and 6 h, respectively. 10-13: Soluble fraction from crude lysate of BL21 (DE3) with pET-41a(+) expression (control). M: EZ Run pre-stained *Rec* protein ladder. White arrows show the expected soluble r-msAdh1 protein bands and black arrows show the expected insoluble r-msAdh1 protein bands

Purification of r-msAdh1 protein was successful, however several non-target protein was also co-eluted (Figure 4). The formation of disulphide bond between cellular host protein and protein in interest could lead to contamination during purification [37]. Formation of inclusion bodies and/or targeted protein tertiary structure, would also block the efficacy of polyhistidine affinity tag [37]. ADH enzyme breaks down ethanol to form acetaldehyde in the presence of NAD^+ as co-enzyme. The catalytic activity of r-msAdh1 can be monitored by the increase of absorbance reading. This is because reduced NAD^+ (NADH) exhibits strong UV absorption at 340 nm while the NAD^+ has almost no absorption at this wavelength. Figure 5 shows catalytic activity of ADH enzyme was detected not only in the soluble fraction of BL21 (DE3) with expressed r-*msAdh1* but also in the control. This is expected because endogenous ADH is known to be present in BL21 (DE3) [38]. Nevertheless, Independent t-test showed a p-value of $0.003 < 0.05$ indicating a significant difference between the catalytic activity of ADH enzyme present in soluble fraction of BL21 (DE3) with expressed r-*msAdh1* and control BL21 (DE3) containing only pET-41a(+).

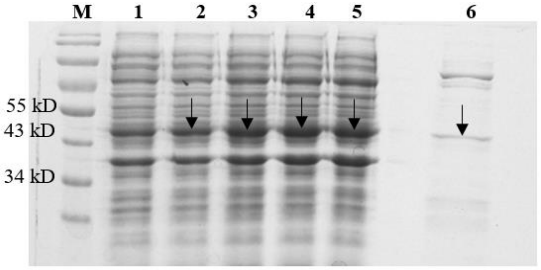

Figure 4. Crude lysate of BL21 (DE3) and Ni-NTA purified r-msAdh1 analyzed on 12% SDS-PAGE stained with Coomassie Brilliant Blue. 1: Soluble fraction of non-induced culture of BL21 (DE3) with r-*msAdh1* expression (0 h). 2-5: Soluble fraction of BL21 (DE3) with r-*msAdh1* expression at 15°C and 27°C for 4 h and 6 h, respectively. 6: Purification of r-msAdh1 protein using 50 mM NaH_2PO_4, 300 mM NaCl and 500 mM imidazole as elution buffer. M: EZ Run pre-stained *Rec* protein ladder. Expected r-msAdh1 bands are shown by black arrows.

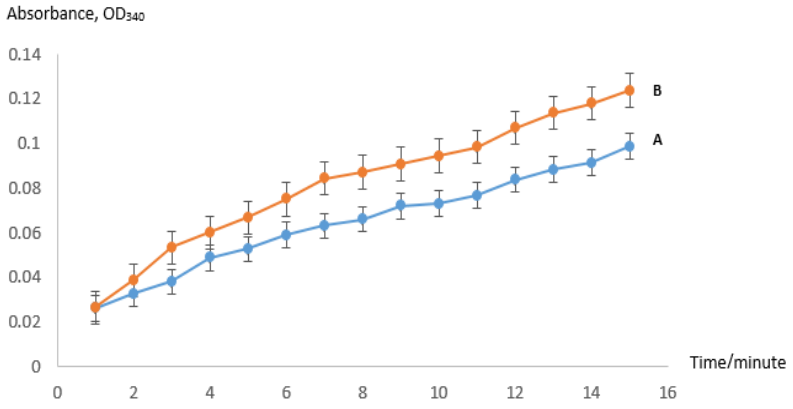

Figure 5. Catalytic activity of ADH enzyme. Absorbance at OD_{340} versus time (min) obtained from (A) soluble fraction of BL21 (DE3) transformed with pET-41a(+) (control) and, (B) soluble fraction of BL21 (DE3) with expressed r-*msAdh1*. Graph plotted with standard deviation (SD) error bar and each point represents the average of triplicate.

3.2 Analysis of r-*msAdh1* and *bar* integration in tomato T_0 and T_1 generations

The use of primers combination; 5_NcoI_msAdh1 and 3_BamHI_msAdh1 in PCR to amplify r-*msAdh1* cDNA resulted in amplification of 1.14 kb fragment on 1% agarose gel electrophoresis (Figure 6). For tomato transformation, the r-*msAdh1* cDNA was cloned after the CaMV35S promoter of the binary vector, pGSA1131. This was confirmed via restriction enzyme analysis and nucleotide sequencing. After seed transformation, a total of 50 seeds germinated but only fifteen putative seedlings (T_0) survived and were used to determine r-*msAdh1* integration. Two negative controls were used in PCR; genomic DNA extracted from wild type tomato and PCR mix without any template, meanwhile a pGSA1131_r-*msAdh1* recombinant plasmid was used as positive control. PCR analysis and sequencing of the PCR fragments of the T_0 seedlings DNA showed five putative transformed plant lines ($T_0$1, $T_0$2, $T_0$4, $T_0$12, $T_0$13) contained the r-*msAdh1* cDNA (Figure 7). Analysis of T_1 generation obtained from $T_0$2, $T_0$12 and $T_0$13 showed that $T_1$1- $T_1$11, also contained r-*msAdh1* (Figure 8). However, r-*msAdh1* in $T_1$4 and $T_1$11 were only detected at annealing temperatures of 60.1°C, 61.1°C and 61.7°C (Figure 9) and using RT-PCR (Figure 12), respectively.

There was no amplification of *bar* gene detected from all tested plants when dimethyl sulfoxide (DMSO) or bovine serum albumin (BSA) was added in PCR reaction. This is possibly due to the high GC content (68%) and the presence of continuous block of GC nucleotides [39] that interferes the annealing of primer to the DNA template [40]. The amplification of *bar* gene was only obtained in gradient PCR by using high fidelity DNA Polymerase enzyme (Thermo Fisher Scientific, USA) at annealing temperatures of 62.4°C, 64.0°C and 65.6°C (Figure 10). Higher annealing is necessary for primer with high GC content [41]. Out of fifteen plants tested, seven putative transformed plant lines: $T_0$1, $T_0$3, $T_0$4, $T_0$5, $T_0$9, $T_0$12 and $T_0$13 were positive for *bar* gene (Figure 11); thus resulting in higher transformation efficiency (46.7%) compared to r-*msAdh1* (33.33%). Perhaps, the *bar* gene is smaller and easier to incorporate into plant genome [42]. Besides, from the result obtained, it showed that both of r-*msAdh1* and *bar* gene did not always co-integrate in transformed plants. The result was in line with other study that found that the copy number of *bar* and *gus* genes on the same T-DNA was different in individual transformants [43] which could be due to rearrangements or truncated T-DNA [44] caused by induction of CaMV35S promoter [45]. The selection of transgenic plant with glufosinate could not be performed as most of transformed plants showed fatality when they reached stage of 4-6 leaves that could be due to overexpression of r-*msAdh1* or excessive cutting during sampling for DNA and RNA extraction.

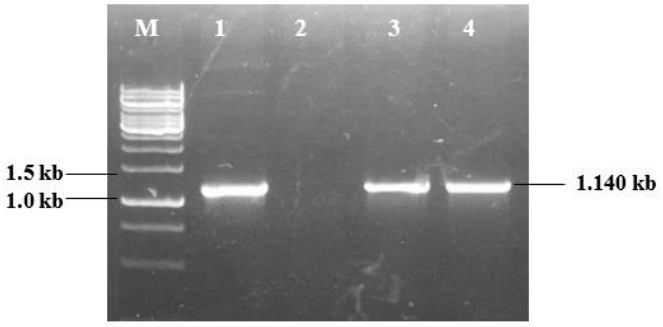

Figure 6. Gel electrophoresis of r-*msAdh1* amplification visualized on 1% of agarose gel stained with EtBr. The used of 5'NcoI_msAdh1 and 3_BamHI_msAdh1 primers in PCR produced r-*msAdh1* band with expected size of 1.14 kb. M: GeneRuler™ 1 kb DNA Ladder (Thermo Fisher Scientific, USA), 2: Negative control, 1, 3 and 4: PCR product

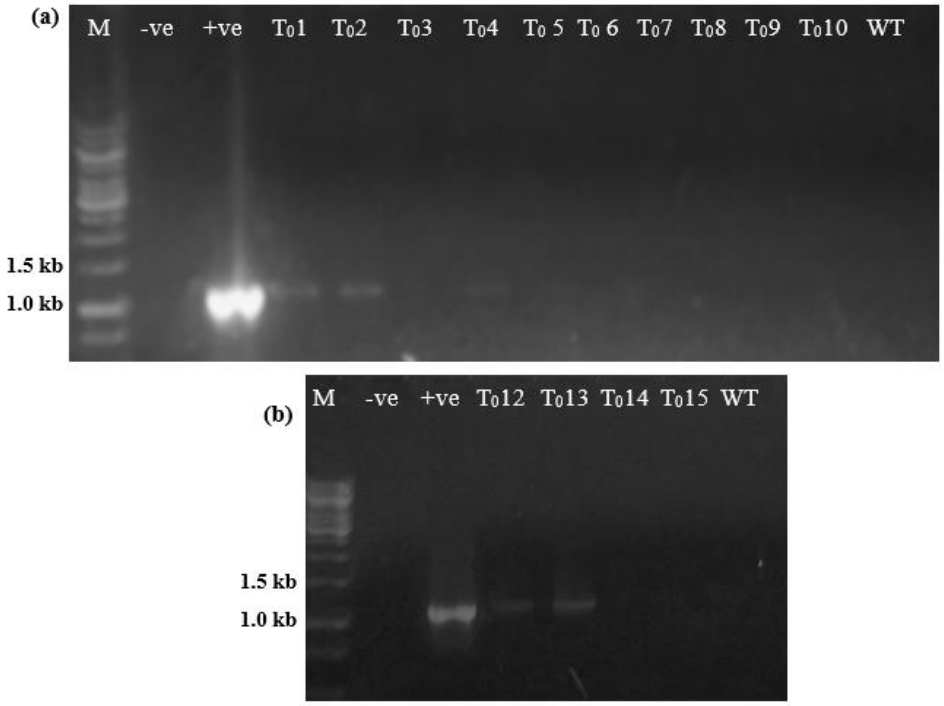

Figures 7. Diagnostic analysis of T_0 generation of tomato seedlings. Gel electrophoresis of PCR product visualized on 1% agarose gel stained with EtBr to detect r-*msAdh1* cDNA in the putative transformed seedling, T_0. The PCR product is the full length of r-*msAdh1* cDNA fragment amplified using 5_Comseq_Adh and 3_Comseq_Adh primers combination. M: GeneRuler™ 1 kb DNA Ladder (Thermo Fisher Scientific, USA), –ve: Negative control (PCR without DNA template), +ve: Positive control, $T_0$1- $T_0$15: Putative transformed seedling 1-15, WT: Wild type control

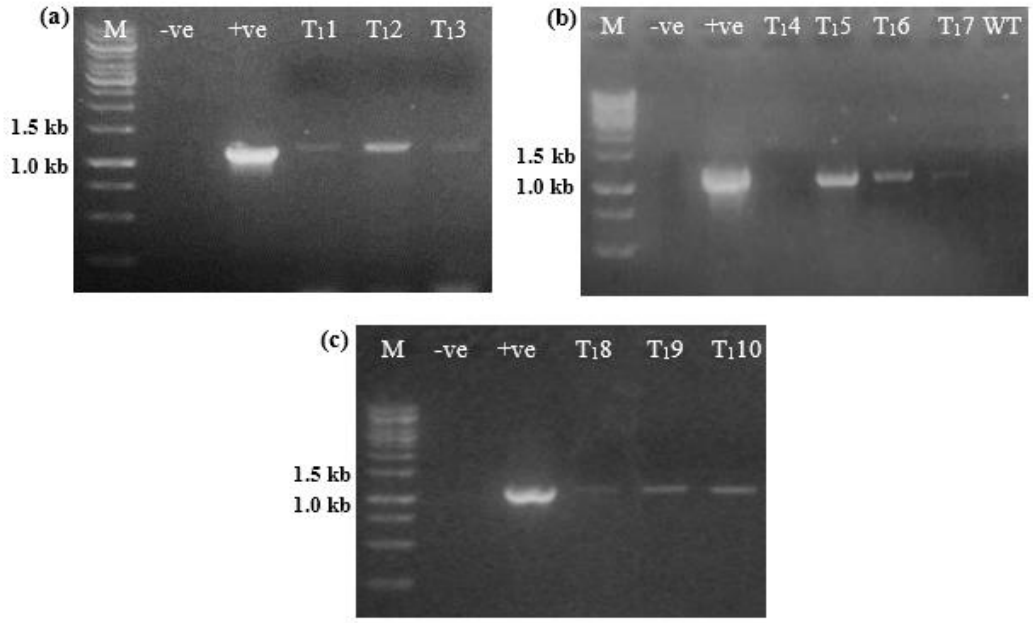

Figure 8. Diagnostic analysis of T_1 generation of tomato seedlings. Gel electrophoresis of PCR product visualized on 1% agarose gel stained with EtBr to detect r-*msAdh1* in T_1 generation from $T_0$12 (a), $T_0$13 (b) and $T_0$2 (c). The PCR product is the full length of r-*msAdh1* cDNA fragment amplified using 5_Comseq_Adh and 3_Comseq_Adh primers combination. M: GeneRuler™ 1 kb DNA Ladder (Thermo Fisher Scientific, USA), –ve: Negative control, +ve: Positive control, $T_1$1-$T_1$10: T_1 generation 1-10, WT: Wild type control

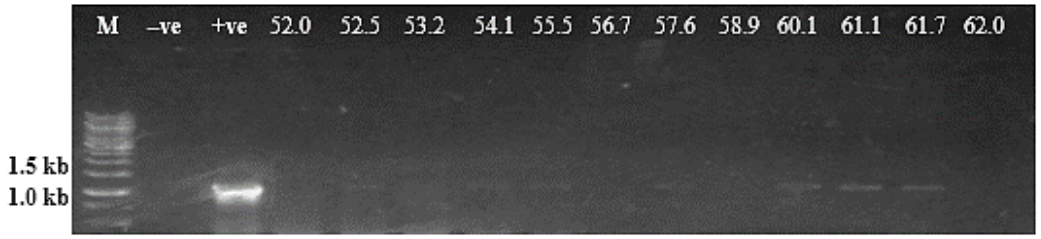

Figure 9. Diagnostic analysis of T_1 generation of tomato seedling. Gel electrophoresis of gradient PCR products on 1% agarose gel stained with EtBr to detect r-*msAdh1* in $T_1$4 generation from $T_0$13. The PCR product is the full length of r-*msAdh1* cDNA fragment amplified using 5_Comseq_Adh and 3_Comseq_Adh primers combination. M: GeneRuler™ 1 kb DNA Ladder (Thermo Fisher Scientific, USA), –ve: Negative control, +ve: Positive control. 52.0°C-62.0°C: Annealing temperatures

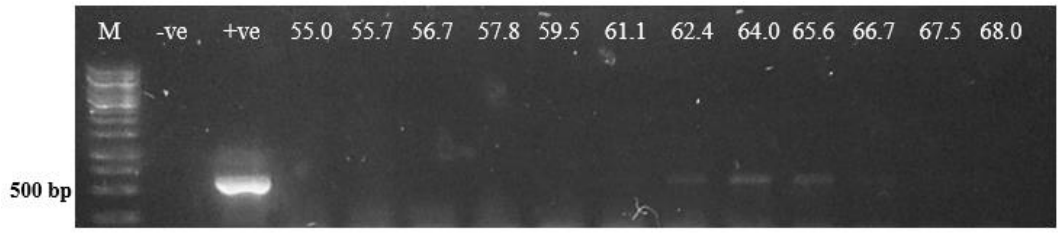

Figure 10. Gel electrophoresis of gradient PCR products for *bar* gene on 1.5% agarose gel stained with EtBr. Genomic DNA extracted from putative transformed seedling; $T_0$1 was used as a template in gradient PCR. M: GeneRuler™ 1 kb DNA Ladder (Thermo Fisher Scientific, USA), –ve: Negative control (PCR without DNA template), +ve: Positive control. 55.0°C-68.0°C: Annealing temperatures

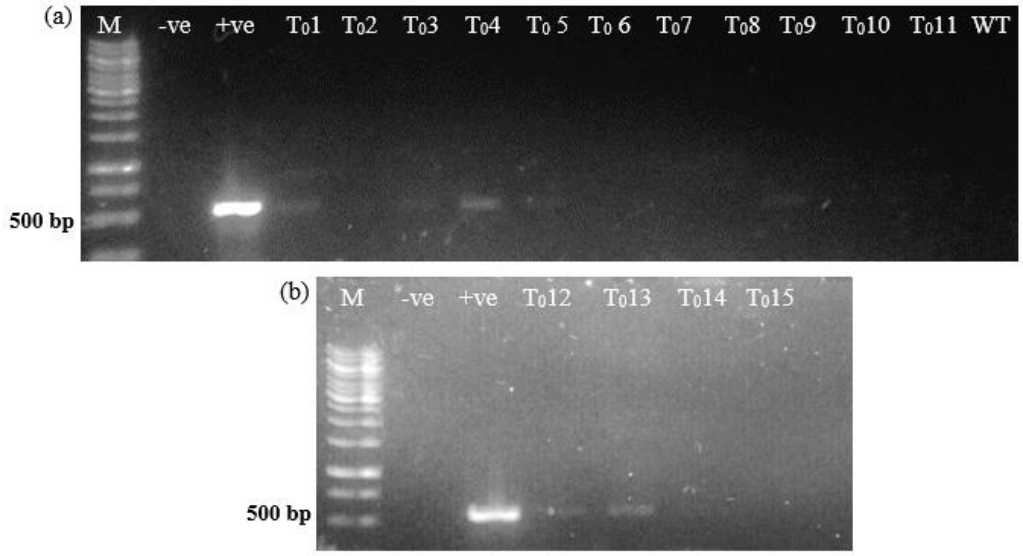

Figures 11. Gel electrophoresis of *bar* gene PCR products from T_0 analyzed on 1.5% agarose gel stained with EtBr. The PCR product is the full length *bar* gene fragment amplified using Bar3_F and Bar3_R primers. M: GeneRuler™ 1 kb DNA Ladder (Thermo Fisher Scientific, USA), –ve: Negative control (PCR without DNA template), +ve: Positive control (PCR using pGSA1131/r-*msAdh1* plasmid as a template), $T_0$1- $T_0$15: Putative transformed seedling, 1-15. WT: Wild type (control).

Transformation efficiency using *A. tumefaciens* differs and is determined by the *Agrobacterium* strains, binary vectors, target tissues used and plant species. Previous works in *in planta* transformation such as in using the technique of *in vitro* tomato fruit injection method, reported transformation efficiency of between 17-68% for tomato infiltrated with *A. tumefaciens* strain EHA105 harboring the plasmid pROKII carrying *Apetala 1* (*Ap1*) and 21% for pROKII carrying *LEAFY* (*LFY*) gene [28, 46]. Meanwhile, tomato infiltrated with *A. tumefaciens* strain LBA4404 plasmid harboring plasmid pPM7 with *HAL1* and *NPTII* genes achieved transformation rate of between 34-42% [29]. All of these experiments used ripened tomato as a target tissue at 48 h incubation after infiltration. On the use of ripen and immature fruits as target tissues using the

in vivo fruit injection method, varying transformation efficiencies were also reported between 35-42% for ripened tomato and 2-5% for immature/green tomato [28]. On the other hand, the floral-dip method targets the ovules, where unopened flowers are introduced to *Agrobacterium* before pollination and subsequently left to develop into flower [28, 39]. Using the floral-dip method, transformation efficiency in range of 12-23% was obtained [28]. This work reports the first *in planta* transformation using tomato seeds as a target tissue and producing a transformation efficiency of between 33.3-46.7%.

3.3 Molecular analysis of r-*msAdh1* expression in transformed seedlings

Most of transformed seedling showed fatality when they reached the stage with 4-6 leaves. Therefore, total RNA was extracted only from four available positive lines; $T_1$8, $T_1$9, $T_1$10 and $T_1$11. RNA purity of between 1.8-2.0 indicates good RNA quality for $T_1$9 and $T_1$11 samples. A lower purity was obtained for samples $T_1$8 and $T_1$10 indicating RNA contamination with protein or phenol. The RT-PCR using r-*msAdh1* specific primers; 5_Comseq_Adh1 and 5_msAdh1_R and subsequent agarose gel electrophoresis produced the expected 500 bp fragment (Figure 11), indicating the presence of r-*msAdh1* transcript in both of the transgenic progeny seedlings of $T_1$9 and $T_1$11. However, no amplification was detected from samples $T_1$8 and $T_1$10, which may be due to the poor RNA quality (data not shown). However, the RT-PCR obtained only when the r-*msAdh1* specific internal specific primer, 5_msAdh1_R, was used to generate the first cDNA strand. This could be because the first cDNA strand was truncated when using the 3_Comseq_Adh1 or 3_BamH1_msAdh1 as primers (Figure 10) due to the presence of mRNA secondary structures that affects the activity of reverse transcriptase enzyme [47].

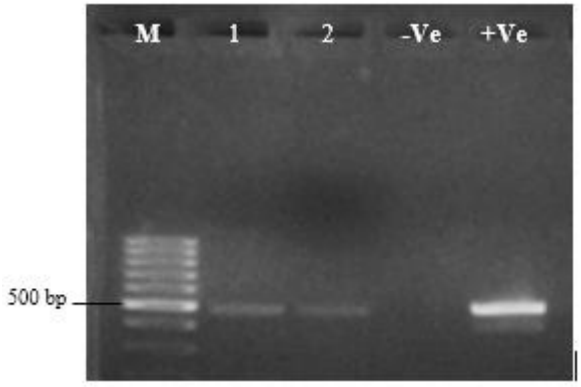

Figure 12. Gel electrophoresis of RT-PCR product visualized on 1.5% agarose gel stained with EtBr to analyze the expression of r-*msAdh1* cDNA in transformed seedlings. Lanes 1 and 2 shows a 500 bp size fragments representing the r-*msAdh1* cDNA amplified using 3_comseq_Adh and 5_msAdh1_R primers. M: GeneRuler™ 1 kb DNA Ladder (Thermo Fisher Scientific, USA), –ve: Negative control (PCR without DNA template), +ve: Positive control, 1: $T_1$9, 2: $T_1$11

4. Conclusions

The r-*msAdh1* cDNA in BL21 (DE3) was highly expressed in *E. coli* system. However, most of the protein formed as insoluble inclusion bodies, even when low temperatures (15°C and 27°C) and low concentration of IPTG were used. We have also demonstrated a successful transformation method by using *Agrobacterium*-mediated *in planta* seed transformation protocol for the transfer of *msAdh1* cDNA into the tomato genome. This method is an alternative for functional analysis of r-msAdh1 protein as the transformation is easy, rapid and economical, with transformation efficiency of between 33.3-46% within two weeks. This simple and easy to perform method can provide a platform for the further characterization of not only r-*msAdh1* but also other eukaryotic genes in plant systems.

5. Acknowledgements

This research project is funded in-part by UNIMAS Tun Openg Research Grant (ORC/08/2011(04)). The authors would also like to thank the Faculty of Resource Science and Technology, Universiti Malaysia Sarawak, for providing the research facilities.

References

[1] Roslan, H.A., Sundaraj, Y. and Awang Husaini, A.A.S., 2008. Multiple form of alcohol dehydrogenase (*Adh*) genes in sago palm: A preliminary study. *BANWA,* 5(1), 30-41.

[2] Kato-Noguchi, H., 2001. Wounding stress induces alcohol dehydrogenase in maize and lettuce seedlings. *Plant Growth Regulation,* 35(3), 285-288.

[3] Dolferus, R., Jacobs, M., Peacock, W.J. and Dennis, E.S., 1994. Differential interactions of promoter elements in stress responses of the *Arabidopsis Adh* gene. *Plant Physiology*, 105(4), 1075-1087.

[4] Garabagi, F., Duns, G. and Strommer, J., 2005. Selective recruitment of *Adh* genes for distinct enzymatic functions in *Petunia hybrida*. *Plant Molecular Biology*, 58(2), 283-294.

[5] Yi, S.Y., Ku, S.S., Sim, H.J., Kim, S.K., Park, J.H., Lyu, J.I., So, E.J., Choi, S.Y., Kim, J., Ahn, M.S., Kim, S.W., Park, H., Jeong, W.J., Lim, Y.P., Min, S.R. and Liu, J.R., 2017. An *alcohol dehydrogenase* gene from *Synechocystis* sp. confers salt tolerance in transgenic tobacco. *Frontier in Plant Science,* 8, 1965.

[6] Jeon, Y.J., Fong, J.C., Riyanti, E.I., Neilan, B.A., Roger, P.L. and Svenson, C.J., 2008. Heterologous expression of *alcohol dehyrogenase* (*Adh1*) gene from *Geobacillus thermoglucosidasius* strain M10EXG. *Journal of Biotechnology,* 135(2), 127-133.

[7] Weckbecker, A. and Hummel, W., 2006. Cloning, expression and characterization of an ®-specific *alcohol dehyrogenase* from *Lactobacillus kefir. Biocatalysis and Biotransformation*, 24(5), 380-389.

[8] Liang, J.J., Zhang, M.L., Ding, M., Mai, Z.M., Wu, S.X., Du, Y. and Feng, J.X., 2014. *Alcohol dehydrogenases* from *Kluyveromyces marxianus*: heterologous expression in *Escherichia coli* and biochemical characterization. *BMC Biotechnology,* 14(45), https://doi: 10.1186/1472-6750-14-45.

[9] Utekal, P., Toth, C., Illesova, A., Kois, P., Bocanova, L., Turna, J., Drahovska, H. and Stuchlik, S., 2014. Expression of soluble *Saccharomyces cerevisiae alcohol dehydrogenase* in *Escherichia coli* applicable to oxido-reduction bioconversions. *Biologia,* 69(6), 722-726.

[10] Wang, N., Shi, H., Yao, Q., Zhou, Y., Kang, L., Chen, H. and Chen, K., 2011. Cloning, expression and characterization of *alcohol dehydrogenases* in the silkworm *Bombyx mori*. *Genetic and Molecular Biology*, 34(2), 240-243.
[11] Yin, J., Li, G., Ren, X. and Herrler, G., 2007. Select what you need: a comparative evaluation of the advantages and limitations of frequently used expression systems for foreign genes. *Journal of Biotechnology*, 127(3), 335-347.
[12] Rosano, G.L. and Ceccarelli, E.A., 2014. Recombinant protein expression in *Escherichia coli*: advances and challenges. *Frontier in Microbiology*, 5, 172.
[13] Joly, J.C., Leung, W.S. and Swartz, J.R., 1998. Overexpression of *Escherichia coli* oxidoreductases increases recombinant insulin-like growth factor-I accumulation. *Proceedings of the National Academy of Science*, 95(6), 2773-2777.
[14] Cario, M.M., Cubarsi, R. and Villaverde, A., 2000. Fine architecture of bacterial inclusion bodies. *FEBS Letters*, 471(1), 7-11.
[15] Slouka, C., Kopp, J., Spadiut, O. and Herwig, C., 2018. Perspective of inclusion bodies for bio-based products: curse or blessing?. *Applied Mirobiology and Biotechnology*, 103(3), 1143-1153.
[16] Lakshmi, G.J., Kotra, S.R., Peravali, J.B., Kumar, P.P.B.S. and Rao, K.R.S.S., 2014. Molecular cloning, high level expression and activity analysis of constructed human interleukin-25 using industrially important IPTG inducible *Escherichia coli* BL21 (DE3). *International Journal of Bio-Science and Bio-Technology*, 6(3), 19-30.
[17] Soltanmohammadi, B., Jalali-Javaran, M., Rajabi-Memari, H. and Mohebodini, M., 2014. Cloning, transformation and expression of proinsulin gene in tomato (*Lycopersicum esculentum* Mill.). *Jundishapur Journal of Natural Pharmaceutical Products*, 9(1), 9-15.
[18] Di Matteo, A., Rigano, M.M., Sacco, A., Frusciante, L. and Barone, A., 2011. Genetic transformation in tomato: novel tools to improve fruit quality and pharmaceutical production. In: M. Alvarez, ed. *Genetic Transformation*. Rijeka: InTech., pp.55.
[19] Barone, A., Chiusano, M.L., Ercolano, M.R., Giuliano, G., Grandillo, S. and Frusciante, L., 2008. Structural and functional genomics of tomato. *International Journal of Plant Genomics*, 2008, 820274.
[20] Fartyal, D., Agarwal, A., James, D., Borphukan, B., Ram, B., Sheri, V., Agrawal, P.K., Achary, V.M.M. and Reddy, M.K., 2018. Developing dual herbicide tolerant transgenic rice plants for sustainable weed management. *Scientific Reports*, 8, 11598, https://doi.org/10.1038/s41598-018-29554-9
[21] Alphey, N. and Bonsall, M.B., 2018. Genetics-based method for agricultural insect pest management. *Agricultural and Forest Entomology*, 20(2), 131-140.
[22] Dong, O.X. and Ronald, P.C., 2019. Genetic engineering for disease resistance in plants: Recent progress and future perspectives. *Plant Physiology*, 180(1), 26-38.
[23] Mehta, R.A., Cassol, T., Li, N., Ali, N., Handa, A.K. and Mattoo, A.K., 2002. Engineered polyamine accumulation in tomato enhances phytonutrient content, juice quality and vine life. *Nature Biotechnology*, 20(6), 613-618.
[24] Klee, H.J. and Giovannoni, J.J., 2011. Genetics and control of tomato fruit ripening and quality attributes. *Annual Review of Genetics*, 45, 41-59.
[25] Baghour, M., Gálvez, F.J., Sánchez, M.E., Aranda, M.N., Venema, K. and Rodríguez-Rosales, P., 2019. Overexpression of *LeNHX2* and *S1SOS2* increases salt tolerance and fruit production in double transgenic tomato plants. *Plant Physiology and Biochemistry*, 135, 77-86.
[26] Ruf, S., Hermann, M., Berger, I.J., Carrer, H. and Bock, R., 2001. Stable genetic transformation of tomato plastids and expression of a foreign protein in fruit. *Nature Biotechnology*, 19(9), 870-875.

[27] Sedeek, K.E.M., Mahas, A. and Mahfouz, M., 2019. Plant genome engineering for targeted improvement of crop traits. *Frontier in Plant Science*, 10, 114, https://doi.org/10.3389/fpls.2019.00114
[28] Yasmeen, A., Mirza, B., Inayatullah, S., Safdar, N., Jamil, M. and Ali, S., 2009. *In Planta* transformation of tomato. *Plant Molecular Biology Reporter*, 27(1), 20-28.
[29] Safdar, N. and Mirza, B., 2014. An experimental comparison of different transformation procedures assessed in tomato cv Rio Grande with yeast *HAL* 1 gene. *Turkish Journal of Biochemistry*, 39(3), 245-252.
[30] Shah, S.H., Ali, S., Jan, S.A. and Ali, U.G., 2015. Piercing and incubation method of *in planta* transformation producing stable transgenic plants by overexpressing *DREB1A* gene in tomato (*Solanum lycopersicum Mill.*). *Plant Cell, Tissue and Organ Culture*, 120(3), 1139-1157.
[31] Miduthuri, S. S., Kumari, A., Pandey, A.K., Sharma, S., Sharma, P., Sreelakshmi, Y. and Sharma, R., 2017. Generation of genetically stable transformants by *Agrobacterium* using tomato floral buds. *Plant Cell, Tissue and Organ Culture*, 129(2), 299-312.
[32] Wee. C.C. and Roslan, H.A., 2012. Isolation of Alcohol Dehydrogenase cDNA and basal regulatory region from *Metroxylon sagu. ISRN Molecular Biology*, 2012, 1-10.
[33] Bergmeyer. H.U., 1986. *Methods of Enzymatic Analysis*. 3rd ed. Weinheim: Verlag Chemie.
[34] Dyson, M.R., Shadbolt, S.P., Vincent, K.J., Perera, R.L. and McCafferty, J., 2004. Production of soluble mammalian proteins in *Escherichia coli*: identification of protein features that correlate with successful expression. *BMC Biotechnology*, 4(32), https://doi.org/10.1186/1472-6750-4-32
[35] Sørensen, H.P. and Mortensen, K.K., 2005. Soluble expression of recombinant proteins in the cytoplasm of *Escherichia coli*. *Microbial Cell Factories*, 4, 1, https://doi.org/10.1186/1475-2859-4-1
[36] Jong, W.S.P., Vikström, D., Houben, D., van den Berg van Saparoea, H.B., de Gier, J.W. and Luirink, J., 2017. Application of an *E. coli* signal sequence as a versatile inclusion body tag. *Microbial Cell Factories*, 16(1), 50, https://doi.org/10.1186/s12934-017-0662-4
[37] Bornhorst, J.A. and Falke, J.J., 2000. Purification of proteins using polyhistidine affinity tags. *Methods in Enzymology*, 326, 245-254.
[38] Jeong, H., Barbe, V., Lee, C.H., Vallenet, D., Yu, D.S., Choi, S.H., Couloux, A., Lee, S.W., Yoon, S.H., Cattolico, L., Hur, C.G., Park, H.S., Ségurens, B., Kim, S.C., Oh, T.K., Lenski, R.E., Studier, F.W., Daegelen, P. and Kim, J.F., 2009. Genome sequences of *Escherichia coli* B strains REL606 and BL21 (DE3). *Journal of Molecular Biology*, 394(4), 644-652.
[39] Desfeux, C., Clough, S.J. and Bent, A.F., 2000. Female reproductive tissues are the primary target of *Agrobacterium*-mediated transformation by the *Arabidopsis* floral-dip method. *Plant Physiology*, 123(3), 895- 904.
[40] Vicker, J.E., Graham, G.C. and Henry, R.J., 1996. A protocol for the efficient screening of putatively transformed plants for*bar*, the selectable marker gene, using the polymerase chain reaction. *Plant Molecular Biology Reporter*, 14(4), 363-368.
[41] Mammedov, T.G., Pienaar, E., Whitney, S.E., TerMaat, J.R., Carvill, G., Goliath, R., Subramanian, A. and Viljoen, H.J., 2008. A fundamental study of the PCR amplification of GC-rich DNA templates. *Computational Biology and Chemistry*, 32(6), 452-457.
[42] Malabadi, R.B. and Nataraja, K., 2007. A biolistic approach for the production of transgenic plants using embryogenic tissue in *Pinus kesiya* Royle Ex. Gord (Khasi pine). Biotechnology, 6(1), 86-92.
[43] Afolabi, A.S., Worland, B., Snape, J.W. and Vain, P., 2004. A large-scale study of rice plants transformed with different T-DNAs provides new insights into locus composition and T-DNA linkage configuration. *Theory and Applied Genetics*, 109(4), 815-826.
[44] Sallaud, C., Meynard, D., van Boxtel, J., Gay, C., Bès, M., Brizard, J.P., Larmande, P., Ortega, D., Raynal, M., Portefaix, M., Ouwerkerk, P.B.F, Rueb, S., Delseny, M. and

Guiderdoni, E., 2003. Highly efficient production and characterization of T-DNA plants for rice (*Oryza sativa* L.) functional genomics. *Theory and Applied Genetics*, 106(8), 1396-1408.

[45] Kohli, A., Miro, B. and Twyman, R.M., 2010. Transgene integration, expression and stability in plants: strategies for improvements. In C., Kole, C. H., Michler, A. G. Abbot, and T. C. Hall, eds. *Transgenic Crop Plants*. Berlin and Heidelberg: Springer Berlin Heidelberg, pp. 201-237.

[46] Hasan, M., Khan, A.J., Khan, S., Shah, A.H., Khan, A.R. and Mirza, B., 2010. Transformation of tomato (*Lycopersicon esculentum* Mill.) with *Arabidopsis* early flowering gene *Apetalai (API)* through *Agrobacterium* infiltration of ripened fruits. *Pakistan Journal of Biotechnology*, 40(1), 161-173.

[47] Brooks, E.M., Sheflin, L.G. and Spaulding, S.W., 1995. Secondary structure in the 30-UTR of EGF and the choice of reverse transcriptases affect the detection of message diversity by RT-PCR. *BioTechniques*, 19(5), 806-812, 814-815.

Phytochemical Screening and GC-MS Analysis of Bioactive Constituents in the Methanolic Extract of *Caulerpa racemosa* (Forssk.) J. Agardh and *Padina boergesenii* Allender & Kraft

Cholaraj Ragunath[1]*, Yohannan Aron Santhosh Kumar[2], Iwar Kanivalan[3] and Sruthi Radhakrishnan[4]

[1]Unit of Aquatic Biotechnology and Live Feed Culture, Department of Zoology, Bharathiar University, Coimbatore, Tamil Nadu, India
[2]Botanical Survey of India, Southern Regional Centre, Coimbatore, Tamil Nadu, India
[3]Department of Botany, Bharathiar University, Coimbatore, Tamil Nadu, India
[4]Department of Biotechnology, Hindustan College of Arts and Science, Coimbatore, Tamil Nadu, India

Received : 22 July 2019, Revised: 8 November 2019, Accepted: 27 April 2020

Abstract

Marine macroalgae (seaweeds) are the potential renewable energy and promising resources of many biologically active compounds. The potential sources of commercial and therapeutic impact of seaweeds are still unaware. In this study, we aim to identify and evaluate the biological activity of *Caulerpa racemosa* (Forssk.) J. Agardh and *Padina boergesenii* Allender & Kraft. The seaweed samples were shade dried and ground. The coarse powdered material was subjected to Soxhlet apparatus and successively extracted with methanol. The phyto-constituents of the seaweeds were analyzed by standard methods and GC-MS. The GC-MS results of *C. racemosa* (Forssk.) J. Agardh and *P. boergesenii* Allender & Kraft revealed the presence of hexadecenoic acid, butanoic acid, arachidonic acid, octadecadienoic acid, cis-vaccenic acid, phytol and eicosatetraenoic acid. The seaweed extracts were subjected to antimicrobial assay by agar-well diffusion. *Padina boergesenii* Allender & Kraft showed the highest inhibition zones (23.6 ± 0.3mm and 22.7 ± 0.5mm) against Gram-positive bacteria *Pseudomonas aeruginosa* and *Staphylococcus aureus*, respectively. *Caulerpa racemosa* (Forssk.) J. Agardh showed the highest inhibition zone (22.0 ± 0.8) against Gram-positive bacteria *Staphylococcus aureus.* Extracts of both seaweeds, *C. racemosa* (Forssk.) J. Agardh and *P. boergesenii* Allender & Kraft, contain potential bioactive compounds with high antibacterial activity and could be deployed in the pharmaceutical applications.

Keywords: seaweeds, phytocompounds, antimicrobial activity
DOI 10.14456/cast.2020.24

*Corresponding author: Tel.: (+91) 96 77 87 42 20
E-mail: ragunath.chola@gmail.com

1. Introduction

Macroalgae are a group of autotrophic, holophytic and complex communites that live in the marine environment. Seaweeds are primitive and they are non-blooming plants, lack a true root, stem-leaves and jacket layer around reproductive structures. Moreover, seaweeds grow extensively in shallow marine water and estuaries and they are usually attached to the bottom or other solid structures by a holdfast, merely used for the attachment of thallus on the substratum and not for the absorption of nutrition [1]. Seaweeds or marine macroalgae are the potential renewable resources in a marine environment.

A total of ten thousand five hundred seaweed species are reported worldwide and 865 species of the seaweeds are found in India. Seaweeds are important for the coastal ecosystems as ocean producers. Seaweed cultivation is the third-largest source of aquaculture production worldwide. It has a portion of human foods exceeding a hundred years [1]. The worldwide seaweed production contributes approximately 20% of total global marine aquaculture production [2]. Seaweed farming signifies an essential component of aquaculture production and accounts for 27.3 million tons in 2014 [3].

Similar to terrestrial plants, macroalgae also synthesise their food by photosynthesis, in the presence of sunlight and seawater. Seaweeds are established in the coastline area, and live between high tide and low tide areas. They contain different types of pigments. Chlorophyta-green algae contains chlorophyll pigment, Phaeophyta-brown algae contains fucoxanthin, and Rhodophyta-red algae contains phycoerythrin and phycocyanin.

Seaweeds are excellent nutritional sources and contain various trace minerals, carbohydrates, vitamins, proteins and other bioactive compound [3]. They yield wide ranges of valuable natural metabolites that can be used in the arenas of the pharmaceuticals and food industries. Various bioactive compounds such as linoleic acid, stearic acid, oleic acid, fucoxanthin, fucophlorethol, loliolide and deschloroelatol have various biological activities [4]. Seaweeds are a rich source of numerous biologically active compounds and those compounds have been possibly exploited as active elements for humans and animal health uses. Although drastic labors have been made to isolate new-fangled compounds with important therapeutic activities, very few such compounds with high potential have been accessed. The bioactive compounds that have been most extensively researched include sulfated polysaccharides laminarin, fucoidan, β-glucans and phlorotannins, which have the ability to inhibit bacterial growth and also possess antioxidant properties [5].

The enormous importance is given to macroalgae due to their broad-spectrum of biological activity [5]. The bioactive compounds have been isolated from macroalgae include sulfated polysaccharides, peptides, sterols, brominates, aromatics, nitrogen-heterocyclic, nitro sulfuric heterocyclic, dibutanoids and proteins [6]. The polymeric carbohydrates are the most important constituents of marine macroalgae. They shows anticoagulant, antitumor and other activities [7]. When compared to telluric plants, macroalgae have innumerable inorganic and carbon-based constituents that have the advantage of the possible use in human food and pharmaceutical industries [8].

The study of the antimicrobial composites from seaweeds is vital as there is increasing demand for therapeutic drugs used for the treatment of pathogenic infection [9]. Recently, seaweeds show stimulatory effects on a wide range of pathogens and this characteristic feature of seaweeds has attracted many researchers to focus on the use of seaweed as an immunostimulant in health improvement and disease prevention in animals, thereby reducing the use of antibiotics and chemotherapeutics. Using these immunostimulants particularly for boosting the immune systems is effective against several opportunistic and secondary pathogens [10]. Immunostimulants can be introduced via the feed and the water. Water-soluble acidic polysaccharides taken from *Ulva rigida*

showed an immune stimulatory response in murine [10], whereas some seaweeds showed immune-suppressive effect [11]. Lipopolysaccharide extracted from seaweeds enhanced the proliferation of hemocytes in *Penaeus monodon* [10].

Extracts of seaweeds help to manage various of diseases in aquatic farm animals. Extracts obtained from the green alga fed to shrimp showed resistance to diseases [12]. Research work on the evaluation of the immunostimulant potential of seaweeds that inhabit the world's oceans and in particular those that live along the Indian coast have not been copious. In recent times, several works have revealed that numerous herbal products having immune-stimulant activities are recommended as herbal biomedicines that can be used in aquaculture as they are easily available, eco-friendly, cost-effective and can also be used in pharmaceutical industries because they can act against a wide range of pathogens [13]. Seaweeds are also used in the various fields of science, such as pharmaceuticals, medicine, tissue culturing, human genetics, microbiology and molecular biology. Although seaweeds are potential sources of compounds for many commercial and therapeutic sectors, the immense impacts of seaweeds are still unaware. Very little reseach has been carried out on the seaweeds *C. racemosa* and *P. boergesenii* from the region of Gulf of Mannar, Rameswaram, India. Therefore, the present study was carried out to assess the phytocompounds, biological activity and antibacterial activity of selected seaweeds.

2. Materials and Methods

2.1 Collection of seaweed sample

The well-grown species of brown and green algae are collected from the coastal area along the Mandapam, Rameshwaram (079° 20`E Long: 09° 25`N Lat) regions, the south-east coast of India during June 2018. After collecting, seaweed was thoroughly washed and cleaned with seawater followed by freshwater and distilled water to remove all epiphytes, sand and calcareous particles including other adhering detritus materials. After that, the seaweed was spread on blotting paper to remove excess water.

2.2 Identification of the seaweed species

The collected seaweed was authentically identified and certificated by the Botanical Survey of India, Southern Regional Center, Coimbatore. Identification was carried out based on morpho-anatomical features.

2.3 Preparation of seaweed extract by Soxhlet apparatus

The fresh materials were shade dried conditions and exposed to pulverization to get a coarse powder. The coarse powdered materials were subjected to Soxhlet extraction and successively extracted with methanol (14 g of algal powder per 250 ml of methanol) for 8 h. These extracts were collected and concentrated in a rotary evaporator (250-280 rpm, pressure 350 mmHg and 70℃) and the extracts were stored (-20℃) in the refrigerator in airtight containers for further use.

2.4 Qualitative phytochemical analysis

The phytochemical screening test was performed as described below by using standard methods [2, 14, 15].

2.4.1 Test of alkaloids by Wagner's test

Five ml of extract are added to 2ml of Wagner's mixture. The formation of magenta-brown precipitate indicates the occurrence of alkaloids.

2.4.2 Test for flavonoids by Shinoda test

A few drops of concentrated HCl are added to 1ml extract followed by addition of 0.5g of magnesium. A pink colouration points out the presence of flavonoids.

2.4.3 Test for saponins by Foam test

One ml of extract is shaken vigorously with 20 ml of distilled water for 10-15 min. The formation of a foam layer indicates the presence of saponins.

2.4.4 Test for phenolic compounds and tannins

One ml of extract is mixed with 2 ml of 5% ferric chloride. The genesis of dark blue or greenish-black colouration points out the occurrence of tannins or phenolic compounds.

2.4.5 Test for glycosides by Keller - Killiani test

An extract (0.5 ml) is added with 2 ml of glacial acetic acid, a few drops of 5% ferric chloride and 1ml of concentrated sulfuric acid. The appearance of a brown ring at the interface shows the presence of glycosides.

2.4.6 Identification of terpenoids by Salkoski test

One ml of the extract is mixed with 2 ml of chloroform along with concentrated sufuric acid. A reddish-brown colouration indicates the presence of terpenoids.

2.4.7 Test for phlobatannins

One ml of extract is mixed with dilute HCl. The formation of a red precipitate indicates the presence of phlobatannins.

2.4.8 Test for protein and free amino acid by Ninhydrin test

For the identification of protein and amino acid, 2 ml of the extract is treated with 1ml of ninhydrin solution and kept in a hot water bath. The appearance of a purple colour indicates the presence of proteins and amino acid.

2.4.9 Test for carbohydrate by Molisch's test

Two ml of the extract is mixed with 1 ml of Molisch's reagent with a few drops of concentrated sulfuric acid along the sides of a test tube. A purple or reddish colour indicates the presence of carbohydrates.

2.5 Gas chromatography-mass spectroscopy analysis

Samples of the brown and green algae were extracted and the extracted fraction was subjected to GC-MS analysis. The phytoconstituents of the seaweed sample were analyzed using a Perkin Elmer Clarus Series Gas Chromatographic System with a capillary column. Identification of products was made by comparison of retention time and fragmentation patterns with known reference complexes as well as with mass spectra in the library search results kept in the software (TurboMass ver 5.4.2) of the GC-MS. The samples were analyzed under the following conditions: Elite-5MS (5% phenyl, 95% dimethylpolysiloxane) fused in a capillary column (30 in length x 250 µm in diameter x 30 µm in thickness of film). The spectroscopic detector for GC-MS involved an electron ionization system in 70 eV with helium as carrier gas flow at 1ml/min and the temperature programmed at 70ºC and 6ºC to 150 ºC for 2 min, 6ºC to 290ºC for 5 min. The split ratio was 10:1, the injection sample volume was 1 µl. The injection and detector temperature were 250ºC. Mass spectra were recorded and the range was m/z 40-500 amu. The GC-MS results were compared with the standard compounds library.

2.6 Collection of bacterial strains

The bacterial strains such as *Pseudomonas aeruginosa*, *Staphylococcus aureus*, *Staphylococcus saprophyticus*, *Streptococcus mutans*, *Bacillus subtilis*, *Streptococcus pyogenes*, *Bacillus cereus*, *Staphylococcus epidermidis*, *Streptococcus pneumoniae*, *Enterococcus faecalis*, *Escherichia coli*, and *Klebsiella pneumoniae* were obtained from PSG Institute of Medical Sciences and Research, Coimbatore, Tamil Nadu. The pathogens were maintained on agar slants at 4ºC.

2.7 Antibacterial assays by well diffusion method

Antibacterial assays were performed using the agar well diffusion method. Muller Hinton agar (pH 7.4) was prepared and sterilized for 15 min. The sterilized medium was poured into sterile Petri dishes and the collected bacterial pathogens were swabbed on the plates. Different concentrations (2.0 to 50 mg/ml) of the algal extract was loaded into the wells (8 mm diameter). Distilled water was used as a negative control [16]. The bacterial plates were then incubated at 37ºC for 24 h and the antibacterial activity was determined by measuring inhibition zone in mm [17-19].

3. Results and Discussion

3.1 Seaweed identification

The collected seaweed samples were identified as green algae: *Caulerpa racemosa* (Forssk.) J. Agardh (Figure 1a) and brown algae: *Padina boergesenii* Allender & Kraft (Figure1b). Identification was based on the morphological and anatomical characteritics of the seaweeds.

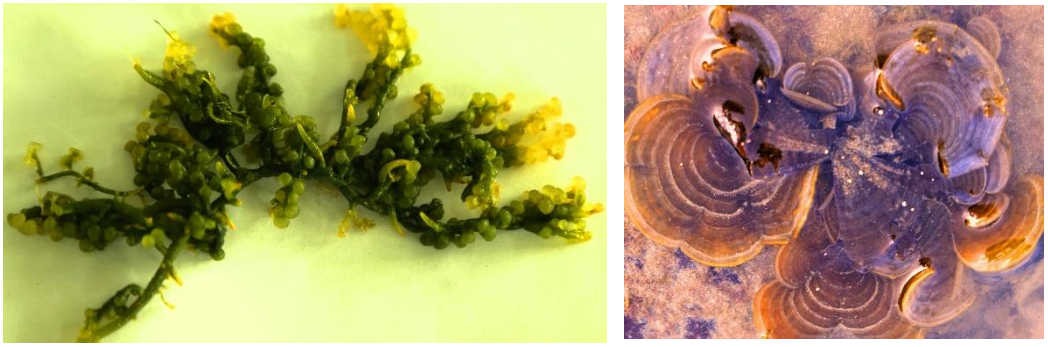

(a) *Caulerpa racemosa* (b) *Padina boergesenii*

Figure 2. Green and brown algae

3.2 Qualitative phytochemical analysis

Secondary metabolites are characterized by a broad spectrum of biological activities. In this study, we observed positive results for flavonoids, saponins, a phenolic compound, terpenoids, phlobatannins and amino acids (Table 1). The identified compounds had cytostatic, antiviral, anthelmintic, antifungal and antibacterial properties [20].

Table 1. Qualitative phytochemical analysis, inference of primary phyto-compound found in *C. racemosa* and *P. boergesenii.*

Phytochemical	Inference	
	C. racemosa	*P. boergesenii*
Alkaloids	-	-
Flavonoids	+	+
Saponins	+	+
Phenolic compound and tannins	+	+
Glycosides	-	-
Terpenoids	-	+
Phlobatannins	+	-
Amino acid and protein	+	+
Carbohydrate	+	-

(+) presence of the compound, (–) absence of the compound

3.3 Gas chromatography-mass spectroscopy analysis

The extracted seaweed (*C. racemosa* and *P. boergesenii*) samples were analyzed with GC-MS to detect phyto-components, various fatty acids and other compounds. GC-MS technique provides the identification and quantification of chemical compounds based on their characteristic fragmentation patterns at specific retention times. The results of GC-MS analysis revealed that a wide range of compounds was identified and these are listed on Table 2 (*C. racemosa*) and Table 3 (*P. boergesenii*). Tables 2 and 3 show the variety of compounds found and also shows their molecular weight and biological activity.

Table 2. The GC-MS analysis of *C. racemosa*, biological activity, molecular formula and molecular weights

Retention time (min)	Peak area (%)	Compound	Molecular weight	Molecular formula	Biological activity
9.766	44.798	Chloroxyletol	156.609	$C_8H_9C_{10}$	Anti-bacterial [21]
17.349	0.476	6-Hydroxy-4, 4,7a-trimethyl-5, 6, 7,7a-tetrahydro-1-benzofuran-2(4H)-one	196.242	$C_{17}H_{32}O_2$	Antipyretic [22, 23]
20.600	2.097	Hexadecanoic acid, methyl ester	270.457	$C_{17}H_{32}O_2$	Anti- fungal and antibacterial [24]
21.256	8.634	n-Hexadecanoic acid	256.430	$C_{17}H_{34}O_2$	Antioxidant [24, 25]
21.811	0.887	Palmitic anhydride	494.845	$C_{17}H_{24}O_5$	Anticancer [24]
22.091	0.308	Rhodovibrin	584.914	$C_4H_7ClO_2$	Anticancer [15]
24.027	1.580	Phytol	296.539	$C_{20}H_{32}O_2$	Anticancer and Anti-inflammatory [26-28]
24.397	1.826	9,12-Octadecadienoic acid (Z, Z)	280.445	$C_{19}H_{34}O_2$	Antimicrobial, Anticancer, Hepatoprotective, Anti-arthritic, anti-asthma and diuretic [29]
24.522	6.069	Oleic acid	282.470	$C_{19}H_{36}O_2$	Antitoxidant [30]
25.342	0.363	Strychane, 1-acetyl-20α-hydroxy-16-methylene	338.443	$C_{20}H_{40}O$	Not reported
27.373	0.607	Methyclothiazide	360.224	$C_{17}H_{32}O$	Not reported
27.428	0.493	Glycidyl palmitate	312.494	$C_{18}H_{34}O_2$	Not reported
29.754	0.410	2-cis,cis-9,12-Octadecadienyloxy ethanol	310.514	$C_{20}H_{34}O_2$	Not reported
29.844	1.083	Glycidyl oleate	338.532	$C_{19}H_{36}O_3$	Not reported
30.084	0.753	1H-Indene, 1-hexadecyl-2,3-dihydro	342.601	$C_{28}H_{38}O_{10}$	Not reported
30.304	0.802	Glycerol 1-palmitate	330.509	$C_{39}H_{78}O_3$	Anticancer [31]
30.373	0.467	1H-cyclopropal	534.600	$C_{21}H_{38}O_3$	Not reported
30.579	0.563	Diisooctyl phthalate	390.564	$C_{25}H_{42}$	Not reported
32.745	0.399	17-Octadecynoic acid, TMS derivative	352.626	$C_{27}H_{56}O_4Si_2$	antioxidant, hepatoprotective, antihistaminic, hypocholesterolemic and anti-eczematic activities [32]

Table 2. (cont.)

32.747	0.398	Linoleic acid ethyl ester	308.498	$C_{26}H_{50}$	Hypocholesterolemic, Nematicide, Antiarthritic, Hepatoprotective Anti-androgenic, Hypocholesterolemic, 5-Alpha reductaseinhibitor, Antihistaminic, Anticoronary, Insectifuge, Anti-eczemic and Anti-acne [19, 22, 33, 34]
32.835	0.623	Glucobrassicin	448.461	$C_{16}H_{20}N_2O_9S_2$	Antioxidant and antimicrobial [17]
33.295	0.410	Oleic acid, eicosyl ester	563.008	$C_8H_9C_{10}$	Antiinflammatory, Cancer preventive, Hypocholesterolemic and Anemia gentic Insectifuge [35]
33.380	0.496	5(α)Pregane-3α,20αdiol	489.600	$C_{17}H_{32}O_2$	Antioxidant and antimicrobial [36]

Table 3. GC-MS analysis of *P. boergesenii*, biological activity and molecular weight and formula

Retention Time (min)	Peak area (%)	Name of the compound	Molecular Weight	Molecular formula	Biological activity
9.731	10.07	Chloroxyletol	156.609	$C_8H_9C_{10}$	Anti-bacterial [21]
20.330	0.35	9-Hexadecenoic acid, methyl ester (Z)	268.434	$C_{17}H_{32}O_2$	Not reported
20.570	3.878	Hexadecanoic acid, methyl ester	270.457	$C_{17}H_{32}O_2$	Anti- fungal and antibacterial [24]
21.111	10.617	n-Hexadecanoic acid	256.430	$C_{17}H_{34}O_2$	Antioxidant [24]
21.776	0.370	Pyrano [4,3-b] benzopyran-1,9-dione, 5a-methoxy-9a-methyl-3 -(1-propenyl) perhydro	308.374	$C_{17}H_{24}O_5$	Antitoxidant [24]
21.921	0.362	Butanoic acid, 4-chloro	122.548	$C_4H_7ClO_2$	Not reported

Table 3. (cont.)

22.651	0.592	Arachidonic acid	304.474	$C_{20}H_{32}O_2$	Antimicrobial activity [24]
23.722	1.416	11,14-Octadecadienoic acid, methyl ester	294.479	$C_{19}H_{34}O_2$	Anticancer [24]
23.862	3.204	9-Octadecenoic acid (Z)-, methyl ester	296.500	$C_{19}H_{36}O_2$	Anticancer and antimicrobial [1, 37]
24.017	0.905	Phytol	296.539	$C_{20}H_{40}O$	Anticancer, anti-inflammatory, antimicrobial, antispasmodic activity and vitamins E, K1 [26, 27]
24.177	1.128	13-Heptadecyn-1-ol	252.442	$C_{17}H_{32}O$	Not reported
25.507	12.631	cis-Vaccenic acid	282.468	$C_{18}H_{34}O_2$	Anticancer [38]
26.678	0.596	5,8,11,14 - Eicosatetraenoic acid, methyl ester, (all-Z)	318.493	$C_{21}H_{34}O_2$	Not reported
27.408	3.511	Glycidyl palmitate,	312.494	$C_{19}H_{36}O_3$	Not reported
28.864	0.369	1H-Cyclopropa [3,4] benz [1,2-e] azulene-4a,5,7b,9,9a (1aH)	534.600	$C_{28}H_{38}O_{10}$	Not reported
28.969	0.448	Stearic acid, 3-(octadecyloxy) propyl	595.050	$C_{39}H_{78}O_3$	Antifungal [39]
29.819	2.799	Glycidyl oleate	338.532	$C_{21}H_{38}O_3$	Not reported
30.069	1.506	(1S)-1-Hexadecyl-2,3-dihydro-1H-indene	342.601	$C_{25}H_{42}$	Not reported
32.720	0.992	2-Oleoylglycerol, 2TMS derivative	500.902	$C_{27}H_{56}O_4Si_2$	Not reported
33.265	0.596	Cyclohexane, 1,1-dodecylidenebis [4-methyl]	362.686	$C_{26}H_{50}$	Not reported
33.340	0.867	Glucobrassicin	448.461	$C_{16}H_{20}N_2O_9S_2$	Not reported

3.4 Antibacterial assays by agar-well diffusion method

The antibacterial activity of seaweed extracts is presented in Table 4. It was found that the *C. racemosa* extract showed the highest inhibition zone (22.0 ± 0.8mm) against Gram-positive bacterium *S. aureus* whereas *P. boergesenii* showed the highest inhibition zone (23.6 ± 0.3mm) against the Gram-positive bacterium *Ps. aeruginosa*. Both *P. boergesenii* and *C. racemosa* showed the highest antibacterial activity at 50 mg/ml concentration.

Table 4. Antibacterial activity of seaweed extracts at 50 mg/ml concentration

Bacterial strain	**Zone of inhibition (mm)**	
	C. racemosa	*P. boergesenii*
Ps. aeruginosa	21.0 ± 0.2	23.6 ± 0.3
S. aureus	22.0 ± 0.8	22.7 ± 0.5
S. saprophyticus	19.8 ± 0.3	21.8 ± 0.5
S. epidermidis	10.5 ± 0.4	13.5 ± 0.8
E. faecalis	No activity	10.1 ± 0.1
E. coli	20.9 ± 0.2	22.2 ± 0.1
B. cereus	12.6 ± 0.1	15.4 ± 0.2
B. subtilis	17.5 ± 0.3	19.7 ± 0.2
S. mutans	17.8 ± 0.9	20.3 ± 0.3
S. pyogenes	14.2 ± 0.5	16.9 ± 0.9
S. pneumoniae	No activity	11.2 ± 0.9
K. pneumoniae	12.2 ± 0.7	18.2± 0.3

3.5 General discussion

In this study, the antibacterial activity of the two macro-algae and their bioactive abilities were assessed. Previous researchers reported that macroalgae are a tremendous source of compounds such as polysaccharides, tannins, flavonoids, phenolic acids, bromophenols, carotenoids and these compounds were responsible for different biological activities [35, 40-42]. In this study the antibacterial activity of extracts of *P. boergesenii* and *C. racemosa* were evaluated. From the results, a higher antibacterial activity was obtained in brown algae *P. boergesenii* compared to green algae *C. racemosa.* Both algae have previously reported higher activity against *Pseudomonas aeruginosa* and *Staphylococcus aureus* pathogens [33, 43].

The outcome of the present study is that preeminent antibacterial activity was exhibited in *C. racemosa* and *P. boergesenii* extracts. Methanol has high antibacterial activity when compared to other organic solvents [20, 44]. Methanolic extracts of macroalgae contains phenolics, alkaloids and amino acids, which may account for the antibacterial activity [43, 45].

Previous reports showed that seaweeds contain momentous amounts of proteins, vitamins, minerals and trace elements. Macroalgae contains phenolic complexes and polysaccharides, which have various biological activities [16]. In the present study, a total of twenty-three chemical constituents from green seaweed and twenty-one chemical constituents from brown seaweed were extracted and identified in methanolic extracts extracts of *C. racemosa* and *P. boergesnii* and included were flavonoids, saponins, phenolic compounds, tannins, amino acids and proteins. While *C. racemosa* showed postive result for phlobatannins and carbohydrates, *P. boergesnii* showed postive result for terpenoids. Both seaweeds showed negative results for glycosides and alkaloids.

4. Conclusions

Collectively, the present data offers great insight and it is the first report of the biological activity of *C. racemosa* and *P. Boergesenii.* Various fatty acids and bioactive compounds present in *C. racemosa* and *P. boergesenii* (Hexadecenoic acid, Hexadecanoic, Butanoic acid, Arachidonic, Octadecadienoic, cis-Vaccenic, Octadecenoic, Phytol and Eicosatetraenoic acid) exhibited effective inhibition against a wide range of pathogens. The research clearly shows that *C. racemosa* and *P. boergesenii* are rich potential sources of many bioactive compounds. From the results, we suggest that *C. racemosa* and *P. boergesenii* could be very beneficial to pharmaceutical and therapeutics applications in future.

References

[1] Bjerregaard, R., Valderrama, D., Radulovich, R., Diana, J., Capron, M., Cedric Amir, M., Cedric, M., Hopkins, K., Charles, Y., Goudey, C. and Forster, J., 2016. *Seaweed Aquaculture for Food Security, Income Generation and Environmental Health in Tropical Developing Countries (English)*. [online] Availabe at: http://documents.worldbank.org/curated/en/ 94783146 9090666344 /Seaweed-aquaculture-for-food-security-income-generation-and-environmental-health-in-Tropical-Developing-Countries

[2] Divyagnaneswari, M., Christybapita, D. and Michael, R.D., 2007. Enhancement of nonspecific immunity and disease resistance in Oreochromis mossambicus by *Solanum trilobatum* leaf fractions. *Fish & Shellfish Immunology*, 23(2), 249-259.

[3] Ghosh, P., Adhikari, U., Ghosal, P., Pujol, C.A., Carlucci, M.J. and Damonte, E.B., 2004. In vitro anti-herpetic activity of sulfated polysaccharide fractions from *Caulerpa racemosa*. *Phytochemistry*, 65(23), 3151-3157.

[4] Bouhla, R., Haslin, C., Chermann, J.C., Colliec-Jouault, S., Sinquin, C., Somin, G., Cerantola, S., Riadi, H. and Bourgougnon, N., 2011. Antiviral activities of sulfated polysaccharides isolated from *Sphaerococcus coronopifolius* (Rhodophyta, Gigartinales) and *Boergeseniella thuyoides* (Rhodophyta, Ceramiales). *Marine Drugs*, 9(7), 1187-209.

[5] Priyadharshini, S., Bragadeeswaran, S., Prabhu, K. and Ran, S., 2011. Antimicrobial and hemolytic activity of seaweed extracts *Ulva fasciata* (Delile 1813) from Mandapam, Southeast coast of India. *Asian Pacific Journal of Tropical Biomedicine*, 1(1), S38-S39.

[6] Kuda, T., Taniguchi, E., Nishizawa, M. and Araki, Y., 2002. Fate of water-soluble polysaccharides in dried *Chorda filuma* brown algae during water washing. *Journal of Food Composition and Analysis*, 15(1), 3-9.
[7] Lavanya, R. and Veerappan, N., 2011. Antibacterial potential of six seaweeds collected from Gulf of Mannar of Southeast Coast of India. *Advances in Biological Research*, 5, 38-44.
[8] Kolanjinathan, K. and Stella, D., 2009. Antibacterial activity of marine macro-algae against human pathogens. *Recent Research in Science and Technology*, 1(1), 20-22.
[9] Holdt, S. and Kraan, S., 2011. Bioactive compounds in seaweed: functional food applications and legislation. *Journal of Applied Phycology*, 23(3), 543-597.
[10] Leiro J.M., Castro R., Arran, J.A. and Lamas, J., 2007. Immunomodulation activities of acidic sulphated polysaccharides obtained from the seaweed *Ulva rigida* C. Agardh. *International Immunopharmacology*, 7 (7), 879-888.
[11] Felix, S., Robins, P. and Rajeev, A., 2004. Immune enhancement assessment of dietary incorporated marine algae *Sargassum wightii* (Phaeophyceae/Punctariales) in tiger shrimp *Penaeus monodon* (Crustacia/penaeidae) through prophenoloxidase (pro PO) systems. *Indian Journal of Marine Science*, 33(4), 361-364.
[12] Kolanjinathan, K., Ganesh, P. and Govindarajan, M., 2009. Antibacterial activity of ethanol extracts of seaweeds against fish bacterial pathogens. *European Review for Medical and Pharmacological Sciences*, 13, 173-7.
[13] Yadav, S., Bajagai, Athol, V., Klieve, Peter, J., Dart., Wayne, L. and Bryden, 2016. Probiotics in animal nutrition. Production, impact and regulation. In: Harinder P.S Makkar, ed. *FAO Animal Production and Health Paper No. 179*, Rome: FAO, pp. 1-170.
[14] Duke, 2016. *Dr. Duke's Phytochemical and Ethnobotanical Databases*. [online] Available at: https://phytochem.nal.usda.gov/phytochem/search/list
[15] El-Baz, F.K, Hassan, A.Z., Abd-Alla, H.I., Aly, H.F. and Mahmoud, K. 2017. Phytochemical analysis, assessment of antiproliferative and free radical scavenging activity of *Morus alba* and *Morus rubra* fruits. *Asian Journal of Pharmaceutical and Clinical Research*, 10(6), 189-199.
[16] Kumar, K.S., Ganesan, K. and Subba Rao, P.B., 2008. Antioxidant potential of solvent extracts of *Kappaphycus alvarezii* (Doty) Doty-edible seaweed. *Food Chemistry*, 107(1), 289-295.
[17] Bischoff, K.L., 2016. Chapter 40-Glucosinolates. [online] Available at : https://doi.org/ 10.1016/B978-0-12-802147-7.00040-1
[18] Priyadharshini, S., Subramanian, B., Prabhu, K. and Ran, S., 2011. Antimicrobial and hemolytic activity of seaweed extract *Ulva fasciata* (Delile 1813) from Mandapam, Southeast coast of India. *Asian Pacific Journal of Tropical Biomedicine*, 1, S38-S39.
[19] Ragunath, C., Komathi, S. and Ragunathan, R., 2018. Molecular Characterization of *Leptospira interorgans*, isolated from animal samples. *International Journal of Pure and Applied Bioscience*, 6(2), 995-1004.
[20] Mozhi, S., Muthuvel, A., Gnanambigai, D. and Thangavel, B., 2009. Total flavanoid and in vitro antioxidant activity of two seaweeds from Rameshwaram Coast. *Global Journal of Pharmacology* 3, 59-62.
[21] Mcdonell, G.E. and Ruseell, A.D., 1999. Antiseptics and disinfectants activity, action and resistance. *Clinical Microbiology Reviews*, 12(1), 147-179.
[22] Igwe, O. and Onwu, F.K., 2015. Leaf essential oil of *Senna alata* Linn from South East Nigeria and its antimicrobial activity. *International Journal of Research in Pharmacy and Chemistry*, 5(1), 27-33.
[23] Lahaye, M., 1991. Marine algae as a source of dietary fibres: determination of soluble and insoluble dietary fibre contents in some sea vegetable. *Journal of the Science of Food and Agriculture*, 54 (4), 587-594.

[24] Chandrasekaran, M., Senthilkumar, A. and Venkatesalu, V., 2011. Antibacterial and antifungal efficacy of fatty acid methyl esters from leaves of *Sesuvium portulacastrum* L. *European Review for Medical and Pharmacological Sciences*, 15, 775-780.
[25] Shahidi, F. Janitha, P.K. and Wanasundara, P.D., 1992. Phenolic antioxidants. *Critical Reviews in Food Sciences and Nutrition*, 32(1), 67-103.
[26] Lee, A.C., Baula, I.U., Miranda, L.N. and Min, S.T. 2015. *A Photographic Guide to the Marine Algae of Singapore.* Singapore: Tropical Marine Science Institute.
[27] Lee, K.L., Lee, S.H. and Park K.Y., 1999. Anticancer activity of phytol and Eicosatrienoic acid identified from Perilla leaves. *Journal of the Korean Society of Food Science and Nutrition*, 28, 1107-1112.
[28] Gideon, V.A., 2015. GC-MS analysis of phytochemical components of *Pseudoglochidion anamalayanum* Gamble: An endangered medicinal tree. *Asian Journal of Plant Science & Research*, 5(12), 36-41.
[29] Tyagi, T. and Agarwal, M., 2017. Phytochemical screening and GC-MS analysis of bioactive constituents in the ethanol extract of *Pistia stratiotes* L. and *Eichhornia crassipes* (Mart.) solms. *Journal of Pharmacognosy and Phytochemistry*, 6(1), 195-206.
[30] Yu, F., Lian, X., Guo, H., McGuire, P.M., Li, R., Wang, R.B. and Yu, F., 2005. Isolation and characterization of methyl esters and derivatives from *Euphorbia kansui* (Euphorbiaceae) and their inhibitory effects on the human SGC-7901 cells. *Journal of Pharmacy & Pharmaceutical Sciences*, 8 (3), 528-535.
[31] Pascual, G., Avgustinova, A., Mejetta, S., Martín, M., Castellanos, A., Attolini, C.S, Berenguer, A., Prats, N., Toll, A., Hueto, J.A., Bescos, C., Di Croce, L. and Aznar Benitah, S.A, 2017. Targeting metastasis-initiating cells through the fatty acid receptor CD36. *Nature*, 541, 41-45.
[32] Fadeyi, O.E., Olatunji, G.A. and Ogundele, V.A., 2015. Isolation and characterization of the chemical constituents of *Anacardium occidentale* cracked bark. *Natural Products Chemistry Research*, 3(5), https://doi:10.4172/2329-6836.1000192
[33] Choi, J.S., Park, N.H., Hwang, S.Y., Sohn, J.S., Kwak, I., Cho, K.K. and Choi, I.S., 2013. The antibacterial activity of various saturated and unsaturated fatty acids against several oral pathogens. *Journal of Environmental Biology*, 34(4), 673-676.
[34] Ogidi, O.C., Oyetayo, V.O. and Akinyele, B.J., 2015. In vitro evaluation of antimicrobial efficacy of extracts obtained from raw and fermented wild macrofungus, *Lenzites quercina*. *International Journal of Microbiology*, 2015, https://www.hindawi.com/journals/ijmicro/2015/106308
[35] Sheela, D. and Uthayakumari, F., 2013. GC-MS analysis of bioactive constituents from coastal sand dune taxon - *Sesuvium portulacastrum* (L.). *Bioscience Discovery*, 4(1), 47- 53.
[36] Altameme, H.J., Hameed, I.M. and Kareem, M.A., 2015. Analysis of alkaloid phytochemical compounds in the ethanolic extract of *Datura stramonium* and evaluation of antimicrobial activity. *African Journal of Biotechnology*, 4(19), 1668-1674.
[37] Bhakuni, D.S. and Rawat, D.S., 2006. Bioactive marine natural products. *Journal of the American Chemical Society*, 128 (13), 4494, https://doi.org/10.1021/ja059852v
[38] Pongprayoon, U., Baeckstreom, P., Jacobsson, U., Lindstreom, M. and Bohlin, L., 1992. Antispasmodic activity of beta-damascenone and e-phytol isolated from *Ipomoea pes-caprae*. *Planta Medica*, 58(1), 19-21.
[39] Abubacker, M.N. and Devi, P.K., 2014. In vitro antifungal potentials of bioactive compound oleic acid, 3-(octadecyloxy) propyl ester isolated from *Lepidagathis cristata* Willd. (Acanthaceae) inflorescence. *Asian Pacific Journal of Tropical Biomedicine*, 7*(*1*)*, S190-S193.

[40] Mahabaleshwara, K., Chandrasekhar, N. and Govindappa, M., 2016. Phytochemical investigations of methanol leaf extracts of *Randia spinosa* using column chromatography, HPTLC and GC-MS. *Natural Products Chemistry & Research*, 4 (2), https://doi:10.4172/2329-6836.1000202

[41] Zaha, A.E., Rajashri, R.N., Ashok, K.S. and Sanaa K.B., 2016. Fatty acid analysis, antioxidant and biological acitivity of fixed oill of *Annona muricata* L. seeds. *Journal of Chemistry*, 2016, 1-6.

[42] Rodriguez, D., Carro, A.M., Cela, R. and Lorenzo, R.A., 2010. Microwave-assisted extraction and large-volume injection gas chromatography-tandem mass spectrometry determination of multi-residue pesticides in edible seaweed. *Analytical and Bioanalytical Chemistry*, 398, 1005-1016.

[43] Kavitha, M. and Vidhya, I., 2014. Antioxidant and antiproliferative activities of extracts of selected red and brown seaweeds from the Mandapam Coast of Tamil Nadu. *Journal of Food Biochemistry*, 38(1), 92-101.

[44] Seenivasan, R., Indu, H., Archana, G. and Geetha, S., 2010. The antibacterial activity of some marine algae from South East Coast of India. *American-Eurasian Journal of Agricultural & Environmental Sciences*, 9(5), 480-489.

[45] Wikfors, G.H. and Ohno, M., 2001. Impact of algal research in aquaculture. *Journal of Phycology*, 37(6), 968-974.

A Simple and Green Approach for Colorimetric Ammonia Determination by Combining Pervaporation with Paper Impregnated Anthocyanins Extracted from Red Cabbage

Jurairat Jongprakobkit, Wannakan Wisaichon and Wiboon Praditweangkum*

Department of Chemistry, Faculty of Science, King Mongkut's Institute of Technology Ladkrabang, Bangkok, Thailand

Received: 21 January 2020, Revised: 9 May 2020, Accepted: 26 May 2020

Abstract

This work reports on the development of a simple, green and inexpensive analytical method utilizing a microwell plate for ammonia determination by combining pervaporation with a paper-based colorimetric sensor. The method is based on the conversion of ammonium ions to ammonia gas by alkalinization of water samples using powdered calcium hydroxide. The generated ammonia gas diffuses freely across the headspace to a paper-based sensor impregnated with natural anthocyanins extracted from red cabbage using deionized water as a non-toxic solvent. The reaction causes the paper sensor to change color from pink to blue, and the sensor is then scanned on a flatbed scanner to quantify ammonia by correlation to the reflectance of the blue spot on the paper sensor. Under the optimal conditions, a working range of 1.0-25.0 mg N l^{-1} was obtained. The limit of detection and the limit of quantification were found to be 0.29 and 0.98 mg N l^{-1}, respectively. The method was successfully applied for determining total ammonia in water samples with recoveries in the range of 89.6-110.5%. No significant difference was observed between this method and the phenate spectrophotometric standard method.

Keywords: ammonia, calcium hydroxide powder, red cabbage anthocyanins, paper-based colorimetric sensor
DOI 10.14456/cast.2020.25

1. Introduction

Ammonia is normally used in fertilizer and animal feedstock production. In agricultural areas, ammonia from fertilizer and animal farming runoff frequently drains into water supplies [1, 2]. The total ammonia nitrogen (TAN) in the form of NH_3 and NH_4^+ is normally analyzed and the results can indicate the water quality [3]. TAN values ranging from 0.53 to 22.8 mg l^{-1} are reported to be initially toxic to freshwater organisms [4, 5].

*Corresponding author: Tel.: +66 87-340-2424
E-mail: wiboon.pra@kmitl.ac.th

Various newly developed methods for the analysis of ammonia, such as a method that involves a fluorescence and colorimetric ammonia sensor based on a metal-organic gel [6], a nondispersive atomic fluorescence spectrometry method based on gas-phase light scattering [7] and a colorimetric detection using smartphones based on localized surface plasmon resonance of silver nanoparticles [8] have been reported, while standard methods for determination of ammonia in waters including titration, ammonia-selective electrode method, spectrophotometry, and flow injection analysis [9] are still being utilized. These spectrophotometry and flow injection analysis (FIA) methods are based on the Berthelot-phenate reaction, which relies on the formation of indophenol blue dye in an alkaline solution from the selective chemical reaction between ammonia and Berthelot's reagents (phenol, hypochlorite, and sodium nitroprusside). The toxic phenol and unstable hypochlorite reagents have been replaced by salicylate and dichloroisocyanurate in the modified Berthelot reaction [10]. Moreover, 1-naphthol has been reported to have been used instead of both phenol and nitroprusside in spectrophotometric FIA [11]. Alternatively, a sequential injection gas diffusion system [12] and a paper-based platform with gas diffusion [13] have been reported for the determination of ammonia in waters using membrane separation of ammonia gas generated from the reaction before its detection using acid-base indicators. The disadvantages of these methods with a gas diffusion system were the wetting, clogging, and leakage of the membrane. Various paper-based visual color change gas sensors for ammonia detection [14-17] have also been developed. Consequently, a membraneless gas-separation [18, 19] and a micro-distillation microfluidic paper-based analytical device [4] were developed for ammonia monitoring in waters. These methods use a pervaporation technique where the ammonia gas is converted from ammonium ions, diffused through a headspace, and reacted with an acid-base indicator to overcome clogging problems of the membrane. Because the detection zone does not contact directly with the sample surface, a membrane does not need to be used. Colorimetric assay employing a well microplate with gas pervaporation and diffusion for determination of ammonia in swine farming wastewater by using natural indicator immobilized on paper sensors [20] has been investigated. This method allows microliter-scale solution handling and offers environmentally friendly chemical analysis in which anthocyanins extracted from butterfly pea flower are applied as a natural indicator. Recently, an increased number of studies concerned with the creation of pH indicators based on anthocyanins [21-23] have appeared in the literature. Fruits and vegetables with purple colors, such as red cabbage, are found to contain phenolic compounds called anthocyanins. Anthocyanins have increasingly attracted the attention of researchers because they are natural, water-soluble, and non-toxic pigments, and because they respond to a wide range of pH [24].

In this work, a simple headspace colorimetric assay based on ammonia gas pervaporation in a microwell plate was investigated. Anthocyanins extracted from red cabbage were applied as a natural indicator immobilized on a paper sensor, and calcium hydroxide was used in the original form of powder solid. Ammonium ions present in the water sample were converted to ammonia gas by reaction with calcium hydroxide in the hole of the microwell plate. Ammonia gas then diffused freely through the headspace and reached to react with the anthocyanins-coated paper covering on the reaction hole, resulting in pink-to-blue color change. A flatbed scanner was used to capture the color images of the tested paper.

2. Materials and Methods

2.1 Chemicals and reagents

All chemicals were of analytical grade and all solutions were prepared in deionized water ($\geq$ 18.2 MΩ cm, Millipore Milli-Q). Ammonium chloride and sodium hydroxide were purchased from Loba Chemie (India). Calcium oxide and calcium hydroxide were obtained from Carlo Erba (Canada). Red cabbage was purchased from a local supermarket (Tops, Central Rama II, Bangkok, Thailand).

A stock solution of ammonia (1000 mg N l^{-1}) was prepared from ammonium chloride, and working standard solutions in the range of 1-100 mg N l^{-1} were then prepared daily by stepwise dilution from the stock solution.

An anthocyanins solution (1:1, w:v) as an acid-base indicator was prepared by adding 100 g of chopped red cabbage into 100 ml of deionized water and heated for 30 min, and then the solution was filtered through a filter paper (Whatman No.1).

2.2 Apparatus

Whatman grade 42 filter paper with a diameter of 125 mm was obtained from GE Healthcare UK limited (UK). A 96-microwell plate (Flat bottom shape, Nunc, Denmark) was used throughout the experiments. A CanoScan LiDE210 flatbed scanner (Canon, Thailand) was used for scanning the images of the detection zone on the tested paper.

2.3 Preparation of anthocyanins impregnated paper

A filter paper (Whatman No.42) was cut into 10×10 mm small pieces and immersed in 10 ml of anthocyanins solution (1:1, w:v) contained in a petri dish for 10 min. Then the impregnated paper was taken out from the solution and dried at room temperature. The prepared paper was later used for the headspace colorimetric detection.

2.4 Analytical procedure

2.4.1 Reaction with sodium hydroxide

For the first procedure, sodium hydroxide was tested as a reagent in solution. A syringe was used to inject 0.10 ml of 2 M sodium hydroxide solution into the reaction hole of a 96-microwell plate and into the same reaction hole, 0.10 ml of ammonium chloride standard solution (50 mg N l^{-1}) was introduced by another syringe. The reaction hole was then immediately covered with a piece of anthocyanins impregnated paper that had just been dipped in deionized water. After 20 min, the test paper was scanned on a flatbed scanner (CanoScan LiPE210, Canon), and then an image of the detection zone on the paper was acquired. Image analysis was performed as described in section 2.5. The effect of sodium hydroxide concentration was examined by use of its solutions in the range of 2-10 M.

For the second procedure, sodium hydroxide was tested as a reagent that was coated on paper. The paper coated with sodium hydroxide was prepared as follows. A piece of filter paper (Whatman No.42) was cut into 0.5×0.5 cm pieces, soaked in a petri dish containing 10 ml of sodium hydroxide (8 M) for 10 min, and then dried at 80ºC in an oven for 3 h. A piece of this prepared sodium hydroxide coated paper was placed into the reaction hole of a 96-microwell plate

and 0.10 ml of ammonium chloride standard solution (50 mg N l^{-1}) was next introduced by a syringe. This reaction hole was immediately covered with a piece of anthocyanins impregnated paper that had just been dipped in deionized water. After 20 min, the test paper was scanned and an image of the detection zone was acquired by the flatbed scanner. Image analysis was performed as described in section 2.5.

2.4.2 Reaction with calcium oxide

Each portion of calcium oxide (examined in the range of 0.0150-0.0250 g) was weighed and put into the hole of 96-microwell plate. The prepared paper which was impregnated with anthocyanins was dipped in deionized water. Afterwards, a syringe was used to introduce a volume of ammonium chloride standard solution (examined in the range of 0.10-0.20 ml) into the reaction hole and this hole was immediately covered with a moistened prepared paper that was exposed to the sample headspace. After a period of reaction time (examined in a range of 15-25 min), the test paper was scanned on the flatbed scanner and an image of the detection zone was achieved. Image analysis was performed as described in section 2.5.

2.4.3 Reaction with calcium hydroxide

The procedure followed was very similar to that described in section 2.4.2, except for the fact that calcium hydroxide was examined instead of calcium oxide.

2.4.4 Calibration curve

Each portion of approximately 20 mg of calcium hydroxide was scooped with a small-sized spatula and put into a hole of a 96-microwell plate. Two empty holes were left in-between each added portion, as shown in Figure 1A. The prepared paper that was coated with anthocyanins was moistened with a drop (50 µl) of deionized water. Afterwards, a syringe was used to introduce 0.10 ml of a standard or sample solution into each reaction hole and the hole was immediately covered with the moistened prepared paper that was exposed to the sample headspace. After 20 min of the reaction, the test paper was scanned on the flatbed scanner and an image of the detection zone on the paper was captured. The color images of the detection zone were analyzed as explained in section 2.5.

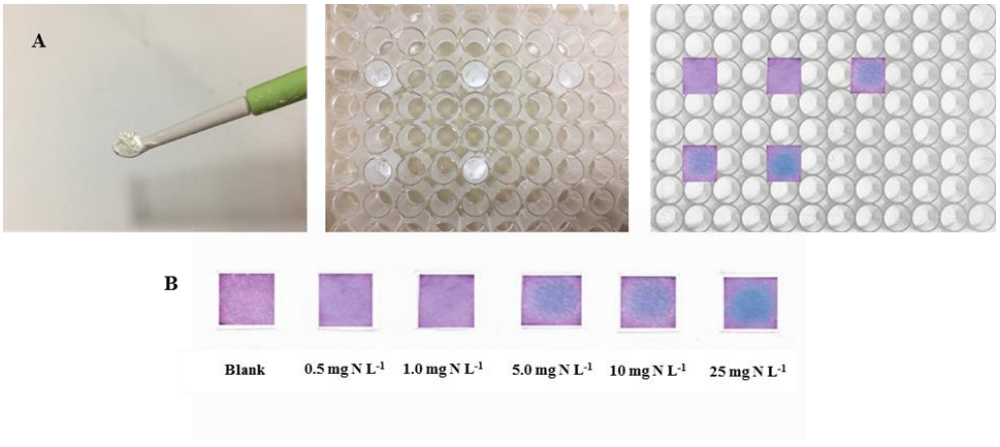

Figure 1. Schematic illustration of the experimental setup (A), and color images of test paper (B)

2.5 Image analysis

Image analysis was performed using ImageJ software (National Institute of Health, USA). The average color intensity was determined within a circular shape (w = 50, h = 50). Red color intensity was chosen as it offered the greatest sensitivity. The intensity values obtained were transformed to pseudo reflectance values: Reflectance = -log (I/I_0), where I refers to the red intensity of the standard or sample, and I_0 refers to the red intensity of the blank (deionized water) [25].

3. Results and Discussion

In this experiment, the reaction involves the generation of ammonia gas by alkalinization of the sample solution. The generated ammonia diffuses into the headspace to react with anthocyanins on the prepared paper sensor covering the top of the reaction hole. The natural dye anthocyanins from red cabbage were extracted into deionized water, which is non-toxic to the environment and thus considered a green solvent. The major structures of anthocyanins in red cabbage are based on a core structure of cyanidin-3-O-diglucoside-5-O-glycoside [24]. Red cabbage's anthocyanins in solution change from red to blue when brought into contact with ammonia gas. The 96-microwell plate was selected as a tool for this application as it is a very simple apparatus normally found in the laboratory and because ammonia gas generation and pervaporation could possibly be controlled within the reaction hole, which has the small volume of 0.36 ml.

3.1 Reaction with sodium hydroxide

First, a sodium hydroxide solution was selected to be used as a reagent for alkalinizing the sample solutions. The effect of sodium hydroxide concentration was examined in the range of 2-10 M. The procedure was as follows. A portion of 0.10 ml of sodium hydroxide solution was injected into a reaction hole, followed by the addition of 0.10 ml of ammonium chloride standard solution (50 mg N l^{-1}). A piece of the prepared paper impregnated with anthocyanins was then immediately placed over the reaction hole. It can be observed from Figure 2A that higher concentrations of sodium hydroxide provided higher reflectance values. To provide more convenience, the system was modified by using a filter paper coated with sodium hydroxide instead of using sodium hydroxide solution. The paper coated with sodium hydroxide was prepared by soaking a small piece of filter paper (0.5 cm x 0.5 cm) in sodium hydroxide solution (8 M) for 10 min and then drying at 80^{o}C in an oven for 3 h. As can be seen in Figure 2B, a higher reflectance value was obtained when sodium hydroxide was coated on the filter paper. This may be a result of increased surface area for the reaction. However, the prepared paper coated with sodium hydroxide seemed to absorb more moisture when contacting the air. This may be a disadvantage in actual use.

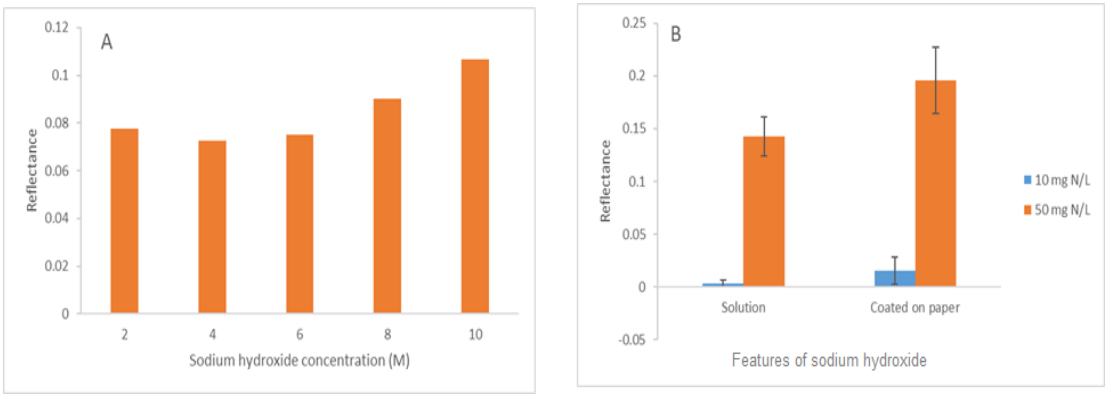

Figure 2. Optimization of reaction with sodium hydroxide: The effect of sodium hydroxide concentration (A), and a comparison of the effect of sodium hydroxide used in solution and coated on paper (B)

3.2 Reaction with calcium oxide

To solve the problem of too much moisture absorbed on the sodium hydroxide coated paper, sodium hydroxide was replaced with calcium oxide in its powdered form, that is without coating it on the filter paper. The experiment was then carried out with the same steps as described above, except for the fact that powdered calcium oxide was used instead of the prepared paper coated with sodium hydroxide. The effect of calcium oxide content, ammonium chloride solution volume, and reaction time were investigated to reach the maximum sensitivity.

Calcium oxide amount was optimized in the range of 0.0150-0.0250 g. From Figure 3A, it can be seen that the signal increased with increasing calcium oxide amount up to 0.0200 g and then slightly decreased at higher calcium oxide amount. When calcium oxide amounts were applied at 0.0150 g and 0.0200 g, the added ammonium chloride solution was able to contact all the powdered calcium oxide and make a thorough reaction. Excessive use of calcium oxide (0.0250 g) caused a thick layer of solid powder to form at the bottom of the reaction hole, and the added ammonium chloride solution was evidently able to contact and react with calcium oxide on the surface of the solid layer. This contact surface was less than that which was available when calcium oxide was applied at 0.0150 g and 0.0200 g, and thus less ammonia gas was generated. Based on the obtained data, a calcium oxide content of 0.0200 g was selected for further experiments.

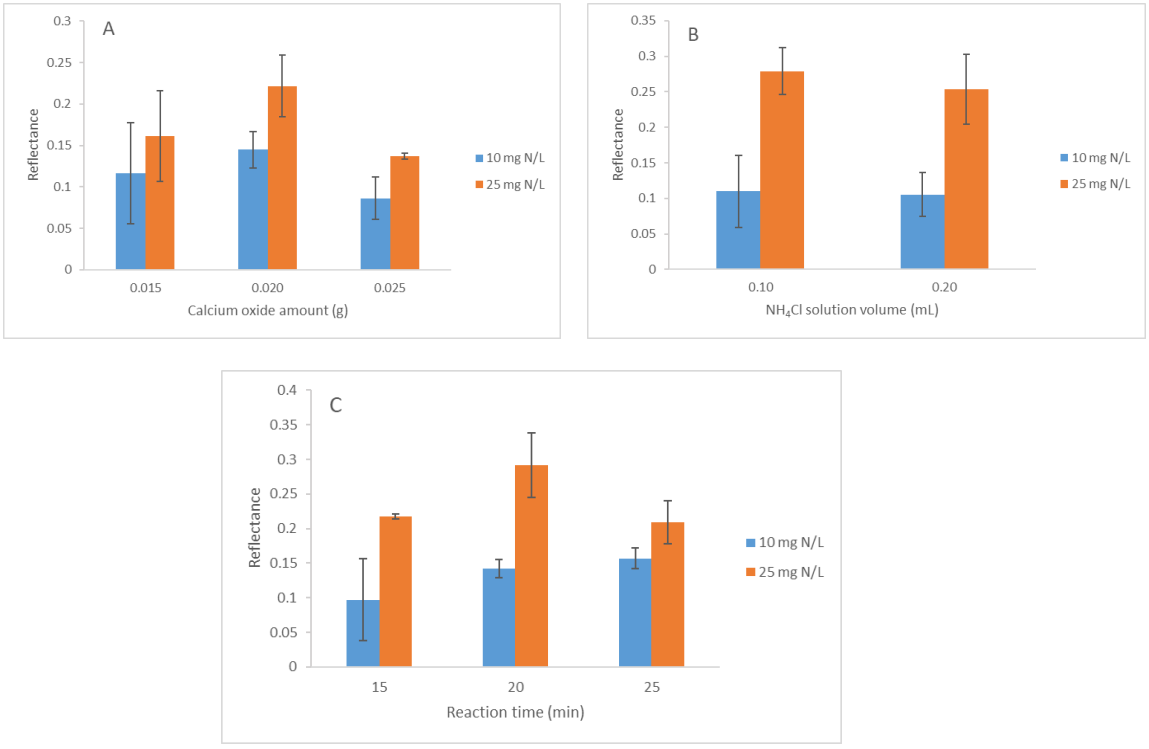

Figure 3. Optimization of reaction with calcium oxide: The effect of calcium oxide amount (A), ammonium chloride solution volume (B), and reaction time (C)

To study the effect of ammonium chloride solution volume on method sensitivity, ammonium chloride standard solution with the volume of 0.10 or 0.20 ml was injected via a syringe into the reaction hole where calcium oxide was initially placed. As can be seen in Figure 3B, the reflectance values were similar when the volume of ammonium chloride solution was either 0.10 or 0.20 ml. When ammonium chloride solution volume was applied at 0.20 ml, the initial volume introduced into the reaction hole was able to mix thoroughly with the presence of calcium oxide, but the volume that was introduced later in the addition caused such a high level of the solution in the reaction hole that some of ammonium chloride at the top could hardly react with calcium oxide. Therefore, some of ammonium chloride was not converted to ammonia gas. Moreover, ammonia gas is highly soluble in water, and this means that the loss of ammonia gas depends on the solution volume. Consequently, an ammonium chloride solution volume of 0.10 ml was selected for further experiments to save the solution and reduce the generated waste.

The effect of reaction time was studied from 15 to 25 min. The initial reaction time was recorded when the moistened anthocyanins coated paper was placed on top of the reaction hole. From Figure 3C, the signal increased with increasing reaction time from 15 min to 20 min and then tended to slightly decrease when the reaction time was 25 min. As a result, 20 min was selected as the optimum reaction time for color development. The decrease in the signal values at longer times was possibly due to the drying up of the anthocyanins coated paper.

The comparison of using sodium hydroxide and calcium oxide as a reagent is shown in Figure 4. The sensitivity was maximum when calcium oxide was used in the form of a powder, while sodium hydroxide that was used as a solution or coated on the filter paper resulted in less sensitivity. For sodium hydroxide used as a solution, the higher concentration caused the higher density. Because of the large difference of density between sodium hydroxide solution and ammonium chloride solution, the injected ammonium chloride solution hardly mixed with the dense under-layer of sodium hydroxide solution and subsequently less ammonia gas was generated. Moreover, when sodium hydroxide coated onto filter paper was used, the sensitivity slightly improved. The disadvantage of using this feature was that sodium hydroxide readily absorbs water. In a later experiment, sodium hydroxide was replaced by calcium oxide in powder form, and better sensitivity was obtained. Even though calcium oxide was less soluble than sodium hydroxide, for the reaction with ammonium chloride solution in this experiment, the use of a little amount of powder calcium oxide resulted in more thorough mixing than did the use of a high-density solution of sodium hydroxide.

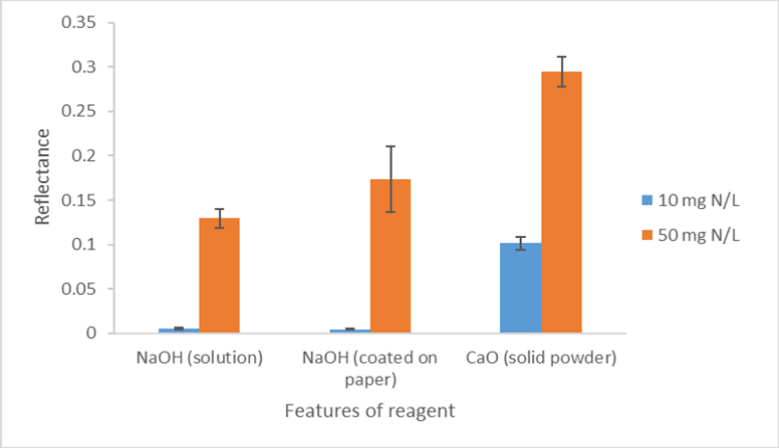

Figure 4. The signal comparison of using sodium hydroxide and calcium oxide as a reagent

3.3 Reaction with calcium hydroxide

Although the use of powdered calcium oxide can help the experiment to proceed more easily, calcium oxide is relatively expensive, so replacing it with calcium hydroxide, which is cheaper, seems to be a good choice. The same procedure as used for the reaction with calcium oxide was conducted except for the point that calcium oxide was replaced by powdered calcium hydroxide. To reach the maximum sensitivity, the influence of calcium hydroxide content, ammonium chloride solution volume, reaction time, and anthocyanins concentration was studied. In all experiments with calcium hydroxide, a portion of 0.10 ml of ammonium chloride standard solution, either at the concentration level of 10 or 25 mg N l^{-1} was used.

The effect of the reagent amount was studied by varying the amount of powdered calcium hydroxide from 0.0150 to 0.0250 g. As can be seen in Figure 5A, the maximum response was obtained when the amount of calcium hydroxide was 0.0200 g. A higher amount of calcium hydroxide (0.0250 g) gave a solid layer at the bottom of the reaction hole, which limited the surface area available to come into contact with ammonium chloride solution, and therefore the production of ammonia gas decreased. For this reason, powdered calcium hydroxide at the amount

of 0.0200 g was selected for further experiments. The ammonium chloride solution volume was investigated by applying various amounts of ammonium chloride standard solution. From Figure 5B, the signal increased with decreasing ammonium chloride solution volume from 0.14 ml to 0.10 ml. Increasing the volume of ammonium chloride solution gave a higher solution level in the reaction hole, making it difficult for the solution injected later to react with calcium oxide. Also, the generated ammonia gas dissolved more into the solution with higher volume. Consequently, an ammonium chloride solution volume of 0.10 ml was selected as the optimum volume. The effect of reaction time was also studied from 15 to 25 min. Considering the data in Figure 5C, 20 min was the optimal reaction time for the test paper to reach the maximum color intensity, and a paler color intensity was observed after longer reaction time because of excessive drying up of the test paper. As a result, 20 min was selected as the optimum reaction time. These three parameters, calcium hydroxide amount, solution volume, and reaction time, provided the same trends as in the reaction with calcium oxide.

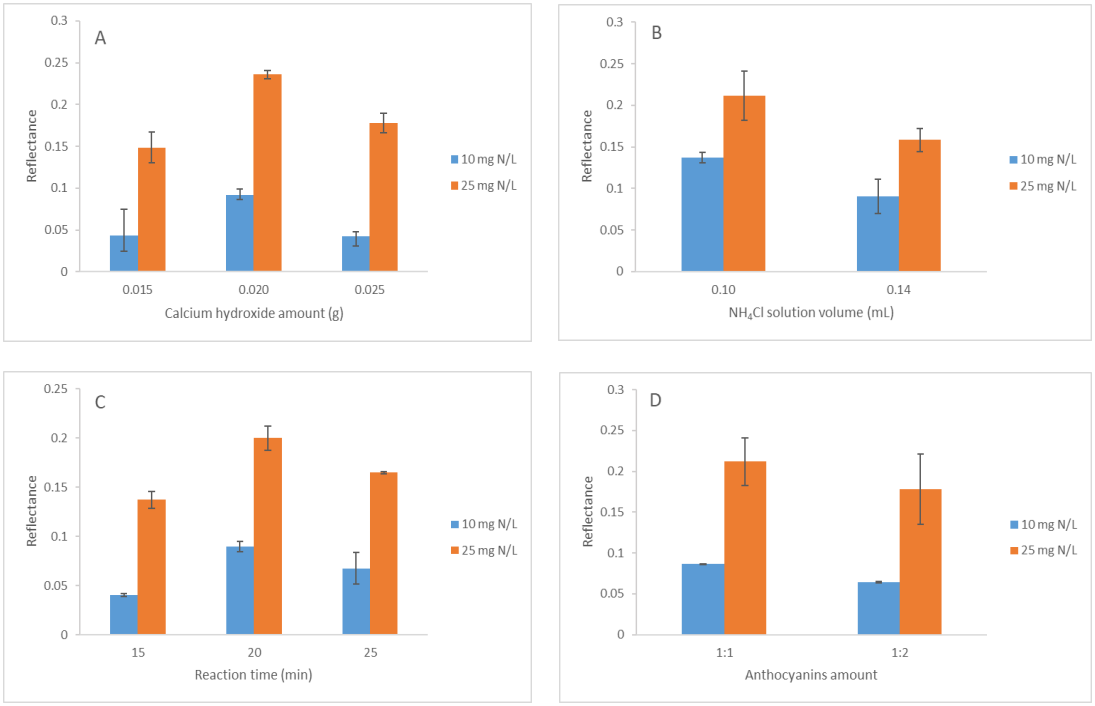

Figure 5. Optimization of reaction with calcium hydroxide: The effect of calcium hydroxide amount (A), ammonium chloride solution volume (B), reaction time (C), and anthocyanins amount (D)

To study the effect of anthocyanin amount on method sensitivity, prepared paper impregnated with anthocyanins that had been extracted from red cabbage in the w:v ratio of 1:1 and 1:2 was examined. As shown in Figure 5D, a higher signal was obtained when anthocyanins extracted with a ratio of 1:1 (w:v) was applied to the paper. Anthocyanins are water-soluble pigments; however, increased deionized water at 1:2 (w:v) makes the extract too dilute. Therefore, extracted anthocyanins in deionized water at the ratio of 1:1 (w/v) were selected for further experiments.

Various conditions of use of the prepared paper impregnated with anthocyanins for the detection process were examined to reach the maximum sensitivity. These conditions included (1) immediate use of the paper after soaking in extracted anthocyanins for 10 min, (2) use after drying the anthocyanins coated paper overnight, (3) use after dropping deionized water [(a) 10 µl and (b) 50 µl] on the dried anthocyanins coated paper, and (4) use after soaking the dried anthocyanins coated paper in deionized water before placing on top of the reaction hole. According to the results shown in Figure 6, the use of dried anthocyanins coated paper with a drop of deionized water (50 µl) resulted in the best sensitivity. When condition (1) and condition (2) were compared, the decrease in the reflectance values was probably due to the drying up of the anthocyanins coated paper. When the prepared paper that had been dried overnight was used, the lowest sensitivity was detected. To improve the sensitivity, deionized water was added on the dried paper before it was placed on the reaction hole. Reflectance values increased when the volume of deionized water was increased from 10 to 50 µl. Even though a higher volume of deionized water (50 µl) would seem to make more dilution, it appears that at this optimized reaction time (20 min), the test paper with a lower volume of deionized water (10 µl) dried more quickly and thus produced a paler color. Immersing the dried anthocyanins coated paper in deionized water caused dissolution of the anthocyanins from the coated paper, so the reflectance value decreased due to the dilution effect. As a result, the dried anthocyanins coated paper with a drop of deionized water (50 µl) was selected as the optimum condition of use.

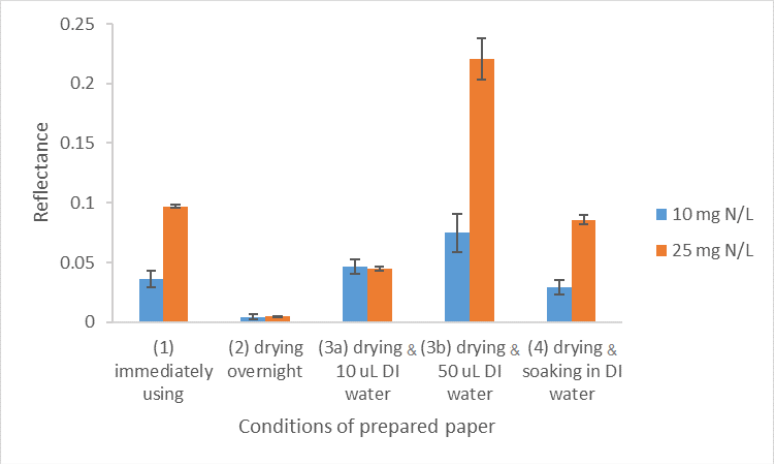

Figure 6. A comparison of signal strength resulting from various conditions of use of prepared paper impregnated with anthocyanins

3.4 Method validation and analytical performance

A validation of the method involving the reaction with calcium hydroxide was conducted, and its analytical characteristics such as the linear range, the limit of detection (LOD), the limit of quantification (LOQ), precision, and recovery were observed when the optimum conditions were applied. The method linearity was explored using various concentrations of ammonium chloride standard solutions. The developed method showed a linear dynamic range of 1.0-25.0 mg N l^{-1} by a calibration curve's equation y = 0.0082x - 0.0086 with the determination coefficients (R^2) of 0.9999 as shown in Figure 7. The LOD and the LOQ of this proposed method defined as $3(SD)_{blank}$ and $10(SD)_{blank}$ divided by the slope of the linear equation were 0.29 and 0.98 mg N l^{-1},

respectively. This sensitivity of detection may be enhanced if the anthocyanins impregnated paper is fabricated by use of a hydrophobic barrier to match the diameter of well and then a controllable color change area established for higher color intensity. The precision of the method was measured by performing replicate experiments (n = 11) of the standard solution at a concentration of 10 mg N l^{-1} and the result was reported by a relative standard deviation of 4.2%. The effect of inter bathes of extracted anthocyanins was also examined by constructing inter-calibration curves and analysis of ammonium chloride standard solution (10 mg N l^{-1}) and the results were presented in Table 1. The precision of the standard solution analysis was reported with %RSD in the range of 5.8-8.0. As extracted anthocyanins from red cabbage may vary from batch to batch, the construction of the calibration curve and analysis of samples should be performed using anthocyanins impregnated paper prepared from the same batch of red cabbage.

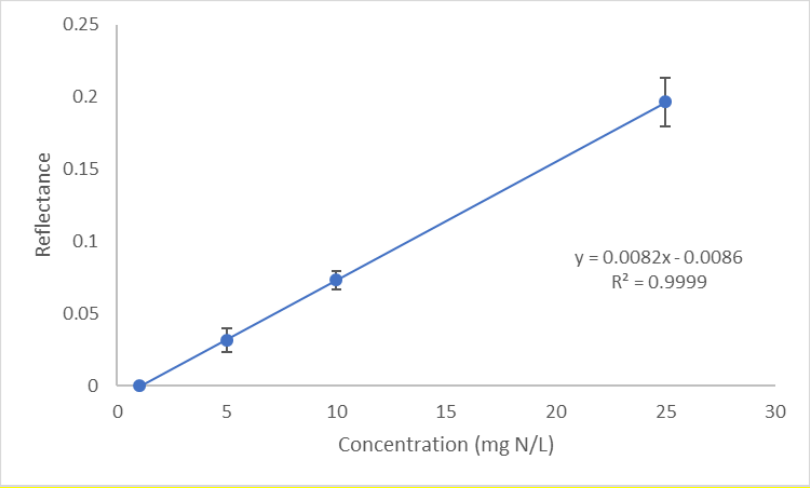

Figure 7. Calibration curve of ammonium chloride (1.0-25.0 mg N l^{-1})

Table 1. The effect of inter bathes of extracted anthocyanins

No.	Calibration curve	R^2	Measured amount[a] (mg N l^{-1})	
			$\bar{x}^b \pm SD$	%RSD
1	y = 0.0076x-0.0013	0.9997	10.1±0.7	7.4
2	y = 0.0083x-0.0067	0.9997	10.2±0.8	8.0
3	y = 0.0079x+0.0019	0.9984	10.0±0.6	5.9
4	y = 0.0086x-0.0049	0.9938	10.1±0.6	5.8

[a]Standard solution (10 mg N l^{-1})
[b]n = 3

The proposed method was applied to determine ammonia in three water samples collected weekly from five sources: agricultural-supplied lagoons A and B (Bang Khun Thian, Bangkok), a canal (Prawet Burirom canal, Ladkrabang, Bangkok), and ponds A and B (Pratep Building Complex, King Mongkut's Institute of Technology Ladkrabang (KMITL), Bangkok). Recoveries were carried out to examine the matrix effect on the analysis of ammonia by the developed method. As reported in Table 2, satisfactory recoveries were found in the range of 89.6-110.5% with good RSDs between 1.7% and 9.8%. As the color change developed on anthocyanins coated paper that covered over the reaction hole and the gas species could only diffuse through headspace and reach the detection paper, possible interferences caused by non-volatile matrices in

the sample were also eliminated. According to prior studies, the only interfering compound is methylamine [26]. Its interference is negligible because it is usually present at μg l^{-1} levels in surface waters [13, 27].

Table 2. Determination of ammonia in water samples

Water samples	Measured amount (mg N l^{-1})		Added amount (mg N l^{-1})	Spiking recovery (%)	RSD[a] (%)
	Developed method	Standard method			
Agricultural supplied lagoon A (Week 1)	4.53±0.16	3.75±0.21	5.00	105.4	1.7
			10.0	89.8	8.1
Agricultural supplied lagoon A (Week 2)	4.64±0.36	5.23±0.13	1.00	92.9	7.6
			10.0	89.6	5.0
Agricultural supplied lagoon B (Week 1)	1.73±0.15	1.10±0.04	1.00	91.8	7.4
			10.0	91.4	3.5
Agricultural supplied lagoon B (Week 2)	2.32±0.08	2.40±0.11	1.00	99.2	8.0
			5.00	96.6	7.7
Canal (Week 1)	8.42±0.34	8.85±0.18	5.00	92.9	2.4
			10.0	98.1	6.9
Canal (Week 2)	8.63±0.28	9.43±0.24	5.00	92.9	5.5
			10.0	91.2	4.3
Canal (Week 3)	4.68±0.50	6.39±0.27	5.00	106.7	9.2
			10.0	95.2	4.1
Pond A (Week 1)	ND[b]	ND	5.00	110.5	6.5
			10.0	107.0	6.5
Pond A (Week 2)	ND	ND	5.00	93.3	7.7
			10.0	92.4	2.3
Pond B (Week 1)	ND	ND	1.00	98.9	9.8
			10.0	103.2	5.1

[a]Relative standard deviation (n = 3)
[b]Not detected

The accuracy of the developed method was further examined using the standard method (4500- NH_3 F. Phenate Method) for ammonia determination in water [9]. This standard method is based on the spectrophotometric measurement of the blue compound indophenol, which is formed by the reaction of ammonia, hypochlorite, and phenol and is catalyzed by sodium nitroprusside. The water samples were filtered before the analysis by the spectrophotometric standard method, whereas the original unfiltered samples were analyzed by the developed method. A paired *t*-test was applied to statistically compare the results obtained by the two methods. The calculated *t*-value was 0.97, while the critical *t*-value was 2.45 (at $p = 0.05$ for a two-tailed test). No significant difference was observed between the two methods.

4. Conclusions

A headspace colorimetric method based on the combination of pervaporation and paper-based sensor was designed to monitor total ammonia in water samples. The most suitable condition selected was reaction with calcium hydroxide. Ammonia gas was generated when 0.10 ml of standard solution or water sample was placed to react with 0.0200 g of calcium hydroxide powder

in the reaction hole of 96-microwell plate that was immediately covered with a moistened anthocyanins impregnated paper for the reaction time of 20 min. A flatbed scanner was used to scan the test paper for color images of the detection zone and ImageJ was applied to evaluate the color intensity. The proposed method was simple and cost-effective because no complicated and expensive apparatus was used. Besides, the method used calcium hydroxide in a powder form, which was more stable than the solution form. Using the powder form also saved analysis time as the solution preparation process was not necessary. Moreover, red cabbage is a source of natural anthocyanins that can be extracted into deionized water. Water is inexpensive and the most environmentally friendly solvent that can be used for separation processes. This simple and green method with adequate analytical performance can be successfully applied in the analysis of total ammonia in water samples.

References

[1] Ghaly, A.E. and Ramakrishnan, V.V., 2015. Nitrogen sources and cycling in the ecosystem and its role in air, water and soil pollution: a critical review. *Journal of Pollution Effects & Control*, 3(2), 136.

[2] Tegeder, M. and Masclaux-Daubresse, C., 2018. Source and sink mechanisms of nitrogen transport and use. *New Phytologist*, 217, 35-53.

[3] Huff, L., Delos, C., Gallagher, K. and Beaman, J., 2013. *Aquatic Life Ambient Water Quality Criteria for Ammonia-Freshwater*. Washington DC: U.S. Environmental Protection Agency.

[4] Peters, J.J., Almeida, M.I.G.S., Šraj, L.O.C., McKelvie, I.D. and Kolev, S.D., 2019. Development of a micro-distillation microfluidic paper-based analytical device as a screening tool for total ammonia monitoring in freshwaters. *Analytica Chimica Acta*, 1079, 120-128.

[5] World Health Organization, 2003. *Ammonia in Drinking-Water: Background Document for Development of WHO Guidelines for Drinking-water Quality*. Geneva : World Health Organization.

[6] Cheng, Y., Feng, Q., Yin, M., Wang, C. and Zhou, Y., 2016. A fluorescence and colorimetric ammonia sensor based on a Cu(II)-2,7-bis(1-imidazole)fluorene metal-organic gel. *Tetrahedron Letters*, 57, 3814-3818.

[7] Duan, X., Fang, J. and Sun, R., 2017. Determination of ammonium in aqueous samples by gas phase light scattering using hydrogen chloride gas as a derivatizing reagent followed by nondispersive atomic fluorescence spectrometry. *Analytical Sciences*, 33, 153-157.

[8] Amirjani, A. and Fatmehsari, D.H., 2018. Colorimetric detection of ammonia using smartphones based on localized surface plasmon resonance of silver nanoparticles. *Talanta*, 176, 242-246.

[9] Eaton, A.D., Clesceri, L.S., Greenberg, A.E. and Franson, M.A.H., 1998. *Standrad Methods for the Examination of Water and Wastewater: 4500-NH_3 Nitrogen (Ammonia)*. 20th ed., Washington DC : American Public Health Association, American Water Works Association, Water Environment Federation.

[10] Krom, M.D., 1980. Spectrometric determination of ammonia: a study of a modified Berthelot reaction using salicylate and dichloroisocyanurate. *Analyst*, 105, 305-316.

[11] Shoji, T. and Nakamura, E., 2009. Flow injection analysis with spectrophotometry for ammonium ion with 1-naphthol and dichloroisocyanurate. *Journal of Flow Injection Analysis*, 26(1), 37-41.

[12] Segundo, R.A., Mesquita, R.B.R., Ferreira, M.T.S.O.B., Teixeira, C.F.C.P., Bordalo, A.A. and Rangel, A.O.S.S., 2011. Development of a sequential injection gas diffusion system for

the determination of ammonium in transitional and coastal waters. *Analytical Methods*, 3(9), 2049-2055.

[13] Jayawardane, B.M., McKelvie, I.D. and Kolev, S.D., 2015. Development of a gas-diffusion microfluidic paper-based analytical device (μPAD) for determination of ammonia in wastewater samples. *Analytical Chemistry*, 87, 4621-4626.

[14] Chen, Y., Zilberman, Y., Mostafalu, P. and Sonkusale, S.R., 2015. Paper based platform for colorimetric sensing of dissolved NH_3 and CO_2. *Biosensors and Bioelectronics*, 67, 477-484.

[15] Hakovirta, M., Aksoy, B., and Hakovirta, J., 2015. Self-assembled micro-structured sensors for food safety in paper based food packaging. *Materials Science and Engineering: C*, 53, 331-335.

[16] Maity, A. and Ghosh, B., 2018. Fast response paper based visual color change gas sensor for efficient ammonia detection at room temperature. *Scientific Reports*, 8, 16851.

[17] Cho, Y.B., Jeong, S.H., Chun, H. and Kim, Y.S., 2018. Selective colorimetric detection of dissolved ammonia in water via modified Berthelot's reaction on porous paper. *Sensors and Actuators B: Chemical*, 256, 167-175.

[18] Phansi, P., Sumantakul, S., Wongpakdee, T., Fukana, N., Ratanawimarnwong, N., Sitanurak, J. and Nacapricha, D., 2016. Membraneless gas-separation microfluidic paper-based analytical devices for direct quantitation of volatile and nonvolatile compounds. *Analytical Chemistry*, 88, 8749-8756.

[19] Almeida, M.I.G.S., Jayawardane, B.M., Kolev, S.D. and McKelvie, I.D., 2018. Developments of microfluidic paper-based analytical devices (μPADs) for water analysis: A review. *Talanta*, 177, 176-190.

[20] Jaikang, P., Paengnakorn, P. and Grudpan, K., 2020. Simple colorimetric ammonium assay employing well microplate with gas pervaporation and diffusion for natural indicator immobilized paper sensor via smartphone detection. *Microchemical Journal*, 152, 104283.

[21] Zhai, X., Shi, J., Zou, X., Wang, S., Jiang, C., Zhang, J., Huang, X., Zhang, W. and Holmes, M., 2017. Novel colorimetric films based on starch/polyvinyl alcohol incorporated with roselle anthocyanins for fish freshness monitoring. *Food Hydrocolloids*, 69, 308-317.

[22] Huang, S., Xiong, Y., Zou, Y., Dong, Q., Ding, F., Liu, X. and Li, H., 2019. A novel colorimetric indicator based on agar incorporated with *Arnebia euchroma* root extracts for monitoring fish freshness. *Food Hydrocolloids*, 90, 198-205.

[23] Zhang, J., Zou, X., Zhai, X., Huang, X.W., Jiang, C. and Holmes, M., 2019. Preparation of an intelligent pH film based on biodegradable polymers and roselle anthocyanins for monitoring pork freshness. *Food Chemistry*, 272, 306-312.

[24] Gachovska, T., Cassada, D., Subbiah, J., Hanna, M., Thippareddi, H. and Snow, D., 2010. Enhanced anthocyanin extraction from red cabbage using pulsed electric field processing. *Journal of Food Science*, 75(6), E323-E329.

[25] Birch, N.C. and Stickle, D.F., 2003. Example of use of a desktop scanner for data acquisition in a colorimetric assay. *Clinica Chimica Acta*, 333, 95-96.

[26] Oms, M.T., Cerdà, A., Cladera, A., Cerdà, V. and Forteza, R., 1996. Gas diffusion techniques coupled sequential injection analysis for selective determination of ammonium. *Analytica Chimica Acta*, 318, 251-260.

[27] Poste, A.E., Grung, M. and Wright, R.F., 2014. Amines and amine-related compounds in surface waters: a review of sources, concentrations and aquatic toxicity. *Science of the Total Environment*, 481, 274-279.

Current Applied Science and Technology Vol. 20 No. 3 (September-December 2020)

Assessment of Some Biochemical Parameters and Dielectric Relaxations in *β*-Thalassemic Children

Yasser Khedr[1]*, Metwally Kotb[2], Samir Abd El-Karem[3] and Omar El-Bayady[4]

[1]Physics Department, Faculty of Science, Damanhur University, Damanhour, Egypt
[2]Medical Biophysics Department, Medical Research Institute, Alexandria University, Alexandria, Egypt
[3]Applied Medical Chemistry Department, Medical Research Institute, Alexandria University, Alexandria, Egypt
[4]Medical Lab, Zagazig University Hospital, Zagazig University, Zagazig, Egypt

Received: 12 March 2020, Revised: 4 May 2020, Accepted: 29 May 2020

Abstract

Thalassemias are considered as a group of inherited disturbances or blood disorders characterized by the formation of abnormal hemoglobin. *β*-thalassemia is the most familiar type of thalassemia worldwide and in Egypt. *β* -thalassemia is classified into three types; minor, intermediate and major. Thalassemia minor resembles anemia with mild iron-deficiency, whilst Thalassemia major is the most severe; patients with the major form need regular blood transfusion stay alive. Patients with the intermediate form show mild to moderate anemia and do not need regular blood transfusion therapy. Therefore, it was thought to be of value to compare the three types on the bases of various biochemical parameters and dielectric properties of blood in the frequency range up to 5 MHz. Sixty children with *β*-thalassemia were involved in the research. They were divided into three equal groups, according to their thalassemia type, in addition to the same group of control. All children were subjected to thorough clinical examination, and the following blood analyses were performed: hemoglobin electrophoresis, complete blood picture "CBC", serum ferritin and creatinine, several vital enzymes, total/direct bilirubin, albumin, and other dielectric parameters. Significant differences were found between thalassemia blood and the control, especially in the case of thalassemia major blood. Dielectric relaxations were also detected in thalassemia blood, indicating possible changes in the RBC membranes of thalassemia blood due to possible variations of the surface charges on the RBC membranes and the reduction of glycophorin sialic acid content. Therefore, the present work reveals significant variations between the biochemical and dielectric properties of the three types of thalassemia blood and control blood, and these differences may be of value in the treatment of thalassemia in children.

Keywords: *β*-thalassemia, antioxidant, CBC, liver enzyme, dielectric, relaxations
DOI 10.14456/cast.2020.26

*Corresponding author: Tel.: (+2) 01 22 67 48 32 6
E-mail: yasserkhedr2001@yahoo.com

1. Introduction

According to Rund and Rachmilewitz [1], thalassemias are a group of inherited disturbances or blood disorders characterized by the formation of abnormal hemoglobin. Disorders of globin constraints (α) or (β) lead to rupture and erythrocyte damage [2]. Deficiency or reduced synthesis in α-globin constraints gives rise to α-thalassemia. β-thalassemia is the most familiar type of thalassemia. It is characterized by decreased synthesis and production of normal adult hemoglobin (HbA), the prevailing type of hemoglobin found in the blood from shortly after birth until death. β-thalassemia is the most common type with 3.5 to ≥ 9% and a gene frequency of 0.03% [3]. The annual total occurrence of symptoms of thalassemia is 1:100 individual population and 1:10,000 individual population in the European countries [4]. In the worldwide population, about 5% has a globin alternative, with only about 1.7% having the α- or β-thalassemia signs, whereas about 4.4 of every ten thousand of live children are affected. Previous research indicates that in Egypt, it was estimated that 1,000:1.5 million live babies born per year would catch thalassemia disease. Galanello and Origa [3] suggested the following classifications of β-thalassemia: thalassemia minor, thalassemia intermedia, and thalassemia major. A thalassemia minor individual is said to be heterozygous because they have as only one of the β-thalassemia gene copies, with one normal gene of the β-chain. Thalassemia minor resembles anemia with mild iron-deficiency, so people who fall into this category do not need treatment. A patient with thalassemia major, on the other hand, is said to be homozygous for β-thalassemia as they have two genes for β-thalassemia and no normal β-chain gene. Accordingly, the individual with thalassemia major is an ill person. A new-born baby with this major type appears completely normal because their hemoglobin at birth is fetal hemoglobin (HbF) that contains two α-chains, similar to HbA, and two γ-chains unlike HbA. Within the first month following birth, anemia however becomes fatal. The baby becomes unable to grow healthily because normal hemoglobin gets replaced by defective hemoglobin and hemolytic anemia results. It is because of this condition that primary thalassemia patients need regular blood transfusions to stay alive and maintain a quality of life. Thalassemia intermedia, on the other hand, shows mild to moderate anemia without the need for regular blood transfusion therapy [4-6]. To bear in mind the items described above will be of value when comparing the biophysical and biochemical parameters and oxidative stress that may be present in some children suffering from the three types of β-thalassemia. Moreover it will be useful when studying the dielectric characteristics of the blood of children in each category as compared to those characteristics of the blood of the children who are controls.

2. Materials and Methods

2.1 The grouping of children with β-thalassemia

Sixty children with β-thalassemia were involved in the study. They were divided into three equal groups; the first group had thalassemia minor, the second group had thalassemia intermedia, and the third group had thalassemia major, in addition to the same group of control. All participants were of the same socio-economic standard. They lived in similar living conditions and had similar dietary habits. All children were first subjected to a thorough clinical examination. Venous blood samples (5 ml) were collected from each subject's antecubital vein under aseptic conditions into two different tubes; a) an EDTA containing tube for dielectric measurement and CBC (automated measurement), and b) an empty tube that was immediately centrifuged at 5000 rpm to obtain serum. The serum of each sample was then frozen at -80°C until further analysis. Blood samples were also obtained from healthy volunteers who served as controls and the control subjects' blood was treated identically.

The blood from each subject was taken by qualified people who performed the following analyses: Haemoglobin Electrophoresis using full automated capillary electrophoresis [7], complete blood picture "CBC" [8], serum ferritin [9], serum creatinine [10], alanine aminotransferase, aspartate aminotransferase, alkaline phosphatase [11], Glutathione-S-Transferase (GST) [12], Total Antioxidant Capacity (TAC) [13], Catalase Assay (CAT) [14], Superoxide Dismutase (SOD), Glutathione Reductase (GR) [15], Glutathione peroxidase (GPx), Gamma-Glutamyl transferase (GGT) [12], Lipid Peroxide (Malondialdehyde; MDA) [16], total/direct bilirubin, and serum albumin [10]. Furthermore, the degree of oxidative stress was assessed by determining total antioxidant activity (Biodiagnostic, Egypt). The principle of this method depends on the reaction of antioxidants in the sample with a defined amount of exogenously provided H_2O_2. The antioxidants in the serum blood sample eliminate a certain amount of the added hydrogen peroxide. The residual H_2O_2 is determined calorimetrically by an enzymatic reaction involving the conversion of the exogenously added 3,5, dichloro-2-hydroxyl benzenesulphonate to a pink-colored product. The absorbance of each sample was read at 505 nm against a blank in which the serum blood sample was replaced with distilled water. In each sample, the total antioxidant concentration was calculated according to the following equation:

$$\text{Total antioxidant concentration (mM/l)} = (\text{Abs of blank-Abs of sample}) \times 3.33 \quad (1)$$

The level of malondialdehyde (MDA) as a measure of lipid peroxidation was also determined by a ready-for-use colorimetric kit (Biodiagnostic, Egypt).

2.2 Dielectric relaxation measurements for the blood

A home-made electric cell takes the shape of a parallel-plate capacitor made of silver containing the sample material (plate distance 1 cm and plate area 0.0001 m^2). The electrodes were connected to an LCR meter (Model Hioki, 3532-50 LCR HiTESTER),which measures the capacitance and resistance with accuracy ± 0.05%, over a frequency range from 42Hz-5MHz.

Capacitance C, and conductance G, were used to calculate the relative permittivity, real (ε') and imaginary (ε") and real conductivity (σ') of RBCs, using the following equations [17].

$$C = \varepsilon' \varepsilon_0 A/d \quad (2)$$

$$G = \sigma A/d \quad (3)$$

Where, C (Farad) and R (Ohm), are the capacitance and resistance of the capacitor between the two measuring electrodes, A (m^2) is the surface area of the electrode, d (m) -the separation distance between the two electrodes, ε'-the relative permittivity (Farad/meter), ε0-the permittivity of vacuum (8.85×10^{-12} F/m), and σ is the electrical conductivity (Siemens/m).The imaginary parts of complex permittivity ε″ and conductivity σ″ were calculated according to the relation [18, 19].

$$\varepsilon'' = (\sigma - \sigma_L)/2\pi f \varepsilon_0 \quad (4)$$

Where σL is the low-frequency limiting conductivity taken at 42 Hz, and εh is the high frequency limiting permittivity taken at 5 MHz.

2.3 Statistical analysis

All values are presented as the mean ± standard deviation (±SD) and were analyzed by the Statistical Package for Social Science (SPSS) version 17. A paired t-test was used to compare two mean parameter values for the same element and the level of significance was set at a P-value of 0.05 or less. All individuals were subjected to full clinical examination and did not show clinical symptoms

or signs of any other problems except thalassemia**.** The study protocol was revised and ethically approved by the Zagazig University Hospital, Zagazig University, Egypt.

3. Results and Discussion

3.1 Variation of hemoglobin (Hb), red blood cells (RBCs) and white blood cells (WBCs)

The results of this study revealed that with respect to the types of hemoglobin that existed in the blood of the control group and thalassemia groups, it is clear that fetal hemoglobin was absent in both the control group and the thalassemia minor group, and was significantly higher in both the thalassemia intermedia and thalassemia major groups. Both Hemoglobin (Hb) and Hemoglobin A (HbA) decreased from the thalassemia minor to thalassemia major groups, while HbA2 increased significantly from T-Minor to TM. All the hemoglobin variations are illustrated in Table 1.

Table 1. Variation of the different hemoglobin in thalassemia groups and control

Type of Hb	Statistic	Groups: n = 20			
		Control	T-Minor	TI	TM
Hb F **%**	Range	00	0.2-1.7	7.9-40	46-95
	Mean±SD	00±00	1.08±0.57*	23.78±9.98*	66.51±15.89*
Hb A **%**	Range	97.6-99.1	92.9-97.3	55-89	0-50
	Mean±SD	98.4±0.47	95.17±1.88*	72.99±10.13*	28.77±15.65*
Hb A2 **%**	Range	0.9-2.4	2.5-6.4	1-7.8	2.1-16
	Mean±SD	1.6±0.47	3.84±1.44*	3.23±1.70*	5.25±3.20*
Hb**%**	Range	11.4-14.3	8-11.9	2.7-9.5	3.5-9
	Mean±SD	12.3±0.93	9.95±1.30*	7.18±1.90*	7.46±1.55*

* Significance at the level ($P < 0.05$)

Fetal hemoglobin, or Hb F, is usually absent in the blood, but it appeared in the blood of thalassemia patients in an increasing order from T-Minor to T-M, with minimum concentration in T-Minor. Hb F is the major oxygen transport protein in the newborn child and it has a much greater exceptional ability to bind oxygen than adult does hemoglobin. Therefore, the higher concentrations of it in T-I and T-M blood types are able to compensate for the cessation of hemoglobin in these patients. Adult hemoglobin or HbA, is the most common form of hemoglobin and comprises about 97% of adult hemoglobin. It exists in erythrocytes to transfer oxygen from the lungs to tissues. In the present data, this hemoglobin was found at 98.4% in the control 'normal' blood and declined gradually from the T-Minor to the T-M bloods. This indicates the need for these patients to have blood transfusion. Hemoglobin A2 is different from other forms of hemoglobins in that it is composed of two α-chains and two δ-chains, and may comprise 1-3% of adult hemoglobin. The average level found in this work for the normal control blood was 1.6%. Elevated concentrations in thalassemia patients are a useful marker of the occurrence of thalassemia, as indicated by Ou *et al*. [20]. Normal hemoglobin, Hb, as analyzed in this work declined across the groups, reaching its lowest level in the T-M group. This indicates the presence of anemia and the need for these patients to have blood transfusion. It must be mentioned that there are several types of anemia produced by different abnormalities in hemoglobin. An example is microcytic hypochromic anemia, which is a standard abnormal hematological parameter in clinical practice and is usually caused by a deficiency in iron and thalassemia traits.

RBCs were not radically changed the in the T-Minor group blood. However, a significant decrease in RBCs occurred in both the TI and TM type bloods when compared to the controls, and this was also seen in the TM type in comparison to the TI blood type. HCT% was observed to be decreased significantly with respect to the control group moving from the T-Minor towards the TM group, with the largest reduction occurring in the TM group whereas MCV was observed to be decreased significantly in TI with respect to the control group. With respect to MCH, it had decreased significantly in the T-Minor group compared to the control but then started to increase in the TI and TM groups, approaching the control level in both cases. The values of MCHC did not change significantly, fluctuating around the control value. On the other hand, the platelets, WBCs and monocytes observed in the T-Minor group had decreased significantly when compared to the controls. Furthermore, significant increases were seen in both the TI and TM groups, results which may be attributable to blood transfusions. The granulocytes and lymphocytes fluctuated around the control value, with non-significant changes. The results of RBCs, WBCs counts and indices variations are illustrated in Table 2.

Table 2. Variation of RBCs indices in thalassemia groups and control

Element type	Statistic	Groups: n = 20			
		Control	**T-Minor**	**TI**	**TM**
RBCs (x 10^6)	Range	3.05-5.31	3.6-6.11	1-4.29	1.43-4.22
	Mean±SD	4.69±0.62	4.91±0.84	2.96±0.90*	3.04±0.68*
HCT%	Range	32.2-38.6	23-33.1	7-26.9	9.8-27.7
	Mean±SD	34.37±2.15	28.51±3.41*	19.84±5.67*	19.76±4.37*
MCV (fl)	Range	61.3-73.6	57.9-77.3	52.9-72.3	67.6-72.7
	Mean±SD	65.96±5.51	67.61±6.06	59.58±8.14*	70.20±1.78
MCH (Pg)	Range	23.8-26.9	17.7-26.3	18.7-28.5	18.6-30
	Mean±SD	25.09±1.05	20.85±3.41*	24.68±3.13	24.78±3.09
MCHC (g/dl)	Range	34.1-36.7	33.5-37.2	32.2-41.8	33.8-44.1
	Mean±SD	35.79±1.15	34.88±1.29	36.42±2.53	37.54±3.01
Plts (x 10^3)	Range	238-387	141-312	100-1096	44.5-1118
	Mean±SD	278.9±44.56	245.9±54.31*	479.0±29.57*	433.32±26.75*
WBCs (x 10^3)	Range	4.2-15	5.3-11	3.9-68.3	3.3-88.2
	Mean±SD	8.61±3.73	7.52±1.69*	24.23±3.08*	29.81±9.83*
Lymphocyte	Range	22-63.1	36.1-50.2	33.6-77.6	34.7-79
	Mean±SD	46.84±12.22	41.59±4.42	50.66±16.52	55.79±15.78
Monocyte	Range	1.9-5.6	1.8-2.7	4-7.7	3.9-13.2
	Mean±SD	3.32±1.19	2.3±0.30*	5.73±1.30*	6.64±2.70*
Granulo-cytes	Range	34.4-76.1	47.7-61.9	14.8-69.1	3.7-13.2
	Mean±SD	49.84±13.19	56.11±4.35	43.57±17.33	37.56±17.04

* Significance at the level ($P < 0.05$)

The RBCs counts (TI and TM) and MCV (TI) in thalassemia patients were decreased significantly which affected the hematocrit value. Moreover, the mean corpuscular hemoglobin level was reduced due to the decrease in Hb concentration, but the mean corpuscular hemoglobin concentration of TM increased. The results of low levels of hemoglobin, HCT, and the change in

hematological parameters are related to the type of thalassemia. The present results are in good agreement with those reported by Mankad *et al.* [21]. According to this report, the clue for thalassemia is the low mean corpuscular volume (MCV) at < 78 fl or the low mean corpuscular hemoglobin (MCH) at <27 pg, which are seen in our results. Platelets show increased levels in T-I and T-M. This increase in platelets can respond to an abnormality on the vessel wall rather than to hemorrhage, resulting in inappropriate platelet adhesion, and the formation of a clot within an intact vessel that may result in arterial obstruction.

For white blood cell counts and differentiation, the increase in WBCs, lymphocytes and monocytes that is accompanied by a reduction in granulocytes is all an indication of internal inflammation, which is produced from anemia and seen in thalassemia patients. However, Mankad *et al.* [21] attributed the increase in WBCs to the probability of the existence of a large number of immature (nucleated) red blood cells, which the cell counter may mistakenly identify as white blood cells.

3.2 Liver enzymes

ALT did not change with respect to the control level except in the case of TM. However, there was a significant difference between T-Minor and TM only. AST increased significantly in the cases of TI and TM, with no variation in T-Minor. Furthermore, there was a significant difference between T-Minor and both TI and TM, with no difference between TI and TM. Albumin did not show any change in concentration in any of the thalassemia groups with respect to the control level. Bilirubin Total increased significantly in the cases of T-Minor and TM, with no variation in TI. There was also a significant difference between T-Minor and TM, with no difference between TI and TM. Bilirubin Direct increased significantly in all thalassemia groups except in the T-Minor group and between each two groups, i.e. between T-Minor and TM, and between TI and TM. Ferritin concentration increased significantly in all thalassemia groups with respect to the control and between each two groups, i.e. between T-Minor and both TI and TM, and between TI and TM. The concentrations in TI and TM were very high, with the concentration in TM the highest. Variations of the afore-said parameters in thalassemia blood and the control groups are illustrated in Table 3.

Table 3. Variation of liver and kidney metabolites in thalassemia groups and control

Parameter	Groups: n = 20			
	Control	**T-Minor**	**TI**	**TM**
Creatinine (mg/dL)	0.74± 0.07	0.78± 0.10	0.79±0.19	0.79± 0.19
GGT(U/L)	7.42±1.64	7.48±1.71	10.90±2.22	10.90± 2.22
ALP(U/L)	269.40±63.76	299.80±29.51	302.00±26.05	302.00±26.05
ALT(U/L)	21.4±6.72	17.81±5.47	60.52±99.33*	60.52±99.33*
AST(U/L)	24.6±5.48	21.57±5.37	60.06±57.23*	60.06±57.23*
Albumin(mg/dl)	4.24±0.25	4.23±0.31	4.02±0.56	4.02±0.56
BilirubinTotal(mg/dl)	0.54±0.06	0.78±0.11*	1.60±0.73	1.60±0.73

* Significance at the level ($P < 0.05$)

Both ALT and AST levels in the thalassemia TI and TM groups increased significantly, with respect to the control level, which indicates that an insult occurred in the liver as judged by the increase of bilirubin T and bilirubin D. These biochemical parameters increase as a result of blocking of the hepatic ducts, which causes leakage into the bloodstream, and which occurs mainly in TI and TM.

Ferritin is a universal protein that stores iron and releases it in a controlled manner. In human beings, ferritin acts as a buffer against iron deficiency and iron overload [22]. In the present

work, ferritin is lowered in the blood of T-Minor patients, indicating the presence of anemia. However, ferritin is raised highly in the blood of TI and TM patients, a condition which affects the heart and causes spleen enlargement. So, ferritin must be removed by using deferoxamine, as reported by Brittenham *et al.* [23]. Of course, the elevated levels of ferritin are due mainly to repeated blood transfusions, on which TI and TM patients are dependent. In some cases, patients may be subjected to splenectomy to reduce the frequency of blood transfusion.

3.3 Oxidative stress markers

Super-Oxide Dismutase (SOD) activity decreased significantly in all thalassemia groups with respect to the control and between each two groups, i.e. between T-Minor and both TI and TM but not between TI and TM. Catalase assay decreased significantly in all thalassemia groups with respect to the control and between each two groups, i.e. between T-Minor and both TI and TM, and between TI and TM. Glutathione Peroxidase (GPx) decreased significantly in all thalassemia groups with respect to the control and between each two groups, i.e. between T-Minor and both TI and TM, and between TI and TM. Glutathione S-transferase (GST) decreased significantly in all thalassemia groups with respect to the control and between each two groups, i.e. between T-Minor and both TI and TM, and between TI and TM. Total antioxidant capacity (TAC) decreased significantly in all thalassemia groups with respect to the control and between each two groups, i.e. between T-Minor and both TI and TM, and between TI and TM. Oxidative stress markers are illustrated in Table 4.

Table 4. Variation of the oxidative stress markers in thalassemia groups and control

Element type	Statistic	Groups: n = 20			
		Control	**T-Minor**	**TI**	**TM**
SOD (U/ml)	Range	98.12-161.16	75.47-118.75	48.32-92.96	36.17-86.83
	Mean±SD	129.64±18.27	97.11±18.21*	70.64±17.88*	61.5±16.52*
CAT (U/l)	Range	38.43-81.07	38.85-61.13	17.88-42.88	15.4-24.28
	Mean±SD	59.75±11.53	49.99±9.63*	30.38±10.42*	19.84±3.03*
GPx (U/l)	Range	12.12-21.22	12.44-14.72	9.06-11.66	4.56-8.05
	Mean±SD	16.67±2.91	13.54±1.27*	10.36±0.93*	6.35±1.42*
GRm (mol/l)	Range	11.67-19.25	11.02-13.89	8.18-11.19	4.66-8.26
	Mean±SD	15.46±2.39	12.33±1.29*	9.58±1.31*	6.46±1.61*
GST (U/l)	Range	20.88-28.46	16.01-23.09	11.15-20.17	6.49-13.09
	Mean±SD	24.67±2.71	19.55±2.64*	9.58±15.66*	9.69±2.62*
TAC (mM/l)	Range	2.4-.51	1.75-.85	1.34-1.45	0.73-.87
	Mean±SD	2.45±0.05	1.77±0.07*	1.39±0.03*	0.82±0.04*
MDA (mmol/ml)	Range	7.29-12.99	10.32-13.69	12.87-15.85	16.85-20.25
	Mean±SD	10.09±2.09	12.42±1.49*	14.33±1.33*	18.55±1.25*

* Significance at the level ($P < 0.05$)

Disturbance of the balance between oxidants and reductants in the body leads to what is known as oxidative stress. This condition arises due to the production of peroxides and free radicals and leads to cellular injuries. Oxidative stress occurs due to increased levels of lipid peroxidation and free-radical formation. Oxidative stress occurs in β-thalassemia patients, who are regularly supplied with blood transfusions, as described by Pavlova *et al*. [24] and Ghone *et al*. [25]. In this

work, ferritin increased significantly in both TI and TM, indicating that the children in these two categories were subjected to iron overload, which in turn made the erythrocytes of these patients vulnerable to peroxidative injury, as reported by Naithanj *et al*. [26].

In a typical normal environment, each cell in the body is subjected to invasion by 100 billion superoxide radicals per day [27]. This account is clear evidence of the size of the risk posed by ROS and the effectiveness of the defense of the biological system toward their damaging effects. The defense of the biological antioxidant system is able to reduce the regular flux state of free radicals, either by blocking their production or by correcting their levels with primary antioxidants, e.g., superoxide dismutase (SOD) and glutathione peroxidase (GPx), which hinder the flow of new unbound root types (ROS) either by modifying present unbound roots by dismutation or by blocking the production of unbound roots from other molecules. In the present work, both (SOD) and (GPx) activities decreased significantly in the TI and TM groups. Moreover, secondary antioxidants, e.g., glutathione (GSH) and bilirubin, work by trapping radicals. GSH, similarly, decreased in the TI and TM groups, indicating either a decrease of the oxidants, or a decrease of the gene responsible for the synthesis of the enzyme protein itself, which is the case in the present work with the TI and TM children's groups.

3.4 Dielectric relaxation

3.4.1 Gross conductivity (σ)

The conductivity of the RBCs increases with increasing frequency and the higher level in the control subjects. The result is shown in Figure 1.

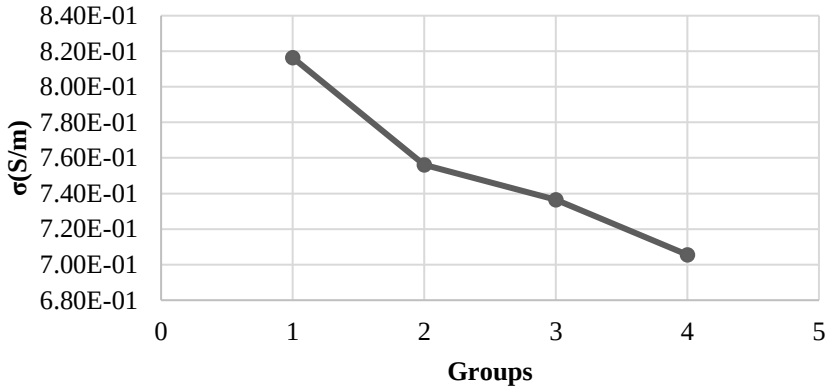

Figure 1. Variation of the conductivity levels in thalassemia and control blood (1: control, 2: T-Minor, 3: TI and 4TM)

3.4.2 Relative permittivity (έ)

The relative permittivity decreases with increasing frequency. The variation of this dielectric parameter reveals that there is a dielectric dispersion occurring at different critical frequencies for each group, as illustrated in Figure 2. The decrease in the relative permittivity at the dispersion point decreases in the order: control >T-Minor > TI > TM.

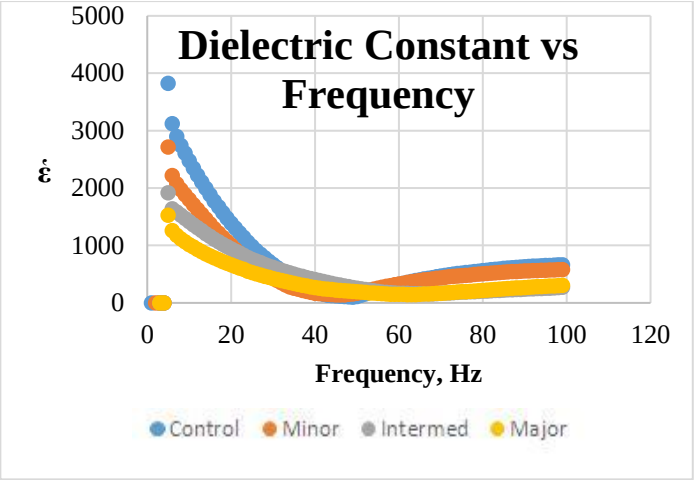

Figure 2. Variation of the relative permittivity (dielectric constant) of the blood groups with frequency

For the impedance Z, the blood impedance decreased with increasing frequency with the minimum level in the case of control blood with a higher value in the case of TM.This variation goes in the reverse direction of the conductivity variation with frequency.

The dielectric strength ($\Delta\dot{\varepsilon} = \dot{\varepsilon} - \dot{\varepsilon}\infty$, the relaxation time, $\tau = 2\pi fc$, where fc is the frequency at the midpoint of dispersion, and the conductivity,σ, at 5 MHz) was calculated and represented in Table 5. The dielectric properties that were used in the comparison between the blood of control children and the blood of the thalassemia patients were numerous. They were namely; the relative permittivity (ε̇), gross conductivity (σ), the dielectric strength (Δε̇), the ac conductivity (σAC) and the relaxation time. Each of these parameters reflects specific differences between the control blood and the thalassemia blood. Importantly, the dielectric properties of the blood are related mainly to the RBCs, which constitute the major component of the blood. Consequently, significant changes in the dielectric properties of the blood are related to the density of the negative charges on RBC membranes. In the present work, increasing frequency was inversely proportional to the relative permittivity of the control and thalassemia blood with gradually reduced levels of (ε̇) from thalassemia minor to thalassemia intermedia and finally to thalassemia major. At the same time, dispersion occurred at different frequencies, as previously described in Table 4. Moreover, the gross conductivity of the control blood was higher than that of the thalassemia blood, and it decreased in the order; σ (control) > σ(T-Minor) >σ (T-intermedia) >σ (T-major), as described in Figure 1. In addition, the blood impedance (z) was lower in the control blood, and increased in an inverse order, i.e. Z (control) < Z (T-Minor) < Z (T-intermedia) <Z (T-major), a result which coincides with the variation in conductivity reported by Haemmerich *et al*. [28]. In our opinion, these variations may be mainly due to the reduction of the sialic acid content on the RBCs. According to Eylar *et al*. [29] and Kahane *et al*. [30], the sialic acid content of glycophorins on thalassemic RBC membranes is about 25% lower than the sialic acid content of glycophorins on healthy RBC membranes. This result means that the carboxyl group, related to sialic acid, is also reduced, resulting in lower conductivity and higher impedance in thalassemia blood. Similarly, there are significant differences between the other dielectric parameters, i.e. the dielectric strength and relaxation time, which are mainly related to the polarization induced in the blood membrane, which differs significantly in the control and thalassemia blood, as described by Desouky *et al*. [31].

Table 5. The dielectric strength, the relaxation time, and the conductivity at 5 MHz

Measure	Control	T-Minor	T-Intermediate	T-Major
Δε	3146.7	2127.2	1633.4	1424.2
τ (S)	7×10^{-7}	7.51×10^{-7}	5×10^{-8}	5.25×10^{-8}
σ(S/m)	0.811	0.742	0.752	0.739

4. Conclusions

The research produced a wide range of data and gave rise to the following conclusions; 1) Most of the measured parameters revealed significant differences between the control blood and the three types of β-thalassemia blood and between each type of thalassemia blood; 2) Patients of thalassemia suffer oxidative stress that strongly affects their activity and quality of life; 3) The β-thalassemia major type shows the maximum differences because patients of this category need regular blood transfusions that slightly improve their quality of life, but increase the toxicity of excess ferritin. Thus, patients within this category needs regular injections of Desferal, which is considered the best agent for the removal of overloaded iron; and 4) Analysis of various dielectric parameters reveal decreased RBC conductivity and related parameters, effects that are mainly due to deformations in RBC membranes due to decreased content of sialic acid in the glycophorins of thalassemic RBC membranes.

5. Acknowledgements

The authors would like to thank all the members of the Medical Biophysics Department and all the staff members in the Faculty of Science, Damanhur University, for their kind help and co-operation.

References

[1] Rund, D. and Rachmilewitz E., 2005. Beta-thalassemia. *New England Journal of Medicine*, 353, 1135-46.

[2] Muncie, J.H. and Campbell, J., 2009. Alpha and beta thalassemia. *American Family Physician*, 80(4), 339-344.

[3] Galanello, R. and Origa R., 2010. Beta-thalassemia. *Orphanet Journal of Rare Diseases*, 5:1-15.

[4] Elbeshlawy, A. and Yossry, I., 2009. Prevention of Haemoglobinopathies in Egypt. *Hemoglobin*, 33, 4-20.

[5] Musallam, K.M., Taher, A.T. and Rachmilewitz, E.A., 2012. β-thalassemia intermedia: a clinical perspective. *Cold Spring Harbor perspectives in medicine*, 2(7), a013482. https://doi: 10.1101/cshperspect.a013482

[6] Camaschella, C., 1995. Thalassemia intermedia. *Haematologica*, 80, 58-68.

[7] Sangkitporn, S., Sangkitporn, S.K., Tanjatham, S., Suwannakan, B., Rithapirom, S., Yodtup, C. and Duangruang, S., 2011. Multicenter validation of fully automated capillary electrophoresis method for diagnosis of thalassmias and hemoglobinpathies in Thailand. *Southeast Asian Journal of Tropical Medicine and Public Health*, 42, 1224-1232.

[8] Bain, B.J., Lewis, S.M. and Bates, I., 2006. Basic haematological techniques. In: Lewis, S.M., Bain, B.J. and Bates I, eds. *Dacie and Lewis Practical Haematology*. 10th ed. Philadelphia: Churchill Livingstone Elsevier, pp. 40-57.

[9] Ikram, N., Hassan, K., Younas, M. and Amanat, S., 2004. Ferritin levels in patients of beta thalassaemia major. *International Journal Pathology*, 2, 71-4.

[10] Burtis, C.A., Ashwood, E.R. and Bruns, D.E., 2008. *Tietz Fundamentals of Clinical Chemistry*. 6th ed. St Louis: Elsevier Saunders Company.

[11] Ohkawa, H., Ohishi, W. and Yagi, K., 2013. Assay for lipid peroxides in animal. *European Scientific Journal*, 9(24), 351-358.

[12] Habig, W.H., Pabst, M.J. and Jakoby, W.B., 1974. Glutathione S-transferases. The first enzymatic step in mercapturic acid formation. *The Journal of Biological Chemistry*, 249, 7130-7139.

[13] Bonnefont-Rousselot, D., Lehmann, E., Jaudon, M.C., Delattre, J., Perrone, B. and Rechke, J.P., 2000. Blood oxidative stress and lipoprotein oxidizability in haemodialysis patients: effect of the use of a vitamin E-coated dialysis membrane. *Nephrology Dialysis Transplantation*, 15, 2020-2028.

[14] Goth, L., 1991. A simple method for determination of serum and erythrocyte catalase activity and the revision of the reference range. *Clinica Chimica Acta*, 196, 143-145.

[15] Marklund, S. and Marklund, G., 1974. Involvement of the superoxide anion radical in the autoxidation of pyrogallol and a convenient assay for superoxide dismutase. *European Journal of Biochemistry*, 47, 469-474.

[16] Draper, H.H. and Hadley, M., 1990. Malondialdehyde determination an index of liquid peroxidation. *Methods in Enzymology*, 186, 421-431.

[17] Polk, C. and Postow, C., 1996. *Handbook of Biological Effects of Electromagnetic Fields.* 2nd ed. London: CRC Press Inc..

[18] Irimajiri, A., Asami, K., Ichinowatari, T. and Kinoshita, Y., 1987. Passive electrical properties of the membrane and cytoplasm of cultured rat basophil leukemia cells. I. Dielectric behavior of cell suspensions in 0.01-500 MHz and its simulation with a single-shell model. *Biochimica et Biophysica Acta (BBA)-Biomembranes*, 896(2), 203-213.

[19] Asamiero, K., Takahashi, Y. and Takashima, S., 1988. Dielectric properties of mouse lymphocytes and erythrocytes. *Biochimica et Biophysica Acta,*1010, 49-55.

[20] Ou, Z., Li, Q., Liu, W. and Sun, X., 2011. Elevated hemoglobin A2 as a marker for β-thalassemia trait in pregnant women. *The Tohoku Journal of Experimental Medicine*, 223(3), 223-226.

[21] Mankad, G.P., Mankad, B. and Singh, S.P., 2013. A study of serological and hematological parameters in thalassaemic patients of Rajkot, Gujarat. *International Journal of Scientific and Research Publications*, 3,(7), 1-4.

[22] Knovich, M.A., Storey, J.A., Coffman, L.G. and Torti, S.V., 2009. Ferritin for the clinician. *Blood Reviews*, 23(3), 95-104.

[23] Brittenham, G.M., Patricia, G.M., Arthur, N.W., Christine, M.E. and Young, N.S., 1994. Efficacy of deferoxamine in preventing complications of iron overload in patients with thalassemia major. *New England Journal of Medicine*, 331(9), 567-573.

[24] Pavlova, L.E., Savov, V.M., Petkov, H.G. and Charova, I.P. 2007. Oxidative stress in patients with beta-thalassemia major. *Prilozi*, 28(1), 145-154.

[25] Ghone, R.A., Kumbar, K.M., Suryakar, A.N., Katkam, R.V. and Joshi, N.G. 2008. Oxidative stress and disturbance in antioxidant balance in beta thalassemia major. *Indian Journal of Clinical Biochemistry*, 23(4), 337-340.

[26] Naithanj, R., Chandra, J., Bhattacharjee, J., Verma, P. and Naravan, S. 2006. Peroxidative stress and antioxidant enzymes in children with beta thalassemia major. *Paediatric Blood Cancer*, 46(7), 780-785.

[27] Percival, M. 1998. Antioxidants. *Clinical Nutrition Insights*, 31(10), 1-4.
[28] Haemmerich, D., Staelin, S.T., Tsai, J.Z., Tungjitkusolmun, S., Mahvi, D.M. and Webster, J.G. 2003. In vivo electrical conductivity of hepatic tumors. *Physiological Measurement*, 24, 251-260.
[29] Eylar, E.H., Madoff, M.A., Brody, O.V. and Oncley, J.L. 1962. The contribution of sialic acid to the surface charge of the erythrocyte. *Journal of Biological Chemistry*, 237, 1992-2000.
[30] Kahane, I., Ben-Chetrit, E., Shifter, A. and Rachmilewitz, E.A. 1980. The erythrocyte membranes in beta-thalassemia. Lower sialic acid levels in glycophorin. *Biochimica et Biophysica Acta*, 596, 10-17.
[31] Desouky, O.S., Selim, N.S., El-Bakrawy, E.M. and El-Marakby, S.M. 2009. Biophysical characterization of β-thalassemic red blood cells. *Cell Biochemistry and Biophysics*, 55(1), 45-53.

The Use of Ozone for Controlling European House Dust Mite, *Dermatophagoides pteronyssinus* (Trouessart)

Jarongsak Pumnuan[1]*, Ammorn Insung[1] and Teerapong Wangapai[2]

[1]Faculty of Agricultural Technology, King Mongkut's Institute of Technology Ladkrabang, Bangkok, Thailand
[2]Faculty of Medicine, Siriraj Hospital, Mahidol University, Bangkok, Thailand

Received: 11 November 2019, Revised: 7 April 2020, Accepted: 1 June 2020

Abstract

Hypersensitivity allergies are mostly caused by house dust mite (HDM), *Dermatophagoides pteronyssinus* (Trouessart). Common control methods for HDM include disposal of bedding sets and fabrics, vacuuming, washing, using plant extracts and applying chemicals. Hence, the application of ozone is a new alternative way to control HDM. The objectives of this experiment were to determine the efficacy of ozone as an HDM killer and to evaluate the allergic levels that remained after the application of ozone. The fumigation method was performed in a laboratory using ozone at the concentrations of 20, 30, 40 and 50 mg l^{-1} in glass chambers (1 m^3) at 1, 2 and 3 h fumigation intervals. The mortality percentages of HDM were observed at 24 h after the treatment. The allergic levels appearing in supernatants were analyzed by an enzyme-linked immunosorbent assay (ELISA) method. Ozone fumigations of 30 mg l^{-1} concentration for 3 h completely killed HDM. In addition, ozone fumigations of $\geq$ 40 mg l^{-1} for 3 h reduced the amount of allergen by >50%, which was a significantly higher reduction than seen at 20-30 mg l^{-1} (35.8-45.8%). The study suggests the ozone fumigation at 30 mg l^{-1} concentration treated for at least 3 h, 40 mg l^{-1} for 2 h, or 50 mg l^{-1} for 1 h could be used as a new alternative method to control HDM.

Keywords: Acari, Pyroglyphidae, *Dermatophagoides pteronyssinis*, ELISA, fumigation, allergies, ozone, *Der p1*
DOI 10.14456/cast.2020.27

1. Introduction

House dust mites (HDM) are classified as members of Arachnida and are related to ticks. They are small in size and typically of 0.2-0.3 mm in length. HDM have translucent bodies under the microscope. The principal HDM species such as *Dermatophagoides pteronyssinus* (Trouessart), *Dermatophagoides farina* (Hughes), *Euroglyphus maynei* (Cooreman) belong to the family Pyroglyphidae, whereas *Blomia tropicalis* (Bronswijk) belongs to Glycyphagidae. The pyroglyphid species are at the top in terms of global frequency and abundance [1, 2]. Remarkably, they are the most common allergy-causing mites found in houses worldwide [3]. Insung *et al.* [4] investigated

*Corresponding author: Tel.: 02 329 8499 Fax: 02 329 8499
E-mail: jarongsak.pu@kmitl.ac.th

the species diversity of HDM in central Thailand and the most abundant species found was *D. pteronyssinus* (69.94%). The incidence of atopic diseases has shown to be increasing all over the world. Allergic rhinitis affects about 10-25% of the population and up to 40% of children, and its incidence is increasing worldwide [5, 6]. In Thailand, the incidence of asthma and allergic rhinitis was 51.4% [7]. The most common sensitizing allergens are HDM. *Dermatophagoides pteronyssinus* and *D. farinae* were major HDM species that were found to be associated with respiratory allergic diseases [7]. In general, sensitization due to house dust mite allergens (HDMAs) appeared in 65 to 130 million people around the world, which is about 50% of the total number of asthmatic patients globally [8]. Recent reports suggested that HDMAs commonly caused allergic diseases found in humans, dogs and cats [9]. Trakultivakorn and Nuglor [10] revealed that *D. pteronyssinus* was one of the major sources of allergy and *Der p1* and *Der p2* were important mite allergens found in Chiang Mai, Thailand.

With the elimination of HDM, the source of HDMAs affecting allergic patients should be reduced. There are many methods of killing HDM; chemical methods such as application of acaricides and physical measures such as heating, freezing and washing of bedding and fabric. However, in the case of the application of acaricides onto carpets, mattresses or furniture, users can come into direct contact with the chemical acaricides. Thus, the use of acaricides is not recommended for controlling HMD. Theoretically, freezing and heating methods should be effective, but no report has demonstrated benefits from such interventions. HDMAs are also effectively removed by washing of bedding and clothing. By this method, mites are killed by drowning [11]. Vinyl fabric is an option for preventing allergic patients coming into contact with HDM. However, further investigation on the efficacy of various kinds and qualities of vinyl fabrics and patient satisfaction with vinyl fabric bed encasing has been recommended [12]. Another alternative method used to control HDM effectively is the application of cloves and cinnamon-based essential oil formulas [13, 14]. Moreover, essential oils from cloves and cinnamon were also extremely effective in reducing HDMAs levels [15-17]. However, there are still some limitations on the use of essential oils. One negative is that some users are not satisfied with the smell of essential oils. Thus, the study of a new appropriate method to control HDM is required in order to address the problems in current methods mentioned above.

Molecules of ozone (O_3) are very unstable and can convert into O_2 rapidly by releasing a single oxygen atom that is extremely reactive [18]. This single oxygen atom displays its reactivity when it comes into contact with the cell membranes of bacteria, viruses and fungal or mycotoxin contaminants. It attacks cellular components and disturbs normal cellular activity [18, 19]. When this free oxygen derived from ozone contacts a volatile organic compound, it can remove the odor of the compound [19]. It can destroy cell membranes or protoplasm, disrupting the cellular reactivation of bacteria, coliforms, viruses and protozoa [20]. Ozone application at low concentrations can effectively reduce microbial populations [21]. To eliminate odors, tastes and color occurring in food or water, ozone treatments are commonly used [22]. Furthermore, a high concentration of ozone for fumigation is a qualified method to control various stored product insects, such as *Sitophilus* spp., *Rhyzopertha dominica*, *Plodia interpunctella*, *Galleria mellonella* and *Tribolium confusum* [19, 23-26]. Therefore, there is a possibility to use ozone to eliminate HDM where the actual area affected requires the use of a fumigation method. In addition, it is also worthwhile to assess its effectiveness in reducing HDMAs. Thus, the objectives of this research were to determine the fumigant toxicity of ozone to house dust mites (*Dermatophagoides pteronyssinus*) and to evaluate its effectiveness in reducing house dust mite allergen (*Der p1* allergen).

2. Materials and Methods

2.1 Mite stock culture

Dermatophagoides pteronyssinus was maintained in mite bottles that were modified from 50 ml cell culture flasks and covered with filter paper. The mite bottles were kept in a mite chamber made from an acrylic sheet (size 30×30×50 cm). Saturated KCl was used to control humidity inside the chamber. The mites were fed on a culture medium with the composition modified from Insung and Boczek [27], i.e. a mixture of rat food, wheat germ and yeast with the ratio of 4:4:1 (by weight). The HDM stock culture was kept at 25±1ºC and 86±1% relative humidity in the laboratory of the Department of Plant Production Technology, Faculty of Agricultural Technology, King Mongkut's Institute of Technology Ladkrabang (KMITL), Thailand.

2.2 Toxicity of ozone fumigation against HDM

Ten adult HDM were introduced into acrylic mite cages adapted from Insung and Boczek [27]. Filter paper was used to close the base holes and glass covers were fixed at the top with wax. All mite cages were placed into a 1 m^3 fumigant glass chamber adapted from Pumnuan *et al*. [28]. Ozone was produced by an ozone generator provided by P.S.C. Trading and Development Co., Ltd., Thailand. The fumigation bioassay was performed by ozone release into the chamber, with the different concentrations of 0 (no ozone), 20, 30, 40 and 50 mg l^{-1}. The fumigation periods were 1, 2 and 3 h, and mortalities of HDM were observed at 24 h thereafter. The death of the mites was confirmed by observing non-movement of their legs when probed with a small hairbrush. The actual death rates were calculated according to Abbot's formula [29]. The completely randomized design (CRD) was applied with five replicates. The percentage of mortality was recorded for each time interval. Lethal concentration (LC_{50} and LC_{90}) and lethal time (LT_{50} and LT_{90}) were determined by the probit method. The analysis of variance (ANOVA) and Duncan's multiple range tests (DMRT) were performed for data analysis.

2.3 Reduction effect to HDMAs

House dust was collected from 20 mattresses that had been used for more than 10 years from different households in Bangkok, Thailand. Afterwards, the house dust was sifted through a fine filtered cloth to sort out the coarse dust. One-gram portions of the house dust were put into petri dishes (10 cm diameter) without a lid. The petri dishes with the house dust material were placed in the 1 m^3 fumigant glass chamber and fumigated with ozone at various concentrations and exposure times following the same method that was used in the fumigation toxicity test against HDM. Then, 0.1 g of material from each treatment was put in a microtube together with 2 ml of phosphate-buffered saline (pH 7) mixed with Tween-20, and the microtubes were placed in a rotator at 4ºC. After 24 h, the contents of the microtubes were homogenized at 2,500 rpm for 15 min. Finally, 1 ml of the supernatant from each tube was removed and kept at 4ºC for further enzyme-linked immunosorbent assay (ELISA). The preparation of house dust material for ELISA test was adapted from Insung *et al*. [15].

2.4 Enzyme-linked immunosorbent assay of the *Der p1* allergen

An enzyme-linked immunosorbent assay (ELISA) was undertaken using the method described by Insung *et al*. [15]. The amount of *Der p1* in the supernatant was measured by an ELISA method using mouse monoclonal antibodies (Indoor Biotechnologies). Three replicates were performed for

each experiment compared with the control group (untreated house dust + spent mite medium). The percentage reductions in the amount of HDMAs were statistically analyzed by applying analysis of variance (ANOVA) and Duncan's multiple range tests (DMRT). The reduction in the amount of *Der p1* was calculated by the following formula:

$$\text{Reduction rate (\%)} = \frac{(\text{Amount of allergen in control} - \text{Amount of allergen in treatment dish}) \text{x} 100\%}{\text{Amount of allergen in control}}$$

3. Results and Discussions

The application of ozone as a fumigant to control HDM in the laboratory at various concentrations and exposure times showed that 3 h fumigation of ozone at ≥ 30 mg l^{-1} completely killed HDM, which was a result of significant difference to 3 h fumigation of ozone at 20 mg l^{-1} , which only reduced HDM by 90.2%. Ozone at 40 mg l^{-1} for 2 h killed HDM by 92.7%, a result which was significantly higher than that for ozone at 30 mg l^{-1} application (68.4%). In addition, the fumigation with 50 mg l^{-1} for 1 h was significantly more effective at killing HDM (81.1%) than was fumigation at 20-40 mg l^{-1}. The appropriate concentration and time of ozone fumigation was 40 mg l^{-1} and 2 h. The LT_{50} and LT_{90} values of ozone fumigation against HDM at 30 mg l^{-1} were 1.30 and 2.35 h, respectively, and 0.99 and 1.67 h, respectively, for 40 mg l^{-1} (Table 1). The result also suggested that ozone fumigation at 20 mg l^{-1} concentration for 3 h was the most effective condition for killing HDM with more than 90% killed, while 1 and 2 h fumigation times presented LC_{50} at 29.98 and 22.96 mg l^{-1}, respectively, and presented LC_{90} at 55.28 and 38.27 mg l^{-1}, respectively. The acaricidal test revealed that ozone fumigation with high concentrations at different periods resulted in a probit regression coefficient (slope) of toxicity regression equation which was higher than that for ozone fumigation at lower concentrations. The concentrations of 40, 30 and 20 mg l^{-1} produced slopes of regression equations with values of 1.788, 1.226 and 0.916, respectively. The slight increment of fumigation time in high ozone concentration resulted in higher HDM mortality rates compared with lower ozone concentration. Likewise, when a longer time of ozone fumigation was used at different concentrations, there was a higher slope of regression equation than for shorter ozone fumigation time. The slopes of regression equations observed were 0.084 and 0.051 at ozone fumigation times at 2 and 1 h, respectively. The result emphasized that a slight increment of ozone concentration used at long fumigation time resulting in higher HDM mortality rate compared with lower ozone fumigation time.

The house dust mite allergen (HDMA), in terms of *Der p1* allergen, was analyzed by the ELISA method. Ozone fumigation at 40 and 50 mg l^{-1} concentration for 3 h reduced the amount of HDMA by 55.4 and 60.3%, results which were not significantly different from each other, but significantly higher than the reduction seen for 20-30 mg l^{-1} (35.8-45.8%). However, ozone application at ≥30 mg l^{-1} with exposure time henceforth 2 h and at 50 mg l^{-1} with exposure time henceforth 1 h resulted in reduction of HDMA by >40%. In contrast, the concentration of ozone at 20 mg l^{-1} with exposure times for 1-3 h reduced the HDMA by only 25.5-35.8%. It was noteworthy that the concentrations of ozone fumigation at 40 and 50 mg l^{-1} resulted in reduction rates of HDMA that were not significantly different, and this was also seen for 30 and 40 mg l^{-1} for 2-3 h fumigation times. All concentrations of ozone fumigation (20-50 mg l^{-1}) for the 2 h fumigation time showed reduction rates of HDMA in the range 34.6-49.2%, with no significant differences among them (Table 2). This study suggests the ozone fumigation at 30 mg l^{-1} concentration treated for at least 3 h or 40 mg l^{-1} for 2 h or 50 mg l^{-1} for 1 h could be used as a new alternative method to control HDM. Those conditions were extremely effective in killing HDM at more than the 80% level, without

significant differences between them and would also reduce the amount of HDMA by >45% effectively.

Table 1. Fumigation toxicities of ozone against house dust mite (*Dermatophagoides pteronyssinus*) (Trouessart) at various concentrations and exposure times

Concentration of ozone (mg l^{-1})	Mortality percentages (means ± S.D.)[1/] Fumigation times			Regression equation	LT_{50} (h)	LT_{90} (h)	Chi-square
	1 h	2 h	3 h				
0 (control)	0.00^{Ea}	0.00^{Da}	0.00^{Ca}	-	-	-	-
20	43.7 ± 3.7^{Db}	49.4 ± 14.1^{Cb}	90.2 ± 6.5^{Ba}	Y=-1.544+0.916x	1.69	3.09	27.99
30	53.0 ± 6.6^{Cb}	68.4 ± 15.8^{Bb}	100.0 ± 0.0^{Aa}	Y=-1.594+1.226x	1.30	2.35	30.15
40	65.4 ± 6.0^{Bc}	92.7 ± 4.3^{Ab}	100.0 ± 0.0^{Aa}	Y=-1.707+1.788x	0.99	1.67	16.51
50	81.1 ± 6.1^{Ab}	97.8 ± 1.8^{Aa}	100.0 ± 0.0^{Aa}	-	-	-	-
Regression equation	Y= -1.518+0.051x	Y= -1.922+0.084x	-	-	-	-	-
LC_{50} (mg l^{-1})	29.98	22.96	-	-	-	-	-
LC_{90} (mg l^{-1})	55.28	38.27	-	-	-	-	-
Chi-square	16.874	7.96	-	-	-	-	-

[1/] Means in column with the same time followed by the same capital letter and means in row followed by the same common letter are not significantly different at the 5% level as determined by DMRT ($P < 0.05$).

Table 2. Percentage reduction of house dust mite (*Dermatophagoides pteronyssinus*) (Trouessart) allergen (*Der p1*) after ozone fumigation at various concentrations and exposure times

Concentration of ozone (mg l^{-1})	Reduction rate (%) (means ± S.D.)[1/] Fumigation times		
	1 h	2 h	3 h
0 (control)	0.00 ± 14.2^{Ca}	0.00 ± 14.2^{Ba}	0.00 ± 14.2^{Da}
20	25.5 ± 3.7^{Ba}	34.6 ± 7.8^{Aa}	35.8 ± 3.2^{Ca}
30	30.0 ± 6.3^{Bb}	40.7 ± 3.3^{Aa}	45.8 ± 3.6^{BCa}
40	39.7 ± 6.3^{Aba}	45.5 ± 3.1^{Aa}	55.4 ± 4.1^{ABa}
50	45.6 ± 1.0^{Ac}	49.2 ± 1.9^{Ab}	60.3 ± 0.2^{Aa}

[1/] Means in column with the same time followed by the same capital letters and means in row followed by the same common letter are not significantly different at the 5% level as determined by DMRT ($P < 0.05$).

Ozone fumigation is a new alternative method for elimination of HDM in households or in accommodation. This study indicates that ozone at 40 mg l^{-1} concentration with 3 h fumigation time could be used to completely control HDM and reduce the amount of HDMA by >50%. This concentration of ozone could also successfully reduce microbial populations. There are many previous reports regarding the efficacy of ozone against many organisms. One finding was that 10 ppm of ozone could remove up to 99% of bacteria and viruses in 10 min. The action of ozone on viruses, even at lower ozone concentrations, compared well to its activity against bacteria at higher concentrations. This is due to the fact that the bacterial wall is more complex than the viral envelope. It was demonstrated that ozone can kill fungi that initiate many human diseases by its oxidizing action, which results in an irreversible cellular effect [20]. Microbial contamination in fresh dates

was able to be completely controlled by ozone application at 5 ppm for at least 1 h [21]. Ozone at <30 ppm concentration was effective in eliminating aflatoxin in contaminated maize feed [19]. Application of 5 ppm ozone showed morphological and mycotoxin inhibition effects on cultures of *Aspergillus flavus* and *Fusarium moniliforme* [30]. Many studies of the control of insect pests in stored products by the use of ozone have been published. Hansen *et al*. [25] reported that ozone fumigation at 135 ppm for 8 days completely killed the young stages of *Sitophilus* spp. and *Rhyzopertha dominica*, while fumigation at 35 ppm for 6 days was a highly effective way to control the adult stages of the insects. The study of Keivanloo *et al*. [26] indicated that the concentrations and exposure times of ozone resulted in different mortality rates of each insect stage. The larval stages were often very much more susceptible than other stages. For example, 5 ppm ozone applied to 12-day-old *Plodia interpunctella* larvae for 2 h produced a 58% mortality rate, and longer exposure times caused higher mortality. However, both egg and pupal stages were more resistant. Continuous ozone treatment at concentration of 13.9 ppm for 2 h was able to kill completely almost all developmental stages of *Ephestia kuehniella* and *Tribolium confusum* [23]. High concentrations of ozone were used to control adult bed bugs with short periods of ozone exposure. When 1800 ppm ozone were applied to bed bugs for 150 min, or 80 ppm applied for 48 h, 100% bed bug mortality resulted [31]. The use of ozone to kill HDM may then also have the further effect of controlling microbial populations, insect pests and other disturbing organisms.

Another good result of the use of ozone for controlling HDM is its direct effect in reducing house dust mite allergen. This study showed that 40 mg l^{-1} ozone fumigation for 3 h completely killed HDM and reduced the amount of HDMA by >50%. Since the allergen is classified as a protein, the characterization of allergens based on a proteomic approach has been introduced [32]. This ability of ozone to reduce the amount of HDMA mentioned above is not surprising in view of Cataldo's work, which shows that ozone causes denaturation of proteins [33]. Besides, the report of Sahab *et al*. [34] indicated that application of 40 ppm ozone for 10 min induced the degradation of aflatoxin by 94%. It also resulted in a reduction in fat and protein content that reached 10.56 and 4.58%, respectively. It is important to note that when ozone fumigation is to take place in the field, care must be taken to avoid its leakage, which could poison organisms outside the desired area. However, in general, ozone decomposes expeditiously. Recommendations for research further to this work could include the study of the insecticidal properties of ozone against other insects, especially insect pests of medical importance such as bed bugs, mosquitoes and cockroaches. The research suggest that ozone fumigation applied at appropriate concentrations could control a number of disturbing organisms effectively.

4. Conclusions

The application of ozone fumigation is a new alternative way for controlling house dust mite. In this experiment, the efficacy of ozone fumigation against HDM and its influence on the reduction of allergen levels were determined. The results indicated that ozone fumigation at concentrations of ≥ 30 mg l^{-1} for 3 h completely killed HDM. In addition, the conditions of 50 mg l^{-1} of ozone fumigation for 1 h, 40 mg l^{-1} for 2 h and 30 mg l^{-1} for 3 h reduced the HDM level by more than 80% and reduced the amount of allergen by more than 45%. This study suggests that ozone fumigation at 30, 40 and 50 mg l^{-1} for at least 3, 2 and 1 h, respectively, could be used as a new alternative methods to control HDM.

5. Acknowledgements

We would like to thank P.S.C. Trading and Development Co., Ltd., Thailand for the utilization of ozone generator throughout the experiment.

References

[1] Colloff, M.J., 2009. *Dust Mites*. Dordrecht: CSIRO Publishing.

[2] Rezk, H.A., Abd El-Hamid, M.M. and Abd El-Latif, M.A., 1996. House dust mites in Alexandria Region. *Alexandria Journal of Agricultural Research*, 41(2), 209-216.

[3] Colloff, M.J. and Spieksma, F.T., 1992. Pictorial keys for the identification of domestic mites. *Clinical & Experimental Allergy*, 22(9), 823-830.

[4] Insung, A., Pumnuan, J. and Konvipasruang, P., 2010. Species diversity of house dust mite in central Thailand. *Entomology and Zoology Gazette*, 28(1), 31-39. (in Thai with English abstract)

[5] Bunjean, K., Sukkasem, K., Noppacroh, N., Yamkaew, N., Janthayanont, D., Theerapancharern, W., Chokkanchitchai, S. and Moungthong, G., 2012. Prevalence of allergic rhinitis and types of sensitized allergen in adult at Wat Intaram community, Hua Raeu, Phra Nakhon Si Ayutthaya District, Phra Nakhon Si Ayutthaya Province, Thailand. *Journal of Medical Association of Thailand*, 95(Suppl. 5), S63-S68.

[6] Sadaka, H., Allam, S., Rezk, H.A., Abo El-Nazer, S.Y. and Shola, A.Y., 2000. Isolation of dust mites from houses of Egyptian allergic patients and induction of experimental sensitivity by *Dermatophagoides pteronyssinus*. *Journal of the Egyptian Society of Parasitology*, 30(1), 263-276.

[7] Visitsunthorn, N., Chirdjirapong, V., Pootong, V., Jirapongsananuruk, O., Pacharn, P., Weeravejsukit, S., Mahakittikun, V. and Vichayanond, P., 2010. The accumulation of dust mite allergens on mattresses made of different kinds of materials. *Asian Pacific Journal of Allergy and Immunology*, 28, 155-161.

[8] Calderón, M.A., Linneberg, A., Kleine-Tebbe, J., De Blay, F., Hernandez Fernandez de Rojas, D., Virchow, J.C. and Demoly, P., 2015. Respiratory allergy caused by house dust mites: What do we really know? *Journal of Allergy and Clinical Immunology*, 136(1), 38-48.

[9] Loft, K.E. and Rosser, Jr. E.J., 2010. Group 1 and 2 *Dermatophagoides* house dust mite allergens in the microenvironment of cats. *Veterinary Dermatology*, 21, 152-158.

[10] Trakultivakorn, M. and Nuglor, T., 2002. Sensitization to *Dermatophagoides pteronyssinus* and *Blomia tropicalis* extracts and recombinant mite allergens in atopic Thai patients. *Asian Pacific Journal of Allergy and Immunology*, 20, 217-221.

[11] Portnoy, J., Miller, J.D., Williams, P.B., Chew, G.L. , Miller, J. D., Zaitoun, F., Phipatanakul, W., Kennedy, K., Barnes, C., Grimes, C., Larenas-Linnemann, D., Sublett, J., Bernstein, D., Blessing-Moore, J., Khan, D., Lang, D., Nicklas, R., Oppenheimer, J., Randolph, C., Schuller, D., Spector, S., Tilles, S.A. and Wallace, D., 2013. Environmental assessment and exposure control of dust mites: a practice parameter. *Annals of Allergy, Asthma and Immunol*ogy, 111(6), 465-507.

[12] Areegarnlert, N. and Malainual, N., 2013. The efficacy of vinyl fabric for protecting house dust mites and their allergens. *Journal of Nursing Science*, 31(2), 82-90. (in Thai with English abstract)

[13] Insung, A. and Pumnuan, J., 2008. Medicinal plant formulation for controlling house dust mites which containing major component of clove essential oil. *Thai Patent Divisional Application*, No. 0801005027. September 30, 2008.

[14] Pumnuan, J. and Insung, A., 2008. Medicinal plant formulation for controlling house dust mites which containing major component of cinnamon essential oil. *Thai Patent Divisional Application*, No. 0801005026. September 30, 2008.
[15] Insung, A., Pumnuan, J., Mahakittikun, V. and Wangapai, T., 2016. Effectiveness of essential oils of medicinal plants at reducing the amounts of allergen produced by the European house dust mite, *Dermatophagoides pteronyssinus* (Trouessart). *Journal of Acarological Society of Japan*, 25(1), 179-184.
[16] Rezk, H.A. and Gadelhak, G.G., 2003. Acaricidal activity of two plant essential oils on the adult stage of the European house dust mite, *Dermatophagoides pteronyssinus* (Acari: Pyroglyphidae). *Journal of Pest Control and Environmental Sciences*, 11(1), 13-27.
[17] Saad, El-Z., Hussein, R., Saher, F. and Ahmed, Z., 2006. Acaricidal activities of some essential oils and their monoterpenoidal constituents against house dust mite, *Dermatophagoides pteronyssinus* (Acari: Pyroglyphidae). *Journal of Zhejiang University Science B*, 7, 957-962.
[18] Mason, L.J., Woloshuk, C.P., Mendoza, F., Maier, D.E. and Kells, S.A., 2006. Ozone: A new control strategy for stored grain. *Proceedings of the 9th International Working Conference on Stored Product Protection*. Campinas, São Paulo, Brazil. October 5-8, 2006, 904-907.
[19] Kells, S.A., Mason, L.J., Maier, D.E. and Woloshuk, C.P., 2001. Efficacy and fumigation characteristics of ozone in stored maize. *Journal of Stored Products Research*, 37, 371-382.
[20] Rojas-Valencia, M.N., 2011. Research on ozone application as disinfectant and action mechanisms on wastewater microorganisms. In: A. Méndez-Vilas, ed. *Science against Microbial Pathogens: Communicating Current Research and Technological Advances.* National Autonomous University of Mexico, Institute of Engineering, Coordination of Environmental Engineering, Mexico.
[21] Habibi Najafi, M.B. and Hadad Khodaparast, M.H., 2009. Efficacy of ozone to reduce microbial populations in date fruits. *Food Control*, 20(1), 27-30.
[22] Kim, J.G., Yousef, A.E. and Dave, S., 1999. Application of ozone for enhancing the microbiological safety and quality of foods: a review. *Journal of Food Protection*, 62(9), 1071-1087.
[23] Isikber, A.A. and Oztekin, S., 2009. Comparison of susceptibility of two stored-product insects, *Ephestia kuehniella* Zeller and *Tribolium confusum* to gaseous ozone. *Journal of Stored Products Research*, 45(3), 159-164.
[24] James, R.R. 2011. Potential of ozone as a fumigant to control pests in honey bee (Hymenoptera: Apidae) Hives. *Journal of Economic Entomology*, 104(2), 353-359.
[25] Hansen, L.S., Hansen, P., Jensen, K.M.V., 2012. Lethal doses of ozone for control of all stages of internal and external feeders in stored products. *Pest Management Science*, 68(9), 1311-1316.
[26] Keivanloo, E., Namaghi, H.S., Hossein, M. and Khodaparast, H., 2014. Effects of low ozone concentrations and short exposure times on the mortality of immature stages of the Indian meal moth, *Plodia interpunctella* (Lepidoptera: Pyralidae). *Journal of Plant Protection Research*, 54(3), 267-271.
[27] Insung A. and Boczek. J., 1995. Effect of some extracts of medicinal and spicy plants on Acarid mites. *Proceedings of Symposium on Advances of Acarology*. Siedlce, Poland. September 26-27, 1995, 211-223.
[28] Pumnuan, J., Chandrapatya, A. and Insung, A., 2010. Acaricidal activities of plant essential oils three plants on the mushroom mites, *Luciaphorus perniciosus* Rack (Acari: Pygmophoridae). *Pakistan Journal Zoology*, 42(3), 247-252.
[29] Abbott, W.S., 1987. A method of computing the effectiveness of an insecticide. 1925. *Journal of the American Mosquito Control Association*, 3, 302-303.

[30] Mason, L.J., Woloshuk, C.P. and Maier, D.E., 1996. Efficacy of ozone to control insects, molds and mycotoxinsin. *Proceedings of the International Conference on Controlled Atmosphere and Fumigation in Stored Products*. Nicosia, Cyprus. April 21-26, 1996, 665-670.
[31] Feston, J., McDonough, M., Mason, L. Gibb, T. and Saltzmann, K., 2011. Effects of ozone on the common bed bug (*Cimex lectularius*). *ESA Annual Meetings Online Program*. November 13-16, 2011.
[32] Nuanlaong, C., Sookrung, N., Reamtong, O., Chaicumpa, W., Saelim, N., Indrawattana, N. and Tungtrongchitr, A., 2016. Protease inhibitor treatment decreases allergenicity of *Dermatophagoides pteronyssinus* allergen evidenced by proteome and allergenome analysis. *Journal of Tropical Medicine and Parasitology*, 39, 12-21.
[33] Cataldo, F., 2003. On the action of ozone on proteins. *Polymer Degradation and Stability*, 82(1), 105-114.
[34] Sahab, A.F., Hassanien, F.R., El-Nemr, S.E., Abdel-Alim, H.A. and Abdel-Wahhab, M.A., 2013. Effect of ozone gaseous on aflatoxin degradation and fat and protein content in peanut seeds. *Journal of Applied Sciences Research*, 9, 2170-2175.

Genetic Diversity of Commercial Field Corn Hybrids in Thailand as Verified by SSR Markers and Their Inbreeding Depression

Terdsak Suwanatape[1], Sansern Jampatong[2] and Choosak Jompuk[1]*

[1]Department of Agronomy, Faculty of Agriculture at Kamphaeng Saen, Kasetsart University, Kamphaeng Saen Campus, Nakhon Pathom, Thailand
[2]National Corn and Sorghum Research Center, Faculty of Agriculture, Kasetsart University, Nakhon Ratchasima, Thailand

Received: 22 January 2020, Revised: 26 April 2020, Accepted: 5 June 2020

Abstract

Commercial field corn hybrids are often used for germplasm or for extracting new inbred lines in hybrid breeding programs. However, the commercial single-cross hybrids should be identified before using their genetic materials to increase the effectiveness of new inbred lines and their hybrids. The objective of this study was to evaluate the genetic diversity of commercial single-cross hybrids as verified by Simple Sequence Repeat (SSR) markers and to assess their inbreeding depression using Troyer's genetic diversity. Fifteen commercial field corn single-cross hybrids were selected from private seed companies and public sector agencies and evaluated for genetic diversity using 40 SSR markers. There was a high correlation between Jaccard's index and simple matching index. The UPGMA dendrogram clustered the hybrids into 8 clusters, which showed hybrids within each of four clusters coming from the same genetic sources, except for a group of CP201 and NS3 hybrids that came from different sources. Besides, Troyer's genetic diversity was applied to analyze the genetic diversity of six single-cross hybrids selected from the previous results. The SSR markers and the Troyer's genetic diversity application gave the same direction of corn genetic diversity with a moderate correlation ($r=0.66$, $P<0.01$). Troyer's genetic diversity ranged from 0.47 to 0.91, with an average of 0.72. The commercial field corn single-cross hybrids used in Thailand are still quite diverse, especially those from different seed companies. Therefore, breeders have a good chance to extract inbreeding lines from the commercial single-cross hybrids, and to make a new hybrid with high yield after the grouping of single-cross hybrids through the use of SSR markers or Troyer's genetic diversity.

Keywords: SSR marker, genetic diversity, inbreeding depression, field corn hybrid
DOI 10.14456/cast.2020.28

*Corresponding author: Tel.: (086) 9818658 Fax: (034) 351887
E-mail: agrcsj@ku.ac.th

1. Introduction

Corn has been an important economic crop for the feed mill business in Thailand, and Thailand was ranked the 20th largest maize producer in the world [1]. Germplasm is an essential key factor in plant breeding programs for yield improvement and the development of new hybrid varieties. For field corn, commercial single-cross hybrids are often used as the source of germplasm from which to extract new inbred lines in hybrid breeding programs in Thailand. For example, Ki21 (Pacific 9-S_8-45), Ki22 ({Pacific 11 × Suwan 1(S)C_6}-S_8-30), and Ki48 (Pioneer 3013-S_8-57-2) were extracted from single-cross hybrids from private companies [2]. On the other hand, sources of germplasm from public sector agencies, such as the National Corn and Sorghum Research Center, Kasetsart University (Ki48 and Ki60) [2] and the Nakorn Sawan Field Crops Research Center, Department of Agriculture (Takfa1 and Takfa3) [3], were successfully used to develop inbred lines that were sold to private seed companies. From 1980 to 2004, in the USA, new corn inbred lines were extracted from different types of crosses including two-parental lines (77%), BC1 (9%), BC2 (2%), three-parental lines (5%), four or more parental lines (2%), synthetic (1%), synthetic × inbred (2%), and commercial hybrid (3%) [4]. Heterotic patterns, or groups of heterosis, play an essential role in the selection of germplasm sources for the development of new sources of inbred lines. Therefore, methods to identify and group germplasm are of importance in breeding programs. Molecular genetic markers are potent tools to separate and assign single-cross hybrids or inbred lines into heterotic patterns [5, 6]. SSR markers offer more cost-effectiveness over other marker types, as well as reliability for the grouping of corn inbred lines [7-9]. Also, in conventional breeding, the grain yield of hybrids, which are a function of inbreeding depression [expressed as Troyer's genetic distance (TGD)], can be used to determine heterotic groups [10, 11]. Various publications have studied the relationship between molecular marker-based genetic distance (MGD) and hybrid grain yield in tropical and temperate corn cultivars, resulting in different levels of correlation [5, 7, 12]. The objective of this study was to evaluate the genetic diversity of commercial single-cross hybrids as verified by SSR markers and to assess their inbreeding depression expressed as Troyer's genetic distance (TGD) for further improvement of corn germplasm.

2. Materials and Methods

2.1 Plant materials

Fifteen commercial field corn single-cross hybrids were selected from private seed companies and public sector agencies in Thailand (Table 1). SSR markers were used to analyze the genetic distance between these 15 varieties directly.

Table 1. Description of fifteen commercial field corn single-cross hybrids from 5 private seed companies and 2 public sector agencies in Thailand

Private seed companies and public sectors	Varieties
1. Charoen Pokphand Produce Co., Ltd.	CP201, CP888
2. Monsanto (Thailand) Co., Ltd.	DK9901
3. Nakorn Sawan Field Crop Research Center	NS3[1/]
4. Syngenta Co., Ltd.	NK6248, NK7328, NK6253
5. Pacific Seeds (Thai), Ltd.	PAC339, PAC559, PAC777
6. Pioneer Hi-Bred Thailand Co., Ltd.	PIO4311, PIO4546, PIO4181
7. National Corn and Sorghum Research Center	KSX5402[2/], KSX5603[3/]

[1/] Takfa × Takfa 3, [2/] Ki 48 × Ki 60, and [3/] Kei1303 × Ki60

Besides, six single-cross hybrids were selected from the previous analysis to study genetic diversity, as described by Troyer genetic diversity (TGD) [10], comprising PAC777, PAC559, PIO4546, PIO4181, NK6248, and NK7328. These six varieties came from the same and different clusters, as shown in Figure 1. PIO4546 and PIO4181 were in cluster 3, while PAC777 and PAC559 were in cluster 5. On the other hand, NK6248 and NK7328 were in clusters 6 and 4, respectively. These varieties were used in Griffing's method IV resulting in fifteen double-cross hybrids and were self-pollinated to obtain six S_1 lines.

2.2 Field experiments

Field trials were conducted in the dry season of 2016 with three locations at Sukhothai, Saraburi, and Phitsanulok provinces and in the rainy season of 2016 with three locations at Saraburi, Phetchabun, and Phitsanulok provinces. Randomized complete block design (RCBD) with two replications was applied in each location. Each plot consisted of four-rows, 5-meters long, with spacing of 0.75×0.25 m^2, and with 21 plants per row. Before sowing, approximately 312.5 kg/ha of basal fertilizer 27-12-6 was applied, and approximately 312.5 kg/ha fertilizer 46-0-0 was applied one month after planting. Herbicide was used according to local practices.

2.3 DNA extraction and genotyping with SSR markers

The leaves of ten-day-old F_1 plants were collected for DNA extraction as described by Sinkangam *et al*. [13]. Two SSR primers, umc1225 (5.08) and bnlg238 (6.00), were used to screen the purity of the sample, which confirmed the purity of DNA, after which it was bulked for the next process. Then, 40 SSR primers were applied to screen the DNA samples that passed the purity test. They were then scored 0 or 1 representing absence or presence of a DNA band, respectively. The SSRs were listed in Table 2. Primer sequences used were sourced from MaizeGDB (www.maizegdb.org; verified 15 September 2019).

2.4 Data analyses

2.4.1 Jaccard's index genetic distance and Cluster dendrogram

The Jaccard's index was calculated based on this formula; $d_{ij} = 1-[a/(a+b+c)]$, where d is the distance between i and j, a attributes both i and j, b attributes only i, and c attributes only j [14]. Moreover, the simple matching's index genetic distance was calculated based on this formula; $d_{ij} = 1-[(a+b)/(a+b+c)]$ [15]. The unweighted pair group method with arithmetic mean (UPGMA) dendrogram of Jaccard's index was obtained from a cluster analysis of fifteen commercial single-cross hybrids using R statistics [16]. For field experiments, average grain yields were measured at 15% moisture content.

2.4.2 Inbreeding depression

The inbreeding depression was analyzed using Troyer's genetic diversity (TGD) as described by Troyer *et al*. [10]. Six single-cross hybrids were selected to study by this method according to the formula; TGD = 1- [(H-C)/ (H-S)], where H is the average yield of the two hybrids, C is the double-cross hybrids, and S is the average yield of the two self-hybrids.

2.4.3 Correlation between Jaccard's index and Troyer's genetic diversity

The Pearson correlation (r) was analyzed between two indices of genetic distances: Jaccard's and Troyer's.

3. Results and Discussion

3.1 SSR primers

3.1.1 Polymorphic information content (PIC)

Forty SSRs were used to analyze 15 single-cross hybrids spanning over ten chromosomes. The number of alleles per SSR locus ranged from 2 to 11, with an average of 5.5 (Table 2). The polymorphic information content (PIC) was significantly different ($P<0.05$), ranging from 0.33 to 0.88. The average PIC was about 0.67, which was more significant than the value reported by Senior *et al*. [17] with an average of 0.59, indicating greater diversity of corn varieties in Thailand.

Table 2. Numbers of alleles, repeat type and polymorphic information content (PIC) values of 40 SSR loci in 15 single-cross hybrids

Number	SSR locus	Bin location no.[a]	No. of alleles	Repeat type[a]	PIC value
1	bnlg1014	1.01	7	AG(14)	0.80
2	umc2232	1.05	2	(CAC)4	0.47
3	bnlg1025	1.07	7	AG(23)	0.78
4	umc1118	1.11	3	(GAGCA)4	0.51
5	bnlg1327	2.02	6	(GA)6	0.75
6	umc2247	2.04	5	CT(25)	0.59
7	bnlg1138	2.06	7	AG(14)	0.81
8	bnlg1940	2.08	11	AG(18)	0.88
9	umc1970	3.01	6	-	0.71
10	umc1501	3.05	4	(AAG)5	0.67
11	bnlg197	3.06	10	-	0.87
12	umc2152	3.09	3	(TG)8	0.51
13	umc2278	4.01	6	(TCTC)4	0.73
14	umc1652	4.04	4	(CCG)5	0.68
15	umc1940	4.09	3	-	0.35
16	bnlg1890	4.11	11	AG(26)	0.86
17	bnlg1879	5.03	8	AG(14)	0.82
18	umc2296	5.03	3	(AGT)4	0.60
19	umc1221	5.04	9	(CT)7	0.88
20	umc1225	5.08	6	(AG)6	0.74

Table 2. (cont.)

21	bnlg238	6.00	7	-	0.84
22	umc1979	6.04	4	-	0.66
23	umc1352a	6.05	2	(GCC)6	0.44
24	umc1490	6.07	2	(AC)6	0.49
25	umc1426	7.00	3	(AGAGG)4	0.33
26	umc1393	7.02	5	(GTC)4	0.68
27	umc1710	7.04	5	(CTG)5	0.73
28	umc2333	7.05	5	(CCGT)4	0.65
29	umc1735	8.03	8	(AG)40	0.85
30	umc1807	8.03	2	(AGC)5	0.49
31	bnlg666	8.05	9	-	0.80
32	umc1005	8.08	6	(GT)15	0.77
33	bnlg2122	9.01	8	AG(17)	0.74
34	umc1170	9.02	5	(TC)12	0.71
35	umc2338	9.05	2	(GCC)4	0.44
36	umc2346	9.06	4	(TA)7	0.61
37	umc1380	10.00	4	(CTG)5	0.59
38	umc2180	10.03	4	(GGCC)4	0.50
39	bnlg1028	10.06	3	AG(12)	0.62
40	bnlg1450	10.07	10	AG(34)	0.86
Total			219		
Mean			5.50		0.67

[a] Loci and repeat class were referred from MaizeGDB

3.1.2 Indices genetic distances and cluster analysis

Genetic distances based upon variation in SSR profiles between 15 single-cross hybrids were shown according to Jaccard's index and the simple matching index (Table 3). Jaccard's index genetic distance ranged from 0.18 to 0.80, with an average of 0.62. On the other hand, the simple matching index genetic distance ranged between 0.06-0.39 with an average of 0.28. However, these indices had a high correlation ($r = 0.98$, $P < 0.01$). Simple matching and Jaccard's indices are rather simplistic and similar in their calculation and have similar metric properties [18]. Nevertheless, the numerator of these indices is different (a vs. a+d) such that the behavior of this similarity index may be data specific [19]. Using SSR-based data to obtain Jaccard's index, the UPGMA dendrogram showed that the fifteen single-cross hybrids could be classified into groups of hybrids on the index of 0.5, separating into eight clusters (Figure 1); CP201 and NS3 in cluster 1, KSX5603 and KSX5402 in cluster 2, PIO4181, PIO4546 and PIO4311 in cluster 3, NK7328 and NK6253 in cluster 4, PAC559, PAC777 and PAC339 in cluster 5, and NK6248, DK9901 and CP888 in clusters 6, 7 and 8, respectively. Four clusters consisted of hybrids coming from the same genetic sources, including

Table 3. Pairwise genetic distance values of 15 single-cross hybrids; Jaccard's index (below diagonal) and simple matching's index (above diagonal)

Hybrids	1	2	3	4	5	6	7	8	9	10	11	12	13	14	15
1. NK6248	-	0.28	0.26	0.31	0.29	0.32	0.3	0.28	0.28	0.27	0.28	0.28	0.27	0.3	0.28
2. NK7328	0.63	-	0.28	0.29	0.25	0.21	0.27	0.26	0.26	0.28	0.26	0.2	0.28	0.22	0.27
3. PAC777	0.59	0.61	-	0.21	0.29	0.34	0.27	0.25	0.33	0.33	0.18	0.24	0.32	0.28	0.36
4. PAC559	0.68	0.66	0.51	-	0.29	0.36	0.35	0.27	0.27	0.28	0.19	0.26	0.31	0.31	0.39
5. PIO4546	0.65	0.59	0.63	0.66	-	0.15	0.29	0.21	0.32	0.30	0.29	0.22	0.06	0.23	0.22
6. PIO4181	0.69	0.53	0.70	0.76	0.40	-	0.33	0.25	0.35	0.34	0.29	0.23	0.16	0.27	0.25
7. CP201	0.65	0.60	0.59	0.72	0.63	0.69	-	0.21	0.26	0.31	0.34	0.27	0.29	0.32	0.28
8. NS3	0.64	0.60	0.57	0.62	0.53	0.60	0.50	-	0.26	0.27	0.29	0.23	0.22	0.25	0.27
9. DK9901	0.63	0.61	0.69	0.62	0.69	0.75	0.58	0.60	-	0.23	0.29	0.29	0.33	0.33	0.32
10. CP888	0.60	0.63	0.69	0.63	0.67	0.72	0.66	0.61	0.55	-	0.31	0.32	0.31	0.31	0.33
11. PAC339	0.63	0.59	0.45	0.48	0.65	0.66	0.70	0.66	0.65	0.67	-	0.27	0.32	0.33	0.36
12. NK6253	0.63	0.49	0.56	0.61	0.53	0.57	0.60	0.57	0.66	0.68	0.61	-	0.23	0.28	0.28
13. PIO4311	0.62	0.63	0.67	0.68	0.18	0.43	0.64	0.53	0.71	0.67	0.68	0.56	-	0.26	0.23
14. KSX5603	0.67	0.54	0.62	0.68	0.56	0.62	0.67	0.59	0.71	0.67	0.70	0.63	0.60	-	0.16
15. KSX5402	0.65	0.63	0.74	0.80	0.55	0.61	0.63	0.64	0.71	0.72	0.76	0.65	0.56	0.43	-

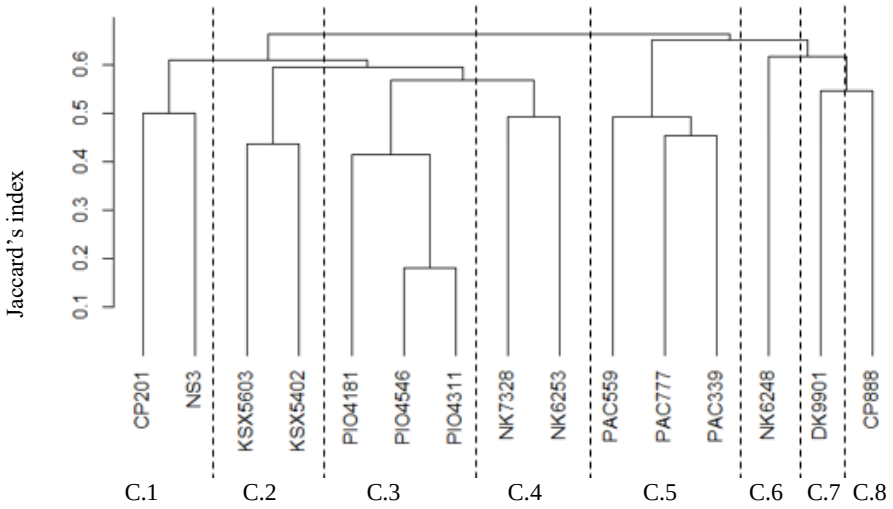

Figure 1. UPGMA dendrogram of 15 single-cross hybrids based on differences in 40 SSR loci of Jaccard's index classified a group of hybrids on the index at 0.5 into eight clusters

hybrids from the National Corn and Sorghum Research Center in cluster 2, Pioneer Hi-Bred in cluster 3, Syngenta in cluster 4, and Pacific Seeds in cluster 5. There was only the group of CP201 and NS3 in cluster 1 that came from different sources, while the remaining three groups of one hybrid each came from each company. These results indicated that hybrids from the same companies or public sector agencies were in the same cluster for at least 4 out of 5 clusters, showing relatedness of the parental lines of hybrids used by each company and public sector agency. For example, hybrids from the public sector, referred to as KSX5603 and KSX5402, used one common parent known as Ki 60 [2]. And Jaccard's index was about 0.43. The highest correlation of genetic distance was between PIO4546 and PIO4311, with an index value of about 0.18, and these hybrids came from the same company. On the other hand, hybrids from different companies were more diverse than those from the same sources, except for CP201 and NS3 in cluster 1. These were more closely related because one parental line of both NS3 (Takfa 3) and CP201 was extracted from the same genetic source, Cargill 5124001 variety (personal communication), indicating the relatedness of these hybrids. Results showed the effectiveness of SSR primers to identify the diversity or relatedness of corn germplasm in Thailand. Based on cluster analysis, six single cross hybrids were selected to study the genetic diversity (GD) as described by Troyer *et al*. [10] including NK6248 (cluster 6), PAC559 and PAC777 (cluster 5), NK7328 (cluster 4) and PIO4546 and PIO4181 (cluster 3). Also, the UPGMA dendrogram from the simple matching index of genetic distance was identical to the dendrogram from Jaccard's index of genetic distance, except for the fact that the value of the index differed.

3.2 Troyer genetic diversity (TGD)

The grain yield of single-cross hybrids (F_1) ranged from 10.26 to 11.67 t/ha and gave an average yield of 11.04 t/ha. At the same time, the grain yield of their selfing (S_1) ranged from 6.48 to 8.36 t/ha and had an average yield of 7.26 t/ha (Table 4). The average grain yield of selfing lines was less than their hybrids by about 34%, indicating inbreeding effect.

Fifteen double-cross hybrids derived from a diallel cross of 6 single-cross hybrids gave grain yields ranging from 8.69 to 10.46 t/ha with an average of 9.54 t/ha (Table 5). The crosses of

PIO4546 × PAC559 and PIO4181 × PAC559 showed the same highest yield of 10.46 t/ha, while the cross of PAC559 × NK7328 gave the lowest yield of 8.69 t/ha.

Table 4. Grain yield (t/ha) of six single-cross hybrids and their selfing (S_1) across 6 environments

	NK6248	**NK7328**	**PAC777**	**PAC559**	**PIO4546**	**PIO4181**	**Mean**
Selfing (S_1)	7.04	6.48	7.22	6.73	8.36	7.73	7.26
Single-cross hybrids (F_1)	11.12	10.79	11.09	11.33	11.67	10.26	11.04

Table 5. The average grain yield (t/ha) of the double-cross hybrids (C) across 6 environments

Hybrids	**NK6248**	**NK7328**	**PAC777**	**PAC559**	**PIO4546**	**PIO4181**
NK6248	-					
NK7328	9.16	-				
PAC777	9.87	9.08	-			
PAC559	9.36	8.69	9.04	-		
PIO4546	9.66	9.41	9.89	10.46	-	
PIO4181	10.18	9.10	10.05	10.46	9.41	-
Mean						**9.54**

To analyze the genetic diversity (GD) as described by Troyer *et al*. [10], the average grain yield of selfing (S_1) and single-cross hybrids (F_1) from Table 4 were taken to measure the average performance of the two hybrids (H), and the two self-hybrids as shown in Table 6.

Table 6. The average grain yield performance (t/ha) of the two hybrids (H) (below diagonal), and the two self-hybrids (S) (above diagonal) across 6 environments

Hybrids	**NK6248**	**NK7328**	**PAC777**	**PAC559**	**PIO4546**	**PIO4181**	**Mean[1/]**
NK6248	-	6.76	7.13	6.89	7.70	7.38	7.17
NK7328	10.96	-	6.85	6.60	7.42	7.10	6.95
PAC777	11.10	10.94	-	6.98	7.79	7.47	7.24
PAC559	11.22	11.06	11.21	-	7.54	7.23	7.05
PIO4546	11.39	11.23	11.38	11.50	-	8.04	7.70
PIO4181	10.69	10.53	10.68	10.79	10.97	-	7.44
Mean[2/]	11.07	10.94	11.06	11.16	11.29	10.73	-

[1/] self-hybrids, and [2/] hybrids

Troyer genetic diversity (TGD) for each pair of single-cross hybrids was presented in Table 7. The TGD ranged from 0.47 to 0.91 and had an average of 0.72. The TGD of hybrids from the same company ranged from 0.47 to 0.57, including NK6248 and NK7328 (TGD=0.57), PAC559 and PAC777 (TGD= 0.49), and PIO4546 and PIO4181 (TGD=0.47). The results indicated that for each pair of hybrids, both hybrids had one common parent, and the other two inbred lines were genetically unrelated [10]. On the other hand, the TGD of hybrids from different companies ranged from 0.47-0.91, indicating that some of the hybrids from various sources were derived from very diverse parents, e.g., PIO4181 × PAC777 (TGD=0.80), NK 6248 × PIO4181 (TGD=0.85), and PIO4181 × PAC559 (TGD=0.91). Theoretically, TGD = 0.75 means that both hybrids have two genetically unrelated parents, and the other two inbred lines are 50% related. Two unrelated hybrids derived from 4 genetically distinct inbred lines have TGD equal to 1 [10]. The TGD of some hybrids from different sources exhibited as hybrids from the same company, e.g., NK6248 × PAC559

(TGD=0.57), NK6248 × PIO4546 (TGD=0.53), NK7328 × PAC777 (TGD=0.55), NK7328 × PAC559 (TGD=0.52), NK7328 × PIO4181 (TGD=0.58), and PIO4546 × PAC777 (TGD=0.58), but the relatedness was not of a high degree. This result may be different from Jompuk *et al*. [11], indicating that some pairs of hybrids from various sources showed a relatively high degree of relatedness of parents (TGD=0.37). However, genetic distance indices have a value ranging from 0-1, which depends upon the percentage of relatedness of the four parents involved in both hybrids, which is a function of inbreeding depression. Furthermore, heterosis is a cumulative effect of dominant genes and the absence of epistasis [10, 11].

Table 7. Troyer's genetic diversity (TGD) of 6 commercial single-cross hybrids in Thailand

Hybrids	NK6248	NK7328	PAC777	PAC559	PIO4546	PIO4181
NK6248	-					
NK7328	0.57	-				
PAC777	0.69	0.55	-			
PAC559	0.57	0.47	0.49	-		
PIO4546	0.53	0.52	0.58	0.74	-	
PIO4181	0.85	0.58	0.80	0.91	0.47	-
Mean	0.64	0.54	0.62	0.64	0.57	**0.72**

3.3 Correlation between Jaccard's index and Troyer's genetic diversity (TGD)

The correlation coefficients between SSR analysis-based Jaccard's index and grain yield-based Troyer's genetic diversity among six single-cross hybrids were significant across six locations ($r=0.66$, $P<0.01$). This result indicated that both Jaccard's index and Troyer's genetic diversity were directionally identical as indications of corn diversity in Thailand. The yield heterosis and DNA-marker based differences had a positive correlation, which agreed with the results of previous studies using tropical corn [20, 21] and temperate corn [5, 22]. Therefore, both SSR-based analysis and Troyer's genetic diversity of grain yield can be used to separate the heterotic groups of single-cross hybrids before using them as germplasm sources, offering breeders the choice of either molecular markers or conventional breeding methods, depending on their facilities. Most of the inbred lines derived from well-adapted germplasm, either from a narrow genetic base synthetic variety or from well-adapted single crosses which in turn ended up with similar hybrids in the market [23]. So, separating heterotic groups of germplasm sources by the methods in this study will help breeders avoid using too narrow a genetic base in their breeding programs.

4. Conclusions

SSR markers and Troyer's genetic diversity (TGD) indicated the same direction of genetic diversity in commercial field corn hybrids in Thailand. There was a moderate correlation between molecular markers and inbreeding depression, as verified by Troyer's genetic diversity. TGD ranged from 0.47 to 0.91, with an average of 0.72. The UPGMA dendrogram clustered the hybrids into 8 clusters, which showed hybrids within each of four clusters coming from the same genetic sources, except for a group of CP201 and NS3, which came from different sources. The commercial field corn hybrids sold in Thailand are still more diverse, especially those from different companies. Therefore, corn breeders have a good chance to extract inbreeding lines from the commercial single-cross hybrids available on the market, and to make a new single-cross hybrid with high yield, after the grouping of single-cross hybrids by SSR markers or by Troyer's genetic diversity method.

5. Acknowledgements

The authors are grateful to the Charoen Pokphand Produce Co., Ltd., Sathorn, Bangkok, Thailand, for supporting this research.

References

[1] Napasintuwong, O., 2015. Structure of maize seed industry in Thailand. *Proceedings of the 37th National Corn and Sorghum Research Conference*. The Greenery Resort Khao Yai, Nakhon Ratchasima, Thailand, August 5-7, 2015, 30-38.

[2] Jampatong, S., 2015. Kasetsart inbred lines released from 1982-2012. Handout of the demonstration field. *Proceedings of the 37th National Corn and Sorghum Research Conference*. The Greenery Resort Khao Yai, Nakhon Ratchasima, Thailand, August 5-7, 2015, 1-10.

[3] Koshawatana, C., Grudloyma, P. and Indan, W., 2010. Inbred planting technique for Nakhon Sawan 3 hybrid maize seed production. *Kasetsart Journal (Natural Science)*, 44, 776-782.

[4] Mikel, M.A. and Dudley, J.W., 2006. Evaluation of North American dent corn from public to proprietary germplasm. *Crop Science*, 46, 1193-1205.

[5] Melchinger, A.E., 1993. Use of RFLP markers for analyses of genetic relationships among breeding materials and prediction of hybrid performance. In: D.R. Buxton, R. Shibles, R.A. Forsberg, B.L. Blad, K.H. Asay, G.M. Paulsen and R.F. Wilson, eds. *International Crop Science I*. Madison: Crop Science Society of America, pp. 621-628.

[6] Smith, J.S.C., 1988. Diversity of United States hybrid maize germplasm: Isozymic and chromatographic evidence. *Crop Science*, 28, 63-69.

[7] Xu, S.-X., Liu, J. and Liu, G.-S., 2004. The use of SSRs for predicting the hybrid yield and yield heterosis in 15 key inbred lines of Chinese maize. *Hereditas*, 141, 207-215.

[8] Xia, X.C., Reif, J.C., Hoisington, D.A., Melchinger, A.E., Frisch, M. and Warburton, M.L., 2004. Genetic diversity among CIMMYT maize inbred lines investigated with SSR markers: Lowland tropical maize. *Crop Science*, 44, 2230-2237.

[9] Xia, X.C., Reif, J.C., Melchinger, A.E., Frisch, M., Hoisington, D.A., Beck, D. and Warburton, M.L., 2005. Genetic diversity among CIMMYT maize inbred lines investigated with SSR markers. II: Subtropical, tropical midaltitude, and highland maize inbred lines and their relationships with elite U.S. and European maize. *Crop Science*, 45, 2573-2582.

[10] Troyer, A.F., Openshaw, S.J. and Knittle, K.H., 1988. Measurement and genetic diversity among popular commercial corn hybrids. *Crop Science*, 28, 481-485.

[11] Jompuk, C., Samphantharak, K. and Chowchong, S., 2000. Genetic diversity of corn hybrids from different sources in Thailand as verified by their heterotic pattern and inbreeding depression. *Kasetsart Journal (Natural Science)*, 34, 205-209.

[12] Barbosa, A.M.M., Geraldi, I.O., Benchimol, L.L., Garcia, A.A.F., Souza Jr., C.L. and Souza, A.P., 2003. Relationship of intra- and inter-population maize single crosses hybrid performance and genetic distances computed from AFLP and SSR markers. *Euphytica*, 130, 87-99.

[13] Sinkangam, B., Stamp, P., Srinives, P., Jompuk, P., Mongkol, W., Porniyom, A., Dang, N.C. and Jompuk, C., 2011. Integration of quality protein in waxy maize by means of simple sequence repeat markers. *Crop Science*, 51, 2499-2504.

[14] Jaccard, P., 1901. Distribution de la flore alpine dans le Bassin des Drouces et dans quelques regions voisines. *Bulletin de la Société Vaudoise des Sciences Naturelles*, 37(140), 41-272.

[15] Everitt, B.S., Landau, S., Leese, M. and Stahl, D. 2011. *Cluster Analysis*. 5th ed. Chichester: John Wiley & Son Inc.

[16] R Core Team., 2019. *R: A language and environment for statistical computing. R Foundation for Statistical Computing, Vienna, Austria*. [online] Available at: https://www.r-project.org/ index.html
[17] Senior, M.L., Murphy, J.P., Goodman, M.M. and Stuber, C.W., 1998. Utility of SSRs for determining genetic similarities and relationships in maize using an agarose gel system. *Crop Science*, 38, 1088-1098.
[18] Jackson, D.A., Somers, K.M. and Harvey, H.H., 1989. Similarity coefficients: Measurements of co-occurrence and association or simply measures of occurrence? *American Naturalist*, 133, 436-453.
[19] Hubalek, Z., 1982. Coefficients of association and similarity based on binary (presence-absence) data: An evaluation. *Biological Reviews*, 57, 669-689.
[20] Betran, F.J., Ribaut, J.M. Beck, D. and Gonzalez de Leon, D., 2003. Genetic diversity, specific combining ability, and heterosis in tropical maize under stress and nonstress environments. *Crop Science*, 43, 491-496.
[21] Phumichai, C., Doungchan, W., Puddhanon, P., Jampatong, S., Grudloyma, P., Kirdsri, C., Chunwongse, J. and Pulum, T., 2008. SSR-based and grain yield-based diversity of hybrid maize in Thailand. *Field Crops Research*, 108, 157-162.
[22] Smith, O.S., Smith, J.S.C., Bowen, S.L., Tenborg, R.A. and Wall, S.J., 1990. Similarities among a group of elite maize inbreds as measured by pedigree, F1 grain yield, grain yield, heterosis, and RFLPs. *Theoretical and Applied Genetics*, 80, 833-840.
[23] Hallauer, A.R., Russell, W.A. and Lamkey, K.R., 1998. Corn breeding. In: G.F. Spraque and J.W. Dudley, J.W., eds. *Corn and Corn Improvement.* Agron. Monogr. 18. ASA, CSSA and SSSA, Madison, WI, pp. 463-564.

Studying the Safety of Instant Noodles Sold in Egyptian Hypermarkets

Eman Trabia[1], Hanaa Ismail[2] and Samar Aborhyem[2]*

[1]Medical Research Institute, Alexandria University, Alexandria, Egypt
[2]Nutrition Department, High Institute of Public Health, Alexandria University, Alexandria, Egypt

Received: 11 March 2020, Revised: 20 April 2020, Accepted: 5 June 2020

Abstract

Instant noodles are one of the staple foods that are popular all around the world. Recently, global demand for noodles has been increasing gradually. This study aims to determine certain safety parameters for spices and liquid seasoning oils that are used in instant noodles available in Egyptian hypermarkets. A total of 90 packets were purchased including four of the main available brands of instant noodles. These samples were categorized as follows: Brand I produced in 7 flavors, Brand II produced in 3 flavors, Brand III produced in 3 flavors and Brand IV produced in 2 flavors. All purchased samples had nearly the same expiry date. The following parameters were measured: aflatoxin content (B1, B2, G1 and G2), heavy metals (Cd, Pb, Hg, As) and oxidation potential. Spices in all brands were free from mercury except for the seafood and shrimp flavors, which had Hg contents of 0.02 and 0.32 ppm, respectively. Cadmium contents of 0.42 and 0.36 ppm were found in shrimp flavor in brands IV and II, respectively, which were higher than the Egyptian standards (0.2 µg/g). Processed tomato flavor had the highest contamination of AFB1 (5.1 ppb). Brand IV Creamy Shrimp flavor and Brand I Special chicken flavor had the highest iodine values of 2.86 ± 0.04 and 1.45 ± 0.02, respectively. Thus consumption of instant noodles is still a risky choice because some flavors contain aflatoxins and heavy metals exceeding the Egyptian standard limits. In addition, extensive studies on experimental animals are needed to evaluate the safety of noodles and health hazards from the consumption of spices and liquid seasonings.

Key words: Aflatoxins, heavy metals, noodles, rancidity parameters, safety
DOI 10.14456/cast.2020.29

1. Introduction

Noodles are widely consumed throughout the world and their global consumption is second only to bread; it is a fast growing sector of the pasta industry. This is because instant noodles are convenient, easy to cook, low cost and have relatively long shelf-lives [1]. The cooking time of noodles is very much lower than that for other types of food products, and fast life styles in the dynamic societies of today have led to the use of this product as an ideal option for people's crucial time management process [2]. During the twentieth century, the consumption of instant noodles grew steadily, and it is still growing. Based on data from the World Instant Noodles Association in 2016, over the span of the five years from 2011-2015,

*Corresponding author: Tel: + 002 03 4285575/6, Fax: + 002 03 4288436; +201224100749,
Email: samaraborhyem@yahoo.com

people around the world consumed 507.570 million servings of instant noodles or 101.514 million servings per year. According to the global demand for instant noodles estimated by World Instant Noodles Association (WINA) in year 2017, Egypt consumption of instant noodles was found to be 150 million servings in year 2012, 170 million servings in 2013, 190 million servings in 2014, 200 million servings in 2015, and 210 million servings in 2016 [3].

Continuous consumption of these noodles may lead to heavy metal toxicity, which can result in impaired neuronal and renal functions such as liver cirrhosis, tubular nephritis dysfunction and reduction in neuropsychological function [4]. Although some of the heavy metals are within the permissible limits, instant noodles consumption could still be unsafe because of the cumulative potential of these contaminants. Moreover, consumers of some brands may be predisposed to carcinogenesis due to the high polycyclic aromatic hydrocarbons (PAH) content in those brands [5]. This study was conducted to determine the chemical composition of instant noodles available in Egyptian hyper markets. Included in the study are analysis of the aflatoxin content of instant noodles' spices and the heavy metals content of spices and liquid seasoning, and measurement of the oxidation potential of liquid seasoning materials.

2. Materials and Methods

2.1 Data collection methods and tools

A pilot study was done over the period of June-July 2017 to screen for the brand availability in the main hypermarkets in Alexandria Governorate, Egypt. The survey clarified the presence of 4 different brands of instant noodles available in markets including local and international brands. There were four different brands of instant noodles available, namely Brand I, Brand II, Brand III and Brand IV, and each brand had various flavors on sale. Six packets of each flavor from each brand were purchased from the main hypermarkets in Alexandria; and two packets of each flavor from each of the following branches; Carrefour hypermarket in Muharum Beek, Metero Hypermarket in Smouha and Fathallah hypermarket in Elmontazah. These branches were considered to be the main distributors to small markets. The collected 6 packets of the same flavor from same brand were homogenized and mixed well in a blender to obtain random and representative samples. The packets contained either spices or seasoning oil or both according to the manufacturing company. All the purchased samples had nearly the same expiry date. A total of 90 packets were purchased from the four main available brands of instant noodles. These samples were categorized as follows: Brand 1 (produced in 7 flavors), Brand 2 (produced in 3 flavors), Brand 3 (produced in 3 flavors) and Brand 4 (produced in 2 flavors).

2.2 Quantification of aflatoxins (B1, B2, G1 and G2)

The determination of the aflatoxins levels in spices packets and dried vegetables packets present in certain flavors was done using HPLC technique [6-8]. The HPLC conditions (Thermo-scientific Ultimate 3000) [8, 9] were as follows:

Mobile phase: Water 54, Methanol 29, Acetonitrile 17

Mobile phase flow: 0.5 ml/m

Column: C_{18}100Rp-18.25 cm

Fluorescence detector: Emissions 460, Excitation 360

2.3 Estimation of heavy metal content

The heavy metals in liquid seasoning, spices and dried vegetables present in some flavors were identified using inductively coupled plasma mass spectrometry (ICP-MS). ICP-MS measurements were performed using a VG Plasma Qua Ex-Cell (Thermo, Courtaboeuf,

France). The sample solutions were pumped by a peristaltic pump from tubes arranged on a CETAC, Varian 720-ES Inductively Coupled Plasma [10]. ICP-MS operating conditions were as follows:

Perkin Elmer Elan DRC II: Spray chamber Cyclonic Nebulizer, Meinhard RF power (W) 1100, Ar nebulizer gas flow (L min1) 0.6-0.9 (optimized daily),

Measures: Scan mode Peak hopping, Resolution (amu) 0.7, Replicate time (s) 1, Dwell time (s) 50 Sweeps/reading 20, Integration time (ms) 1000 and Replicates.

2.4 Sample preparation

Noodles were ground using a grinder. One hundred mg of each sample was treated with 10 ml of HNO_3 (65%), and heated up to 130°C till dryness. After cooling, 5 ml of H_2O_2 (40%) was added to the sample and then it was heated at 130°C till dryness. After cooling, the sample was then diluted with 20 ml distilled water [11-14] and filtered twice through Whatman filter paper grade II into a glass bottle [15].

Five ml of each sample of seasoning liquid oil was added to 5 ml of HNO_3 in a flask, which was then placed on hot plate at 100°C until almost complete volume reduction took place (almost to dryness). The sample was then cooled and 5 ml of HCL was added. It was then heated at 100°C till dryness. Each sample was cooled and diluted with distilled water (20 ml) and filtered twice through Whatman filter paper grade II into a glass bottle [15].

2.5 Rancidity parameters

Purchased packets of oil were taken from the samples to check rancidity which was expressed as the acid value and the iodine value [16-18].

Calculation for acid value:

$$\text{Acid value (mg KOH/g)} = \frac{\text{titration (ml)} \times 5.61}{\text{weight of sample used (g)}}$$

Calculation for Iodine value:

$$\text{Iodine value} = \frac{\text{(b-a) x 1.269}}{\text{weight of sample (g)}}$$

Where a= titration of sample (ml) and b= titration reading of blank (ml).

3. Results and Discussion

There is not much recent information available on safety of instant noodles sold in Egyptian markets. Analysis of heavy metal content in spices (Table 1) showed there was an elevated Cd concentration in Brand I with shrimp flavor (0.36µg/g), which is higher than the Egyptian Standard (ES) 7136/2010 for Cd, which is 0.2 µg/g [19]. Abou-Arab and Abou Donia [20] studied the contamination of Egyptian spices and medicinal plants with heavy metals, and found that the maximum level of Cd was 2.44 µg/g, which is in contrast to the results of the present study. In addition, Krejpcio *et al*. [21] found an elevated content of Cd in basil (0.47 mg/kg) and savory (0.40 mg/kg). However, Sharma *et al*. [22] revealed that the concentration of cadmium (Cd) in spices ranged from 0.194-3.17 ppm, which was higher than the maximum level in this study, and may have been due to the use of different types of spices; spices that may have come from different agro-ecological regions and which may have been stored differently.

Sattar *et al*. [23] found that mixed spices generally exhibited high values for trace metals, especially cadmium (0.65-1.34 µg/g), values which were higher than the maximum concentration found in the present study (Table 1). However, the highest content of trace metals found in the present study was for lead at 0.42 ppm, in Brand (IV) with shrimp flavor, which was higher than Egyptian Standard (ES) 7136/2010 (0.3 ppm). According to the Codex

Table 1. Heavy metals content (µg/g, ppm) in spices present in different studied brands of instant noodles

Spices	Unit	N	Cd	(ES) No 7136/2010	Pb	(ES) No 7136/2010	Hg	EC) No 1881/2006	As	(ES) No 7136/2010
Brand I										
Chicken flavor			0.12 ± 0.02		0.19 ± 0.03		0.0 ± 0.0		0.02 ± 0.02	
Paprika flavor			0.23 ± 0.03		0.13 ± 0.02		0.0 ± 0.0		0.01 ± 0.01	
Chicken curry flavor			0.14 ± 0.04		0.09 ± 0.01		0.0 ± 0.0		0.01 ± 0.01	
Special chicken flavor		6	0.12 ± 0.02		0.14 ± 0.01		0.0 ± 0.0	Not mentioned	0.02 ± 0.02	Not mentioned
Shrimp flavor			0.36* ± 0.02	0.20	0.26 ± 0.01		0.05 ± 0.01	in	0.03 ± 0.02	in (ES) No
Beef flavor			0.24* ± 0.03		0.18 ± 0.01	0.30	0.0 ± 0.0	(ES) No	0.02 ± 0.02	7136/2010
Vegetable flavor			0.11 ± 0.02		0.14 ± 0.04		0.0 ± 0.0	7136/2010	0.09 ± 0.02	
Super me vegetable flavor			0.16 ± 0.02		0.11 ± 0.04		0.0 ± 0.0		0.0 ± 0.0	
Brand II										
Tomato flavor	µg/g		0.18 ± 0.04		0.24 ± 0.03	0.30	0.0 ± 0.0	Not mentioned	0.0 ± 0.0	Not mentioned
Processed tomato flavor		6	0.17 ± 0.01		0.14 ± 0.03		0.0 ± 0.0	in	0.0 ± 0.0	in (ES) No
Cheese flavor			0.14 ± 0.03	0.20	0.10 ± 0.03		0.0 ± 0.0	(EC) No 1881/2	0.01 ± 0.01	7136/2010
Paprika flavor			0.15 ± 0.02		0.09 ± 0.01		0.0 ± 0.0		0.0 ± 0.0	
Brand III										
Beef flavor			0.12 ± 0.02		0.14 ± 0.04		0.0 ± 0.0	Not mentioned	0.0 ± 0.0	Not mentioned
Paprika flavor		6	0.11 ± 0.02	0.20	0.18 ± 0.04	0.30	0.0 ± 0.0	in	0.0 ± 0.0	in (ES) No
Chicken flavor			0.13 ± 0.02		0.08 ± 0.03		0.0 ± 0.0	(ES) No	0.0 ± 0.0	7136/2010
Vegetable flavor			0.19 ± 0.04		0.14 ± 0.03		0.0 ± 0.0	7136/2010	0.0 ± 0.0	
Brand IV										Not mentioned in
Sea food flavor		6	0.33* ± 0.03	0.20	0.21 ± 0.04	0.30	0.02 ± 0.02	0.50	0.04 ± 0.03	(ES) No
Shrimp flavor			0.31* ± 0.02		0.42* ± 0.04		0.02 ± 0.02		0.05 ± 0.04	7136/2010

Detection Limit: 0.01µg/g
Accuracy: 98.6%
Precision: 0.97.2%
Bias: -0.04 µg/g

standard 193-1995 toxicological guidance values, it was previously established that provisional tolerable weekly intake (PTWI) of 25 µg/kg.bw was associated with a decrease of at least 3 intelligence quotient (IQ) points in children and an increase in systolic blood pressure of approximately 3 mm Hg in adults [24].

Sattar *et al*. [23] also found that mixed spices generally exhibited high values for trace metals, especially lead (6.6-9.2 µg/g), which is in contrast to the results of the present study. Sharma *et al*. [22] stated that lead was 1.52-2.92 ppm, which is very much higher than the result of the present study. Krejpcio *et al.* [21] found elevated amounts of lead in cinnamon (6.24 mg/kg), basil (2.25 mg/kg) and savory (1.29 mg/kg). Abou-Arab and Abou Donia [20] stated that the maximum level of lead in Egyptian spices and medicinal plants in studied samples was 14.4 µg/g, which is much higher than results of the present study. All tested brands were free from mercury (Hg,) except for Brand I with shrimp flavor (0.05 ppm) and Brand (IV) with seafood and shrimp, which showed a content of 0.02 ppm, which might have been due to the presence of traces of powdered fish in the spices. Interestingly, the concentration of Hg is not mentioned in Egyptian Standards (ES) 7136/2010. Sharma *et al.* [22] revealed that mercury (Hg) concentration ranged from 0.1-0.3 ppm, which is more than double the results of this study. On the other hand, Nkansah and Amoako [25] examined the concentrations of Hg in fifteen spices available at local markets in the Kumasi Metropolis and stated that the maximum level for Hg was 0.025 mg/kg, which is nearly the same as the results of the present study.

Arsenic (As) was found at high level in Brand I with vegetable flavor (0.09 ppm), which may be attributed to the presence in the spices of traces of dried vegetables that had been irrigated with contaminated water and industrial wastes. Meanwhile, arsenic is mentioned in Egyptian Standards (ES) 7136/2010 [19]. According to Codex standard 193-1995 and toxicological guidance values, the intake of arsenic should not exceed 3.0 µg/kg bw/day (2-7 µg/kg bw/day based on the range of estimated total dietary exposure) [24].

Soliman [26] stated that the concentration of arsenic in spices and herbs available in the Egyptian market ranged from 0.02 (in paprika) to 0.11mg/kg in cloves, results which are similar to the results of this study. Research in Mumbai revealed that the concentration of arsenic (As) in fennel seed samples was 0.92 ppm [22], which was much higher than we found. Spices in Brand (I) had the highest content of Cd in shrimp flavor and Asenic in the vegetable flavor, while Brand (IV) had the highest content of Hg in shrimp flavor. The latter may be attributable to the shrimp having been raised in sea water or irrigation water that had been contaminated by heavy metals from sewage or industrial wastes.

The comparison of heavy metals content in liquid seasonings (oil) present in some of the brands of instant noodles (Table 2) revealed that Brand (IV) had the highest content of Cd (0.29 ppm) in the shrimp flavor variant, followed by seafood flavor (0.27ppm). However, Cd is not mentioned in Egyptian Standards (ES) 7136/2010. Cadmium is known to be toxic if its level exceeds the Codex toxicological guidance values, and the Cd provisional tolerable monthly intake (PTMI) is 25 µg/kg bw. The presence of metals in vegetable oils is either due to plant metabolism or contamination during the agronomic techniques of production and collection of seeds during oil extraction and treatment processes. It may also be due to materials used for packaging and storage [27].

The presence of metals in oil can facilitate oxidative degradation of the oil and decrease shelf life. It may also have adverse effects on the flavor, color and odor [28]. The concentrations of heavy metals in oil-producing plants depend on many factors, such as plant species, soil types, anthropogenic pressure, fertilization and hydrological conditions (irrigation) [29]. Szyczewski *et al*. [30] concluded that concentration of Cd in different types of oils ranges from 0.03-0.65 ppm, numbers which are in line with the present results (Table 2). Mohammed *et al*. [31] found concentrations of heavy metals in sesame oil (0.11 mg/kg) that were in line with our results. Karthik and Vijayarekha [32] found the level of mercury in sunflower oil ranged from 71.44-87.94 ppm, which is contrary to the results of the present study that indicates low Hg contamination. Differences could be due to different types of spices being added to liquid seasoning oil. Aflatoxin B1 is responsible for both toxicity and carcinogenicity. It was classified as a group I carcinogen by the International Agency for

Table 2. Heavy metals content (µg/g, ppm) in liquid seasoning oils present in different studied brands of instant noodles

Oil	unit	N	Cd	(ES) No 7136/2010	Pb	(ES) No 7136/2010	Hg	(ES) No 7136/2010	As	(ES) No 7136/2010
Brand I										
Chicken curry			0.13±0.01		0.12*±0.02		ND	Not mentioned in (ES) No 7136/2010	0.06±0.01	Not mentioned in (ES) No 7136/2010 0.1 mg/kg according to Codex
Special chicken			0.14±0.02		0.08±0.01		ND		0.02±0.01	
Vegetable	µg/g	3	0.12±0.03	Not mentioned in (ES) No 7136/2010	0.21*±0.04	0.10	ND		0.01±0.01	
Brand IV										
Sea food			0.27±0.02		0.28*±0.03		0.03±0.01	0.50	0.04±0.02	
Shrimp			0.29±0.02		0.24*±0.01		0.32±0.03		0.03±0.02	

ND: Not detected
Detection Limit: 0.01µ/g
Accuracy: 98.6%
Precision: 0.97.2%
Bias: -0.04 µ/g

Research on Cancer (IARC). The disease caused by the consumption of aflatoxins is known as aflatoxicosis, and it can lead to cancer, immune suppression and other slow pathological conditions. Acute aflatoxicosis leads to death. The liver is the main target organ [33].

The comparison of the aflatoxin B1 content of spices and paprika in different brands of instant noodles (Tables 3) revealed that processed tomato flavor in Brand (II) had the highest content of AFB1 (5.1 µg/kg), and was followed by Brand (I) vegetable flavor (4.6 µg/kg). This may be attributable to the high level of moisture in tomato and vegetables flavors during production of spices, which enhances the growth of fungus producing aflatoxins [19]. The level of AFB1 in paprika in Brand I was high (0.6 µg/kg), but less than the Egyptian Standard (ES) 7136/2010 (5 µg/kg), and thus it lies within the safe limit.

In Algeria, Azzoune *et al*. [34] reported that 23 of 36 samples of spices contained AFB1 ranging from 0.2 to 26.50 µg/kg, while Sugita-Konishi *et al*. [35] found that only one sample of 6 red pepper samples was contaminated with aflatoxins, but it was at the level of 16.7 µg/kg, which was very much higher than our results. Martins *et al*. [36] studied twelve different pre-packaged spices marketed in Portugal and found 43% of the samples including paprika and chili powder were contaminated with aflatoxin B1 in the ranges of 1-18.2 µg/kg and 1.9-2.5µg/kg, respectively, which is in line with the results of the present study .

El-Kady *et al*. [37] studied a total of 120 different samples of 24 kinds of spices and reported the presence of AFB1 (8± 35 mg/kg). Another study by Selim *et al*. [38] found the prevalence of AFB1 in 10 samples of Egyptian spices was 40%, with a mean value of 25 mg/kg, which was very much higher than results of this study. This may have been due to El-Kady *et al*. [37] studying different types of spices to those analyzed in the present research, and /or due to differences in the storage conditions [39].

The highest aflatoxins content reported in this work was in Brand (II) processed tomato flavor (10.74 µg /kg) (Table 4). A UK study found that nine samples from eighteen different spices were contaminated with total aflatoxins above the recommended level for aflatoxins in the UK (10 µg/ kg), and the highest level was 48 µg /kg in chili powder, which was much higher than results of the present study [40]. Contamination of spices starts mainly in the field due to the humidity and high temperature in which plants are grown, and it can continue during handling and processing because of drying on bare ground. Contamination can be prevented by growing and harvesting spices according to good agricultural practices in areas free from harmful chemicals. Appropriate quality control measures in accordance with the principals of good handling practice, good manufacturing practice, hazard analysis and critical control points should be implemented at all stages after harvesting.

Aflatoxin B1 in dried vegetables in Brand IV seafood flavor, which was the only brand containing dried vegetables, was 0.17 µg /kg (Table 5). A study on aflatoxins in dried vegetables in Benin, Mali and Togo showed dried vegetables were contaminated with fungi, which led to mycotoxin development and the presence of aflatoxin B1 and aflatoxin B2 in dried okra to the extent of 5.4 µg /kg and 0.6 µg/kg, respectively. Total aflatoxins content was 6 µg /kg in okra and 3.2 µg /kg in hot chili [41], which is in line with results for chili powder in the present study. The assessment of aflatoxins in dried vegetables from selected markets in Kaduna Metropolis revealed that the highest aflatoxin content was in dried baobab at 31.6µg/kg, while 27.00 µg/kg were found in dried okra and 26.40 µg/kg in red chili pepper. Tomatoes had the lowest aflatoxin content (6.50 µg /kg) [42]. The results were much higher than our results. This could be due to different items to ours being analyzed.

High iodine values indicate high degrees of unsaturation and high susceptibility to rancidity. Brand IV shrimp flavor had the highest iodine value (2.86 µg/g), while Brand I vegetable flavor (0.96 µg/g) contained the least unsaturation and susceptibility to rancidity (lipid oxidation) (Table 6) and thus offered a longer shelf life. High unsaturated fats under conditions of high temperature and humidity are liable to bacterial attack. The bacteria can secret lipase enzymes which break double bonds giving free fatty acids responsible for off flavor, bad taste and rancidity [43]. The comparison of acid values for liquid seasoning present in different studied brands of instant noodles clarified that Brand I vegetable flavor had the highest acid value (5.8 mg/g) (Table 7), indicating a high degree of rancidity with

liberation of free fatty acid. The lowest amount was found in Brand IV shrimp flavor (1.96 mg/g). However, there is not enough information about rancidity parameters in liquid seasoning oils in noodles from previous studies.

Table 3. Aflatoxin B1 content (µg/kg) in spices and paprika in different brands of instant noodles

Spices	**Aflatoxin B1 (µg/kg)**	**(ES) No 7136/2010 (µg/Kg)**
Brand I (Indomie)		
Chicken flavor	0.9	
Paprika	0.6	
Chicken curry flavor	0.15	
Special chicken flavor	0.11	
Shrimp flavor	0.18	
Beef flavor	0.12	
Vegetable flavor	3.4	
Super me vegetable flavor	4.6	
Brand II (El Maleka)		
Tomato flavor	2.8	5
Processed tomato flavor	5.1*	
Cheese flavor	3.2	
Paprika flavor	0.19	
Brand III (Kelloges)		
Beef flavor	0.6	
Paprika	0.15	
Chicken flavor	0.18	
Vegetable flavor	2.2	
Brand IV (FF)		
seafood flavor	0.14	
Creamy shrimp flavor	0.17	

Detection Limit: 0.5µg/kg
Accuracy: 99.1%
Precision: 0.98.4%
Bias: -0.2 µg/kg

Table 4. Aflatoxins content (µg/kg) in spices and paprika of different brands of instant noodles

Spices	Aflatoxins (µg/kg)					
	AFB1	**AFB2**	**AFG1**	**AFG2**	**AFB1+ AFB2+ AFG1+ AFG2**	**(ES) No 7136/2010**
Brand I (Indomie)						
Chicken flavor	0.9	0.5	0.42	0.38	2.2	
Paprika	0.6	0.33	0.5	0.28	1.71	
Chicken curry flavor	0.15	0.16	0.12	0.19	0.62	
Special chicken flavor	0.11	0.18	0.23	0.13	0.65	
Shrimp flavor	0.18	0.7	0.5	0.28	1.66	
Beef flavor	0.12	0.09	0.17	0.15	0.53	
Vegetable flavor	3.4	1.6	1.1	0.7	6.8	
Super me vegetable flavor	4.6	0.15	0.7	0.41	5.86	
Brand II (El Maleka)						
Tomato flavor	2.8	1.7	0.15	0.19	4.84	10
Processed tomato flavor	5.1	4.1	1.4	0.14	10.74*	
Cheese flavor	3.2	1.2	1.8	0.14	6.34	
Paprika flavor	0.19	0.15	0.11	0.24	0.69	
Brand III (Kelloges)						
Beef flavor	0.6	0.21	0.5	0.34	1.65	
Paprika	0.15	0.33	0.24	0.19	0.91	
Chicken flavor	0.18	0.11	0.19	0.28	0.76	
Vegetable flavor	2.2	0.8	0.12	0.6	3.72	
Brand IV (FF)						
seafood flavor	0.14	0.19	0.28	0.36	0.97	
Creamy shrimp flavor	0.17	0.22	0.18	0.19	0.76	

Detection Limit: 0.5µg/kg
Accuracy: 99.1%
Precision: 0.98.4%
Bias: -0.2 µg/kg

Table 5. Aflatoxins content (µg/kg) in dried vegetables

dried vegetables	Results (µg/kg)					
	AFB1	**AFB2**	**AFG1**	**AFG2**	**AFB1+ AFB2+ AFG1+ AFG2**	**(ES) No 7136/2010**
Brand IV (FF) Seafood flavor	0.17	0.25	0.16	0.17	0.75	4

Detection Limit: 0.5µg/kg
Accuracy: 99.1%
Precision: 0.98.4%
Bias: -0.2 µg/kg

Table 6. Iodine values for liquid seasoning present in different studied brands of instant noodles

Palm oil	Iodine (µg/g)	Codex Standard 210-1999 for palm oil
Brand IV, Creamy shrimp flavor	2.86 ± 0.04	50-55 g/100 g = 0.5-0.55 g/g
Brand I, Chicken curry flavor	1.13 ± 0.03	
Brand I, Special chicken flavor	1.45 ± 0.02	
Brand I, Vegetable flavor	0.96 ± 0.03	

Table 7. Acid values (mg/g) for liquid seasoning present in different studied brands of instant noodles

Palm oil	Acid value(mg/g)	Codex Standard 210-1999 for palm oil
Brand IV, Creamy Shrimp flavor	1.96 ± 0.02	10 mg KOH/g
Brand I, Chicken curry flavor	3.8 ± 0.02	
Brand I, Special chicken flavor	4.6 ± 0.03	
Brand I, Vegetable flavor	5.8 ± 0.03	

4. Conclusions

The seafood flavor and shrimp flavor of Brands I and IV were the most contaminated flavors with respect to heavy metals. Cadmium (Cd) and lead (Pb) contents of Brand IV exceeded the Egyptian standards (ES No. 71361/2010). Brands I and IV were the only brands that included liquid seasoning oil in various flavors. Brand IV had the highest contamination of Cd, Pb, and Hg in its two flavors, while the highest As contamination was found in the chicken curry flavor of Brand I. There was no available data in (ES) No 7136/2010 about heavy metals in liquid oil seasoning except for Pb, which had the limit of 0.10 ppm. In any case, the studied samples fell above this limit, except for Brand I with special chicken flavor. Brand II, with processed tomato flavor, had the highest contamination of aflatoxins, a level which was higher than (ES) No 7136/2010. Other brands were below that limit. Brand I with special chicken flavor had the lowest aflatoxin contamination, and can thus be considered as the safest brand for aflatoxin contamination. Brand IV shrimp flavor had the highest iodine value, while the least value for it was found in Brand I vegetable flavor, which was below the limit stated by the Codex (0.5-0.55 g/g). Brand I vegetable flavor had the highest acid value of 5.8 ± 0.03mg/g, while Brand IV shrimp flavor had the lowest acid value. Brand IV had a high iodine value and low acid value, which suggested no rancidity and no lipid peroxidation when compared to Brand I, with low iodine value and high acid value, suggesting it would be more susceptible to rancidity and lipid peroxidation. The consumption of instant noodles is still a risky choice because some flavors contain aflatoxins and heavy metals at levels exceeding the Egyptian standard limits. In addition, the risk of lipid oxidation for liquid seasoning oils is evident. Extensive studies on experimental animals are recommended to evaluate noodle safety and health hazards associated with consumption of spices and liquid seasoning oils.

5. Acknowledgements

The authors wish to thank the Central Laboratory's staff, High Institute of Public Health, Alexandria University, for facilitating the analysis of the samples.

References

[1] Onyema, C., Ekpunobi, U., Edowube, A., Odinma, S. and Sokwaibe, C., 2014. Quality assessment of common instant noodles sold in Nigeria markets. *American Journal of Analytical Chemistry*, 5, 1174-1177.

[2] Navaratne, S.B, 2015. *Pasta Products Technology*. [online] Available at: https://www.researchgate.net/publication/284725118_PASTA_PRODUCTS_TECHNOLOGY.

[3] World Instant Noodles Association (WINA), 2020. *Global Demand for Instant Noodles*. [online] Available at: https://instantnoodles.org/en/ noodles/market.html.

[4] Jarup, L., 2003. Hazards of heavy metal contamination. *British Medical Bulletin*, 68, 167-182.

[5] Charles, I.A., Ogbolosingha, A.J. and Afia, I.U., 2018. Health risk assessment of instant noodles commonly consumed in Port Harcourt, Nigeria. *Environmental Science and Pollution Research International*, 25(3), 2580-2587.

[6] Qiang, X., Weiss, M., Kogel, K.H. and Schafer, P., 2012. *Piriformospora indica*-a mutualistic basidiomycete with an exceptionally large plant host range. *Molecular Plant Pathology*, 13(5), 508-518.

[7] Wang, B. and Zhou, S.F., 2009. Synthetic and natural compounds that interact with human cytochrome P450 1A2 and implications in drug development. *Current Medicinal Chemistry*, 16(31), 4066-4018.

[8] Wogan, G.N., Kensler, T.W. and Groopman, J.D., 2012. Present and future directions of translational research on aflatoxin and hepatocellular carcinoma. A review. *Food Additives & Contaminants. Part A, Chemistry, Analysis, Control, Exposure & Risk Assessment*, 29(2), 249-257.

[9] Ghasemi-Kebria, F., Joshaghani, H., Taheri, N.S., Semnani, S., Aarabi, M., Salamat, F. and Roshandel, G., 2013. Aflatoxin contamination of wheat flour and the risk of esophageal cancer in a high risk area in Iran. *Cancer Epidemiology*, 37(3), 290-293.

[10] Noel, L., Chekri, R., Millour, S., Vastel, C., Kadar, A., Sirot, V. and Guerin, T., 2012. Li, Cr, Mn, Co, Ni, Cu, Zn, Se and Mo levels in foodstuffs from the second French TDS. *Food Chemistry*, 132(3), 1502-1513.

[11] Molan, A., Flanagan, J., Wei, W. and Moughan, P., 2009. Selenium-containing green tea has higher antioxidant and prebiotic activities than regular green tea. *Food Chemistry*, 114(3), 829-835.

[12] Muntean, N., Muntean, E., Creta, C. and Duda, M., 2013. Heavy metals in some commercial herbal teas. *ProEnvironment*, 6, 591-594.

[13] Adamczyk-Szabela, D., Anielak, P. and Wolf, W.M., 2017. Influence of digestion procedure and residual carbon on manganese, copper, and zinc determination in herbal matrices by atomic absorption spectrometry. *Journal of Analytical Methods in Chemistry*, 2017, 1-11.

[14] Choi, Y., Kim, J., Lee, H.S., Kim, C., Hwang, I.K., Park, H.K. and Oh, C.H., 2009. Selenium content in representative Korean foods. *Journal of Food Composition Analysis*, 22(2), 117-122.

[15] Khan, N., Jeong, I.S., Hwang, I.M., Kim, J.S., Choi, S.H., Nho, E.Y. and Kim, K.S., 2014. Analysis of minor and trace elements in milk and yogurts by inductively coupled plasma-mass spectrometry (ICP-MS). *Food Chemistry*, 147, 220-224.

[16] Egan H., Kirk R.S. and Sawyer, R., 1981. *Pearson's Chemical Analysis of Foods*. New York: Churchilli Livingstone.

[17] Malcolmson, L.J., Przybylski, R. and Daun, J.K., 2000. Storage stability of milled flaxseed. *Journal of the American Oil Chemists' Society*, 77(3), 235-238.

[18] Kalantari, F., Bahmaei, M., Ameri, M. and Shoaei, E., 2010. Effect of vegetable oil oxidation on the hydrogenation reaction process. *Grasas y Aceites*, 61(4), 361-368.

[19] Egyptian Organization for Standardization and Quality, 2010. *Maximum levels for certain contaminants in foodstuffs, ICS: 67.020 Egyptian standards ES: 7136/2010*. Egypt: Egyptian Organization for Standardization and Quality.

[20] Abou-Arab, A.A. and Abou Donia, M.A., 2000. Heavy metals in Egyptian spices and medicinal plants and the effect of processing on their levels. *Journal of Agricultural and Food Chemistry*, 48(6), 2300-2304.
[21] Krejpcio, Z., Krol, E. and Sionkowski, S. 2007. Evaluation of heavy metals contents in spices and herbs available on the Polish market. *Polish Journal of Environmental Studies*, 16, 97-100.
[22] Sharma, N., More, B., Bhandari, D. and Wavhal, D., 2012. Analysis of heavy metals content in spices collected from local market of Mumbai by using atomic absorption spectrometer. *Global Journal for Research Analysis*, 3, 56-57.
[23] Sattar, A., Wahid, M. and Durrani, S.K., 1989. Concentration of selected heavy metals in spices, dry fruits and plant nuts. *Plant Foods for Human Nutrition*, 39(3), 279-86.
[24] CODEX, 2009. *CODEX General Standard for Contaminants and Toxins in Food and Feed (CODEX STAN 193-1995)*. [online] Avilable at: http://www.fao.org/fileadmin/user_upload/livestockgov/documents/1_CXS_193e.pdf.
[25] Nkansah, M. and Amoako, C., 2010. Heavy metal content of some common spices available in markets in the Kumasi metropolis of Ghana. *American Journal of Scientific and Industrial Research*, 1, 158-163.
[26] Soliman, N.F., 2015. Metals contents in spices and herbs available on the Egyptian market: Assessment of potential human health risk. *The Open Conference Proceedings Journal*, 6(1), 24-29.
[27] Dantas, T.N.C., Neto, A.A.D., Moura, M.C.P.A., Neto, E.L.B., Forte, K.R. and Leite, R.H.L., 2003. Heavy metals extraction by microemulsions. *Water Research*, 37(11), 2709-2717.
[28] Sahan, Y. and Basoglu, F., 2008. *Trace Metals in Olive Oil*. [online] Available at: https://DOI:10.17660/ActaHortic.2008.791.109
[29] Mendil, D., Uluozlu, O.D., Tuzen, M. and Soylak, M., 2009. Investigation of the levels of some element in edible oil samples produced in Turkey by atomic absorption spectrometry. *Journal of Hazardous Materials*, 165(1-3), 724-728.
[30] Szyczewski, P., Frankowski, M., Ziola-Frankowska, A., Siepak, J., Szyczewski, T. and Piotrowski, P., 2016. A comparative study of the content of heavy metals in oils: Linseed oil, rapeseed oil and soybean oil in technological production processes. *Archives of Environmental Protection*, 42(3), 37-40.
[31] Mohammed, F., Abdulwali, N., Guillaume, D., Tenyang, N., Ponka, R., Al-Gadabi, K. and Naji, K., 2018. Chemical composition and mineralogical residence of sesame oil from plants grown in different Yemeni environments. *Microchemical Journal*, 140, 269-277.
[32] Karthik, D. and Vijayarekha, K., 2015. Tracing mercury and cadmium sources in edible sunflower oil. *Rasayan Journal of Chemistry*, 8(4), 448-451
[33] Santini, A. and Ritieni, A., 2013. Aflatoxins: risk, exposure and remediation. In M. Razzaghi-Abyaneh, ed. *Aflatoxins-Recent Advances and Future Prospects*, Rijeka: In Tech, pp. 343-376.
[34] Azzoune, N., Mokrane, S., Riba, A., Bouras, N., Verheecke, C., Sabaou, N. and Mathieu, F., 2016. Contamination of common spices by aflatoxigenic fungi and aflatoxin B1 in Algeria. *Quality Assurance and Safety of Crops & Foods*, 8(1), 137-144.
[35] Sugita-Konishi, Y., Sato, T., Saito, S., Nakajima, M., Tabata, S., Tanaka, T. and Sugiyama, K., 2010. Exposure to aflatoxins in Japan: risk assessment for aflatoxin B1. *Food Additives and Contaminants*, 27(3), 365-372.
[36] Martins, M.L., Martins, H.M. and Bernardo, F., 2001. Aflatoxins in spices marketed in Portugal. *Food Additives & Contaminants*, 18(4), 315-319.
[37] El-Kady, I., El-Maraghy, S. and Mostafa, M.E., 1995. Natural occurrence of mycotoxins in different spices in Egypt. *Folia Microbiologica*, 40(3), 297-300.
[38] Selim, M.I., Popendorf, W. and Ibrahim, M.S., 1996. Aflatoxin B1 in common Egyptian foods. *Journal of AOAC International*, 79(5), 1124-1129.

[39] Elshafie, A.E., Al-Rashdi, T.A., Al-Bahry, S.N. and Bakheit, C.S., 2002. Fungi and aflatoxins associated with spices in the Sultanate of Oman. *Mycopathologia*, 155(3), 155-160.
[40] Macdonald, S. and Castle, L., 1996. A UK retail survey of aflatoxins in herbs and spices and their fate during cooking. *Food Additives & Contaminants*, 13(1), 121-128.
[41] Hell, K., Gnonlonfin, B., Kodjogbe, G., Lamboni, Y. and Abdourhamane, I., 2009. Mycoflora and occurrence of aflatoxin in dried vegetables in Benin, Mali and Togo, West Africa. *International Journal of Food Microbiology*, 135(2), 99-104.
[42] Nafisa, A., Datsugwai, M.S.S. and Zakari, L., 2017. Assessment of aflatoxins and aflatoxigenic fungi associated with dried vegetables from selected markets within Kaduna Metropolis. *Industrial Engineering*, 1(2), 68-73.
[43] Okparanta, S., Daminabo, V. and Solomon, L., 2018. Assessment of rancidity and other physicochemical properties of edible oils (mustard and corn oils) stored at room temperature. *Journal of Food and Nutrition Sciences*, 6(3), 70-75.

The Relationships Between Extreme Precipitation and Rice and Maize Yields Using Machine Learning in Sichuan Province, China

Jun Fan[1]*, Attachai Jintrawet[2] and Chanchai Sangchyoswat[2]

[1]Agricultural System Resource Management Program, Center for Agricultural Resources System Research, Chiang Mai University, Chiang Mai, Thailand
[2]Department of Plant and Soil Sciences and Center for Agricultural Resource System Research, Chiang Mai University, Chiang Mai, Thailand

Received: 26 February 2020, Revised: 20 May 2020, Accepted: 10 June 2020

Abstract

Rice and maize are two staple crops that play a critical role in food security in the southwest of China. They are sensitive to extreme climate events such as drought and flood. Therefore, the assessment of the future production of these crops in an era of climate change is essential. However, current assessment tools are time consuming and require extensive input datasets and expert knowledge. This study is an attempt to provide an alternative tool for prefecture level users using an aggregate Z-index which uses precipitation as an input. A machine learning algorithm (Random Forest) was introduced to build and train the model. Finally, future precipitation projected from Global Climate Models (GCMs) was used as an input to assess the future rice and maize yield variations. This tool outperformed other conventional statistical tools and was especially suitable for assessing extreme cases. Crop yields are significantly affected by drought in the study area. Z-indexes derived from three GCMs on decadal time scales were used for assessing future yield variations. Under the lower emission Representative Concentration Pathway (RCP) 4.5, average maize yields and rice yields are likely to be reduced by -0.58% and -1.49%, respectively, over the next three decades in Mianyang prefecture compared to the baseline period. Similarly, under the higher emission (RCP) 8.5, maize yields and rice yields may decrease by -0.75% and -1.30%, respectively. This assessment tool can be applied in other locations, providing that datasets are available to meet the user's needs.

Keywords: extreme precipitation, machine learning, climate scenarios, yield forecasting, random forest
DOI 10.14456/cast.2020.30

*Corresponding author: Tel: 053-221275, Fax: 053-210000
Email: thebestone2007@sina.com

1. Introduction

Rice and maize are the dominant crops in Sichuan province, accounting for about 90% of the total cereal grain output and about 83% of the food crop sown in the area in 2017 [1]. Rice is fully irrigated, while maize is mostly rainfed in this area. Rice is the staple food for human consumption and maize is the major animal feedstuff. Thus, the production of rice and maize is critical for food security and the national self-sufficiency policy [2-4]. However, rice and maize production is sensitive to extreme climate events. For example, the big droughts in 1994 and 2006 severely damaged crop production [5, 6].

Extreme climate events are projected to be more frequent and intensive in the future due to climate change [7]. Although extreme climate events are defined by different criteria and thresholds, abnormal temperature and extreme precipitation are the main extreme climate events and are widely studied [8, 9]. In the southwest part of China, droughts and floods, which are related to extreme precipitation, are key extreme climate events [10, 11]. Extreme climate events inevitably affect an ecosystem's quality and productivity. Chen *et al.* [12] found that extreme climate events have decreased Gross Primary Productivity by 2.8% annually in China over the past three decades. They also highlighted that Gross Primary Productivity is more sensitive to drought than to other factors. Moreover, that extreme climate events directly damage crop yields has been reported by many researchers using different methods such as crop models and econometrics [13-17]. Drought, heat and heavy rain are the three main extreme events that affect crop production [18].

The effects of extreme climate events on agricultural systems are expected to increase in the future [19]. Therefore, anticipating and assessing the influence of extreme climate events on crop yield is important for better decision making. When studying the effects of future extreme climate events on crop yield, two crop model families, namely DSSAT (Decision Support System for Agrotechnology Transfer) and APSIM (Agricultural Production Systems Simulator) are widely used for simulating crop yield and other variables. However, these crop models do not fully capture the impact of extreme events [18]. Moreover, the use of crop models often requires expert knowledge and an extensive number of input datasets, which are lacking at the prefecture level [20]. The aim of this study is to provide a reliable alternative assessment tool that captures the impact of key extreme climate events (extreme precipitation) on rice and maize production. Consequently, the decision makers at prefecture level can apply the tool to gain better understanding of the relationships between crop production and extreme precipitation and adjust their policies accordingly.

2. Materials and Methods

2.1 Study areas

Mianyang, Dazhou and Leshan prefecture-level cities in Sichuan province, China (Figure 1) were chosen to be the study areas as they are typical crop production areas distributed in the eastern Sichuan province (the western Sichuan province is one part of the Tibet Plateau and has a different agricultural system). Mianyang was chosen to be the main study area, while Dazhou and Leshan were used to validate the assessment method. The climate zone of the study areas was warm temperate, winter dry and hot summer. Historic annual precipitation for Mianyang, Dazhou and Leshan are 546-1237 mm, 874-1693 mm, 769-1720 mm, respectively [1]. The main crops in the study areas are rice, maize and wheat.

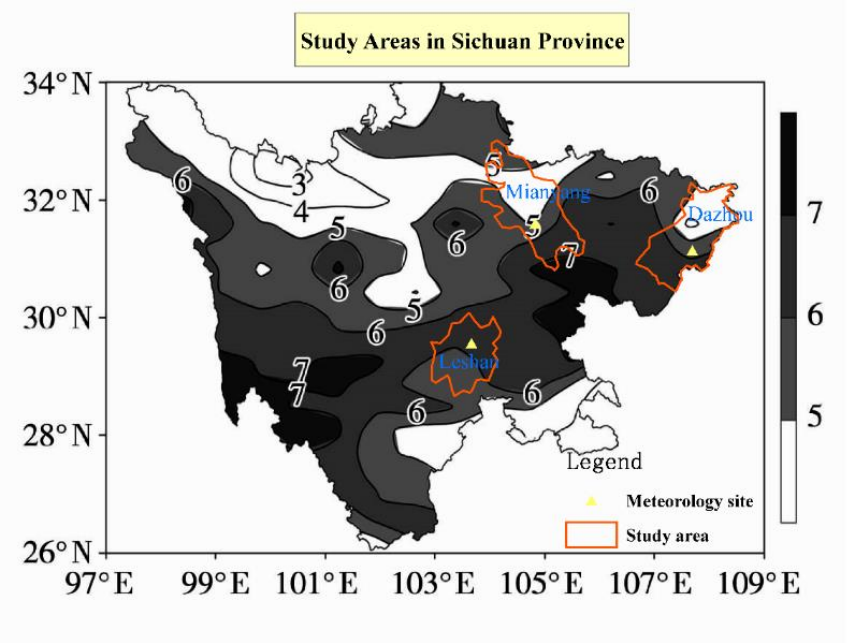

Figure 1. Location of the study areas (red polygon) in Sichuan province. The background map is the drought map in 2006 summer based on Z-index [23], the darker and the higher number is the drier zone

2.2 Defining extreme precipitation by the aggregate Z-index

This study focused on precipitation-related extreme events because the frequency of temperature-related extreme events such as maximum temperatures showed little change in the study area, and the intensity of heat waves was even decreasing. On the other hand, precipitation-related events such as droughts were increasing in terms of frequency [21, 22]. The Palmer Z-index is a method to calculate short-term drought, and it was applied in Sichuan province, China [23]. Assuming monthly precipitation follows a generalized gamma distribution, it can be transformed to normal distributions [23]. The transformation process is as follows:

$$Z_i = \frac{6}{C_s}\left(\frac{C_s}{2}\varphi_i + 1\right)^{\frac{1}{3}} - \frac{6}{C_s} + \frac{C_s}{6} \quad (1)$$

$$C_s = \frac{\sum_{i=1}^{n}(X-\bar{X})^3}{n\sigma^3} \quad (2)$$

$$\varphi_i = \frac{X-\bar{X}}{\sigma} \quad (3)$$

Where Z_i is the index value, C_s is a coefficient, φ_i is the normalized precipitation variable, X is the monthly precipitation amount, n is the number of total samples, and $\bar{X}$ and σ are the mean and standard deviation of X respectively.

After calculating the Z-index, the extreme events can be classified into seven categories by distribution quantiles. These seven categories are 'Extreme dry', 'Severe dry', 'Moderate dry', 'Normal', 'Moderate wet', 'Severe wet' and 'Extreme wet'. Table 1 lists the details of all the seven categories.

Table 1. The categories of extreme events based on monthly precipitation and its Z-index values

Category	Value Range	Quantile
Extreme dry	Z<-1.65	less than 5%
Severe dry	-1.65<Z<-1.04	5%--15%
Moderate dry	-1.04<Z<-0.52	15%--30
Normal	-0.52<Z<0.52	30---70%
Moderate wet	0.52<Z<1.04	70%--85%
Severe wet	1.04<Z<1.65	85%--95%
Extreme wet	Z>1.65	greater than 95%

Using precipitation data, we first calculated the monthly Z-index during the crop growing period, which is from April to August in the region. Next, except for the Z-index values which fell into the normal category, all remaining negative Z-index values were aggregated into a drought class, and all remaining positive Z-index values into a flood class. For example, the Z-index values for April to August 1987 were 0.36, -1.02, 1.9, 0.66, -0.09, so the aggregated wet value which denoted flood was 1.9 + 0.66 = 2.56. We did not add 0.36 into the aggregate wet value as it fell into the Normal category. Likewise, the aggregate dry value was -1.02, as -0.09 was in the Normal class.

2.3 Historic and future precipitation data

Historic daily precipitation data for the three study areas from the years 1985 to 2017 were obtained and cross-checked from the China Academic of Agricultural Engineering's greenhouse data program (http://data.sheshiyuanyi.com/WeatherData/), Statistical Bureau of Sichuan (http://tjj.sc. gov.cn/tjcbw/tjnj) and the Statistical Bureau of Mianyang (http://tjj.my.gov.cn/myoldfiles/mytjnj/index.html). Daily precipitation data was accumulated into monthly precipitation to calculate the Z-index, then monthly Z-indices were aggregated to the yearly dataset to match the crop yield dataset. A total of 180,675 historic daily precipitation records were collected in the three study areas.

Output from three Global Climate Models (GCMs), the BCC_CSM1_1_M, the CESM1_CAM5, and the IPSL_CM5A_MR models, were bias-corrected [24] to provide projected future precipitation for Mianyang prefecture for the period 2020 to 2050. The data simulated by these models were based on the Coupled Model Inter-comparison Project phase five (CMIP5), and two future scenarios were considered: RCP 4.5 and RCP 8.5. The simulated precipitation from these three GCMs were used to calculate the future Z-index separately. We defined the future periods into three decades, namely the 2020s (2020-2029), 2030s (2030-2039), and 2040s (2040-2050) to compare and check if the simulated precipitation and corresponding Z-index were consistent. All the bias-corrected daily precipitation data were obtained from the research program on Climate Change, Agriculture and Food Security (http://www.ccafs-climate.org/data_bias_correction/) and accumulated into monthly precipitation data to calculate the Z-index. Then, the monthly Z-indices were aggregated to a yearly dataset for predicting crop yield. In total, 407,340 daily precipitation records from three GCMs were collected, and it should be noted that the data from September to the following March were not used.

2.4 Predicting crop yield by Random Forest

Machine learning algorithms such as Artificial Neural Network (ANN), Support Vector Machine (SVM) and Random Forest (RF) have been introduced for predicting crop yield in recent years. Choosing the right algorithm depends on the data and research objective. ANN and SVM require a stationary dataset, carefully scaled input data, and a large training dataset [25, 26]. However, crop yield data are typically nonstationary time-series data, so the use of ANN requires data transformation. Moreover, it has been reported in the literature that RF outperformed simple ANN, SVM, Generalized Additive Models, and K-Nearest Neighbors in the predictions that involve extreme events [13, 27]. Since the extreme cases are the focus of this study, and requirements are that the model should be simple and easy to use, and that the data size is not large, the Random Forest was chosen as the main machine learning algorithm. To evaluate the Random Forest prediction, this study also applied Multiple Linear Regression (MLR) and SVM as the benchmark.

Random Forest is one of the fundamental Machine Learning algorithms. It was invented by Breiman [28], and it is an effective statistical tool for prediction. The algorithm derives from a decision-making tree that works by asking a sequence of queries about the available data until it arrives at a decision. Random Forest decision trees randomly sample training data to build each tree and randomly set features when splitting nodes. Random Forest can be used for both classification and regression. There are many open-source packages that provide the Random Forest algorithm in different programing languages. Here, we used the Python programing language version 3.7 and the Random Forest regression algorithm available in the scikit-learn package [29]. The maximum depth parameter (max_depth) was set to 10 to avoid over-fitting, and all the other parameters were set at their default values initially. For example, the number of trees in the forest (n_estimators) was '10' and the minimum number of samples required to be at a leaf node (min_samples_leaf) was '1'. These parameters were then adjusted during the training process to find the best performance. Feature Importance is a built-in function that is used for measuring the relative importance among the input features in Random Forest. Its value for a specific feature ranges from zero to one (the higher the value, the more important the feature is), while the sum of all values is one. The value is calculated by the number of samples that reached a node divided by the total number of samples. Detailed calculations can be found in Ronaghan [30] and Louppe [31].

Similarly, SVM regression was performed using the scikit-learn package with all the parameters initially set at their default values (kernel='rbf', C=1, epsilon=0.1 and so on). They were then tuned to find the best performance.

Aggregate Z-index values (both drought and flood classes) and time were used as the input features (independent variables), whereas crop yields of each year were used as the output feature (dependent variable). Time (years) was chosen to be an input variable because temporal yield increased due to technology and management improvement [32]. Alternatively, accumulated precipitation in the crop growing season and time were also used as input features to check if using the Z-index was better than using precipitation in crop yield prediction. Historic data in Mianyang prefecture was firstly used to train and generate the model. In order to validate the model, the dataset was divided into two parts randomly: one for training, the other one for testing. Empirically, the training was set to 70-80% of the total dataset. If the percentage is too high, the model can be overloaded, and thus lack prediction capability. On the other hand, if the percentage is too low, the low number of samples cannot generate a good model. Considering our dataset, we tried the proportions of 70%, 75% and 80%, and they all generated similar results. Therefore, 75% of data was used for training. Indeed, this ratio was the default value of the split function in scikit-learn. To make the result reproduceable and accountable for the extreme dry/wet years in the training part, we set the split random state to eight. This study used R^2 and Root Mean Square

Error (RMSE) as the model's performance criteria during the comparison between observed data and model predictions. After the model was generated and tested in Mianyang, we applied this method (Z-index plus Random Forest) to another two areas (Dazhou and Leshan) to check if this method was applicable in other places.

Finally, the future aggregate Z-index values of Mianyang that were derived from bias-corrected GCMs were used to predict the future yields in Mianyang prefecture. We used the average yields from 2011 to 2017 (2010s) as the baseline to analyze the yield variations of future periods, namely, the 2020s, 2030s and 2040s.

2.5 Crop yield data

Rice and maize are two economic and staple crops in the main growing season in the study areas. Each year, crop production data as well as the harvest area at prefecture level were obtained, and then crop yields were calculated. Thirty-three years (from 1985 to 2017) of rice and maize yields for Mianyang were obtained from the Statistical Bureau of Mianyang (http://tjj.my.gov.cn/myoldfiles/mytjnj/index.html), and 19 years (from 1999 to 2017) of rice yields for Dazhou and Leshan were obtained from the Statistical Bureau of Sichuan (http://tjj.sc.gov.cn/tjcbw/tjnj). For the few years of missing data for Dazhou and Leshan prefectures, provincial yield data were used to estimate prefectural-level yield, assuming that prefectural-level yield would increase/decrease by the same proportion as the provincial yield in that year. For example, the rice yield of Dazhou in 2004 was missing. However, the yield of previous year was 7.77 (ton/ha) and the provincial yield had decreased 0.3% in 2004. Therefore, the estimate for the rice yield of Dazhou in 2004 was $7.77 \times (1\text{-}0.3\%) = 7.75$. In total, there are 104 crop yield records in the three study areas, of which 66 records are in Mianyang (rice 33, maize 33), 19 records are in Dazhou (only rice), and 19 records are in Leshan (only rice).

3. Results and Discussion

3.1 Historic crop yield, precipitation, and Z-index in Mianyang

Both rice and maize yields generally increased over the past three decades. However, yields were very low in years 1994, 2001 and 2006, mainly due to the extreme dry events. Interestingly, maize yield was low in 1986, while rice yield was not affected. Figure 2A shows the yield changes of both rice and maize from 1985 to 2017 with the aggregate Z-index values. Every significant drop in yield occurred when there was a large negative aggregate Z-index [6].

Over the past three decades, the average precipitation was 592 ± 161 mm during the rice and maize growing seasons. Typically, April and May have the lowest precipitation and July and August have the highest precipitation. The historic monthly precipitation in Mianyang prefecture (Figure 2B) roughly showed that extreme dry years happened in 1994, 2000, and 2015, while extreme wet years happened in 1988, 1998, and 2017. The Aggregate Z-index values gave more accurate assessment of the extreme dry/wet events as they were designed and accounted for the abnormal precipitation. For example, the years 2006, 1994 and 2001 were the top three extreme dry years, whereas the years 1998, 2004 and 1990 were the three wettest years (Figure 2A).

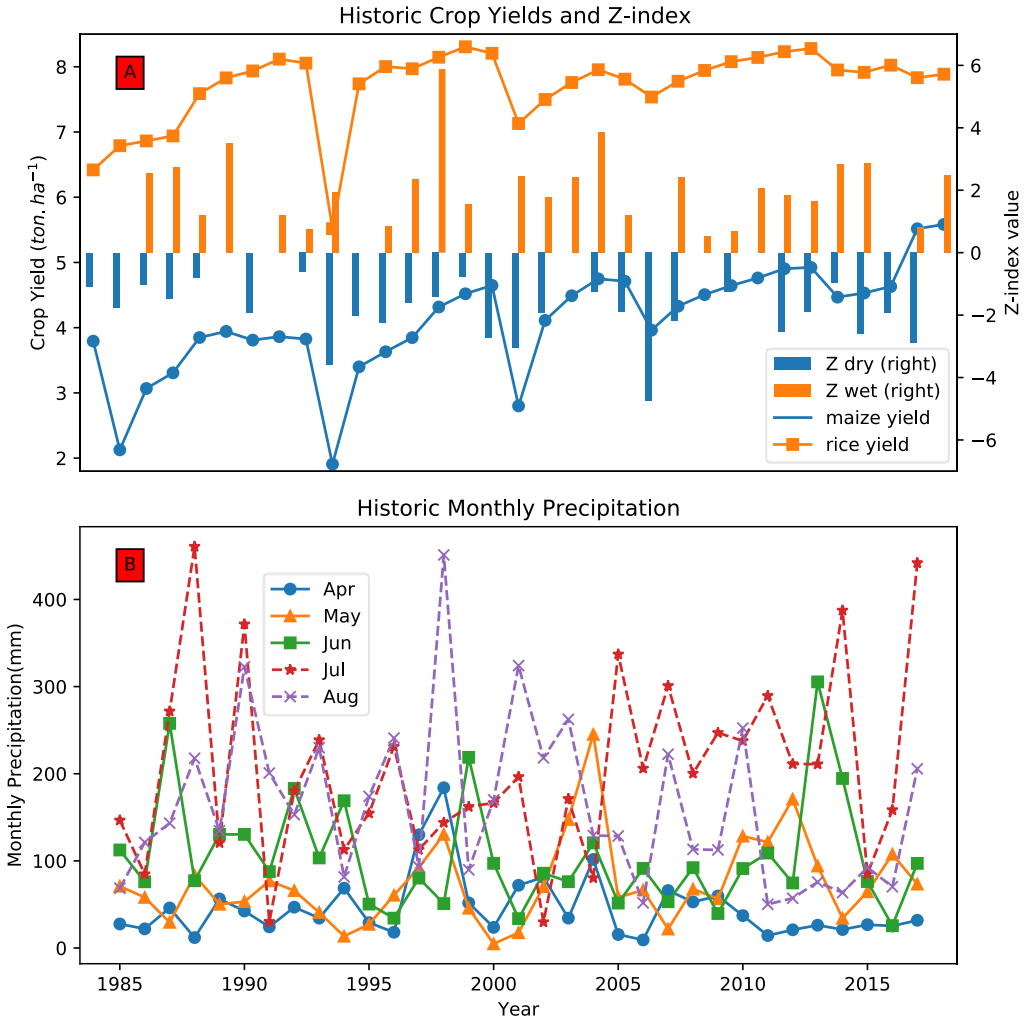

Figure 2. Historic rice and maize yields (A, left axis) and aggregate Z-index values (A, right axis) in Mianyang prefecture. The negative aggregate Z-index values represent dry events while the positive aggregate Z-index values denote wet events. B is the historic monthly precipitation from 1985 to 2017, Apr=April, May=May, Jun=June, Jul=July, Aug=August.

3.2 Performance of the models for predicting crop yield

Using the dataset in Mianyang prefecture, the various models used were trained and tested. The best parameters for the RF regression model were the default values, while the RF regression models were sensitive to the number of trees (n_estimators). For the SVM model, the kernel function parameter (kernel) was tuned to 'linear', the regularization parameter (C) was tuned to 0.9, and the error penalty parameter (epsilon) was adjusted to 0.47, with all the other parameters kept at the default values.

The performance of all the models is reported in Table 2. The RF+Z-index outperformed other methods, as it had the highest R^2 and the smallest RMSE for both the rice dataset and the maize dataset. The SVM models were not very different from the MLR models. Moreover, using the Z-index as input was better than using accumulated precipitation as input in the prediction. For example, the RMSE of RF+Z-index for predicting maize yield was 0.33, while the RMSE of RF+Precipitation for prediction maize yield was 0.39. RF models could capture the extreme dry years such as 1994 and 2001, which made it a favorable method to predict extreme yield variations (Figure 3).

Table 2. Performance of models, when comparing predicted crop yields to observed crop yields in Mianyang. RF represents Random Forest regression, MLR represents Multiple Linear Regression, and SVM stands for Support Vector Machine regression. RMSE means Root Mean Square Error

Method	Maize		Rice	
	R^2	RMSE (ton/ha)	R^2	RMSE (ton/ha)
RF+Z-index	0.83	0.33	0.79	0.27
MLR+Z-index	0.66	0.47	0.33	0.49
SVM+ Z-index	0.67	0.47	0.36	0.48
RF+ Precipitation	0.77	0.39	0.67	0.34
MLR+ Precipitation	0.56	0.54	0.27	0.51
SVM+ Precipitation	0.48	0.59	0.22	0.53

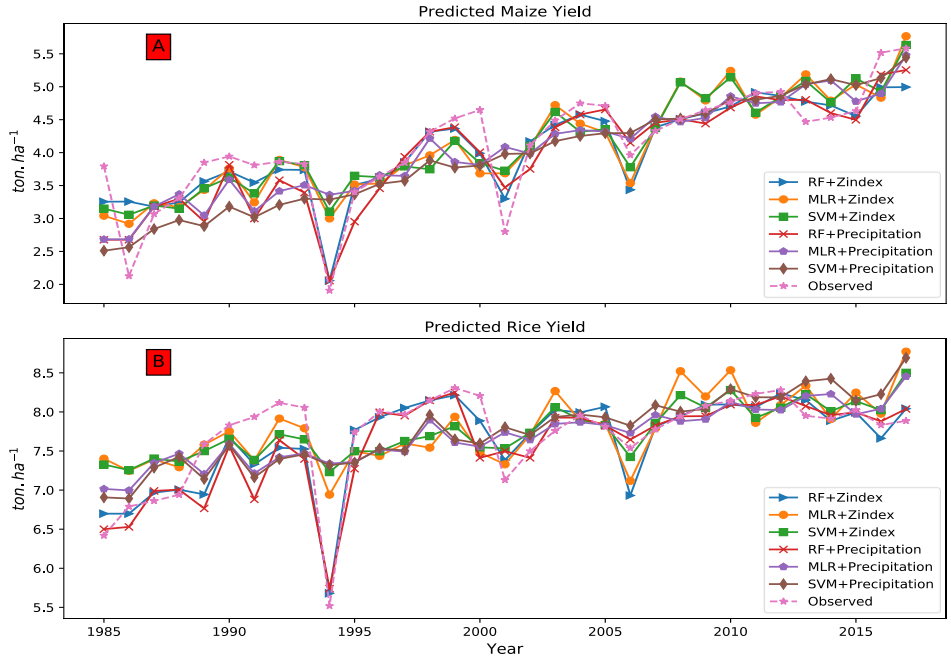

Figure 3. Predicted maize yield (A) and rice yield (B) in Mianyang by different methods. RF represents Random Forest regression, MLR represents Multiple Linear Regression, SVM represents Support Vector Machine regression. '+Zindex' means using Z-index as input, '+Precipitation' means using accumulated precipitation as input

In terms of relative feature importance for RF+Z-index models, drought could explain 38% of the maize yield change, while flood could only explain 3% of the maize yield change. Similarly, drought could explain 57% of the rice yield change while flood could only explain 6% of the rice yield change.

Since the RF+Z-index had been proven to be a favorable extreme precipitation assessment tool in Mianyang, the rice dataset in Leshan and Dazhou prefectures were used to check if the RF+Z-index was applicable in other places. After training the model, the parameter number of trees (n_estimators) was tuned to 100, and all the other parameters were kept at their default values. Figure 4 shows the predicted rice yield and the model's performance. In both places, RF+Z-index had the ability to predict rice yield with high R^2 and small RMSE values.

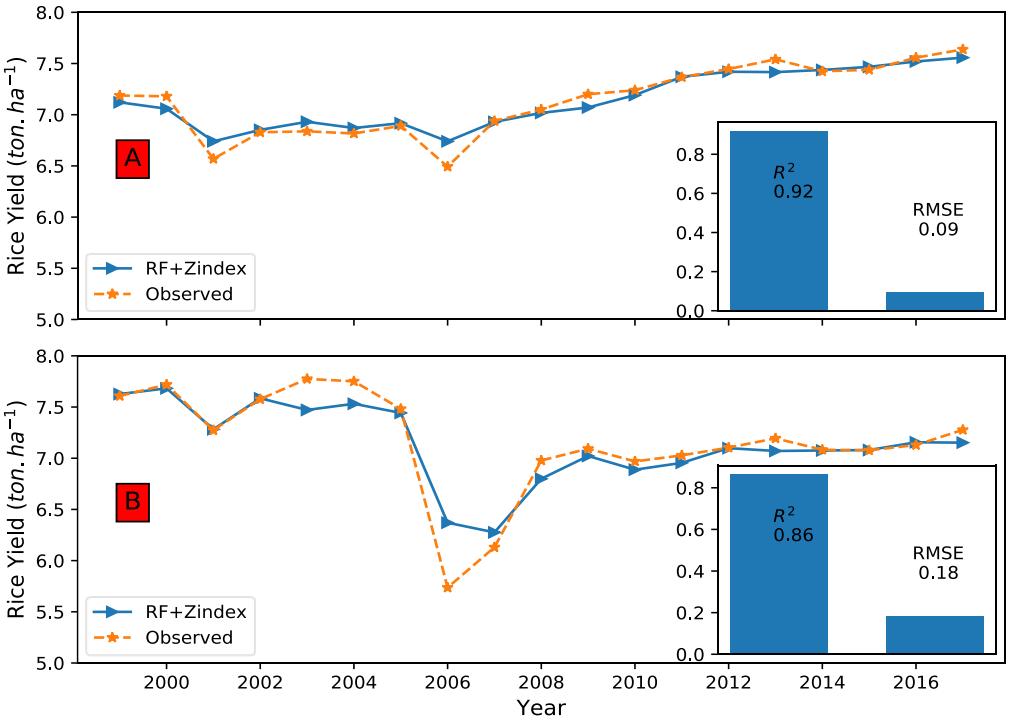

Figure 4. Application of Random Forest plus Z-index for predicting rice yield in Leshan (A) and Dazhou (B). RF represents Random Forest regression. RMSE means Root Mean Square Error.

3.3 Future precipitation and Z-index in Mianyang

Over the next three decades, the annual mean precipitation simulated by the three GCMs under RCP 4.5 tended to decline slightly, while the simulated annual mean precipitation under RCP 8.5 deceased significantly, compared to the 2010s baseline (Figure 5). From Figure 6, the precipitation simulated by three GCMs on decadal time scales were consistent, as they had similar changes in means. In addition, the variation among these simulations became even smaller after the precipitation data were transformed to Z-index.

However, there were some differences among the three GCM simulations. In terms of precipitation, under RCP 4.5, the IPSL_CM5_MR model simulated the highest annual mean

precipitation as well as the highest variation of precipitation throughout the 2020s-2040s. On the other hand, CESM1_CAM5 simulated the median annual mean precipitation and the smallest variation of precipitation throughout the 2020s-2040s. Under RCP 8.5, small precipitation variations were seen in 2020s for all three GCMs. However, larger precipitation variations were seen in the 2030s, and 2040s. The Z-index under RCP 4.5, CESM1_CAM5 had the smallest negative aggregate Z-index spread in the 2040s, while IPSL_CM5_MR had the highest negative aggregate Z-index spread in the 2040s. Under RCP 8.5, the values of the Z-indexes were similar among the three GCMs over the next three decades, however, BCC_CSM1_1_M had the smallest negative aggregate Z-index spread compared to the other two GCMs in the 2020s.

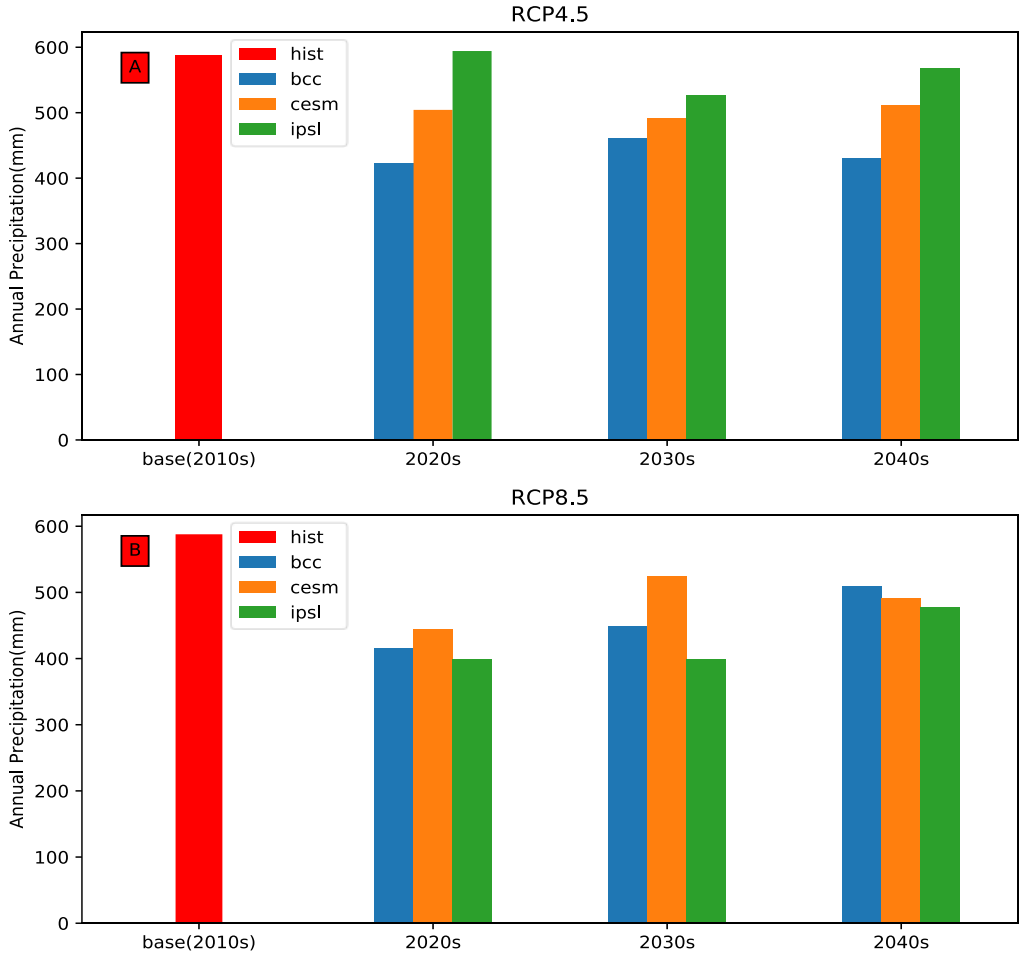

Figure 5. Precipitation in the growing season of rice and maize in Mianyang prefecture. A is the future annual mean precipitation simulated by three Global Climate Models from 2020 to 2050 under RCP4.5, while B is under RCP8.5. 'bcc' means data simulated by BCC_CSM1_1_M, likewise, 'cesm' = CESM1_CAM5, 'ipsl' = IPSL_CM5A_MR. 'hist' means data obtained from history.

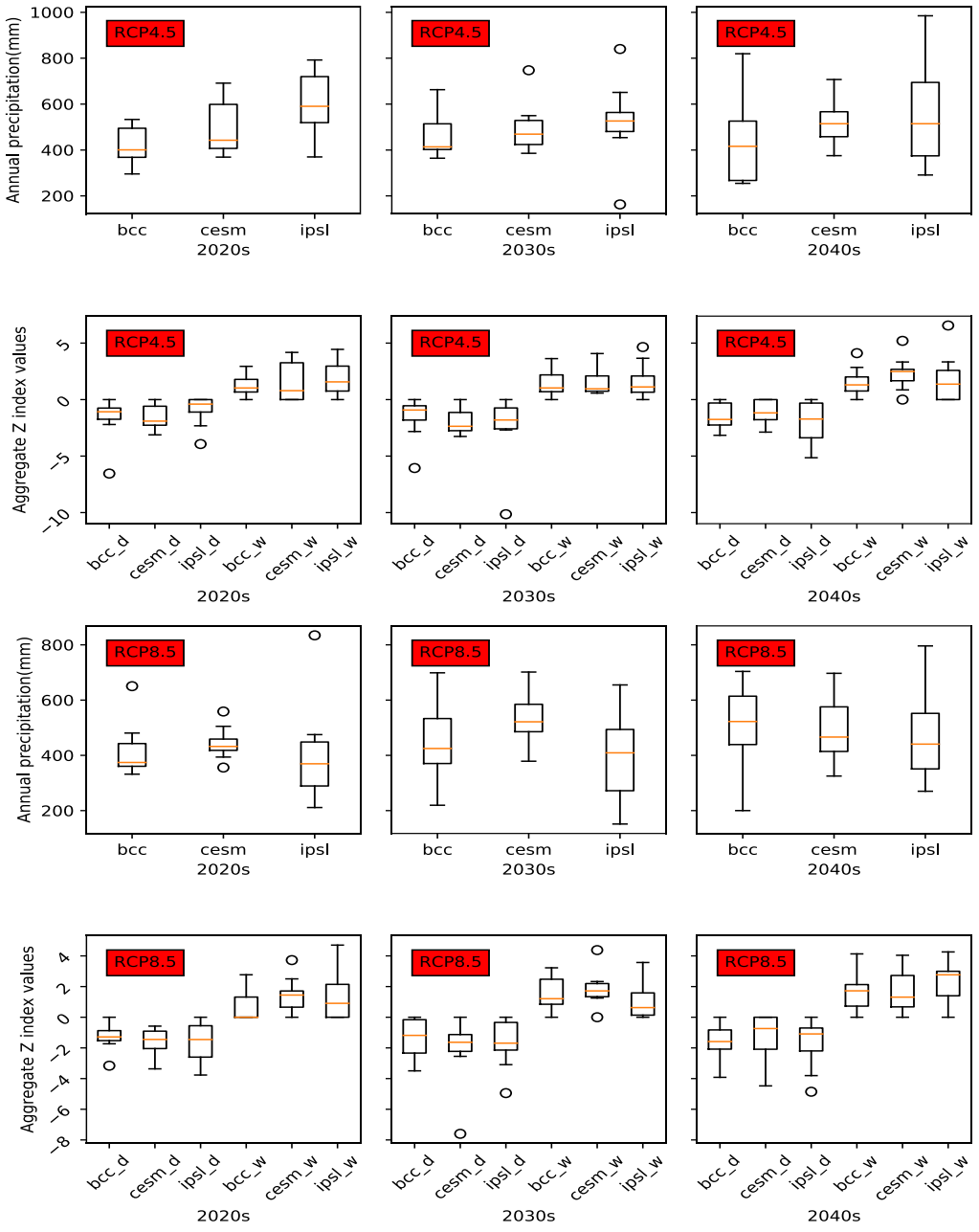

Figure 6. Consistency of future precipitation and Z-index derived from Global Climate Models in Mianyang prefecture. 'bcc' means data simulated by Global Climate Model BCC_CSM1_1_M. Likewise, 'cesm' = CESM1_CAM5, 'ipsl' = IPSL_CM5A_MR. Negative Z-index values represent dry events, while positive Z-index values represent wet events. 'bcc_d' means dry events based on BCC_CSM1_1_M, and 'bcc_w' means wet events based on BCC_CSM1_1_M. So 'cesm_d', 'cesm_w', 'ipsl_d', and 'ipsl_w' have similar meanings.

3.4 Future crop yield variations in Mianyang under climate scenarios

Predicted future crop yields were compared to the base line (2010s). Generally, future crop yields were likely to decline throughout the 2020s-2040s under both the RCP 4.5 and RCP 8.5 climate scenarios, with rice yield reductions larger than maize yield reductions (Figure 7). Under RCP 4.5, the average maize yields tended to decline by -0.27%, -0.65%, and -0.82% in the 2020s, 2030s, and 2040s, respectively. A similar pattern was seen in rice yield reduction, with average rice yields decreasing by -0.93%, -1.59%, and -1.94% in the 2020s, 2030s, and 2040s, respectively. An abnormal case was noted in the 2040s, with maize and rice yields slightly increased based on CESM1_CAM5. Under RCP 8.5, the average maize yields were likely to decrease by -0.69%, -0.64%, and -0.91% in the 2020s, 2030s, and 2040s, respectively, while the average rice yields would drop by -0.95%, -1.23%, and -1.72% in the 2020s, 2030s, and 2040s, respectively. Again, one special case was recorded in the 2020s, when rice yield increased by a small proportion using the simulation data from BCC_CSM1_1_M.

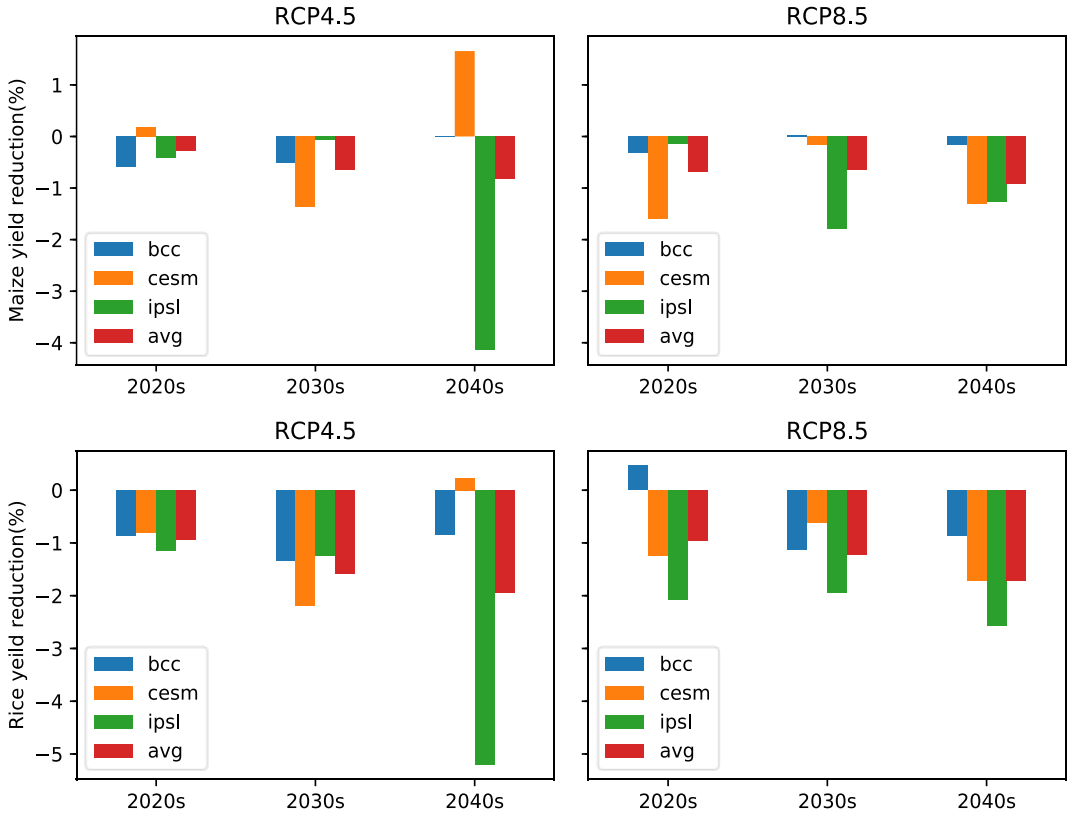

Figure 7. Future rice and maize yield variations compared to the base line period (2011-2017) under climate scenarios RCP4.5 and RCP8.5 in Mianyang prefecture. 'bcc' means yield variations using the precipitation data that simulated by Global Climate Model (GCM) BCC_CSM1_1_M as input. Similarly, 'cesm' = CESM1_CAM5, 'ipsl' =IPSL_CM5A_MR, and 'avg' means the average of yield variations based on those three GCMs.

3.5 Results interpretation

By coupling the aggregate Z-index and RF regression, a new and reliable assessment tool was created for studying and assessing the impacts of extreme precipitation events on rice and maize yields at the local administrative organization level. RF regression does not need careful normalization of input variables or extensive parameter tuning, which makes it easy for other non-professionals to use. Another advantage of RF regression is that variable collinearity does not affect its ability [32]. Moreover, this assessment tool does not require the conduction of long-term experiments, thus making it more efficient to use. This method can be applied to other crops and other locations if training data is provided.

In this study, RF regression outperformed MLR and SVM regression. This was consistent with the studies by Jeong *et al*. [32] and Feng *et al*. [33]. The main reason is that RF is a decision tree-based algorithm. Therefore, it has the ability not only to capture non-linear relationships but also to capture extreme cases. For example, 1994 was an extreme dry year and the RF model was able to simulate the extreme small yield value. Other methods may not have simulated this situation. SVM regression and MLR had similar results in this study because the input variables had some linear relationship with the output variables, and therefore, the kernel parameter was tuned as 'linear' in the SVM model to transform the input data, making it similar to MLR. Using the aggregated Z-index as input to train models was better than using the accumulated precipitation because the Z-index could account for both drought and flood, while accumulated precipitation might have ignored some events due to an uneven precipitation distribution. For example, 2001 is a normal year for accumulated precipitation (Figure 2B), but the aggregated Z-index (Figure 2A) portrays it as a dry year, with corresponding to significantly reduced crop yield.

The Z-index was able to be accurately used to capture the extreme dry and wet events during the historic period, which is consistent with a previous study [23]. The RF+Z-index model indicates that drought affects the crop yield significantly in Mianyang. This is because water is essential in the photosynthesis process, turgidity, solvent nutrients, medium bio-chemical process, and other crop growing processes, so insufficient water may affect these processes and eventually affect crop yield [34]. Time also contributes to the crop yield variation through technology change and management improvements [32, 35]. Flood may affect the respiration of the crop and harm the crop roots, leading to yield loss. However, flood in Mianyang only contributes a small proportion of crop-yield variation. This study implies that drought is more critical for rice yield variation than for maize yield variation. This is mainly due to maize being classified as a C4 crop, which means it is more resilient to drought than rice, which is classified as a C3 crop [36]. Indeed, predicted future yield variations under climate scenarios revealed that maize yield reduction was smaller than rice yield reduction in Mianyang prefecture.

The three GCMs were used to simulate the future precipitation, and the mean change in precipitation predicted was consistent on decadal time scales, especially when the precipitation was transformed to a Z-index. The average future crop yields were decreasing over the next three decades compared to the baseline period. Similar decreasing patterns were reported in the study of Xu *et al*. [16] in Sichuan province using crop models, although their results showed larger reductions. This indicates that our assessment tool can be used as an alternative for local policy makers and other researchers. The abnormal yield increases in the 2040s based on CESM1_CAM5 under RCP 4.5 were due to an annual average aggregate negative Z-index value of -1.12, which was smaller than the other two GCMs' results and suggests that droughts were not that strong. The predicted rice yield increased, while maize yield decreased in the 2020s based on BCC_CSM1_1_M under RCP 8.5, possibly due to the different patterns between historic rice yield and historic maize yield in the training datasets.

3.6 Limitations and future research

Using the Z-index and time as input, RF regression assessed the yield variation impacted by extreme dry and wet conditions. However, the predicted future yield might not be accurate, as it is beyond the training data's boundary. If we want to improve yield prediction, an improved Machine Learning method (for example, combined RF and Linear models) and more relevant input variables are needed. These variables could be technical variables such as research investment and innovations, natural variables such as land quality, and social variables such as social learning platform, labor education and policy intervention at the local level. Moreover, since the Z-index assumes that the precipitation follows a statistical distribution, if the precipitation samples are too small it may not satisfy this assumption and lead to a biased result. Therefore, other users should use the Z-index for future projections with caution. This study had 33 years of precipitation records for all three study areas; however, the longer the record, the more robust the result [37].

In addition, future studies should focus more on specific local variables, and those variables should be modified appropriately (as was done in this study when we used the aggregate Z-index rather than raw precipitation data), and then be inputted into the Machine Learning models. Our future yield variation prediction was heavily based on the GCMs, although we had used three GCMs from different countries and institutions to capture plausible errors and analyzed their consistency. There could be some modifications that might improve our predictions, since projection of future precipitation is so complex, and the confidence of precipitation estimation is smaller than for other climate variables such as temperature [38]. Future research at the local level needs national and international cooperation and research collaboration in the areas of climate change, agriculture, food security, sustainable livelihood, and ecosystem improvement. The establishment of well-organized research infrastructures and a collaboration network to implement these tools needs both private and public support in China and at the global level.

4. Conclusions

The aggregate Z-index accurately captured extreme dry and wet events. The Random Forest regression model was determined to be a good method to assess the impact of extreme events on crop yield. This assessment approach was applicable in different places and showed how crop yield was affected by drought and flood and varied over plant variety, time, and place. The Z-indices derived from three GCMs provided consistent results for predicting future yield variations. In Mianyang prefecture, under climate scenario RCP 4.5, maize yields were likely to decrease by -0.27 to -0.82% and rice yields by -0.93 to -1.94%, compared to the baseline period, over the next three decades. Similarly, under RCP 8.5, maize yields and rice yields could decrease by -0.64 to -0.91% and -0.95 to -1.72% respectively compared to the baseline period, over the next three decades. Both the Z-index and Random Forest model were simple and practical to use for decision makers and practitioners at the prefecture level to gain understanding of the relationships between crop production and extreme events, and to facilitate policy adjustment for local adaptation.

5. Acknowledgements

We thank the China Academic of Agricultural Engineering and Research Program on Climate Change, Agriculture and Food Security for supplying the historic and future precipitation data. We express our appreciation to Dr. Jack Katzfey, CSIRO Australia, for his technical and language editing. We also acknowledge the work of three anonymous reviewers and editorial staff, who provided valuable suggestions, attention, and time.

References

[1] Statistical Bureau of Sichuan, 2018. *Sichuan Statistical Yearbook.* [online] Available at: http://tjj.sc.gov.cn/tjcbw/tjnj/

[2] Zhan, S., 2017. Riding on self-sufficiency: Grain policy and the rise of agrarian capital in China. *Journal of Rural Studies*, 54, 151-161.

[3] Huang, J.K., Wei, W., Cui, Q. and Xie, W., 2017. The prospects for China's food security and imports: Will China starve the world via imports? *Journal of Integrative Agriculture*, 16(12), 2933-2944.

[4] He, Z.H. and Bonjean, A.P.A., 2010. *Cereals in China*. [e-book] Mexico, D.F.: CIMMYT. Available through: Sematic Scholar <https://www.semanticscholar.org>

[5] Wu, M.X. and Lu, H.Q., 2016. A modified vegetation water supply index (MVWSI) and its application in drought monitoring over Sichuan and Chongqing, China. *Journal of Integrative Agriculture*, 15(9), 2132-2141.

[6] Pan, N., Wei, R.J., Zhan, C. and Liang, C., 2017. Applicability analysis of drought indexes in Sichuan Province. *South-to-North Water Transfers and Water Science & Technology*, 15(4), 71-78. (in Chinese).

[7] Sui, Y., Lang, X.M. and Jiang, D.B., 2018. Projected signals in climate extremes over China associated with a 2°C global warming under two RCP scenarios. *International Journal of Climatology*, 38(S1), e678-e697.

[8] Easterling, D.R., Kunkel, K.E., Wehner, M.F. and Sun, L., 2016. Detection and attribution of climate extremes in the observed record. *Weather and Climate Extremes*, 11, 17-27.

[9] Camuffo, D., Valle, A.D. and Becherini, F., 2020. A critical analysis of the definitions of climate and hydrological extreme events. *Quaternary International*, 538, 5-13.

[10] Cheng, Q., Gao, L., Zuo, X. and Zhong, F., 2019. Statistical analyses of spatial and temporal variabilities in total, daytime, and nighttime precipitation indices and of extreme dry/wet association with large-scale circulations of Southwest China, 1961-2016. *Atmospheric Research*, 219, 166-182.

[11] Jia, J.Y., Han, L.Y., Liu, Y.F. and He, N., 2016. Drought risk analysis of maize under climate change based on natural disaster system theory in Southwest China. *Acta Ecologica Sinica*, 36(5), 340-349.

[12] Chen, W.Z., Zhu, D., Huang, C.J. and Ciais, P., 2019. Negative extreme events in gross primary productivity and their drivers in China during the past three decades. *Agricultural and Forest Meteorology*, 275, 47-58.

[13] Feng, P.Y., Wang, B., Liu, D.L. and Yu, Q., 2019. Machine learning-based integration of remotely-sensed drought factors can improve the estimation of agricultural drought in South-Eastern Australia. *Agricultural Systems*, 173, 303-316.

[14] Liu, X.F., Pan, Y.Z., Zhu, X.F. and Yang, T.T., 2018. Drought evolution and its impact on the crop yield in the North China Plain. *Journal of Hydrology (Amsterdam)*, 564, 984-996.

[15] He, Q.J., Zhou, G.S., Lü, X.M. and Zhou, M.Z., 2019. Climatic suitability and spatial distribution for summer maize cultivation in China at 1.5 and 2.0 °C global warming. *Science Bulletin*, 64(10), 690-697.
[16] Xu, C.C., Wu, W.X. and Ge, Q.S., 2018. Impact assessment of climate change on rice yields using the ORYZA model in the Sichuan Basin, China. *International Journal of Climatology*, 38(7), 2922-2939.
[17] Powell, J.P. and Reinhard, S., 2016. Measuring the effects of extreme weather events on yields. *Weather and Climate Extremes*, 12, 69-79.
[18] Rötter, R.P., Appiah, M., Fichtler, E. and Kersebaum, K.C., 2018. Linking modelling and experimentation to better capture crop impacts of agroclimatic extremes-A review. *Field Crops Research*, 221, 142-156.
[19] Harrison, M.T., Cullen, B.R. and Rawnsley, R.P., 2016. Modelling the sensitivity of agricultural systems to climate change and extreme climatic events. *Agricultural Systems*, 148, 135-148.
[20] Perondi, D., Fraisse, C.W., Staub, C.G. and Cerbaro, V.A., 2019. Crop season planning tool: Adjusting sowing decisions to reduce the risk of extreme weather events. *Computers and Electronics in Agriculture*, 156, 62-70.
[21] Ma, Z.F., Liu, J., Zhang, S.Q. and Chen, W.X., 2013. Observed climate changes in Southwest China during 1961-2010. *Advances in Climate Change Research*, 4(1), 30-40.
[22] Xu, C.X., An, W.L., Wang, S.Y.S., Yi, L., Ge, J., Nakatsuka, T., Sano, M. and Guo, Z.T., 2019. Increased drought events in southwest China revealed by tree ring oxygen isotopes and potential role of Indian ocean dipole. *Science of the Total Environment*, 661, 645-653.
[23] Qi, D.M., Li, Y.Q., Wang, Y. and Deng, M.Y., 2017. Temporal-spatial abnormity characteristics of drought in Sichuan province based on Z index. *Journal of Arid Meteorology*, 35(5), 734-744. (in Chinese)
[24] Racines, N.C., Tarapues, J., Thornton, P., Jarvis, A., and Villegas, J.R., 2020. High-resolution and bias-corrected CMIP5 projections for climate change impact assessments. *Scientific Data*, 7(1), 1-14.
[25] Chlingaryan, A., Sukkarieh, S. and Whelan, B., 2018. Machine learning approaches for crop yield prediction and nitrogen status estimation in precision agriculture: A review. *Computers and Electronics in Agriculture*, 151, 61-69.
[26] Butler, M. and Kazakov, D., 2011. The effects of variable stationarity in a financial time-series on Artificial Neural Networks. *Proceedings of the 2011 IEEE Symposium on Computational Intelligence for Financial Engineering and Economics (CIFEr)*, Paris, France, April 11-15, 2011, 1-8.
[27] Vogel, E., Donat, M.G., Alexander, L.V., Meinshausen, M., Ray, D.K., Karoly, D., Meinshausen, N. and Frieler, K., 2019. The effects of climate extremes on global agricultural yields. *Environmental Research Letters*, 14(5), 054010, https://doi.org/10.1088/1748-9326/ab154b
[28] Breiman, L., 2001. Random Forests. *Machine Learning*, 45, 5-32. [online] Available at: https://doi.org/10.1023/A:1010933404324
[29] Pedregosa, F., Varoquaux, G., Gramfort, A., Michel, V. and Thirion, B., 2011. Scikit-learn: machine learning in python. *Journal of Machine Learning Research*, 12(2011), 2825-2830.
[30] Ronaghan, S., 2018. *The Mathematics of Decision Trees, Random Forest and Feature Importance in Scikit-learn and Spark.* [online] Available at: https://towardsdatascience.com/the-mathematics-of-decision-trees-random-forest-and-feature-importance-in-scikit-learn-and-spark-f2861df67e3
[31] Louppe, G., 2015. *Understanding Random Forests: From Theory to Practice*. Ph.D. University of Liège.

[32] Jeong, J.H., Resop, J.P., Mueller, N.D. and Fleisher, D.H., 2016. Random forests for global and regional crop yield predictions. *Plos One*, 11(6), e0156571, https://doi.org/10.1371/journal.pome.o156571

[33] Feng, S.F., Hao, Z.C., Zhang, X. and Hao, F.H., 2019. Probabilistic evaluation of the impact of compound dry-hot events on global maize yields. *Science of the Total Environment*, 689, 1228-1234.

[34] Aslam, M., Maqbool, M.A. and Cengiz, R., 2015. Effects of drought on maize. In: M.L. Zea, ed. *Drought Stress in Maize*. Cham: Springer, pp. 5-17.

[35] Crane-Droesch, A., 2018. Machine learning methods for crop yield prediction and climate change impact assessment in agriculture. *Environmental Research Letters*, 13(11), 114003, https://doi.org/10.1088/1748-9326/aae159

[36] Liu, X.L., Li, X., Dai, C.C. and Zhou, J.Y., 2017. Improved short-term drought response of transgenic rice over-expressing maize C4 phosphoenolpyruvate carboxylase via calcium signal cascade. *Journal of Plant Physiology*, 218, 206-221.

[37] Wu, H., Hayes, M.J., Wilhite, D.A. and Svoboda, M.D., 2005. The effect of the length of record on the standardized precipitation index calculation. *International Journal of Climatology*, 25(4), 505-520.

[38] Randall, D.A., Wood, R.A., Bony, S. and Colman, R., 2007. Climate models and their evaluation. In: S. Solomon, D.H. Qin, M. Manning and Z. Chen, eds. *Climate Change 2007: The Physical Science Basis*. Cambridge and New York: Cambridge University Press, pp. 591-662.

Micropropagation of *Koelreuteria bipinnata* Using Juvenile and Mature Explants

Azza A. Tawfik*, Omer H. Ibrahim and Mona A. Taha

Department of Horticulture, Faculty of Agriculture, Assiut University, Assiut, Egypt

Received: 20 January 2020, Revised: 13 May 2020, Accepted: 9 June 2020

Abstract

An efficient micropropagation protocol for *Koelreuteria bipinnata*, an ornamental tree, from mature and juvenile phase tissues was described. Nodal explants from one-year-old branches of a field-grown mature tree (mature phase) and from *in vitro* growing seedlings (juvenile phase) were used. The nodal explants from mature explants cultured on Murashig and Skoog (MS) medium supplemented with or without growth regulators did not show any axillary shoot development. However, 6-benzylaminopurine (BAP) at 1.5 mg/l induced axillary shoots from all juvenile explants (100%). It also produced the highest number of shoots (2.5 shoots per explant), the highest rooting percentage (100%), the maximum number of roots (2.80 roots/shoot) and the longest roots (5.87 cm) when it was added as a supplement to the half-strength MS medium culture that included 15 g/l sucrose. Plantlets were successfully acclimatized and transferred to the field with 60% survival rate.

Keywords: BAP, Chinese flame tree, Juvenile nodal explants, mature nodal explants, sucrose, woody plants
DOI 10.14456/cast.2020.31

1. Introduction

Koelreuteria is a genus of small to medium-sized ornamental trees, indigenous to East Asia. The members of the genus *Koelreuteria* have been widely cultivated as ornamental trees because of their large showy inflorescences of yellow flowers [1]. *Koelreuteria bipinnata* (Figure 1), also known as the Chinese flame tree, the Bougainvillea golden rain tree, and the Chinese golden rain tree, belongs to the family Sapindaceae [2]. It is often used as a tree along streets and highways, and in parking lots. It is grown to provide shade in gardens and is a fine display tree. The trees bloom in summer from July to August, and in some regions in Europe, they flower in September. The flowers are small with four yellow petals which have a touch of red color at the base. The flowers can yield a yellow dye. The three-sided seed pods of *K. bipinnata* look like red Chinese paper lanterns that hang all over the tree in the late autumn forming a spectacular picture. So, the trees are commonly used as a focal point in landscape design in regions where they flourish [3].

*Corresponding author: Tel.: 020882412559
E-mail: azza7799@yahoo.com

Figure 1. *Koelreuteria bipinnata* tree growing in the nursery of ornamental plants, Faculty of Agriculture, Assiut University, Assiut, Egypt

The conventional propagation method for the golden rain tree (*Koelreuteria* spp.) is usually via seeds. However, seeds germination is slow because seeds have physical dormancy [4, 5]. Seeds can germinate best if the seed coats are scarified for about one hour in sulfuric acid, followed by stratification for about 3 months at 2 to 4°C, which overcomes embryo dormancy [6]. For *K. bipinnata*, the seed germination percentage was 55% (unpublished data). Moreover, no reports on using other methods for propagation of *K. bipinnata* could be found and it seems that the tree cannot be propagated by conventional vegetative propagation methods such as making stem cuttings. These problems could possibly be overcome by the application of plant tissue culture techniques such as micropropagation, and thus a protocol for in the vitro propagation of these ornamental trees should be established. However, most of the previous investigations of woody plants utilized seeds and juvenile tissues were more responsive to *in vitro* manipulations than tissues from mature plants [7, 8]. Moreover, the degree of maturity affects the efficiency and production of a forest tree species.

There is scarce information available in the literature about the use of tissue culture technique for *Koelreuteria bipinnata* [9]. Thus, the aim of the study was to establish a simple procedure for *in vitro* propagation of *K. bipinnata* tree from juvenile and mature explants.

2. Materials and Methods

2.1 Explant collection, disinfection and culture establishment

Seeds and mature nodal explants of *Koelreuteria bipinnata* were obtained from an approximately 20 year-old tree growing in the nursery of ornamental plants, Faculty of Agriculture, Assiut University, Egypt. The healthy seeds were thoroughly cleaned in running tap water for 30 min and disinfected by submerging them in 70% (v/v) ethanol for 3 min. Then, the seeds were rinsed three times using sterile distilled water and cultured in 250 ml jars containing 30 ml of Murashig and Skoog (MS) medium [10] supplemented with 3% (w/v) sucrose, 0.75% (w/v) agar and without growth regulators for seed germination. The pH of the medium was adjusted to 5.8 prior to autoclaving at 121ºC and 1.5 kg/cm^2 for 30 min. The cultures of all experiments were incubated at 25 ±2°C under 16 h light from cool white fluorescent tubes.

After 5 weeks of seed germination, nodal explants were excised from *in vitro* grown seedlings (juvenile explants) and used for further experiments. Mature nodal explants were taken from one-year-old branches collected from the same tree grown in the nursery. The branches were cleaned under running tap water for 15 min, cut into pieces with 1-2 nodes, and the surfaces were disinfected for 20 min in 30 % (v/v) commercial bleach (~5% sodium hypochlorite).

Finally, in a laminar air flow hood, the nodes were rinsed three times using sterile distilled water and 1.5-2 cm nodal explants were cultured in jars (250 ml) that contained 30 ml of plant growth regulators (PGRs)-free basal MS medium which had been supplemented with 3% (w/v) sucrose and 0.75% (w/v) agar. The pH of the medium was adjusted to 5.8 prior to autoclaving at 121º C and 1.5 kg/cm^2 for 30 min. The cultures of all experiments were incubated at 25 ±2°C under 16 h light from cool white fluorescent tubes.

2.2 Effect of 6-benzylaminopurine (BAP) concentration on shoot multiplication

For the juvenile phase, nodal segments (~1cm containing 2 nodes) were taken from *in vitro*-growing seedlings. For the mature phase, nodal segments (~1.5-2 cm with 1-2 nodes) were excised from recent branches of the tree and the following experiment was conducted to study the effect of BAP on both types of explants.

Mature and juvenile explants were cultured in 250 ml baby food jars containing 30 ml MS basal salt medium. The medium was supplemented with 6-benzylaminopurine (BAP) at 0, 0.5, 1, 1.5 and 2 mg/l. A completely randomized design (CRD) with three replicates was used. The data were analyzed according to the multiobservation approach where each treatment per replicate contained five jars. The following data were recorded after 3 weeks culturing on media: percentage of axillary shoots induction (%), average number of shoots per explant, average length of shoots (cm), and number of leaves/shoot

2.3 Effect of sucrose concentration on root formation

Proliferated axillary shoots were excised and transferred to half-strength MS medium without PGRs to allow rooting, and the following experiment was conducted to study the effect of sucrose on root formation.

Uniform individual shoots (each ~3-4 cm long) derived from the multiplication stage were transferred to PGRs-free half-strength MS medium supplemented with four concentrations of sucrose (15, 20, 25 and 30 g/l).

A completely randomized design (CRD) was used with three replicates and each treatment per replicate contained five jars. Data were recorded after two weeks for rooting percentage (%), number of roots per explant, and root length (cm).

2.4 Acclimatization stage

After four weeks, the rooted plantlets (~3- 4 cm) were gently removed from the medium, and the roots were rinsed using tap water to remove the excess medium. Finally, the plantlets were transplanted into small plastic pots (10-cm dia.) that contained a 1:1 mixture of peat moss and perlite. Data on the survival rate was calculated after four weeks.

2.5 Statistical analysis

The data from all experiments were subjected to analysis of variance (ANOVA) and mean comparison was performed using the least significant difference (LSD) method with a significant level of 5%, which was adapted from Gomez and Gomez [11].

3. Results and Discussion

3.1 Establishment stage (initiation stage)

All the nodal explants (1.5 -2 cm) taken from the mature phase did not respond and turned brown when cultured on PGRs-free MS medium. Under *in vitro* conditions, the explant proliferation depends on the specific balance of PGR's, auxins and cytokinins [12]. However, the establishment of explants for micropropagation of woody plants and the induction of adventitious shoots and roots is greatly influenced by the maturation status of the tissue used for the primary explant [8]. Young plant material from mature woody plants can be obtained in two ways, the first being the use of new growth parts of the mature plants, and the second way being the renovation of the mature parts of the woody plants themselves. In this work, seeds of *K. bipinnata* that were cultured on plant growth regulators (PGRs)-free MS basal medium germinated after four weeks of culture. The nodal explants, which were approximately 1 cm in length, had two nodes, and which had been taken from the *in vitro* growing seedlings (juvenile phase), were used for the multiplication stage.

3.2. Axillary shoots multiplications

3.2.1 Effect of BAP on mature nodal segments

All nodal explants (1.5-2 cm) taken from the mature phase did not respond and turned brown when cultured on MS medium supplemented with different concentrations of BAP (0, 0.5, 1.0, 1.5, and 2 mg/l). Browning is a common and often severe problem in plant tissue culture that is caused by the accumulation and oxidation of phenolic compounds and is frequently observed in tissue cultures of woody plants [13-15]. This may be due to high oxidative stress during culture and strong wound reactions accompanied by increase in phenolic compounds [16].

Most of the studies carried out on woody plants have utilized seeds and juvenile tissues that were more responsive to *in vitro* manipulations than tissues from mature plants [6, 7, 14, 15]. It is well known that 6-benzylaminopurine (BAP) and/or kinetin (6-furfurylaminopurine, Kin) are often used as cytokinins [17-19] in plant tissue culture proliferation. However, they both have a

limited success in woody plant regeneration [20]. Many reports stated that Thidiazuron (TDZ) induces regeneration via axillary shoot proliferation, adventitious shoot organogenesis, and somatic embryogenesis in many woody plant species [21-25].

3.2.2 Effect of BAP on juvenile nodal segments

The data presented in Table 1 and Figure 2 (E) showed that increasing BAP concentration up to 1.5 mg/l increased all the measurement parameters of nodal explants taken from the germinated seedlings (juvenile explant). Nodal explants significantly responded to all concentrations of BAP in comparison to the control treatment (BAP-free medium). Nodal segments gave the highest shoot number (2.5 shoots /explant), shoot length (4 cm) and leaves number (5 leaves/shoot) when cultured on MS medium supplemented with 1.5 mg/l BAP. The promoting effect of BAP on shoot proliferation of *Koelreuteria* spp and other members of family Sapindaceae was reported by several investigators [8, 9, 25, 26]. Groach *et al.* [26] reported that using BAP at 1.5 mg/l in the multiplication stage of *Koelreuteria elegans* gave the highest shoot regeneration (70%) and the highest number of shoots (4.35 shoots) from calli explants.

Table 1. Effect of different concentrations of BAP on axillary shoots induction from nodal explants (juvenile phase) of *Koelreuteria bipinnata*.

Treatment	**Measurements**			
BAP mg/l	**Axillary shoots induction (%)***	**No. of axillary shoots/ explant**	**Shoot length (cm)**	**Leaves number/ shoot**
0.0	50.00	1.00	2.10	2.00
0.5	90.00	1.25	2.30	2.23
1.0	90.00	2.00	2.70	3.33
1.5	100.00	2.50	4.00	5.00
2.0	70.00	1.90	3.80	3.68
LSD at 5%*	11.50	0.11	0.62	0.74

***Means were compared using Least Significant Difference (LSD) test at 5% level of probability

3.3 *In vitro* rooting

In the present study, shoots were easily rooted (100%) after two weeks when cultured on half-strength MS medium supplemented with sucrose at either 15 or 20 g/l (Table 2). A similar result was found by Yang *et al.* [27], who reported that the greatest number of roots (3.8 roots per explant) was formed when shoot tips of the *Melaleuca* tree were cultured on MS medium supplemented with 20 g /l sucrose. As shown in Table 2, using 15 and 20 g sucrose/l gave the highest root number (2.80 and 1.90 roots /explant) and root length (5.87 and 5.30 cm) respectively. Increasing sucrose concentration up to 30g/l significantly decreased rooting percentage, root number/shoot and root length. The results also demonstrated that the addition of auxins is

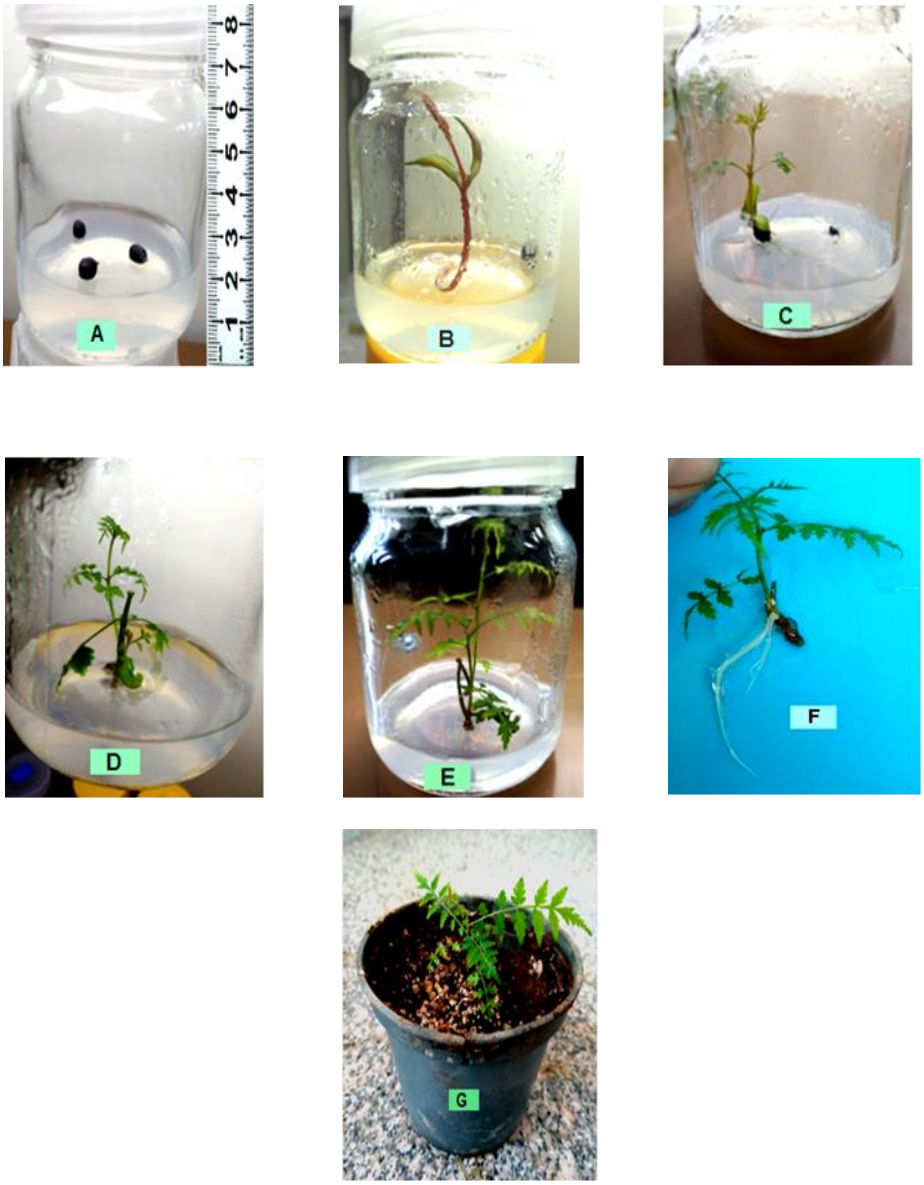

Figure 2. Micropropagation of *Koelreuteria bipinnata* from *in vitro* germinated seeds (juvenile phase). (A) aseptically cultured seeds on PGRs-free MS medium; (B and C) germinated seeds after 4 weeks; (D) cultured nodal explants on PGRs-free MS medium for axillary shoot induction; (E) shoot multiplication on MS medium with 1.5 mg/l BAP after 3 weeks; (F) Rooting of isolated single shoot on 1/2 MS medium with 15 g sucrose/l after 2 weeks; (G) Acclimatized plantlets transferred to plastic pots with peat moss and perlite (1:1) after 4 weeks

unnecessary. Similar results were reported by Tawfik [28] on *Melaleuca* where the explants formed roots in auxin-free medium. Also, Tawfik *et al*. [29] reported that the best interaction effect on rooting percentage (61.00%), highest number of roots/shoot (5.12) and root length (3.33 cm) were observed when the shoots of *Rosa* spp cv Eiffel Tower were cultured on hormone-free MS medium and pH level was adjusted to 5.5.

Table 2. Effect of different concentrations of sucrose on rooting percentage, root number and root length of *Koelreuteria bipinnata*

Sucrose g/l	**Measurements**		
	Rooting %*	**Roots number/ shoot**	**Root Length (cm)**
15	100.00	2.80	5.87
20	100.00	1.90	5.30
25	90.00	1.00	4.83
30	90.00	1.00	4.35
LSD at 5%*	9.41	0.27	0.68

***Means were compared using Least Significant Difference (LSD) test at 5% level of probability

3.4 Acclimatization stage

Acclimatization of plantlets is a vital step in the micropropagation of any plant species. It involves the transfer of plantlets from tissue culture containers to *ex vitro* conditions. In the present study, a plantlet of *K. bipinnata* is shown in Figure 2 (G). Acclimatized plantlets were transferred to plastic pots with peat moss and perlite (1:1) after four weeks. Plantlets were successfully acclimatized and transferred to the field with 60% survival rate.

4. Conclusions

Nodal segments of *Koelreuteria bipinnata* from *in vitro* growing seedlings (juvenile phase) were used for mass production of good-looking trees. The best medium for axillary shoot multiplication was MS supplemented with BAP at 1.5 mg/l. The highest rooting percentage (100%) was obtained on half MS medium supplemented with 15 g/l sucrose. Plantlets were successfully acclimatized on peat moss and perlite (1:1) with a survival rate of 60%.

References

[1] Xia, N. and Gadek, P.A., 2007. Sapindaceae. In: Z.Y. Wu, P.H. Raven and D.Y. Hong, eds. *Flora of China. Vol. 12. (Hippocastanaceae through Theaceae).* Beijing: Science Press/ Missouri Botanical Garden Press, pp. 5-24.

[2] Gilman, E.F. and Watson, D.G., 1993. *Koelreuteria bipinnata Chinese Flame-Tree*. [online] Available at https://hort.ifas.ufl.edu/database/documents/pdf/tree_fact_sheets/koebipa.pdf

[3] Urban Forest Ecosystem Institute, 2020. *SelecTree. "Koelreuteria bipinnata Tree Record." 1995-2020*. [online] Available at https://selectree.calpoly.edu/tree-detail/koelreuteria-elegans

[4] Cook, A., Turner, S.R., Baskin, J.M., Baskin, C.C., Steadman, K.J. and Dixon, K.W., 2008. Occurrence of physical dormancy in seeds of Australian Sapindaceae: a survey of 14 species in nine genera. *Annals of Botany*, 101(9), 1349-1362.

[5] Park, I.-H. and Rehman, S., 1999. Studies on seed dormancy: seeds maturation in relation to dormancy in golden rain tree *(Koelreuteria paniculata Laxm.)*. *Acta Horticulturae*, 504(21), 199-208.

[6] Hartmann, H.T., Kester, D.E., Davies, F.T. and Geneve, R.L. 2009. Propagation of ornamental trees, shrubs, and woody vines. In: H.T. Hartmann, D.E. Kester, F.T. Davies and R.L. Geneve. *Hartmann and Kester's Plant Propagation Principles and Practices*. Harlow: Pearson Education Limited, pp. 774-839.

[7] Bonga, J.M., 1987. Clonal propagation of mature trees: problems and possible solutions. In: J.M. Bonga and D.J. Durzan, eds. *Cell and Tissue Culture in Forestry*. Dordrecht: Springer, pp. 249-271.

[8] Hackett, W.P. and Murray, J.R., 1993. Maturation and rejuvenation in woody species. In: M.R. Ahuja, ed. *Micropropagation of Woody Plants*. Dordrecht: Springer, pp. 93-105.

[9] Feng, D.-L., Meng, Q.-R., Li, W.-P., Hu, Y.-H., Li, M. and Gu, A.-X., 2010. Morphology of somatic embryogenesis and plantlet formation in tissue cultures of lantern tree (*Koelreuteria bipinnata var. integrifoliola*). *Forestry Studies in China*, 12(1), 31-36.

[10] Murashige, T. and Skoog, F., 1962. A revised medium for rapid growth and bioassays with tobacco tissue cultures. *Physiologia Plantarum*, 15, 473-497.

[11] Gomez, K.A. and Gomez, A.A., 1984. *Statistical Procedures for Agricultural Research*. 2nd ed. New York: JohnWiley.

[12] Hartmann, H.T., Kester, D.E., Davies, F.T. and Geneve, R.L., 2011. *Plant Propagation: Principles and Practices*. 8th ed. New Jersey: Prentice-Hall.

[13] Andersone, U. and Ievinsh, G., 2002. Changes of morphogenic competence in mature *Pinus sylvestris* L. buds *in vitro*. *Annals of Botany*, 90(2), 293-298.

[14] Borthakur, A., Das, S.C., Kalita, M.C. and Sen, P., 2011. *In vitro* plant regeneration from apical buds of *Albizzia odoratissima* (L.f.) Benth. *Advances Applied Science Research*, 2, 457-464.

[15] Hung, C.D. and Trueman, S.J., 2011. *In vitro* propagation of the African mahogany *Khaya senegalensis*. *New Forests*, 42(1), 117-130.

[16] Jones, A.M.P. and Saxena, P.K., 2013. Inhibition of phenylpropanoid biosynthesis in *Artemisia annua* L.: a novel approach to reduce oxidative browning in plant tissue culture. *PloS One*, 8(10), e76802, https://doi.org/10.1371/journal.pone.0076802

[17] Kieber, J.J. and Schaller, G.E., 2014. Cytokinins. *The Arabidopsis Book*, 12, https://doi.org/ 10.1199/tab.0168.

[18] Tawfik, A.A. and Read P.E., 1991. Effect of benzyladenine on the oil constituents of rosemary plants regenerated from callus. *Plant Growth Regulator Society of America*, 37-39.

[19] Tawfik, A.A., 1997. Micropropagation and plant regeneration of neem tree (*Azadirachta indica* Juss). *Assiut Journal of Agriculture Science*, 28(2), 3-14.

[20] van Staden, J., Zazimalova, E. and George, E.F., 2008. Plant growth regulators II: cytokinins, their analogues and antagonists. In: E.F. George, M.A. Hall and G.-J. De Klerk, eds. *Plant Propagation by Tissue Culture*. *Vol 1. The Background*. 3rd ed. Dordrecht : Springer, pp. 205-226

[21] Huetteman, C.A. and Preece, J.E., 1993. Thidiazuron: a potent cytokinin for woody plant tissue culture. *Plant Cell, Tissue and Organ Culture*, 33(2), 105-119.

[22] Tawfik, A.A., Read, P.E. and Cuppett, S.L., 1998. *Rosmarinus officinalis* L. (Rosemary): In vitro culture, regeneration of plants, and the level of essential oil and monoterpenoid constituents. In: Y.P.S. Bajaj, ed. *Medicinal and Aromatic Plants X. Biotechnology in Agriculture and Forestry Vol. 41*. Berlin: Springer-Verlag, pp. 349-365.

[23] Tawfik, A.A., 2002. Adventitious meristem organogenesis and shoot proliferation of *Salvia officinalis* L. in split-nodal culture. *Assiut Journal of Agriculture Science*, 33(2), 99-114.

[24] Tawfik, A.A. and Mohamed, M.F., 2006. Shoot differentiation and plant regeneration from thidiazuron-induced callus of *Salvia officinalis*. *Acta Horticulture*, 723, 309-313.

[25] Wang, Y. and Yao, R., 2017. Plantlet regeneration of adult *Pinus massoniana* Lamb. Trees using explants collected in March and thidiazuron in culture medium. *Journal of Forestry Research*, 28(6), 1169-1175.

[26] Groach, R., Dar, M.H., Badgal, K.C., Pal, P., Singh, N. and Yadav, K.U.M., 2014. Plantlet regeneration through indirect organogenesis of flame gold tree (*Koelreuteria elegans* Laxm.). *Journal of Ornamental Plants*, 4(3), 175-180.

[27] Yang, X., Yang, X., Guo, T., Gao, K., Zhao, T., Chen, Z. and An, X., 2018. High-efficiency somatic embryogenesis from seedlings of *Koelreuteria paniculata* Laxm. *Forests*, 9(12), 769, https://doi.org/10.3390/f9120769

[28] Tawfik, A.A., 1995. *In vitro* propagation of *Melaleuca armillaris*. *Assiut Journal of Agriculture Science*, 26(4),137-149.

[29] Tawfik, A.A., Ibrahim, O.H.M., Abdul-Hafeez, E.Y. and Ibrahim, S.A., 2018. Optimizing micropropagation protocol for *Rosa hybrida* cv. Eiffel Tower with improved *in vitro* rooting ability. *Egypt Journal of Horticulture*, 45(2), 323-335.

Identification and Plant Growth-Promoting Activities of Proteobacteria Isolated from Root Nodules and Rhizospheric Soils

Kingchan Malisorn[1], Supunnee Chanchampa[1], Pawina Kanchanasin[2] and Somboon Tanasupawat[2]*

[1]Department of Biology, Faculty of Science, Udon Thani Rajabhat University, Udon Thani, Thailand
[2]Department of Biochemistry and Microbiology, Faculty of Pharmaceutical Sciences, Chulalongkorn University, Bangkok, Thailand

Received: 26 February 2020, Revised: 21 May 2020, Accepted: 16 June 2020

Abstract

Phosphate solubilization, zinc solubilization, nitrogen fixation and indole-3-acetic acid (IAA) production are plant growth-promoting activities that occur in certain kinds of bacteria. In particular, the rod-shaped proteobacteria isolated from root nodules and rhizospheric soil are considered to be plant growth-promoting. This study aimed to screen and identify plant growth-producing bacteria and included a study of the IAA optimization of the selected isolates. A total of twelve Gram-negative, rod-shaped bacteria were isolated from *Leguminosae* root nodules and *Leguminosae* rhizospheric soils. The samples were collected in Udon Thani, Nong Bua Lumphu and Nakhon Phanom provinces, Thailand. Based on the phenotypic characteristics and 16S rRNA gene sequence similarities (99.2-100% similarity), the isolates were characterized as relatives of *Rhizobium pusense* (2 isolates), *Ochrobactrum oryzae* (1 isolate), *Pseudomonas aeruginosa* (1 isolate), *Acinetobacter pittii* (1 isolate), *Klebsiella pneumoniae* subsp. *rhinoscleromatis* (1 isolate), and *Pseudomonas geniculata* (6 isolates). The isolates were screened for their plant-growth-promoting activities. The results revealed that 8 isolates exhibited phosphate solubilization (10.9 ± 0.00 to 17.0 ± 1.40 Solubilization Index, SI), zinc solubilization (21.5 ± 0.70 to 33.0 ± 1.40 SI) and indole-3-acetic acid production (1.0 ± 0.2 to 113.4±3.5 µg/ml), and 2 isolates showed their nitrogen-fixing activities. The isolates SN1, SN3-3, SN5, PN1-1 and LS1 were selected and optimized for IAA production.

Keywords: proteobacteria, phosphate solubilizing, zinc solubilizing, indole-3-acetic acid
DOI 10.14456/cast.2020.32

*Corresponding author: Tel.: Tel +66-2-218-8376. Fax +66-2-254-5195
E-mail: Somboon.T@chula.ac.th

1. Introduction

Proteobacteria including Gram-negative, rod-shaped bacteria in genera *Acinetobacter*, *Achromobacter*, *Aerobacter*, *Agrobacterium*, *Azospirillum*, *Burkholderia*, *Chryseomonas*, *Curtobacterium*, *Enterobacter*, *Erwinia*, *Flavimonas*, *Ralstonia*, *Pseudomonas*, *Enterobacter*. *Ralstonia*, *Rhizobium*, *Pantoea*, and *Sphingomonas* strains were found in soils, soybean cultivars, legume tissues and root nodules [1, 2]. They are plant growth promoters and can be used in place of chemicals in agriculture, horticulture, silviculture, and environmental clean-up [3]. Solubilized phosphate and zinc sulfate, which can be supplied via fertilization, are essential nutrients for plant growth [4, 5]. Indole-3-acetic acid (IAA) is one of the most physiologically active auxins produced by plant growth-promoting rhizobacteria [6]. *Rhizobium* strains that present within the root nodules are involved in fixing atmospheric nitrogen for the host plant [3]. This research deals with the identification, screening and optimization of plant growth-promoting activities of bacteria from root nodules and rhizospheric soils.

2. Material and Methods

2.1 Sample collection and isolation of isolates

Eight plant root nodules and 2 rhizospheric soils were randomly collected from Udon Thani, Nong Bua Lamphu and Nakhon Phanom provinces in Thailand (Table 1). All samples were separately kept in sterile plastic bags and then preserved at 4°C. The plant root samples were pretreated as described by Riker and Riker [7]. Each rod nodule was squeezed and streaked on yeast extract-mannitol-congo red (YMC) agar plates and incubated at 30°C for 3-5 days. Then, a 10-fold (10^{-3} and 10^{-4}) dilution of each soil sample was prepared, and 0.1 ml of each dilution was spread onto YMC agar plates. After incubation, the colonies were selected and purified on nutrient agar (NA, Difco) plates. The selected isolates were preserved in 20% (v/v) glycerol at -20°C and in 10% (w/v) skim milk as lyophilized ampoules.

2.2 Identification methods

2.2.1 Phenotypic characterization

Cell morphology, colony appearance, oxidase, catalase, hydrolysis of aesculin, arginine, gelatin, casein, starch and Tween 80; indole, Methyl Red-Voges-Proskauer (MR-VP), nitrate reduction, citrate utilization, and acid production, and growth in NaCl (3%, 5%, w/v) at pH (pH 5 and 9) and temperature at 30, 37, 40 and 48ºC, of the isolates were determined as reported by Barrow and Feltham [8] and Tanasupawat *et al*. [9].

2.2.2 Genotypic characterization

The 16S rRNA gene sequences were amplified using primers 27F (5'-AGAGTTTGATCMTGGC TCAG-3') and 1492R (5'-TACGGYTACCTTGTTACGACTT-3')[10], and their PCR products were analyzed by Macrogen, Korea. The EzBiocloud server [11] was used for the analysis of sequence similarity among the closest strains.

The sequences of isolates were aligned with selected type strain sequences obtained from GenBank. Multiple alignments of the sequences determined were performed using CLUSTAL_X version 1.81. Gaps and ambiguous bases were eliminated prior to construction of a phylogenetic

tree. A phylogenetic tree was reconstructed by the neighbor joining method [12] with the program MEGA 6 [13], and the confidence values of individual branches were also determined using bootstrap analyses based on 1000 replications as described by Felsenstein [14].

2.3 Screening of plant promoting activities

The culture, cultivated in nutrient broth (NB) and incubated at 30ºC for 24 h, was used as an inoculum in this study.

2.3.1 Phosphate solubilizing activity on Pikovskaya's (PVK) agar

The suspension of cultures in NB was swabbed on nitrogen free (NF) agar plates [15] and incubated at 30ºC for 2 days. The culture on the NF agar plates was prepared as inoculum using a cork-borer technique and then inoculated on PVK agar plates [16**]** and incubated at 30ºC for 3-5 days. Phosphate solubilization ability was observed by the formation of a transparent halo around the colonies on the PVK agar plates supplemented with tricalcium phosphate [$Ca_3(PO_4)_2$]. After incubation, a clear halo formed, and the colony diameter and clear zone were measured. The solubilization index was calculated per the following equation [17]:

$$\text{Solubilization index (SI)} = \frac{\text{Colony diameter + clear zone diameter (mm)}}{\text{Colony diameter (mm)}}$$

2.3.2 Zinc solubilizing activity on Mineral salt agar (MSA)

The suspensions of cultures were swabbed on NF agar plates [15] and incubated at 30°C for 2 days. The culture on NF agar was prepared as the inoculum using a cork-borer technique as mentioned above. Then it was inoculated on MSA as described by Saravanan *et al*. [5] and incubated at 30ºC for 3-5 days. The isolates produced transparent halos around the colonies indicating positive zinc solubilization ability. The clear zones formed by the isolates were determined as described by Saravanan *et al*. [5] using the equation mentioned above.

2.3.3 Nitrogen fixing characterization

The nitrogen fixing activity was determined using Nessler's reagent assay [18]. The isolates were cultivated in NF broth and incubated on a shaker (180 rpm) at 30ºC for 48 h. The broth was centrifuged at 3000 rpm for 10 min and the supernatant was tested with Nessler's reagent under dark conditions. It was then subject to colorimetric analysis by microplate reader (CLARIOstar Plus, BMG Labtech) at 560 nm after 20 min incubation.

2.3.4 Indole-3-acetic acid (IAA) production

The isolates were cultivated in NF broth with 1% tryptophan on a shaker (180 rpm) at 30ºC for 48 h. IAA production was evaluated by the Salkowski's method [19] with Salkowski's reagent. The broth was centrifuged at 4000 rpm for 10 min and the supernatant was estimated using colorimetric technique, in the dark. The optical density (OD) of samples was measured at 530 nm after 120 s by microplate reader [20]. The production of the isolate was determined and expressed as µg/ml based on a standard curve of IAA [21].

2.4 Optimization of IAA production

The carbon sources (glucose, mannitol, sucrose, glucose with mannitol and glucose with sucrose), nitrogen sources ($NaNO_3$, KNO_3, peptone, $NaNO_3$ with peptone or KNO_3 with peptone), and tryptophan concentration (0.1%, 0.5%. 1% and 1.5%) were optimized. Effects of pH (5-9) and temperature (30-37°C) on IAA production were also tested. Phosphate buffer was used to maintain the pH value of the medium. Yeast extract-Malt Extract-Dextrose (YMD) broth supplemented with tryptophan was used as basal medium for optimization of IAA production [22].

2.5 Statistical analysis

The data were statistically analyzed by Statistical Package for the Social Sciences (SPSS, Statistics version 24.0.0.0) using one-way analysis of variance (ANOVA) and the grouping was obtained by Duncan's multiple range tests at *p*-value 0.05 [23]. The data were expressed as mean values of triplicates ± standard deviation.

3. Results and Discussion

3.1 Identification of isolates

Twelve Gram-negative, rod-shaped bacteria were isolated from the root nodules of 8 selected plant species and 2 rhizospheric soil samples (Table 1). They were divided into 6 groups based on their phenotypic characteristics (Figure 1). All the isolates grew at pH 5 and 9. They were positive for catalase, nitrate reduction and arginine hydrolysis but were negative for MR-VP. They produced acids from glucose, mannitol and sucrose but did not produce acids from lactose and xylose. The various characteristics are presented in Table 2. The isolates that belonged to genera *Rhizobium* [24], *Ochrobactrum* [25], *Pseudomonas* [26, 27], *Acinetobacter* [28] and *Klebsiella* [29] were designated as Group I to VI (Table 1).

Group I consisted of 2 isolates, LN4-2 and LS1. Colonies were creamy-white, irregular, smooth, flat and opaque on NA agar. All isolates grew in 3% NaCl and at 37°C. They were positive for oxidase, starch, indole, nitrate, and Simmons citrate utilization (Table 2). Based on 16S rRNA gene sequence similarity (100%) and phylogenetic tree analysis (Figure 2), isolate LN4-2 (1299 bp) was identified as *Rhizobium pusense*, while isolate LS1 (1340 bp) was most closely related to *Rhizobium pusense* LMG 25623^T with 99.5% sequence similarity.

Group II consisted of one isolate, which was SN1. The colonies were white, irregular, smooth, flat and opaque on NA agar. The isolate was positive for oxidase. It did not grow in 3 or 5% NaCl and at 40°C. Based on 16S rRNA gene sequence and phylogenetic tree analysis (Figure 2), isolate SN1 (1278 bp) was most closely related to *Ochrobactrum oryzae* MTCC 4195^T with 99.5% sequence similarity.

Group III consisted of one isolate, SN2. The colonies were white, irregular, smooth, flat and opaque on NA agar. All isolates grew in 3 or 5% NaCl and at 40°C. The isolate was positive for oxidase, indole, nitrate reduction, hydrolysis of casein and gelatin, and Simmons citrate utilization. Based on 16S rRNA gene sequence and phylogenetic tree analysis (Figure 2), isolate SN2 (1310 bp) was closely related to *Pseudomonas aeruginosa* JCM 5962^T with 100% sequence similarity. Therefore, it was identified as *Pseudomonas aeruginosa* [26].

Table 1. Samples, location, isolate number, 16S rRNA gene similarity (%) and nearest relatives

Plant/ Soil	Province	Isolate no.	Group	Similarity (%)	Nearest relatives
Indigofera tinctoria	Nong Bua Lamphu	LN4-2	I	100	*Rhizobium pusense*
Macroptilium lathyroides (L.) Urb. Soil	Nong Bua Lamphu	LS1	I	99.5	*Rhizobium pusense*
Sesbania javanica	Udon Thani	SN1	II	99.5	*Ochrobactrum oryzae*
Samanea saman	Udon Thani	SN2	III	100	*Pseudomonas aeruginosa*
Vigna unguiculata sesquipedalis (L.) Verdc	Udon Thani	SN6-2	IV	100	*Acinetobacter pittii*
Tamarindus indica	Udon Thani	SN3-3	VA	99.2	*Pseudomonas geniculata*
Arachis hypogaea	Udon Thani	SN5	VA	100	*Pseudomonas geniculata*
Mimosa pudica	Nong Bua Lamphu	LN1-4	VA	99.9	*Pseudomonas geniculata*
Mimosa pudica	Nong Bua Lamphu	LN1-2	VA	99.4	*Pseudomonas geniculata*
Mimosa pudica	Nong Bua Lamphu	LN1-8	VB	100	*Pseudomonas geniculata*
Mimosa pudica Soil	Nakhon Phanom	PS1-5	VB	99.8	*Pseudomonas geniculata*
Pueraria phaseoloides (Roxb.) Benth	Nakhon Phanom	PN1-1	VI	99.9	*Klebsiella pneumoniae* subsp. *rhinoscleromatis*

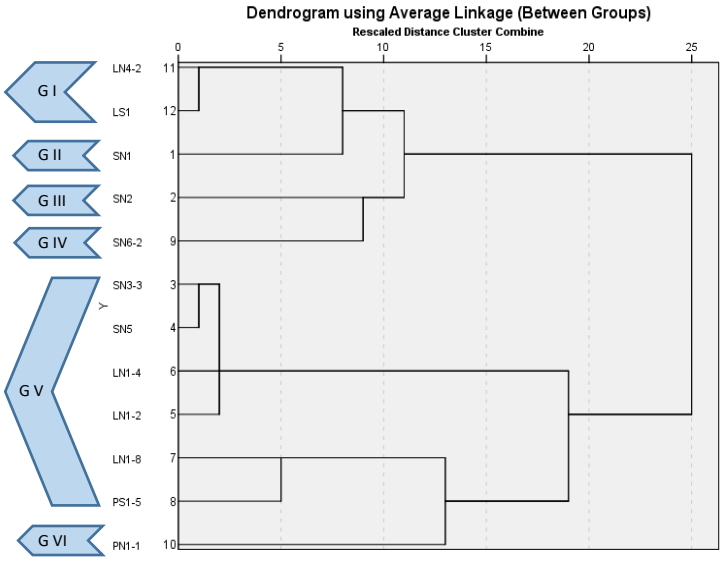

Figure 1. Dendrogram analyzed by SPSS version 24.0.0.0 showing the hierarchical cluster of isolates based on their phenotypic characteristics

Table 2. Phenotypic characteristics of the isolates

Characteristic	I	II	III	IV	VA	VB	VI
	2	1	1	1	4	2	1
Colony color							
Growth in NaCl 3%	+	-	+	+	+	+	+
NaCl 5%	-	-	+	+	+	+	+
Growth at 40°C	-	-	+	+	+	+	+
at 48°C	-	-	-	-	-	-	+
Oxidase	+	+	+	-	-	+	-
Indole	+	-	+	+	+	+	+
Tween 80	-	-	-	-	-	+	-
Citrate utilization	+	-	+	+	+	+	+
Hydrolysis of:							
Aesculin	-	-	-	+	+	+	+
Casein	-	-	+	-	+	+	+
Gelatin	-	-	+	-	+	+	-
Starch	+	-	-	-	-(+2)	+(-1)	+
Acid production from:							
Arabinose	-	-	-	-	+	+(-1)	+
Cellobiose	-	-	-	-	+	+	+
Fructose	-	-	-	-	+	+	+
Galactose	-	-	-	-	+	+	+
Maltose	-	-	-	-	+	+	+
Raffinose	-	-	-	-	-	-	+
Ribose	-	-	-	-	+	-	+
Sorbitol	-	-	-	-	+	+(-1)	+
Trehalose	-	-	-	-	+	-	+

+ positive reaction, - negative reaction

Group IV consisted of one isolate, SN6-2. Its colonies were white, irregular, smooth, flat and opaque on NA agar. It grew in 3 or 5% (w/v) NaCl and at 40ºC. It was positive for indole, nitrate reduction, aesculin hydrolysis and Simmons citrate utilization. Based on 16S rRNA gene sequence and phylogenetic tree analysis (Figure 2), isolate SN6-2 (1383 bp) was closely related to *Acinetobacter pittii* CIP 70.29^T with 100% sequence similarity. Therefore, it was identified as *A. pittii* [28].

Group V consisted of 6 isolates (VA for SN3-3, SN5, LN1-4 and LN1-2; VB for LN1-8 and PS1-5). Colonies were creamy-white, irregular, smooth, flat and opaque on NA agar. All isolates grew in 3 or 5% NaCl and at 40ºC. They were positive for aesculin, casein and gelatin hydrolysis, indole, nitrate reduction and Simmons citrate utilization. Oxidase, starch, and Tween hydrolysis were variable. Four isolates in Groups VA and VB showed differences for oxidase activity, hydrolysis of Tween 80 and acid production from trehalose. On the basis of their 16S rRNA gene sequence and phylogenetic tree analysis (Figure 2), isolates SN3-3 (1207 bp), SN5 (1297 bp), LN1-4 (1249 bp), LN1-2 (1237 bp), LN1-8 (1170 bp) and PS1-5 (1403 bp) were most closely related to *Pseudomonas geniculata* ATCC 19374^T with 99.2, 100, 99.4, 99.3, 100 and 99.8% sequence similarity, respectively [27]. Isolates SN3-3, LN1-2 and LN1-4 exhibited low sequence similarity (99.2%, 99.3% and 99.4%); however, their taxonomic positions were in the same cluster. Further genomic sequence analysis is required for identification.

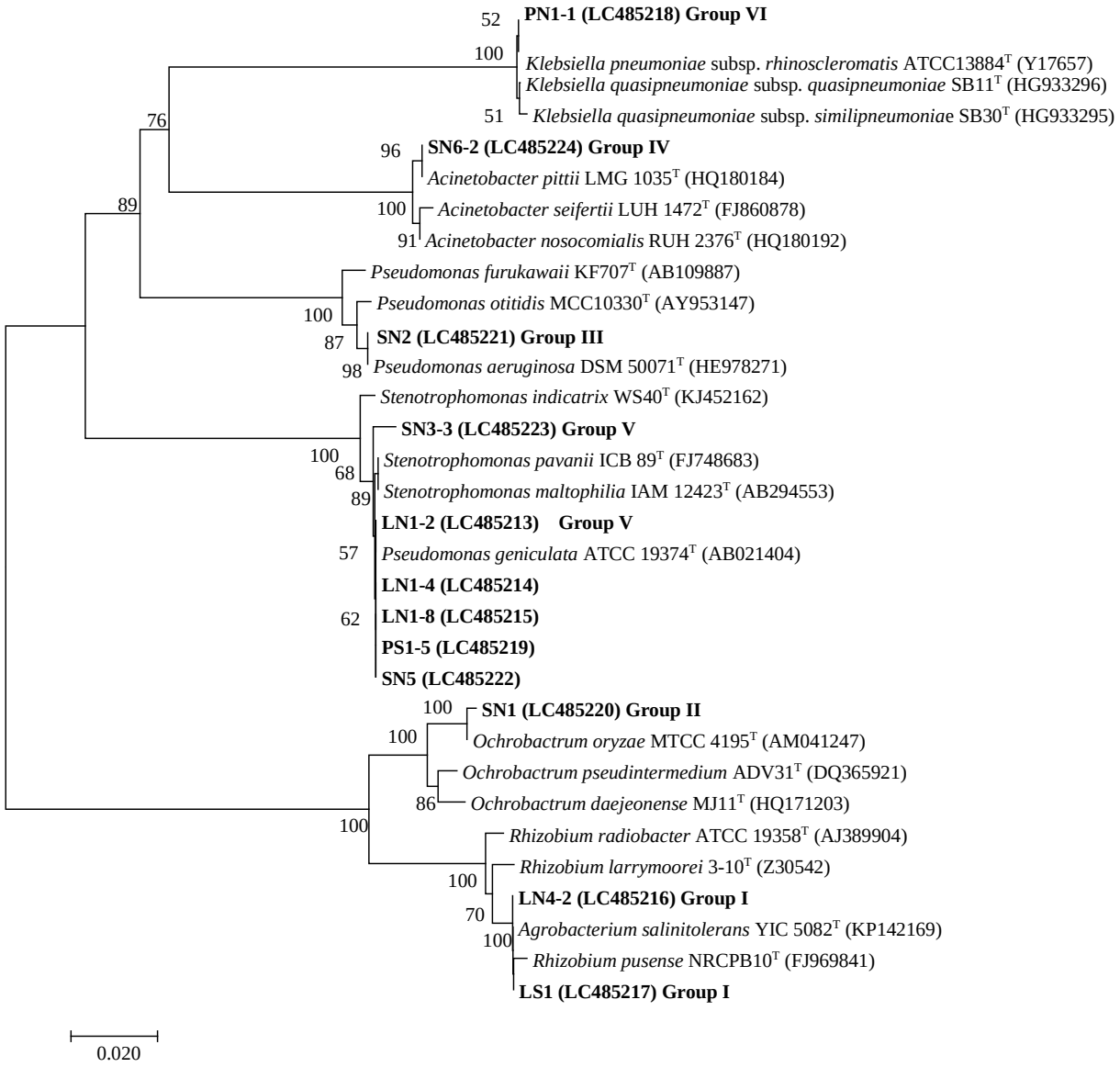

Figure 2. Neighbor-joining tree based on the 16S rRNA gene sequences showing relationships of the isolates. The numbers on the branches indicate the percentage bootstrap values of 1,000 replicates; only values higher than 50% are indicated. Bar, 0.02 substitutions per nucleotide position

Group VI consisted of one isolate, PN1-1. Its colonies were white, irregular, smooth, flat, and opaque on NA agar. The isolate was able to grow in 3 or 5% NaCl and at 40 or 48ºC. It was positive for catalase, indole, nitrate reduction, Simmons citrate utilization, aesculin, casein and starch hydrolysis. On the basis of 16S rRNA gene sequence and phylogenetic tree analysis (Figure 2), isolate PN1-1 (1383 bps) was most closely related to *Klebsiella pneumoniae* subsp. *rhinoscleromatis* 01A030^{T} with 99.9% sequence similarity.

3.2 Screening of plant-growth-promoting activities

The phosphate solubilizing ability in Pikovskaya medium varied from 12.8 ± 7.00 to 17.0 ± 1.40 (Table 3). Isolate LN1-8 exhibited the highest level of solubilized phosphorus (17.0 ± 1.40 mm). Zinc solubilizing ability varied from 21.5 ± 0.70 to 33.0 ± 1.40 mm using ZnO^{3+} as a source of insoluble Zn. Isolate PS1-5 exhibited the highest solubilized zinc (33.0 ± 1.40) (Table 2). The isolates produced IAA (1.0 ± 0.2 to 113.4±3.5 µg/ml) in NF medium with 1% L-tryptophan. Isolates PN1-1 and SN3-3 produced the highest levels of IAA, 113.4±3.5 and 110.8±17.1µg/ml, respectively (Table 2). Among the 12 isolates, only LN1-4 and LN1-8 were able to fix nitrogen (Table 3).

Table 3. Phosphate solubilizing, zinc solubilizing, indole-3-acetic acid (IAA) production and nitrogen fixing activities of the isolates

Isolate no.	Group	Phosphate solubilizing SI*	Zinc solubilizing SI*	IAA (µg/ml)	N_2 fixing (NH_4^+)
LN4-2	I	-	-	27.3±2.3^{b,c}	-
LS1	I	-	-	33.7±8.8^{c}	-
SN1	II	12.8±7.00	-	56.8±2.4^{d}	-
SN2	III	10.9±0.00	21.5±0.70	1.8±0.2^{a}	-
SN6-2	IV	-	21.5±0.70	2.9±0.8^{a}	-
SN3-3	VA	14.6±0.70	29.5±0.70	110.8±17.1^{e}	-
SN5	VA	-	30.5±0.70	12.6±7.6^{a,b}	-
LN1-2	VA	13.4±6.40	21.5±2.10	8.1±0.3^{a}	-
LN1-4	VA	14.6±1.40	-	8.1±0.3^{a}	+
LN1-8	VB	17.0±1.40	-	-^{a}	+
PS1-5	VB	14.9±0.00	33.0±1.40	1.0±0.2^{a}	-
PN1-1	VI	13.0±1.40	30.0±0.00	113.4±3.5^{e}	-

SI*, solubilization index. +, positive reaction; -, negative reaction or no activity.
The clustering result of IAA (µg/ml) from each isolate was a group of a, b, c, d and e, respectively, and was separated by multiple comparisons with the statistical program by Duncan's method at *p*-value 0.05.

3.3 Optimization of IAA production

3.3.1 Effect of different carbon and nitrogen sources on IAA production

The significant differences of IAA production from various carbon sources of each isolate revealed that isolate SN1 produced the maximum IAA (11.8±0.6 µg/ml) when glucose was used, but a low yield of IAA was obtained when sucrose was used (Figure 3). Based on the statistical analysis, glucose was a suitable carbon source for IAA production. However, the amount of IAA produced was not significant when glucose coupled with mannose, and glucose coupled with sucrose were

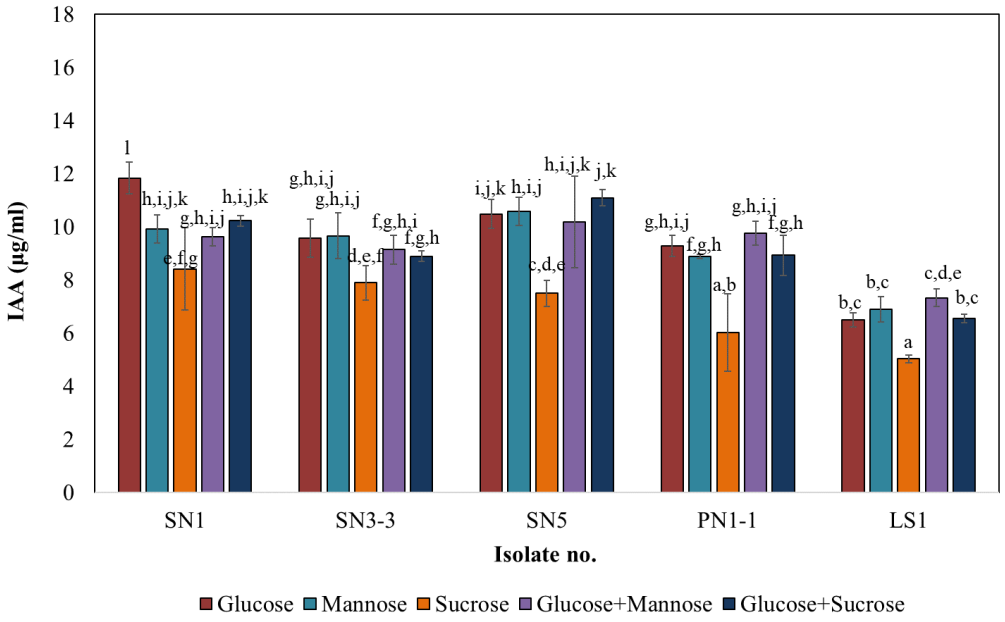

Figure 3. Effect of various carbon sources on IAA production by the selected isolates. The vertical bars represent the standard deviation with triplicates experiment. The clustering result of carbon sources on IAA production defined groups a, b, c, d, e, f, g, h, i, j, k, and l. The values marked by the same letter are not significantly different (*p*-value more than 0.05)

used as carbon sources. In addition, among 5 sources of nitrogen, peptone was clearly the best nitrogen source for IAA production for all isolates. The maximum IAA (13.7±1.6 µg/ml) was obtained from isolate SN5, followed in decreasing order of IAA production by LS1, SN1, SN3-3, and PN1-1 (11.4±0.3, 10.9±0.1, 10.6±0.2, and 10.5±0.1 µg/ml, respectively) (Figure 4). The results from multiple comparisons of different nitrogen sources were divided into 3 groups, and it was confirmed that peptone was the best nitrogen source. The degree of IAA production depending on the isolates, the carbon sources (glucose, mannitol, and sucrose) and the nitrogen sources (peptone, $NaNO_3$ and KN O_3) was also reported by Mohite [22].

3.3.2 Effect of L-tryptophan concentration on IAA production

L-Tryptophan concentrations, 0.1% to 1.5%, affected the production of IAA (Figure 5). Tryptophan was an important variable factor for promoting IAA production of proteobacteria. This result was supported by the research of Costacurta and Vanderleyden [30], who noted that tryptophan was generally considered as an IAA precursor used by bacterial cultures to enhance IAA biosynthesis. However, when the concentration of tryptophan was maintained at 1.0%, isolate PN1-1 was able to produce sufficient IAA with the maximum of 56.7±1.0 µg/ml (Figure 5).

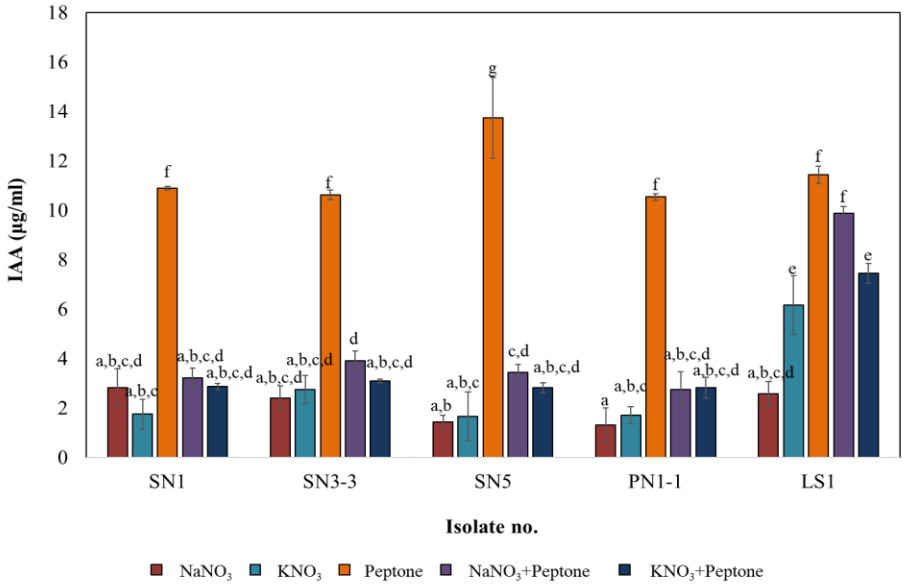

Figure 4. Effect of various nitrogen sources on IAA production by the selected isolates. The vertical bars represent the standard deviation with triplicates experiment. The clustering result of carbon sources on IAA production defined groups a, b, c, d, e, f, and g. The values marked by the same letter are not significantly different (*p*-value more than 0.05).

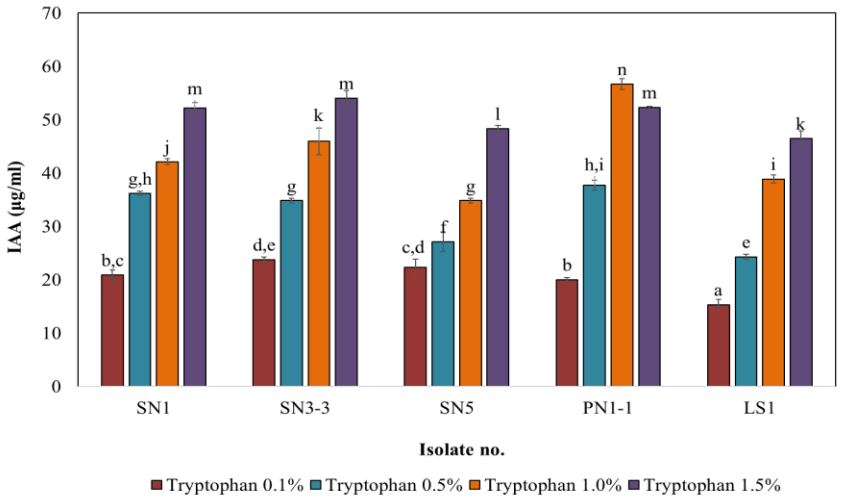

Figure 5. Effect of various tryptophan concentrations on IAA production by the selected isolates. The vertical bars represent the standard deviation with triplicates experiment. The clustering result of carbon sources on IAA production defined groups a, b, c, d, e, f, g, h, i, j, k, l, m, and n. The values marked by the same letter are not significantly different (*p*-value more than 0.05).

3.3.3 Effect of pH and temperature on IAA production

The maximum amount of IAA (70.1±2.2 µg/ml) was produced by isolate SN5 at pH 9. Similarly, IAA was also produced at high concentration at pH 9 by isolates PN1-1, SN1, SN3-3, and LS1 (66.5±2.3, 65.0 ±1.3, 64.6±0.2, and 64.6±0.4 µg/ml, respectively). IAA production was reduced when the pH value was reduced to 8, and further suppressed when the pH value decreased to 5-7. (Figure 6). Therefore, the result was elucidated that pH value is a significant factor for IAA production. The weak alkaline (pH value of 8-9) supported the production of IAA of selected isolates. The result from statistical analysis confirmed that a low concentration IAA was produced at pH value in the range 5-7 and was not significantly different within the group (*p*-value 0.052).

In the comparison of the IAA production at 30 and 37 °C, the results showed that IAA production was favored at 37 °C compared to 30 °C. The isolate SN5 produced the maximum IAA concentration of 8.6±0.9 µg/ml, and it was followed in decreasing order by isolates PN1-1, SN3-3, LS1, and, SN1, which produced 8.4±0.9, 7.1±1.0, 6.5±0.9, and 6.3±1.3 µg/ml of IAA, respectively at 37°C (Figure 7).

According to Sudha *et al*. [31] and Mandal *et al*. [32], *Rhizobium* strain VMA 301 produced high concentrations of IAA in a medium at pH 7.2, while Khamna *et al*. [33] reported that the conditions most suitable for maximum IAA production by *Streptomyces* sp. were at 30°C and pH 7.0. Low pH limits plant growth because the concentrations of metals (Al^{3+} and Mn^{2+}) in the soil solution can reach toxic levels. In addition, *Bacillus* strains produced the maximum amount of IAA when the pH of the medium was at 7, 8 and 9 [22, 34].

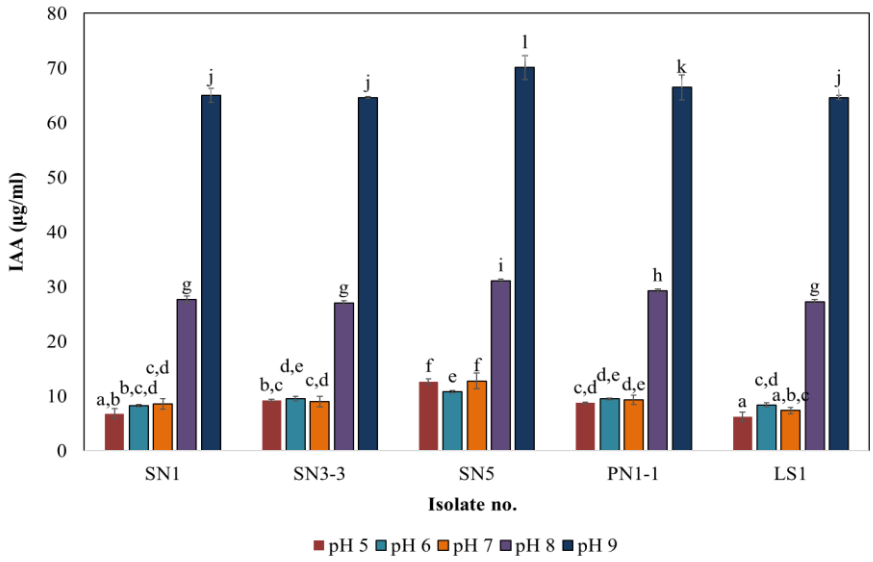

Figure 6. Effect of various pH on IAA production by the selected isolates. The vertical bars represent the standard deviation with triplicates experiment. The clustering result of carbon sources on IAA production defined groups a, b, c, d, e, f, g, h, i, j, k, and l. The values marked by the same letter are not significantly different (*p*-value more than 0.05).

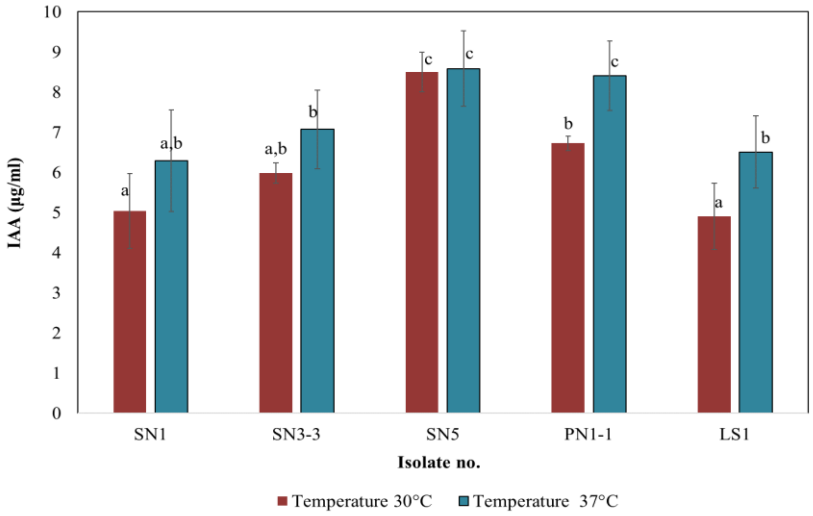

Figure 7. Effect of various temperatures on IAA production by the selected isolates. The vertical bars represent the standard deviation with triplicates experiment. The clustering result of carbon sources on IAA production defined groups a, b, and c. The values marked by the same letter are not significantly different (*p*-value more than 0.05).

Gram-negative bacteria, *Pantoea, Pseudomonas, Rahnella* and *Rhizobium* strains, were reported to produce IAA [35, 36], and they were isolated from rhizospheric soil [22]. Our strains produced different amounts of IAA that was influenced by culture conditions and substrates as reported in *Streptomyces* strains by Matsukawa *et al*. [37]. Moreover, the isolates from the rhizospheric soil were found to be more effective in auxin production, a result which was in agreement with the conclusions of Sarwar and Kremer. [38].

In this study, SN1, SN3-3, SN5, PN1-1, and LS1 proved to be potential isolates for IAA production. The study of the effects of medium components (YMD) on IAA production by selected isolates using statistical analysis indicated that glucose and peptone were the most suitable sources of carbon and nitrogen, respectively. The optimum physical factors at pH 9 and 37ºC were elucidated. In addition, IAA production was further optimized when the culture medium was supplemented with 1.0% L-tryptophan.

4. Conclusions

In this study, isolates LN4-2 and LS1 in Group I, isolate SN1 in Group II, isolate SN2 in Group III, isolate SN6-2 in Group IV, isolates SN3-3, SN5, LN1-4, LN1-2, LN1-8 and isolate PS1-5 in Group V, and isolate PN1-1 in Group VI, were most closely related to *Rhizobium pusense, Ochrobactrum oryzae, Pseudomonas aeruginosa, Pseudomonas geniculata, Acinetobacter pittii* and *Klebsiella pneumoniae* subsp. *rhinoscleromatis*, respectively. They belong to the gamma proteobacteria group. The SN1, SN5 and SN3-3, PN1-1 and LS1 isolates were able to produce IAA effectively when optimized for media components, pH, and temperature.

5. Acknowledgements

This study was supported by the Grant for International Research Integration, Research Pyramid, Ratchadaphiseksomphot Endowment Fund (GCURP_58_01_33_01), Chulalongkorn University and research facilities were provided by the Pharmaceutical Research Instrument Center, Faculty of Pharmaceutical Sciences, Chulalongkorn University. The authors would like to thank Dr.Sukanya Phuengjayaem for the statistical analysis and the revision of Figures.

References

[1] Kuklinsky-Sobral, J., Araujo, W., Mendes, R., Geraldi, I., Pizzirani-Kleiner, A. and Azevedo, J., 2004. Isolation and characterization of soybean-associated bacteria and their potential for plant growth promotion. *Environmental Microbiology*, 6, 1244-1251.

[2] Blaha, D., Prigent-Combaret, C., Mirza, M.S. and Moënne-Loccoz, Y., 2006. Phylogeny of the 1 aminocyclopropane-1-carboxylic acid deaminase-encoding gene acdS in phytobeneficial and pathogenic proteobacteria and relation with strain biogeography. *FEMS Microbiology Ecology*, 56, 455-470.

[3] Shahzad, F., Shafee, M., Abbas, F., Babar, S., Tariq, M.M. and Ahmed, Z., 2012. Isolation and biochemical characterization of *Rhizobium meliloti* from root nodules of Alfalfa (*Medica sativa*). *Journal of Animal and Plant Sciences*, 22, 522-524.

[4] Chen, Y.P., Rekha, P.D., Arun, A.B., Shen, F.T., Lai, W.A. and Young, C.C., 2006. Phosphate solubilizing bacteria from subtropical soil and their tricalcium phosphate solubilizing abilities. *Applied Soil Ecology*, 34, 33-41.

[5] Saravanan, V.S., Madhaiyan, M. and Thangaraju, M., 2007. Solubilization of zinc compounds by the diazotrophic, plant growth promoting bacterium *Gluconacetobacter diazotrophicus. Chemosphere*, 66, 1794-1798.

[6] Lynch, J.M., 1985. Origin, nature and biological activity of aliphatic substances and growth hormones found in soil. In: D. Vaughan and R.E. Malcom, eds. *Soil Organic Matter and Biological Activity*. Dordrecht, Boston, Lancaster: Martinus Nijhoff/Dr. W. Junk Publishers, pp.151-174.

[7] Riker, A.J. and Riker, R.S., 1936. *Introduction to Research on Plant Diseases. A Guide to the Principles and Practice for Studying Various Plant-disease Problems*. St. Louis, Chicago, New York and Indianapolis: John's Swift Co.

[8] Barrow, G.I. and Feltham, R.K.A., 1993. *Cowan and Steel's Manual for the Identification of Medical Bacteria*. New York: Cambridge University Press.

[9] Tanasupawat, S., Okada, S. and Komagata, K., 1998. Lactic acid bacteria found in fermented fish in Thailand. *Journal of General and Applied Microbiology*, 44, 193-200.

[10] Lane, D. J., 1991.16S/23S rRNA sequencing. In: E. Stackebrandt and M. Goodfellow, eds. *Nucleic Acid Techniques in Bacterial Systematics*. New York: John Wiley & Sons, pp.115-175.

[11] Kim, O.S., Cho, Y.J., Lee, K., Yoon, S.H., Kim, M., Na, H., Park, S.C., Jeon, Y.S., Lee, J.H., Yi, H. and Won, S., 2012. Introducing EzTaxon-e: a prokaryotic 16S rRNA gene sequence database with phylotypes that represent uncultured species. *International Journal of Systematic and Evolutionary Microbiology*, 62, 716-721.

[12] Saitou, N. and Nei, M., 1987. The neighbor-joining method: a new method for reconstructing phylogenetic trees. *Molecular Biology and Evolution*, 4, 406-425.

[13] Tamura, K., Stecher, G., Peterson, D., Filipski, A. and Kumar, S., 2013. MEGA6: Molecular evolutionary genetics analysis version 6.0. *Molecular Biology and Evolution*, 30, 2725-2729.

[14] Felsenstein, J., 1985. Confidence limits on phylogenies: an approach using the bootstrap. *Evolution*, 39, 783-791.
[15] Tariq, S., Amin, A. and Latif, Z., 2015. PCR based DNA fingerprinting of mercury resistant and nitrogen fixing *Pseudomonas* spp. *Pure and Applied Biology*, 4, 129-136.
[16] Pikovskaya, R.I., 1948. Mobilization of phosphorus in soil connection with the vital activity of some microbial species. *Microbiology*, 17, 362-370.
[17] Nautiyal, C.S., 1999. An efficient microbiological growth medium for screening phosphate solubilizing microorganisms. *FEMS Microbiology Letters*, 170, 265-270.
[18] Vogel, A.I. and Svehla, G., 1979. *Vogel's Textbook of Macro and Semimicro Qualitative Inorganic Analysis*. London: Longman.
[19] Ehmann, A., 1977. The Van Urk-Salkowski reagent-a sensitive and specific chromogenic reagent for silica. *Journal of Chromatography A*, 132, 267-276.
[20] Vaghasiat, H.L., Patel, G.M., Chudasama, R.S. and Bhott, K.R., 2011. Screening of IAA from rhizosphere microflora of field crops. *Bioscience Discovery*, 2, 94-100.
[21] Chibani, H.R., Bouznad, A., Bellahcene, M. and Djibaoui, R., 2017. Screening and characterization of plant growth promoting traits of phosphate solubilizing bacteria isolated from wheat rhizosphere of Algerian saline soil. *Malaysian Journal of Microbiology*, 13, 124-131.
[22] Mohite, B., 2013. Isolation and characterization of indole-3-acetic acid (IAA) producing bacteria from rhizospheric soil and its effect on plant growth. *Journal of Soil Science and Plant Nutrition*, 13, 638-649.
[23] Duncan, D.B., 1955. Multiple range and multiple F tests. *Biometrics*, 11, 1-42.
[24] Panday, D., Schumann, P. and Das, K.S., 2011. *Rhizobium pusense* sp. nov., isolated from the rhizosphere of chickpea (*Cicer arietinum* L.). *International Journal of Systematic and Evolutionary Microbiology*, 61, 2632-2639.
[25] Tripathi, K.A., Verma, C.S., Chowdhury, P.S., Lebuhn, M., Gattinger, A. and Schloter, M., 2006. *Ochrobactrum oryzae* sp. nov., an endophytic bacterial species isolated from deep-water rice in India. *International Journal of Systematic and Evolutionary Microbiology*, 56, 1677-1680.
[26] Kersters, K., Ludwig, W., Vancanneyt, M., De Vos, P., Gillis, M. and Schleifer, K-H., 1996. Recent changes in the classification of the pseudomonads: an overview. *Systematic and Applied Microbiology*, 19, 465-477.
[27] Anzai, Y., Kim, H., Park, J.Y., Wakabayashi, H. and Oyaizu, H., 2000. Phylogenetic affiliation of the pseudomonads based on 16S rRNA sequence. *International Journal of Systematic and Evolutionary Microbiology*, 50, 1563-1589.
[28] Chang, C.H., Wei, F.U., Dijkshoorn, L., Vaneechoutte, M., Tang, T.C. and Chang, C.T., 2005. Species-Level identification of isolates of the *Acinetobacter calcoaceticus-Acinetobacter baumannii* complex by sequence analysis of the 16S-23S rRNA gene spacer region. *Journal of Clinical Microbiology*, 43, 1632-1639.
[29] Corelli, B., Almeida, S., Sonego, F., Castiglia, V., Fevre, C., Brisse, S., Sansonetti, J.P. and Tournebize, R., 2018. *Rhinoscleroma pathogenesis*: The type K3 capsule of *Klebsiella rhinoscleromatis* is a virulence factor not involved in Mikulicz cells formation. *PLoS Neglected Tropical Diseases*, 12, e0006201, https://doi.org./10.1371/journal.pntd.0006201.
[30] Costacurta, A. and Vanderleyden, J., 1995. Synthesis of phytohormones by plant associated bacteria. *Critical Reviews in Microbiology*, 21, 1-18.
[31] Sudha, M., Shyamala, G.R., Prbhavati, P., Astapritya, P., Yamuna Devi, Y. and Saranya, A., 2012. Production and optimization of Indole-3-acetic acid by indigenous microflora using agro waste as substrate. *Pakistan Journal of Biological Sciences*, 15, 39-43.
[32] Mandal, S.M., Mondal, K.C., Dey, S. and Pati, B.R., 2007. Optimization of cultural and nutritional conditions for indole-3-acetic acid (IAA) production by a *Rhizobium* sp. isolated

from root nodules of Vigna mungo (L.) Hepper. *Research Journal of Microbiology*, 2, 239-246.

[33] Khamna, S., Yokota, A., Peberdy, J.F. and Lumyong, S., 2010. Indole-3-acetic acid production by *Streptomyces* sp. isolated from some Thai medicinal plant rhizosphere soils. *EurAsian Journal of BioSciences*, 4, 23-32.

[34] Acuña, J.J., Jorquera, M.A., Martínez, O.A., Menezes-Blackburn, D., Fernández, M.T., Marschner, P., Greiner, R. and Mora, M.L., 2011. Indole-3-acetic acid and phytase activity produced by rhizosphere bacilli as affected by pH and metals. *Journal of Soil Science and Plant Nutrition*, 11, 1-12.

[35] Lindow, E., Desurmont, C., Elkins, R., Mccourty, G., Clark, E. and Maria, T.B., 1998. Occurrence of Indole-3-acetic acid-producing bacteria on pear trees and their association with fruit russet. *Phytophathology*, 88, 1149-1157.

[36] Datta, C. and Basu, P., 2000. lndole acetic acid production by a *Rhizobium* species from root nodules of a leguminous shrub *Cajanus cojan*. *Microbiological Research*, 155, 123-127.

[37] Matsukawa, E., Nakagawa, Y., Iimura, Y. and Hayakawa, M., 2007. Stimulatory effect of indole-3-acetic acid on aerial mycelium formation and antibiotic production in *Streptomyces* spp. *Actinomycetologica*, 21, 32-39.

[38] Sarwar, M. and Kremer, R.J., 1992. Determination of bacterially derived auxins using a microplate method. *Letters in Applied Microbiology*, 20, 282-285.

Oil Removal from Produced Water Using *Imperata cylindrica* as Low-Cost Adsorbent

Hind J. Hadi[1], Khalid M. Mousa Al-zobai[1] and Mohammed Jaafar Ali Alatabe[2]*

[1]Department of Chemical Engineering, Al-Nahrain University, Al-Jaderyah, Baghdad, Iraq
[2]Department of Environmental Engineering, College of Engineering, University of Al Mustansiriya, Bab-al-Mu'adhem, Baghdad, Iraq

Received: 29 November 2019, Revised: 2 June 2020, Accepted: 17 June 2020

Abstract

Produced water is wastewater that is generated as a byproduct of the extraction of oil and natural gas from underground reservoirs. It contains emulsified oil, organic compounds, inorganic compounds, suspended solids, and dissolved solids. Untreated produced water can cause serious environmental problems. In this research, batch adsorption of produced water that came from the Iraqi Midland Oil Company using *Imperata cylinderica* as adsorbent was investigated. All the experiments were done with 100 ml of produced water in a 250 ml beaker. The factors investigated were pH of the solution (3, 5, 7 and 9), temperature (20, 40, 50 and 60°C), adsorbent dosage (0.05, 0.1, 0.2 and 0.4 g), contact time (15, 30, 60 and 90 min), and the rotational speed of the mixer (150 rpm). The Taguchi method was used to determine the operating conditions. The experimental data were analyzed using statistical optimization and the aim was to develop a general model for determining the optimum conditions that would lead to 97% oil removal, which turned out to be at 30°C, pH 9, adsorbent dose of 0.1g, and 90 min contact time. The Langmuir equation fitted the experimental data for the equilibrium isotherm of oil removal better than did other equations. A pseudo-first-order adsorption was predominant from the kinetics and thermodynamic studies.

Keywords: batch adsorption, *Imperata cylindrica*, produced water
DOI 10.14456/cast.2020.33

1. Introduction

A huge volume of produced water is generated by the Iraqi Midland Oil Company. The disposal of this water into the environment without treatment has the potential to cause serious environmental problems. The treatment process to be used in such a situation depends on nature and the quality of water needed [1]. The most often used methods for treatment of oily wastewater are skimming, gravity separation, neutralization, flotation [2], adsorption, membrane separation [3], coagulation and flocculation [4], electrochemical treatment [5], emulsion breaking [6], biochemical and biological treatment [7, 8], and activated sludge processing [9]. The low molar mass of organic

*Corresponding author: Tel.: 009647706391499
E-mail: mohammedjjafer@uomustansiriyah.edu

pollutants means they cannot be removed efficiently when using coagulation and flocculation processes [10]. Ion exchange processes are too slow kinetically [11]. Membrane technologies require too much power [3]. Most techniques that have been tried to date are not efficient at lower concentrations [12].

Adsorption stands out for being effective and efficient [13]. Adsorption remains the best candidate for this important task because of its simplicity, high efficiency, and easy recovery [12]. One of the keys to making biosorption a viable technology is to have a cost-effective biosorbent. By using renewable or waste raw materials, this technology has the potential to be more economically attractive than conventional technologies [13].

Developments in the field of low-cost adsorbents have led to interest in their use in water treatment processing [14]. Sorbents may be either natural, based on plants or minerals (cotton [15], turf [16], peat-moss [17], sawdust [18], wood shavings [19], wood flour [20], hemp [21], straw [22], clay [23]), or artificial or synthetic materials based on viscose, hydrated cellulose [24], synthetic fibers, thermoplastic materials, and polyurethane foam [25].

Several researchers studied the removal of oil from oily water. Muhammad *et al*. [26] used eggshell to remove oil from oil-contaminated water. The removal rate was almost 100% at a concentration of 1.8 g eggshell/l of produced water and oil concentration as high as 194 mg/l. Wang *et al*. [27] improved the efficiency of kapok fiber for oil absorbency. Kapok fiber was treated by $NaClO_2$, HCl and NaOH. The effects of time and temperature on oil recovery were studied. The oil adsorption capacity of modified sugarcane bagasse in treating oil spills within the water was examined [28]. Oil was also removed from water using *Auricularia polytricha* as adsorbent [29]. Other researchers used eggshell as adsorbent and the process was able to remove 91.21% of the oil [30].

In this research, *Imperata cylindrica,* here considered as agricultural waste, was used. *Imperata cylindrica* has increasingly been recognized as one of the world's most problematic invasive plants [31]. Figure 1 shows the general distribution of *Imperata cylindrica* throughout the world. Its use has presented as worthy of study because biosorbants have come to be seen as a viable technology due to their low cost, renewability and availability [32].

The aims of this research is to study the removal of oil (by the use of harmful, invasive and natural growing plants as adsorbents) from produced water that results from the Iraqi Midland Oil Company, by optimizing the conditions of pH, contact time, adsorbent dose and temperature, and by finding a general equation that relates these conditions to give an optimum value for adsorption. Included are the study of the adsorption isotherms, kinetics and thermodynamics.

Figure 1. The general distribution of *Imperata cylindrica* throughout the world, depicted by areas of white [26].

2. Materials and Methods

2.1 *Imperata cylindrica*

Imperata cylindrica, as an agriculture waste, was collected from roadsides and abandoned farmland around Baghdad, Iraq. Its properties were determined by FTIR, SEM, and EDX tests, the results of which appear in Figures 2 to 4 in the next section. It was washed and milled into 150-210 µm mesh size to use in experiments.

2.2 Experimental procedure

A coagulation/flocculation process was conducted using 70 mg/l of KlarAid CDP 1326 and 2.5 mg/l of Zetag 8140 to treat produced water. The oil content was reduced to 54.6 mg/l as reported in previous work [33]. After that, 100 ml of the produced water was used as a sample to study the ability of *Imperata cylinderica* to adsorb oil. The parameters investigated were pH of the solution (3, 5, 7 and 9), temperature (30, 40, 50 and 60 °C), adsorbent dose (0.05, 0.1, 0.2 and 0.4 g) and contact time (15, 30, 60 and 90 min). The rotational speed of the mixer was 150 rpm. The oil concentration of the samples was analyzed by TD-500, as described in previous work [34].

2.3 Instruments

The equipment and instrumentation utilized to complete the experiments of this research included the following:

(1) A sensitive balance with accuracy down to 0.00001g
(2) Shaker with a perforated platform, Tablar 2000, Heidolph
(3) Hot plate with a magnetic stirrer and controlling thermostat.
(4) Water bath, model WNB, Memmert company.
(5) UV-visible spectrophotometer, model GenesysTM 10, Thermo company
(6) X-ray diffraction device (XRD-6000, Shimadzu, device for qualitative analysis and energy- dispersion X-ray spectroscopy (EDX-7000, Shimadzu, device for quantitative analysis).

2.4 Adsorption isotherms models

The distribution of the contaminant between the solid and liquid is the Adsorption isotherm [35, 36].

2.4.1 The Langmuir model

The Langmuir isotherm assumes monolayer adsorption. Equation 1 was used to describe this type of isotherm [37-39]:

$$q_e = \frac{K_l C_e}{1+a_l C_e} \quad (1)$$

where K_l (l/g) and a_l (l/mg) represent Langmuir constants.

2.4.2 The Freundlich model

In this type of isotherm, the adsorption sites are distributed exponentially [38], and the isotherm is represented by equation 2 [40, 41]:

$$q_e = a_f C_e b_f \quad (2)$$

where q_e is the oil adsorbed (mg/g), a_f (mg/g) is the capacity of multilayer adsorption, and b_f an empirical number that indicates the intensity of adsorption.

2.4.3 Temkin isotherm model

This model was obtained with consideration of adsorption interaction and adsorption substances [42], and in this model the heat of adsorption decreases linearly with coverage. Equation 3 describes this relation:

$$q_e = \frac{RT}{b} \ln AC_e \quad (3)$$

where ($\frac{RT}{b}$)= B(j/mol), which is the Temkin constant, A (L/g) is the equilibrium binding constant, R is the universal gas constant and T (^oK) is absolute solution temperature.

2.4.4 Harkins-Henderson model

This model assumes a multilayer adsorption [43]. Equation 4 describes the Harkins-Henderson isotherm:

$$q_e = \frac{K_{H-H}^{1/n}}{c_e^{1/n}} \quad (4)$$

Here, n and K_{H-H} are isotherm constants.

2.5 Adsorption kinetics

The study of the adsorption kinetics shows the adsorbed rate of adsorbate on the adsorbent. It is therefore required for finding the best-operating conditions for the batch process [44]. There are many kinetic models that analyze adsorption kinetics data.

2.5.1 Pseudo-first-order kinetic model

This model was proposed by Lagergren [45]. The linearized form is shown in equation (5).

$$\text{Log}(q_e - q_t) = \log q_e - k_1 t/2.303 \quad (5)$$

In this equation, qe (mg/g) and qt (mg/g) are the adsorption capacities at equilibrium and at time t, respectively, where k_1 is the rate constant of pseudo-first-order adsorption (min^{-1}) [46].

2.5.2 Pseudo-second-order kinetic model

The pseudo-second-order kinetic model can be represented as follows [47]:

$$\frac{dq_t}{dt} = k_s(q_e - q_t)^2 \quad (6)$$

where k_s is the rate constant of adsorption, g/(mg.min).

2.5.3 Intra particle diffusion study

In the intraparticle diffusion model, adsorption occurs on the surface of the adsorbent initially, then the sorbate diffuses into the interior pores of the adsorbent. The following relationship describes this process:

$$q_t = k_{id}\, t^{1/2} + C \quad (7)$$

where k_{id} and C are the intra-particle diffusion rate constants.

2.5.4 Elovich model

Heterogeneous chemisorption is assumed in the Elovich model. It is widely used in liquid-solid adsorption [47]. Equation 8 describes this type:

$$q_t = 1/\beta \ln(\alpha\beta) + 1/\beta \ln t \quad (8)$$

where α is the initial bio-sorption rate (mg/g.min) and β is related to the extent of surface coverage and the activation energy for chemisorption (g/mg).

2.6 Adsorption capacity

Equation 9 was used to calculate the adsorption capacity (q) [32]:

$$Q = \frac{V(C_0 - C_e)}{M} \quad (9)$$

where Q is the capacity of adsorption (mg/g), C_o is the initial concentration (mg/l), C_e is the equilibrium concentration, *M* is the dosage of adsorbent (g), and *V* is the volume of solution (l). The percentage of the oil removal is calculated using equation 10:

$$(\%)\ \text{Oil removal} = \frac{C_0 - C_e}{C_0} \times 100 \quad (10)$$

3. Results and Discussion

3.1 Produced water

The specification of the sample supplied by the Midland Oil Company was TDS= 157,790 mg/l and TSS = 21.6 mg/l. The other substances' concentrations in produced water are shown in Table 1.

3.2 Fourier transforms infrared spectroscopy (FT-IR) investigation

The FT-IR spectra images of *Imperata cylinderica* were recorded and shown in Figure 2. The medium-length two peaks observed at 2,916 cm^{-1} and 2,849 cm^{-1} are attributed to the presence of C-H asymmetrical stretching and symmetrical stretching, respectively. The peak at 1,731.91 cm^{-1} was assigned to C=O stretching of the carboxylate group, and the peak at 1,462 cm^{-1} is related to C=C stretching of the alkene group. Chowdhury *et al.* [41] indicated that the main functional groups

responsible for the adsorption process are the alkene, aldehyde, carboxylic acid, nitro compound, and phosphate groups [48].

Table 1. Analyses of produced water

Compounds	Concentration (mg/l)
Calcium	7,840
Magnesium	2,352
Chloride	107,192
Sulphate	3,763
Bicarbonate	263.5
Carbonate	n.d.
Oil and grease	550
Iron	<0.02
Manganese	3
Chrome	<0.2
Zinc	1.1
Nickel	<0.2

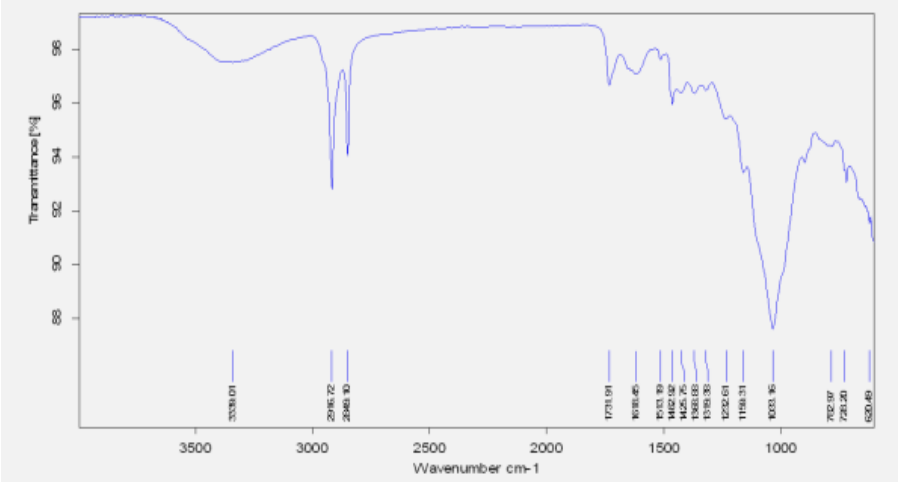

Figure 2. Fourier transforms infrared spectroscopy of *Imperata cylindrica*

3.3 Scanning Electron Microscopic (SEM) and Energy Disperse X-ray spectra (EDX) investigations

The SEM images and EDX spectra of *Imperata cylinderica* surface are shown in Figures 3 and 4. It is clear from the images that the surface was irregular and rough, and had many creases. The white region in the SEM spectrum indicated the presence of large amounts of silica (Si) can possibly enhance the adsorption capacity of adsorbent. Furthermore, EDX is a very good tool for identifying elements on the adsorbent surface. The presence of C, O, and Si ions on *Imperata cylinderica* surface was confirmed by the peaks at 0.2, 0.5, and 1.7 keV, respectively.

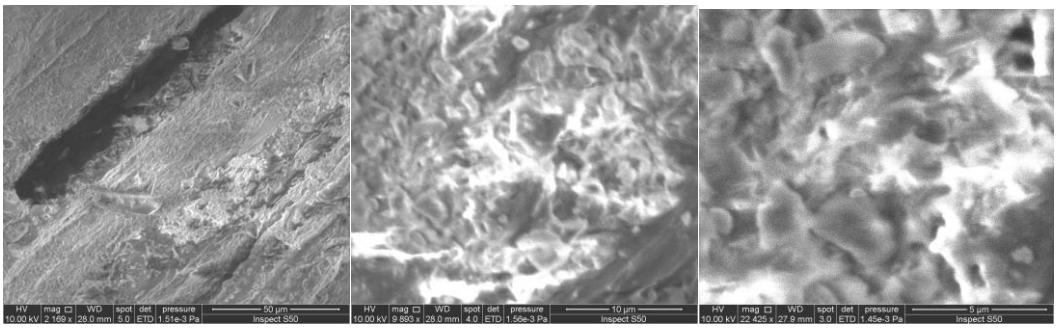

Figure 3. Scanning Electron Microscopic (SEM) of *Imperata cylinderica*

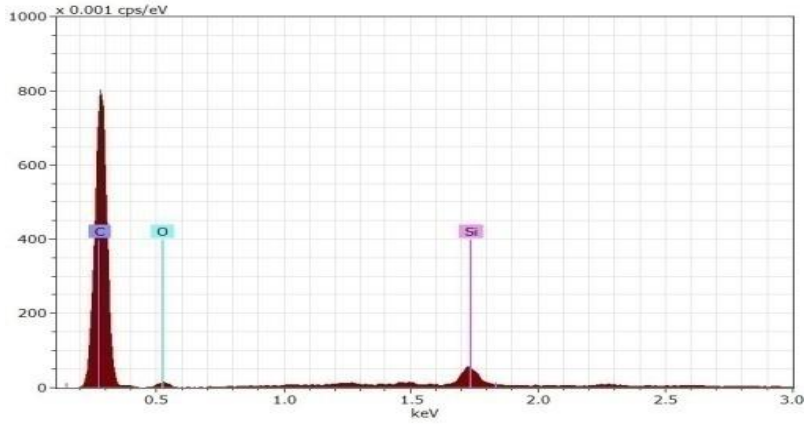

Figure 4. EDX spectra of *Imperata cylinderica*

3.4 Modeling

The main objective of this study was to find the optimal conditions for the adsorption process. The Taguchi method was used to determine the best operating conditions, as shown in Table 2. Statistical optimization was used to analyze experimental data and to develop the general model equation 11:

$$y = (68.96738-(1.02744*x_3) + (0.0136*x_2*x_3) + (1.34999*x_3*x_4)-(2.328*x_2*x_4)) \quad (11)$$

where: X_2 = Temperature , X_3 = Time , and X_4 = adsorbent dose.

3.4.1 Effects of variables

The effects of different conditions on oil adsorption by *Imperata cylinderica* using the combined variables are shown in Table 2. Sixteen experiments were conducted using the Taguchi method to design the batch adsorption experiments, then various models were used to study the isotherm and the kinetics.

The pH(X_1) has no significant effect on the adsorption process due to previous treatment using coagulation and flocculation which neutralized the produced water. Figure 5 proves that the data was distributed close to linearly (R^2 = 0.972), showing a good relationship between the observed and predicted oil concentrations.

Table 2. Experimental design for batch process

No.	pH	Temperatue (°C)	Time (min)	Adsorbent dosage (g)	Oil concentration (ppm)
1	3	30	15	0.05	32.0
2	3	40	30	0.10	13.4
3	3	50	60	0.20	6.8
4	3	60	90	0.40	8.3
5	5	30	30	0.20	22.4
6	5	40	15	0.40	15.8
7	5	50	90	0.05	2.60
8	5	60	60	0.10	5.80
9	7	30	60	0.40	32.0
10	7	40	90	0.20	12.0
11	7	50	15	0.10	19.2
12	7	60	30	0.05	14.3
13	9	30	90	0.1	1.5
14	9	40	60	0.05	9.9
15	9	50	30	0.40	14.8
16	9	60	15	0.20	8.2

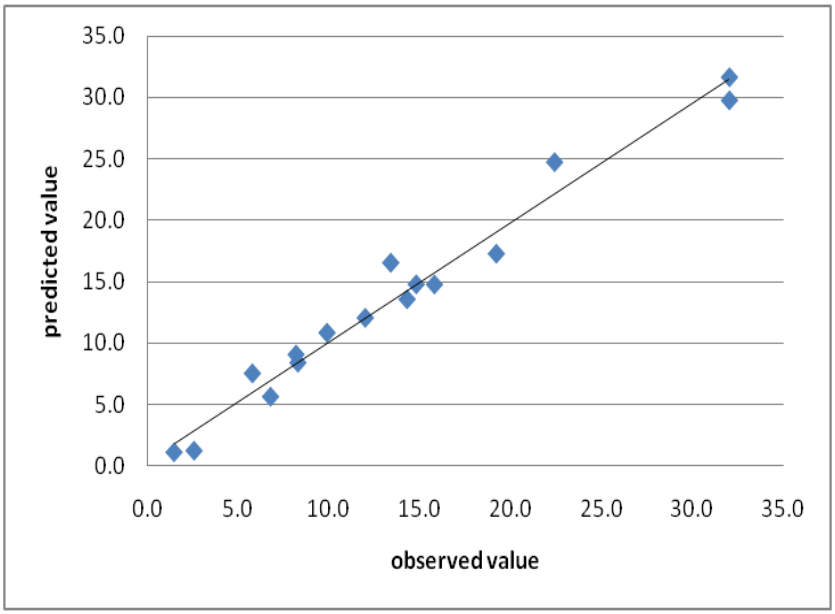

Figure 5. Observed and predicted oil concentration

Table 3 shows that the F-value is 56.65872 and the probability value (p) is 0.00016, indicating the significance of the model.

Table 3. ANOVA test results

P-value	F-value	Mean Squares	DF	Sum of Squares	Effect
Regression	4204.430	11.0000	382.2209	56.65872	0.00016
Residual	33.730	5.0000	6.7460		
Total	4238.160	16.0000			

3.4.2 Effect of contact time on oil removal

The relationship between contact time and oil removal by *Imperata cylindrica* was tested through batch experiments to achieve equilibrium as shown in Figure 6. Oil removal increased with contact time. The rapid adsorption in the first 5 to 30 min can be attributed to the high availability of vacant surface sites during the initial stages. After around 45 min, the adsorption rate started to decline as there were less available adsorption sites [49].

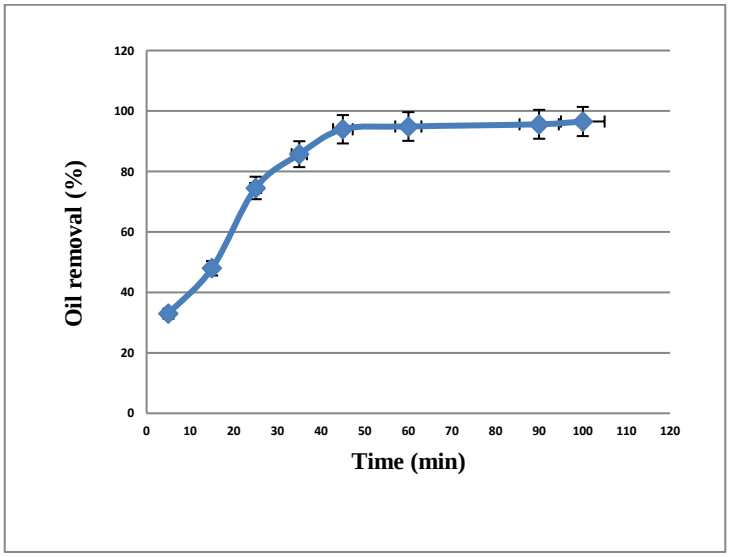

Figure 6. The effect of contact time on percent oil removal by *Imperata cylinderica* at T = 60ºC, Adsorbent dose = 0.5 g/100 ml

3.5 Finding the optimal conditions by Taguchi experimental design

3.5.1 Effect of adsorbent dose on oil removal

The effect of adsorbent dosage at specific conditions on the percentage removal of oil is shown in Figure 7. It can be seen that the removal of oil increased with increasing adsorbent dosage and attained a maximum value of 100% at an adsorbent dosage of 0.753 g/100 ml. The adsorption process increased with an increase in sorbent dosage due to the increase of unsaturated oil binding sites [26].

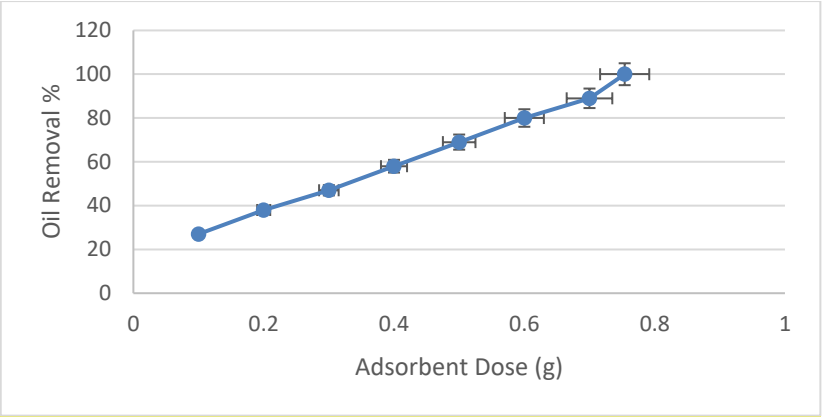

Figure 7. The effect of adsorbent dose on percent oil removal at T = 60°C and t = 45min

3.5.2 Effect of temperature on oil removal

The effect of temperature on oil removal is shown in Figure 8. It is known that oil is sticky and hydrophobic. Temperature affects the solubility of liquids. Increasing the temperature will increase the solubility, hence it improves the mass transfer processing, and the removal of oil should increase [50, 51].

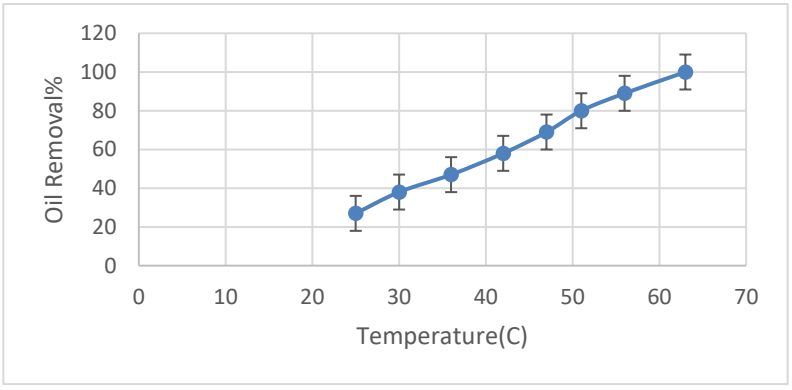

Figure 8. The effect of temperature on percent oil removal at t = 45min and adsorbent dose = 0.753 g/100ml

3.6 Adsorption isotherm results

The linearized forms of the Langmuir, Freundlich,Temkin and Harkins-Henderson isotherm models, as shown in equations (1), (2), (3) and (4), respectively, were analyzed using Microsoft Excel Software to find the isotherm constants. These constants are presented in Table 4, and it can be seen that the regression correlation coefficient (R^2) of the Langmuir equation (R^2 = 0.998) is more linear when compared with that of other equations, implying that the adsorption isotherm data are well fitted by the Langmuir isotherm. Figure 9 shows the experimental curve and isotherm model curves.

Table 4. The constants of isotherm models

Isotherms	Parameters	Values
Langmuir	q_L	0.1404
	K_L	1.17
	R^2	0.998
Freundlich	b_f	0.77
	a_F	1.89
	R^2	0.966
Temkin	B	0.931
	A	34.47
	R^2	0.931
Harkins-Henderson	n	1.2987
	K_{H-H}	2.29
	R^2	0.966

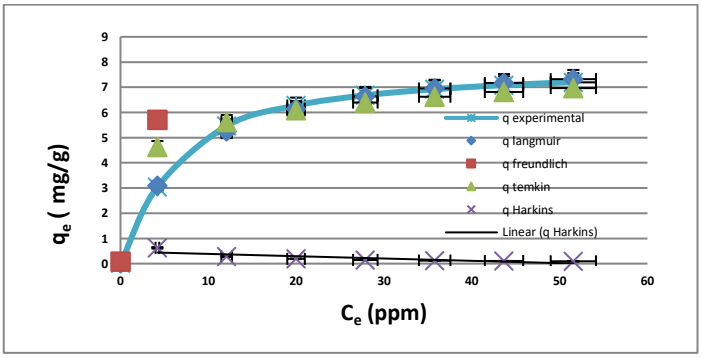

Figure 9. Adsorption isotherm of oil content adsorbed onto *Imperata cylinderica*

The experimental data fit the Langmuir isotherm very well, which means that the process is a single-layer one and the maximum adsorption of oil molecules is only on the surface of *Imperata cylinderica* [42]. The Langmuir isotherm assumes a finite number of active sites available over the surface of the adsorbent and there is no interaction among adsorbed molecules. The same finding was observed by Sarkheil *et al.* [28].

3.7 Adsorption kinetics results

The instantaneous adsorption of the batch process was investigated using four different models. These kinetic models included the pseudo-first-order, pseudo-second-order, intra-particle diffusion, and Elovich models. The experimental results were employed to derive the kinetic parameters using these models. The contacts for these models were obtained using Microsoft Excel Software. Table 5 shows the results of these analyses and Figures 10 to 13 represent the adsorption capacity with the fitted model. Figure 10 represents the relation of log (q_e-q_t) and time for a pseudo-first-order model. Figure 11 represents the relation of (time/q_t) and time for a pseudo-second-order model, Figure 12

represents the relation of q_t and (time) 0.5 for an intra-particle diffusion model, and Figure 13 represents the relation of q_t and ln (time) for the Elovich model.

Table 5. Kinetic models constants for the adsorption of oil onto *Imperata cylinderica*

Model	Parameters	Values
Pseudo-first order equation (5)	q_e	142.2
	K_1	0.0207
	R^2	0.984
Pseudo-second order equation (6)	q_e	0.543
	K_s	1.826
	R^2	0.938
Intra-particle diffusion equation (7)	K_{id}	0.967
	C	0.474
	R^2	0.979
Elovich equation (8)	α	2.895
	β	0.515
	R^2	0.912

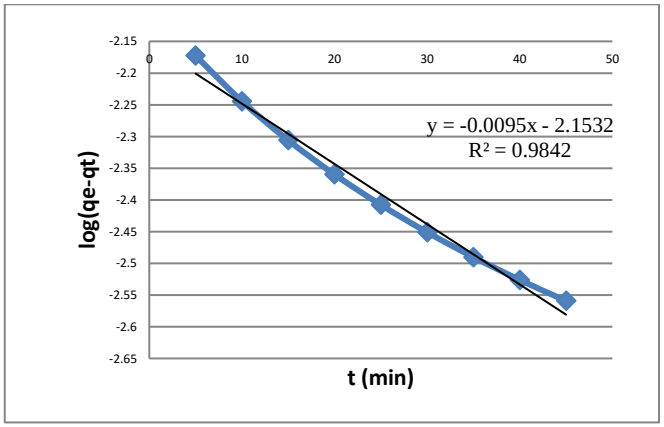

Figure 10. Pseudo-first-order adsorption kinetics of produced water onto *Imperata cylinderica*

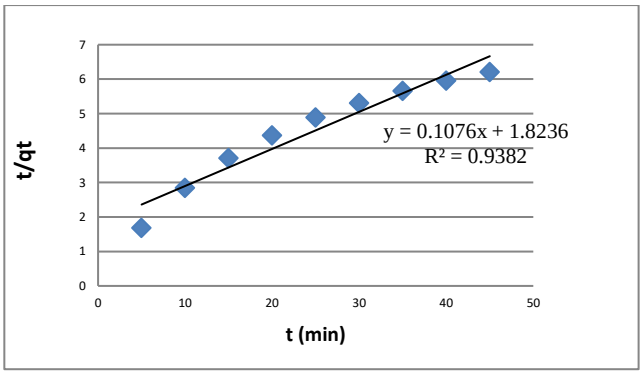

Figure 11. Pseudo-second-order adsorption kinetics of produced water onto *Imperata cylinderica*

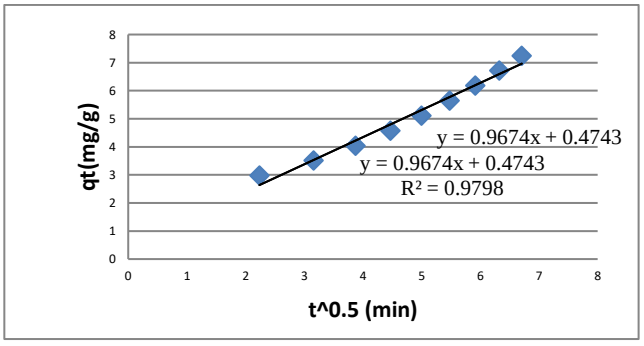

Figure 12. Intra-particle adsorption kinetics of produced water onto *Imperata cylinderica*

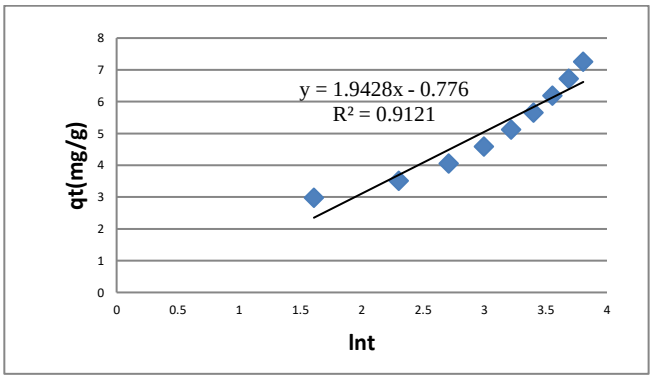

Figure 13. Elovich model for adsorption kinetics of produced water onto *Imperata cylinderica*

By comparing the correlation coefficient (R^2) values of each curve for all five models listed in Table 5, it seems that the kinetics of the oil content adsorption onto *Imperata cylinderica* was a better fit with a pseudo-first-order model than it was with other models. This indicates the applicability of the Lagergren kinetic model to describe the adsorption process of oil onto *Imperata cylindrical*. Moreover, this result is in agreement with Alam *et al*. [32].

3.8 Adsorption thermodynamic results

The effect of temperature on oil adsorption was studied at temperatures ranging from 20 to 60°C. The Gibbs energy change (ΔG°) indicates the degree of the spontaneity of an adsorption process, and a higher negative value reflects more energetically favorable adsorption [52, 53]. Thermodynamic parameters such as standard free energy change (ΔG°), standard enthalpy change (ΔH°) and standard entropy change (ΔS°) were calculated using the following relations [24]:

$$\Delta G^\circ = -RT\text{lin}Kc \quad (12)$$

$$\Delta G^\circ = \Delta H^\circ - T\Delta S^\circ \quad (13)$$

where R is the universal gas constant (8.314 J/mol. K), T is the temperature (°K) and Kc is the thermodynamic equilibrium constant without units. The enthalpy change (ΔH°) and entropy change (ΔS°) of adsorption are obtained from the following equation

$$\text{lin}Kc = (\Delta S^\circ)/R - (\Delta H^\circ)/RT \quad (14)$$

According to Equation (9), (ΔH°) and (ΔS°) parameters can be calculated from the slope and intercept of a plot of linKc versus 1/T, respectively (Figure 14).

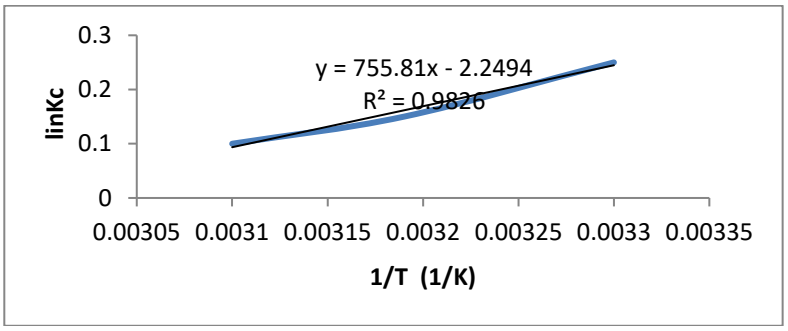

Figure 14. Thermodynamic parameters for oil adsorption onto *Imperata cylinderica*

These thermodynamic parameters can offer insight into the type and mechanism of an adsorption process. Values of free energy change ΔG° are negative confirming that oil adsorption is spontaneous and thermodynamically favorable since ΔG° became more negative (-0.27,-0.39 and-0.63 KJ/mol) with an increase in temperature at 20, 30 and 60°C, respectively, indicating a high driving force and hence resulting in higher adsorption capacity at higher temperatures. The positive value of ΔH° indicated the endothermic adsorption process (0.756 KJ/mol.). A small but positive value of ΔS° (0.0225 KJ/mol.K) in the temperature range 20-60°C suggested increased randomness at the solid-solution interface because some water molecules were dislodged during adsorption of oil [54, 55].

4. Conclusions

This study found that the *Imperata cylinderica* tested, which is one of the numerous kinds of agriculture waste, was very effective in removing oil from produced water through adsorption at low and high initial concentrations and at different temperatures. *Imperata cylinderica* was studied using X-ray diffraction and energy dispersion X-ray spectroscopy techniques, and by other techniques as well. The results showed that *Imperata cylinderica* is effective as an oil adsorbent from produced water due to the availability of effective functional groups, and the presence and nature of these groups was confirmed by FTIR. Very high oil removal efficiencies of the order of 97% were reached at temperature 30°C, pH 9, adsorbent dose 0.1 g, and 90 min contact time. The main objective of this study was to find the optimal conditions for the adsorption of oil.The Taguchi method was used to determine the best operating conditions. The method was used to design the batch adsorption experiments, and then to study the isotherm, and the kinetics. Next, statistical optimization was used to analyze experimental data and develop the general model. The adsorption isotherm was studied, and the linearized forms of the Langmuir, Freundlich, Temkin, and Harkins-Henderson isotherm models were analyzed using Microsoft Excel Software in order to find the relevant isotherm constants. The regression correlation coefficient (R^2) of the Langmuir equation (R^2 =0.998) was more linear when compared with that of other models, implying that the adsorption isotherm data fitted the Langmuir isotherm well. The instantaneous adsorption of the batch process was investigated using four different models: the pseudo-first-order, pseudo-second-order, intra-particle diffusion, and Elovich models. The experimental results were employed to derive the kinetic parameters using these models, and the kinetics of oil adsorption onto *Imperata cylinderica* was found to be best fitted with a pseudo-first-order model. Thermodynamic parameters such as standard free energy change ($\Delta G°$), standard enthalpy change ($\Delta H°$) and standard entropy change ($\Delta S°$) were studied at a temperature ranging from 20 to 60 °C. Finally, we recommend that the oil adsorbed by *Imperata cylindrica* from the produced water should be burned in oil-fired power stations as a heating source.

5. Acknowledgements

The authors are thankful to the technical support of Chemical Engineering Department, Al-Nahran University and Environmental Engineering Department, Al-Mustansiriyah University for giving their investigative services.

References

[1] Igwe, C.O., Saadi, A.A.L. and Ngene, S.E., 2013. Optimal options for treatment of produced water in offshore petroleum platforms. *Journal of Pollution Effects and Control*, 1(2), 1-5.

[2] Ran, J., Liu, J., Zhang, C., Wang, D. and Li, X., 2013. Experimental investigation and modeling of flotation column for treatment of oily wastewater. *International Journal of Mining Science and Technology*, 23(5), 665-668.

[3] Soleimani, R., Shoushtari, N.A., Mirza, B. and Salahi, A., 2013. Experimental investigation, modeling and optimization of membrane separation using artificial neural network and multi-objective optimization using genetic algorithm. *Chemical Engineering Research and Design*, 91(5), 883-903.

[4] You, Z., Zhang, L., Zhang, S., Sun, Y. and Shah, K.J., 2018. Treatment of oil-contaminated water by modified polysilicate aluminum ferric sulfate. *Processes*, 6(7), 95, https://doi.org/

10.3390/pr6070095
[5] Ibrahim, D.S., Sakthipriya, N. and Balasubramanian, N., 2012. Electro-coagulation treatment of oily wastewater with sludge analysis. *Water Science and Technology*, 66(12), 2533-2538.
[6] Cai, Q., Zhu, Z., Chen, B. and Zhang, B., 2019. Oil-in-water emulsion breaking marine bacteria for demulsifying oily wastewater. *Water Research*, 149, 292-301.
[7] Rahman, M.M. and Al-Malack, M.H., 2012. Biochemical kinetics of cross flow membrane bioreactor processes in the treatment of refinery wastewater. *International Journal of Environmental Research*, 6(1), 285-296.
[8] Yu, L., Han, M. and He, F., 2017. A review of treating oily wastewater. *Arabian Journal of Chemistry*, 10, S1913-S1922.
[9] Jafarinejad, S., 2017. Activated sludge combined with powdered activated carbon (PACT process) for the petroleum industry wastewater treatment: A review. *Chemistry International*, 3, 268-277.
[10] Lee, C.S., Robinson, J. and Chong, M.F., 2014. A review on application of flocculants in wastewater treatment. *Process Safety and Environmental Protection*, 92(6), 489-508.
[11] Naghizadeh, A., Nasseri, S., Mahvi, A.H., Nabizadeh, R., Kalantary, R.R. and Rashidi, A., 2013. Continuous adsorption of natural organic matters in a column packed with carbon nanotubes. *Journal of Environmental Health Science and Engineering*, 11(1), 14, http://doi.org/10.1186/2052-336-11-14
[12] Patel, C.V., 2005. *Management of Produced Water in Oil and Gas Operations*. M.Sc. Texas A&M University.
[13] da S. Grem, I.C., Lima, B.N.B., Carneiro, W.F., de C. Queirós, Y.G. and Mansur, C.R.E., 2013. Chitosan microspheres applied for removal of oil from produced water in the oil industry. *Polímeros*, 23(6), 705-711.
[14] Al-Razaq, A.A.A-H. 2012. Oilfield produced water management: treatment, reuse and disposal. *Baghdad Science Journal*, 9(1), 124-132.
[15] Wu, J., Jiang, Y., Jiang, D., He, J., Cai, G. and Wang, J., 2015. The fabrication of pH-responsive polymeric layer with switchable surface wettability on cotton fabric for oil/water separation. *Materials Letters*, 160, 384-387.
[16] Sirotkina, E.E. and Novoselova, L.Y., 2005. Materials for adsorption purification of water from petroleum and oil products. *Chemistry for Sustainable Development*, 13(3), 359-375.
[17] Mathavan G.N. and Viraraghavan, T., 1989. Use of peat in the treatment of oily waters. *Water, Air and Soil Pollution*, 45(1-2), 17-26.
[18] Ortea, E., Cambiella, A., Rios, G., Benito, J.M., Pazos, C. and Coca, J., 2006. Treatment of oil-in-water emulsions: Performance of a sawdust bed filter. *Journal of Hazard Materials*, 131(1-3), 195-199.
[19] Bagrovskaya, N.A., Nikiforova, T.E., Kozlov, V.A. and Lilin, S.A., 2006. Sorption properties of modified wood chips. *Chemistry for Sustainable Development*, 14(1), 1-7.
[20] Ahmad, A.L., Bhatia, S., Ibrahim, N. and Sumathi, S., 2005. Adsorption of residual oil from palm oil mill effluent using rubber powder. *Brazilian Journal of Chemical Engineering*, 22(3), 371-379.
[21] Wahi, R., Chuah, L.A., Choong, T.S.Y., Ngaini, Z. and Nourouzi, M.M., 2013. Oil removal from aqueous state by natural fibrous sorbent: an overview. *Seperation and Purification Technology*, 113, 51-63.
[22] Ibrahim, S., Wang, S. and Ang, H.M., 2010. Removal of emulsified oil from oily wastewater using agricultural waste barley straw. *Biochemical Engineering Journal*, 49(1), 78-83.
[23] Moazed, H. and Viraraghavan, T., 2005. Use of organo-clay/anthracite mixture in the separation of oil from oily waters. *Energy Sources*, 27(1-2), 101-112.
[24] Rohrbach, K., Li, Y., Zhu, H., Liu, Z., Dai, J., Andreasen, J. and Hu, L. 2014. A cellulose based hydrophilic, oleophobic hydrated filter for water/oil separation. *Chemical*

Communications, 50(87), 13296-13299.
[25] Rajakovic, V., Aleksic, G., Radetic, M. and Rajakovic, L., 2007. Efficiency of oil removal from real wastewater with different sorbent materials. *Journal of Hazard Materials*, 143(1-2), 494-499.
[26] Muhammad, I.M., El-Nafaty, U.A., Abdulsalam, S. and Makarfi, Y.I., 2012. Removal of oil from oil produced water using eggshell. *Civil and Environmental Research*, 2(8), 52.
[27] Wang, J., Zheng, Y. and Wang, A., 2012. Effect of kapok fiber treated with various solvents on oil absorbency. *Industrial Crops and Products*, 40(1), 178-184.
[28] Sarkheil, H., Tavakoli, J. and Behnood, R., 2014. Oil by-product removal from aqueous solution using sugarcane bagasse as absorbent. *International Journal of Emerging Science and Engineering*, 2(9), 48-52.
[29] Yang, X., Guo, M., Wu, Y., Wu, Q. and Zhang, R., 2014. Removal of emulsified oil from water by fruiting bodies of macro-fungus (*Auricularia polytricha*). *PLoS One*, 9(4), e95162, https://doi.org/10.1371/journal.pone.0095162
[30] Muhammad, I.M., El-Nafaty, U.A., Abdulsalam, S., Makarfi, Y.I., Ibarahim, M. and Abdulkarim, A., 2015. Oil removal from produced water using surfactant modified eggshell. *2015 4th International Conference on Envirnomental. Energy and Biotechnology*, 85, 84-92.
[31] Hagan, D.L., Jose, S. and Lin, C.-H., 2013. Allelopathic exudates of cogongrass (*Imperata cylindrica*): Implications for the performance of native pine savanna plant species in the southeastern US. *Journal of Chemical Ecology*, 39(2), 312-322.
[32] Alam, M.Z.,. Muyibi, S.A and Toramae, J., 2007. Statistical optimization of adsorption processes for removal of 2, 4-dichlorophenol by activated carbon derived from oil palm empty fruit bunches. *Journal of Environmental Science*, 19(6), 674-677.
[33] Mousa, K.M. and Hadi, H.J., 2016. Coagulation/flocculation process for produced water treatment. *International Journal of Current Engineering and Technology*, 6(2), 551-555.
[34 Mousa, K.M. and Arafat, A.S, 2016. Treatment of oily water containing different salts using surfactants. *Journal of Petroleum Research and Studies*, 120(12th), 75-92.
[35] Al-atabe, M.J.A., 2018. A novel approach for adsorption of copper (II) ions from wastewater using cane papyrus. *International Journal of Integrated Engineering*, 10(1), 96-102.
[36] Shahmohammadi-Kalalagh, S., 2011. Isotherm and kinetic studies on adsorption of Pb, Zn and Cu by kaolinite. *Caspian Journal of Environmental Sciences*, 9(2), 243-255.
[37] Langmuir, I., 1918. The adsorption of gases on plane surfaces of glass, mica and platinum. *Journal of the American Chemical Society*, 40(9), 1361-1403.
[38] Al-atabe, M.J.A. and Hussein, A.A, 2017. Isotherm and kinetics studies, adsorption of chromium (III) ions from wastewater using cane papyrus. *Themed Section: Engineering and Technology*, 3(6), 676-686.
[39] Li, W., Zhang, L., Peng, J., Li, N., Zhang, S. and Guo, S., 2008. Tobacco stems as a low cost adsorbent for the removal of Pb (II) from wastewater: Equilibrium and kinetic studies. *Industrial Crops and Products*, 28(3), 294-302.
[40] Freundlich, H.M.F., 1906. Over the adsorption in solution. *The Journal of Physical Chemistry*, 57, 385-471.
[41] Chowdhury, Z.Z., Zain, S.M., Khan, R.A. and Ahmed, A.A., 2011. Equilibrium kinetics and isotherm studies of Cu (II) adsorption from wastewater onto alkali activated oil palm ash. *American Journal of Applied Sciences*, 8(3), 230-237.
[42] Al-atabe, M.J.A., and Hussein, A.A., 2018. Adsorption of nickel ions from aqueous solution using natural clay. *Al-Nahrain Journal for Engineering Science*, 21(2), 223-229.
[43] Vadi, M., Abbasi, M., Zakeri, M. and Yazdi, B.J., 2010. Application of the Freundlich Langmuir Temkin and Harkins-Jura adsorption isotherms for some amino acids and amino acids complexation with manganese ion (II) on carbon nanotube. *Journal of Physical and Theoretical Chemistry*, 7(2),95-104.

[44] Sulaymon, A.H., Abbood, D.W. and Ali, A.H., 2011. Competitive adsorption of phenol and lead from synthetic wastewater onto granular activated carbon. *Journal of Environmental Science and Engineering*, 5(2011), 1389-1399.
[45] Lagergren, S.K., 1898. About the theory of so-called adsorption of soluble substances. *Kungliga Svenska Vetenskapsakademiens. Handingar*, 24(4), 1-39.
[46] Al-atabe, M.J.A. and Hussein, A.A., 2018. Adsorption of nickel ions from aqueaus solution using natural clay. *Al-Nahrain Journal for Engineering Science*, 21(2), 223-229.
[47] Ho, Y.S. and McKay, G., 1999. Pseudo-second order model for sorption processes. *Process Biochemistry*, 34(5), 451-465.
[48] Alatabe, M.J.A. and Al-sharify, Z.T., 2019. Utilization of low cost adsorbents for the adsorption process of lead ions. *International Journal of Modern Research in Engineering and Technology*, 4(11), 29-48.
[49] Thajeel, A.S., 2013. Isotherm, kinetic and thermodynamic of adsorption of heavy metal ions onto local activated carbon. *Aquatic Science and Technology*, 1(2), 53-77.
[50] Abdulnabi, W.A., Abdulmajeed, Y.R. and Hadi, H.J., 2013. Adsorption of heavy metals from aqueous solution using agricultural wastes. *International Journal of Current Engineering and Technoogy*,3(4),1467-1472.
[51] Sharan, R., Singh, G. and Gupta, S.K., 2009. Adsorption of phenol from aqueous solution onto fly ash from a thermal power plant. *Adsorption Science and Technology*, 27(3), 267-279.
[52] Liu, Y., 2009. Is the free energy change of adsorption correctly calculated? *Journal of Chemical and Engineering Data*, 54(7), 1981-1985.
[53] Alatabe, M.J.A,, 2018. Crystallization in phase change materials. *International Journal of Scientific Research in Science, Engineering and Technology*, 4(1), 93-99.
[54] Liu, M., Zhang, H., Zhang, X., Deng, Y., Liu, W. and Zhan, H., 2001. Removal and recovery of chromium (III) from aqueous solutions by a spheroidal cellulose adsorbent. *Water Environmental Research*, 73(3), 322-328.
[55] Alatabe, M.J.A., 2018. Adsorption of copper (II) ions from aqueous solution onto activated carbon prepared from cane papyrus. *Pollution*, 4(4), 649-662.

Semi-field Application of a New Formulation Based on *Spodoptera litura* Nuclear Polyhedrosis Virus and *Bacillus thuringiensis* subsp. *mexicanensis* Against Cotton Leaf Worm, S*podoptera littoralis* and Root Knot Nematode, *Meloidogyne incognita* in Egypt

Hanan Alfy[1]*, Rehab Y. Ghareeb[2] and Wesam Z. Aziz[3]

[1]Field Crop Pests Department, Plant Protection Research Institute, Agricultural Research Center, Giza, Egypt
[2]Plant Protection and Biomolecular Diagnosis Department, Arid Lands Cultivation Research Institute, City of Scientific Research and Technology Applications, Borg El-Arab, Alexandria, Egypt
[3]Vegetables Pests Department, Plant Protection Research Institute, Agricultural Research Center, Giza, Egypt

Received: 7 March 2020, Revised: 1 June 2020, Accepted: 17 June 2020

Abstract

In this study, new biopreparations based on *Spodoptera litura* nuclear polyhedrosis virus (*Slitura*NPV) and *Bacillus thuringiensis* subsp. *mexicanensis* (Btm) were evaluated against two important pests: cotton leaf worm, *Spodoptera littoralis,* and the root knot nematode, *Meloidogyne incognita,* in 2017 and 2018. The mortality of treated *S. littoralis* larvae occurred, with combination treatments of *Slitura*NPV and Btm at two concentrations (20 and 30%), without significant differences between the two tested concentrations (87.9 and 94.0, respectively). Deformities among pupae were the highest in Btm treatments, followed by *Slitura*NPV treatments, then the fewest deformed pupae were recorded in the combined treatment. Increases of the soybean mean seed weights were highly significant with combined treatment when compared to the controls, in both years, and the greatest expansion was seen with combination treatment. The treatment of *M. incognita* with Btm was highly effective for nematode J_2-mortality. Furthermore, the mean numbers of all recorded parameters for tomato showed significant differences.

Keywords: nuclear polyhedrosis virus, bacteria, cotton leaf worm, nematode, field application
DOI 10.14456/cast.2020.34

*Corresponding author: Tel.: (+20) 1229257322
E-mail: alfyhanan@gmail.com

1. Introduction

The Egyptian cotton leaf worm, *Spodoptera littoralis* (Boisd.) (Lepidoptera: Noctuidae) is certainly one of the most damaging agricultural lepidopteran pests within the subtropics and tropics [1]. It is a hugely polyphagous pest, which presents in almost the whole of Africa, as well as in parts of the Middle East and southern Europe [2, 3]. This insect uses at least 112 species, in 44 plant families, as host plants, for food or for oviposition. In Egypt, it can attack many economically important crops throughout the year, especially cotton and some vegetables [1, 3, 4]. The level of invasion may reach up to 119,048 egg-mass ha^{-1}, inflicting a great harm to all parts of plants [5-9]. Despite the introduction of several management procedures, this pest is still inflicting significant damage.

Meloidogyne incognita (Kofoid and White) (Nematoda; Meloidogynidae), which is a plant parasitic nematode of the root knot nematode type, is an important pathogen in many crops around the world, such as onion, soybean, rice, olive, cucumber, tomato and potato [10-13]. Yield losses of up to 50% may be incurred from intense infestations of the nematode [14].

Although pesticides still play a crucial role in the control of plant pathogenic nematodes and insect pests such as root-knot nematodes and cotton leaf worm, the massive-scale application of such chemicals causes many environmental problems that cannot be ignored. Furthermore, many pests have developed resistance to the pesticides used, and an example of this is the case of *S. Littoralis,* which has developed resistance to many pesticides [15]. The use of pesticides poses acute and chronic hazards to human and non-target organisms. Such chemicals can pollute the environment, challenge wildlife populations, and cause serious public health and food safety problems [7, 16].

Biological control is a successful method that can be used to manage damage from many pests. In fact, biopesticides production and use is growing at an annual rate of 10-20%, a rate that shows it is outpacing the chemical pesticide products industry [17]. Several studies have revealed much about the insecticidal and nematicidal effects of *Bacillus thuringiensis* (Bt) against economically important insect pests and phytoparasitic nematodes. This bacterium represents an important and useful group for microbial control of lepidopteran pests including the Egyptian cotton leafworm *S. littoralis* (Boisd.), tobacco cutworm *S. litura* (F.), fall armyworm *S. frugiperda* Smith, beet armyworm *S. exigua* (Hübner) [18], corn borers *S. nonagrioides* (Lef.) and *Ostrinia nubilalis* (Hübner), cotton bollworm *Helicoverpa armigera* (Hübner), corn earworm *Helicoverpa zea* (Boddie) and soybean looper *Chrysodeixis includens* (Walker) [18-21]. The toxicity of Bt towards phytoparasitic nematodes such as potato cyst nematode (*Globodera pallida*) and root knot nematode (*Meloidogyne incognita, M. javanica*) [22-24], has also been demonstrated.

Baculoviridae is a family of viruses with circular, covalently closed, double-stranded DNA genomes that range in extremely tiny size from 100 to 180 kbp. The virion (an infective baculovirus particle) is occluded into large proteinaceous capsules or occlusion bodies that are rod-shaped polyhedrons. Two genera have been recognized, Nucleopolyhedrovirus (NPV) and Granulovirus (GV), known as Alphabaculoviridae and Betabaculoviridae, respectively [25]. Baculoviruses show a scanty host limit, generally infecting only closely related species. These baculoviruses are potentially useful as biological control agents and have been used effectively to manage different insect pests [26, 27]. NPVs have an impact on a massive range of insect pests and can cause lethal epizootics in susceptible species. The bacterial biopreparations demand around 74% of the market whilst the viral ones around 5% [28]. This study aims to evaluate the biological aspects of new biopreparation upon field application, and to illustrate their impact on Egyptian cotton leafworm and root knot nematodes.

2. Materials and Methods

2.1. Microbial agents

In the present study, *S. litura* nuclear polyhedrosis virus (*Slitura*NPV) and *B. thuringiensis* subsp. *mexicanensis* (Btm) were used. The Btm was isolated in 2003 from the citrus mealybug, *Planococcus citri* (Risso) on a sour orange tree, at the courtyard of Faculty of Agriculture, El-Shatby, Alexandria University, Alexandria, Egypt [29]. Serotyping of this local strain was kindly confirmed by Prof. Lecadet Marguerite, Pasteur Institute, Paris, France. The tested virus was originally isolated from moribund larvae of the cotton leafworm *S. littoralis*, collected in 2017, from fields of the Agricultural Research Station Farm, Nubaria, 47 km west of Alexandria City, Egypt. The NPV was propagated in *S. littoralis* larvae. NPV-murdered larvae were amalgamated in sterile water and then refined through four layers of cotton fabric [30] to obtain a suspension of 7.93×10^8 polyhedra g^{-1} of the dry preparation. The virus particles were then partially purified and subjected to a molecular identification using specific primers [31]. The formulation was produced by adding the suspensions of Btm and virus to a suitable proprietary adjuvant (Patent no. 473/2014). The biopreparation of Btm was produced by adding the adjuvant into other ingredients after sterilizing. The initial Btm preparation contained 1.23×10^9 CFU g^{-1} of the dry preparation.

2.2. Isolation and PCR amplification of the viral DNA

The viral DNA was obtained from the infected *S. littoralis* using DNA virus isolation kit (Qiagene, USA) according to the manufacturer's procedures. A 1 µl (100 ng) sample of the purified DNA was used for PCR amplification of the *Slitura*NPV-polyhedrin gene using specific primers. The PCR reaction mixture consisted of 1 µl DNA sample, 12.5 Master mix (Fermentas, USA), and 1 µl (20 pmol) of each primers of the polyhedrin gene; forward: 5' TA(CT) GTG TA(CT) GA(CT) AAC AA T 3' and reverse: 5' TTG TA(GA) AAG TT(CT) TCC CA(AG) AT 3' in a final volume of 25 µl. The cycling conditions for polymerase chain reaction were as follows: 1 cycle at 94°C for 5 min., followed by 35 cycles of; 94°C for 30 s; 49°C for 1 min and 72°C for 1 min, and an extension cycle at 72°C for 10 min. Amplification was accomplished using a DNA thermal cycler (Eppendorff, USA). The PCR amplified product was clarified by a PCR clean-up column kit (QIAGEN, Germany) and examined on agarose gel electrophoresis. After the sequencing process, the annotated nucleotide sequence was analyzed using NCBI-BLAST (http://blast.ncbi.nlm.nih.gov/Blast.cgi), and compared with those of previously reported *Slitura*NPVs. The sequence was deposited in GenBank with the accession number MN649826 Spodoptera_LAST Spodopera.

2.3. Semi-field application test against *S. littoralis*

The experiment was carried out at Nubaria Agriculture Research Station, km. 47 Cairo-Alexandria road during 2017 and 2018. The experimental area was divided into plots of 3.5m x 3m (10.5 m^2), each arranged in a randomized complete block design with three replicates for each treatment. The common soybean variety Giza 111 was planted in mid-May each year and normal agriculture practice was followed. Treatments consisted of (1) Btm alone, (2) *Slitura*NPV alone, (3) a combination of the two entomopathogens and (4) an untreated control. The microbial agents, alone and in combination, were prepared with each of two concentrations, 20% and 30% (W/V), for a total of 7 treatments.

The preparations were sprayed at a rate of 494 l ha^{-1} using a manually pressurized 10 l backpack sprayer after observing the first egg mass in field, and after two weeks, untreated plants were sprayed by water only. Sprays were applied thoroughly to cover the plants. Some egg masses

of *S. littoralis* were taken to the laboratory for hatching and rearing. Everyday, soybean leaves were collected at random from each plot for feeding larvae in the laboratory. Each container contained ten middle-sized leaves, and one egg mass was placed on sprayed leaves after counting the eggs in the mass. Percent mortality of larvae was determined after five days; adjusted mortality rate (P) was calculated based on the following formula [32]:
where P = [P observed - P expected/control / (1- P expected/control] x 100.
At harvest, the seed weights per plot were recorded as proper indicator of yield.

2.4. Root-knot nematode preparation

The root-knot nematode *M. incognita* used in this study was supplied by the Plant Pathology Department, Faculty of Agriculture, Alexandria University. The nematodes were propagated on tomato plants, *Solanum lycopersicum* cv. Alisa, cultivated in sandy clay soil. Inocula of *M. incognita* were prepared by extracting nematode eggs from nine-week-old nematode-infected tomato roots. Active juveniles (J_2) of *M. incognita* were obtained by using Baermann plate technique [33, 34].

2.5. Nematicidal bioassay of Btm

2.5.1. *In vitro* effect

The microbial agent (Btm) was tested on second-stage juveniles (J_2) of *M. incognita* under laboratory conditions. Two rates (20 and 30%, w/v) of each treatment as described earlier were prepared in distilled water. Five replicates of each rate were used with about 150 *M. incognita* juveniles. The assays were conducted in 6-well plastic ELISA plates, with the plates incubated in the lab at room temperature ($27^{o}\pm 2^{o}C$). The control treatment was distilled water. The mortality of J_2s was determined after 24 h, 48 h and 72 h of exposure.

2.5.2. *In planta* effect

The nematicidal activity of Btm towards *M. incognita* was examined *in planta*, using tomato plants (*S. lycopersicum* cv. Alisa). The assay was performed in 15 plastic pots, 15 cm in diameter and 14 cm in depth, filled with 1 kg of an autoclaved mixture of a sandy loam soil (1:1, sand: loam). Three weeks after sowing, each pot was thinned to one plant. The pots were then each inoculated with close to 3000 second-stage juveniles (J_2) of *M. incognita* by running 10 ml of a nematode suspension into an aperture having a 3-5 cm depth around the plant stem. Each treatment consisted of 5 pots and an additional 5 pots were left to serve as controls. The pots were arranged in a completely randomized design, one plant per pot. Infested pots were kept on a bench in the greenhouse and maintained for two months at 25°C±5°C. After this incubation period, the root groups were harvested and assessed for galling (number of galls per root system), and egg masses per root using an aqueous solution of phloxine-B stain (0.15 g l^{-1} tap water) for 15-20 min, and then the roots were rinsed in tap water to remove residual stain [34]. The percent reduction was calculated using the Abbott correction [31].

2.6. Data analysis

Data were analyzed using IBM SPSS software package version 20.0 (Armonk, NY: IBM Corp). The Kolmogorov-Smirnov test was used to verify the normality of distribution of variables. Comparisons of categorical variables between groups were assessed using Chi-square test (Fisher or Monte Carlo). Smirnov, Shapiro, and D'agstino tests were used to verify the normality of distribution of

variables, Student t-test was used to compare two groups for normally distributed quantitative variables, while ANOVA was used to compare more than two groups for normally distributed quantitative variables. This was followed by Post Hoc test (Tukey) for pairwise comparison. Spearman coefficient was used to correlate between quantitative variables. Significance of the obtained results was judged at the 5% level.

3. Results and Discussion

Viral identification involved the use of PCR with specific polyhedrin gene primers, and an amplicon with a molecular size of ~1200 bp was detected (Figure 1). After PCR product purification and sequencing, the DNA sequence was delivered to the GenBank database under the accession number of MN649826. NCBI-BLAST alignment and phylogenetic analysis (Figure 2) indicated that our virus isolate was closely linked to the two isolates (*Spodoptera litura* NPV) of Chinese and Australian origin (AF037262, AF068189), respectively, with a similarity of 86% to viral isolates of *S. litura* from 4 countries. An Indian isolate of *Sl*NPV (Y10254) was considered an outlier for all the examined genes in the constructed tree. On the other hand, when the analysis performed, using the deduced amino acid sequences, it was observed that our isolate showed only 50% similarity with a French isolate of *Sl*NPV (X99073).

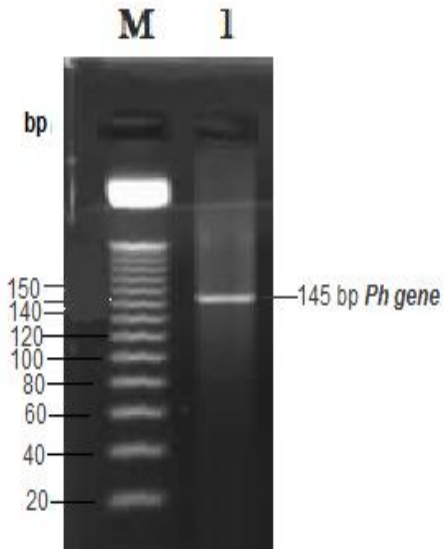

Figure 1. PCR amplification of the polyhedrin gene from the DNA extracted from the cotton leaf worm *S. littolaris* infected with the *Slitura*NPVs

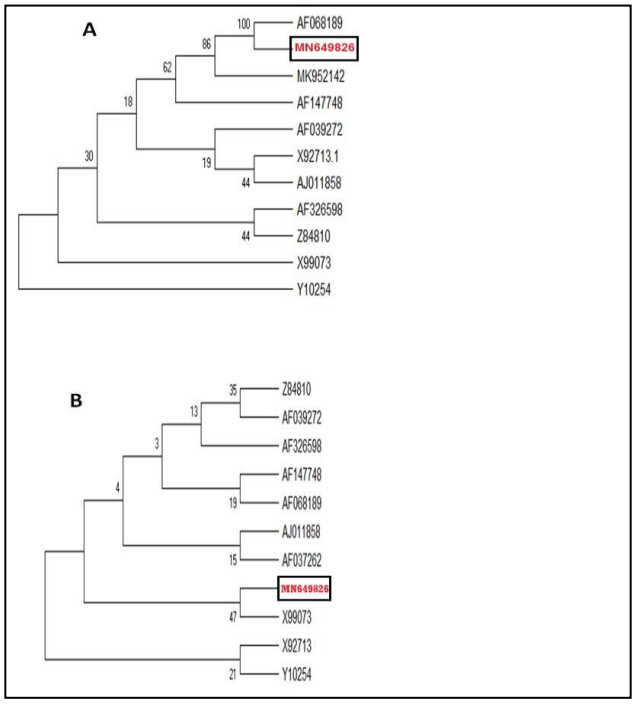

Figure 2. Phylogenetic tree of the isolated polyhedrin genes compared with the others published in the GenBank. The phylogenetic trees were constructed using the Mega 5 program using UPGMA type. A: phylogeny was constructed based on the nucleotide DNA sequence; while B: the phylogeny was constructed based on the deduced amino acid sequences

Data presented in Tables 1 and 2 illustrate the insect stage effect on responses of *S. littoralis* after foliar application by the treatments (Btm, *Slitura*NPV and both *Slitura*NPV and Btm) in 2017 and 2018. The percentage mortality of the treated *S. littoralis* larvae is presented in Table 1. Our results reveal that the impact of the combined *Slitura*NPV and Btm at 20% and 30% gave the highest activity of 87.9% and 94.0%, respectively, without any significant differences between these two concentrations. Mortality of *S. Littoralis* larvae treated with *Slitura*NPV alone, at 20% and 30%, was 73.6% and 77.3%, respectively, which was higher than the corresponding mortality of larvae treated with Btm alone, which was 60.2% and 63.8%, respectively, in 2017. In 2018, similar results were obtained (Table 2).

In both years, the results of all treatments showed a numerical but not statistically significant increase in the mortality percentage of *S. littoralis* larvae with highly significant differences between the type of treatments; but there were no significant differences between the concentrations of the same treatment used in 2017 and 2018 (Tables 1 and 2). According to the high percentage of mortality, the treatments of the combinations of Btm and SliturаNPV were highly effective. In 2017, after application of SliturаNPV or Btm (20 and 30%), the percentage of abnormal pupae of S. littoralis was 11.9 and 5.7%, respectively while it was 25.1% and 22.5% after the treatment with SliturаNPV (20 and 30%). However, the abnormal pupae percentage of the target insect, treated with Btm 20% was 37.1%, and with Btm 30% was 34.4% (Table 1). The pupal abnormality was the highest with Btm treatment, followed by SliturаNPV, and the lowest abnormal

Table 1. Biological parameters of *S. littoralis* after field foliar application in 2017

Biological parameters	**Btm**		***Slitura*NPV**		***Slitura*NPV and Btm**		**Untreated (control)**	χ^2	**p**
	20%	**30%**	**20%**	**30%**	**20%**	**30%**	**0%**		
Total number of eggs	1820	1914	1911	1857	1853	1912	1862		
Number of dead larvae	1095^{a} (60.2%)	1221^{a} (63.8%)	1406^{b} (73.6%)	1436^{b} (77.3%)	1629^{c} (87.9%)	1798^{d} (94.0%)	21^{e} (1.1%)	4714.052^{*}	$\leq 0.001^{*}$
Number of abnormal pupae	675^{a} (37.1%)	658^{a} (34.4%)	480^{b} (25.1%)	418^{b} (22.5%)	221^{c} (11.9%)	109^{d} (5.7%)	3^{e} (0.2%)	1419.329^{*}	$\leq 0.001^{*}$
Number of abnormal adult moths	41^{a} (2.3%)	27^{ab} (1.4%)	18^{bc} (0.9%)	3^{d} (0.2%)	3^{d} (0.2%)	5^{cd} (0.3%)	0^{d} (0.0%)	106.382^{*}	$\leq 0.001^{*}$
Number of normal adult moths	9^{a} (0.5%)	8^{ab} (0.4%)	7^{ab} (0.4%)	0^{b} (0.0%)	0^{b} (0.0%)	0^{b} (0.0%)	1838^{c} (98.7%)	12738.011^{*}	$\leq 0.001^{*}$

Different superscripts are statistically significant at $p<0.05$ in the same row.

Table 2. Biological parameters of *S. littoralis* after field foliar application in 2018

Biological parameters	Btm		*Slitura*NPV		*Slitura*NPV and Btm		Untreated (control)	χ^2	p
	20%	30%	20%	30%	20%	30%	0%		
Total number of eggs	1789	1852	1848	1798	1836	1817	1839		
Number of dead larvae	1228^{a} (68.6%)	1349^{a} (72.8%)	1431^{b} (77.4%)	1437^{b} (79.9%)	1695^{c} (92.3%)	1625^{c} (89.4%)	19^{d} (1.0%)	4944.390^{*}	$\leq 0.001^{*}$
Number of abnormal pupae	508^{a} (28.4%)	432^{b} (23.3%)	409^{b} (22.1%)	350^{b} (19.5%)	138^{c} (7.5%)	184^{c} (10.1%)	0^{d} (0.0%)	849.150^{*}	$\leq 0.001^{*}$
Number of abnormal adult moths	38^{a} (2.1%)	45^{a} (2.4%)	5^{b} (0.3%)	6^{b} (0.3%)	3^{b} (0.2%)	7^{b} (0.4%)	0^{b} (0.0%)	138.699^{*}	$\leq 0.001^{*}$
Number of normal adult moths	15^{ab} (0.8%)	26^{b} (1.4%)	3^{ac} (0.2%)	5^{ac} (0.3%)	0^{c} (0.0%)	1^{c} (0.1%)	1820^{d} (99.0%)	12232.302^{*}	$\leq 0.001^{*}$

χ^2: Chi square test
Different superscripts are statistically significant at $p<0.05$ in the same row.

pupae were in the combination treatment. There were no significant differences between different concentrations in the same treatment; with the except of the combination treatment where the result recorded at a high concentration (30%) was less significant than a lower one (20%). On the other hand, there was the difference between the two concentrations of Btm treatment in 2018 (Table 2), hence it was 28.4 and 23.3%, respectively, for Btm (20%) and (30%). Other treatments in 2017 revealed the same significance in pupa abnormality. There were significantly different percentages of abnormal moth after treatment, where the Btm (20 %) treatment gave the highest abnormal moth numbers, while the lowest was the combination (30 %) treatment.

In the two years of this study, significant differences were found in the number of normal and abnormal moths of *S. littoralis* after foliar application with the current treatments. Furthermore, all treatments used showed a clear effect on numbers of dead larvae, abnormal pupae, abnormal moths and normal moths of the target insect *S. littoralis* compared with the untreated control (Tables 1 and 2).

Some of the obvious symptoms in infected larvae, in addition to deformed pupae, are illustrated in Figure 3. These are the results after exposure to both bacteria and virus. The symptoms of viremias differed from those killed by the Btm bacteria. Infection with the virus led to build-up of fluid in the body of the larva and rupture of the cuticle upon touching with a probe; at the beginning of the injury, the bodies had a rubbery consistency. However, the action of the bacteria lead to harder cadavers and dark body colors due to paralysis and cessation of nutrition, in addition to septicemia.

Figure 3. Adverse effects of the tested biological control agents on *S. littolaris*-treated individuals

All biological parameters in both seasons showed that the treatment was very effective in the case of larval mortality, while it has had a weak effect on abnormal pupae or moths and vice versa. In addition to the presence of different significance between two seasons, the percentage of larval mortality was higher in the second season than in the first one, as shown in Table 3. There was no correlation between the number of mortality larvae and the number of abnormal pupae in the two seasons, where the Spearman coefficient was -0.250.

Table 3. Biological parameters of *S. littoralis* after field foliar application in 2017 and 2018 seasons

Biological parameters	2017	2018	χ^2	p
	No. (%)	No. (%)		
No. of dead larvae				
Btm at 20%	1095 (60.2%)	1228 (68.6%)	28.265*	≤0.001*
Btm at 30%	1221 (63.8%)	1349 (72.8%)	35.548*	≤0.001*
*Slitura*NPV at 20%	1406 (73.6%)	1431 (77.4%)	7.566*	0.006*
*Slitura*NPV at 30%	1436 (77.3%)	1437 (79.9%)	3.652	0.056
*Slitura*NPV and Btm at 20%	1629 (87.9%)	1695 (92.3%)	20.107*	≤0.001*
*Slitura*NPV and Btm at 30%	1798 (94.0%)	1625 (89.4%)	26.223*	≤0.001*
Untreated	21 (1.1%)	19 (1.0%)	0.078	0.781
No. of abnormal pupae				
Btm at 20%	675 (37.1%)	508 (28.4%)	30.935*	≤0.001*
Btm at 30%	658 (34.4%)	432 (23.3%)	55.904*	≤0.001*
*Slitura*NPV at 20%	480 (25.1%)	409 (22.1%)	4.638*	0.031*
*Slitura*NPV at 30%	418 (22.5%)	350 (19.5%)	5.098*	0.024*
*Slitura*NPV and Btm at 20%	221 (11.9%)	138 (7.5%)	20.420*	≤0.001*
*Slitura*NPV and Btm at 30%	109 (5.7%)	184 (10.1%)	25.205*	≤0.001*
Untreated	3 (0.2%)	0 (0.0%)	2.965	0.250
No. of abnormal moth				
Btm at 20%	41 (2.3%)	38 (2.1%)	0.070	0.792
Btm at 30%	27 (1.4%)	45 (2.4%)	5.213*	0.022*
*Slitura*NPV at 20%	18 (0.9%)	5 (0.3%)	6.963*	0.008*
*Slitura*NPV at 30%	3 (0.2%)	6 (0.3%)	1.102	0.336
*Slitura*NPV and Btm at 20%	3 (0.2%)	3 (0.2%)	0.000	1.000
*Slitura*NPV and Btm at 30%	5 (0.3%)	7 (0.4%)	0.445	0.505
Untreated	0 (0.0%)	0 (0.0%)	–	–
No. of normal moth				
Btm at 20%	9(0.5%)	15 (0.8%)	1.616	0.204
Btm at 30%	8(0.4%)	26 (1.4%)	10.226*	0.001*
*Slitura*NPV at 20%	7(0.4%)	3 (0.2%)	1.473	0.344
*Slitura*NPV at 30%	0(0.0%)	5 (0.3%)	5.171*	0.029*
*Slitura*NPV and Btm at 20%	0(0.0%)	0 (0.0%)	–	–
*Slitura*NPV and Btm at 30%	0(0.0%)	1 (0.1%)	1.053	0.487
Untreated	1838(98.7%)	1820 (99.0%)	0.527	0.468

χ^2 = Chi square test

* = Statistically significant at $p \leq 0.05$

Table 4 shows a comparison between the different treatment groups based on seed weight. In 2017, the mean weight ranged from 803.3±12.6 g/plot when treated with Btm at 20% to 847.7±4.0 g/plot when treated by the combination treatment at the 30% rate, compared with the untreated which was 545.7d±5.5 g/plot; and ranged from 807.0±4.4 g/plot when treated with Btm at 20% to 842.3±2.5 g/plot when treated with *Slitura*NPV and Btm at 30%, compared to the untreated which was 560±2.0 g/plot in 2018. Statistically, according to ANOVA test significant differences were showed in both years.

Treatments with Btm showed high efficacy against Juvenile (J_2) *M. incognita* after 24, 48 and 72 h of exposure in vivo, compared with the control (Table 5). This illustrated a highly significant difference in the percentage of mortality compared with the untreated control, which were the same for two concentrations (20 and 30%) after 24, 48 h at 87.5%, 90.6%, respectively and were 94%, 97% after 72 h for the two concentrations.

Table 4. Comparisons between the different studied treatments according to seed weight

Treatment	Weight of seed by g/plot				T	p
	2017		2018			
	Mean ± S.D.	% Increasing	Mean ± S.D.	% Increasing		
Btm at 20%	803.3^{c}±12.6	47.2	807.0^{d}±4.4	44.1	0.477	0.658
Btm at 30%	829.3^{b}±1.5	52.0	820.0^{c}±1.0	46.4	8.854*	≤0.001*
*Slitura*NPV at 20%	822.7^{b}±2.5	50.8	808.0^{d}±7.5	44.3	3.192*	0.033*
*Slitura*NPV at 30%	829.0^{b}±3.6	51.9	827.3^{bc}±1.5	47.7	0.737	0.502
*Slitura*NPV and Btm at 20%	846.0^{a}±3.6	55.0	836.0^{ab}±2.0	49.3	4.201*	0.014*
*Slitura*NPV and Btm at 30%	847.7^{a}±4.0	55.3	842.3^{a}±2.5	50.4	1.940	0.124
Untreated (control)	545.7^{d}±5.5		560.0^{e}±2.0		4.237*	0.013*
F	1029.080*		2262.120*			
P	<0.001*		<0.001*			

Data with the same letter(s) in each column, are not significantly different

Table 5. Evaluation of the nematicidal effects of *Bacillus thuringiensis* on mortality (M%) of juvenile (J2) *Meloidogyne incognita* for different exposure periods

Treatments	Juvenile (J2) mortality					
	24 h		48 h		72 h	
	L	M %	L	M %	L	M %
Control (distilled water)	6.4 ±1.08^{a}	0	6.4± 1.09^{a}	0	6.4±1.57^{a}	0
Btm at 20%	0.8 ±0.24^{b}	87.5	0.6±1.38 ^{b}	90.6	0.4±1.20^{b}	94
Btm at 30%	0.8± 0.44^{b}	87.5	0.6±0.47 ^{b}	90.6	0.2 ±1.43^{b}	97

Data of means with the same letter(s) in each column, are not significantly different at P ≤0.05.
M% (% Mortality) = [(Total number of J2 in control - No. of alive (L) J2 in treatment) ÷ No. of Total J2 in control] × 100

In Table 6, there were significant differences in the mean number of the root fresh weight, number of galls/ roots, number of egg masses/ root and number of egg /egg masses between the two Btm concentrations and the untreated control and among each other, the treatment with Btm 30%

showing the highest effectiveness in all parameters. The percentage reduction due to Btm at 20% and Btm at 30% ranged from 77%, 83% for galls/root; 67%, 80% for egg masses/root and 39%, 61% egg/egg masses.

Table 6. The effect of *Bacillus thuringiensis* on root-knot nematode *M. incognita* in tomato plants

Treatments	Nematode parameters and percent reduction (R)						
	Root fresh wt. (g)	Galls per Root	% Reduction	Egg masses per root	% Reduction	Eggs per egg mass	% Reduction
Untreated (control)	32.0[c]	129.7[a]	0	441.2[a]	0	510[a]	0
Btm at 20%	57.0[b]	30[b]	77	145[b]	67	312[b]	39
Btm at 30%	65.0[a]	21.5[c]	83	88[c]	80	200[c]	61

Data are means of 10 replicates, means with the same letter(s) in each column are not significantly different

The bacterium (Btm) and virus (*Slitura*NPV) gave the highest larval *S. litoralis* mortality when used in combination at 30%. The other treatments in order of decreasing efficacy were Btm/*Slitura*NPV combined at 20%, *Slitura*NPV alone at 30%, then 20%, and finally Btm alone at 30 and 20%. Çakici *et al*. [35] mentioned that *B. thuringiensis* subsp. *kurstaki* (MnD) and *B. thuringiensis* subsp. *kurstaki* (BnBt) were found to be the foremost successful of the strains tested, causing 100% mortality within 10 days of treatment, whereas in this study *Bacillus thuringiensis* serovar *mexicanensis* (Btm) had a mean efficacy of 68.3% efficacy, in both seasons, only 5 d after treatment. The efficacy appears to be due to the formula, which provided more protection to spores and crystals under conditions of continuous sun exposure [27, 36].

Nathan *et al*. [37] found that bacterial Cry toxin affected the lactate dehydrogenase (LHD) activity and this effect was more severe at low concentrations in *Cnaphalocrocis medinalis* (rice leaf folder). Similar results occurred in our study, hence the lower rate had better efficacy.

Sarker and Mahbub [38] reported that several *B. thuringiensis* strains were very effective for suppressing many insect pests. In addition, Konecka *et al*. [39] obtained results that are consistent with another effect of Bt toxicity in lepidopteran species.

Abad *et al*. [40] indicated the importance of NPV in controlling insect pests, especially lepidopteran pests. As the same in the studies of Eroglu *et al*. [41], when testing neonate, 3rd, and 5th instar larvae of *H. armigera*, the highest dose (8×10^6 PIBs ml^{-1}) of *Helicoverpa armigera* nucleopolyhedrovirus (HearNPV-O1) caused 92, 88 and 57% mortality, respectively, within 14 days.

Raghunandan *et al*. [42] revealed that NPV infected *S. frugiperda* larvae on maize could cause high mortality ratio after 3 days; while Luna-Espino *et al*. [43] demonstrated that the biological efficacy of the local Mexican *Se*MNPV isolates was identical to the activity of the foreign isolate (SeUS2), and these native viruses are appropriate for the microbial control of *S. exigua* in Mexico. The native virus gave 92-100% mortality whereas the exotic virus gave only 78%.

Regarding nematode efficacy of Bt, Mohammed *et al.* [44] demonstrated that Bt7N reduced the number of egg masses by 78%, and the number of eggs by 84% compared to their control. These results were similar to those shown in Table 6, which had 80 and 67% from treatment with Btm at both 30% and 20% rates. Ashoub and Amara [45] confirmed that all their tested bacteria (*Bacillus thuringiensis, Pseudomonas fluorescens,* and *Rhizobium leguminosarum*) showed a significant efficacy in suppressing *M. incognita* in vivo and *in vitro* [46]. In evaluating three Egyptian-isolates

of *B. thuringiensis*, significant positive correlations between percentage reduction in the nematode populations and bacterial doses were found. *Bacillus thuringiensis* was also reported to suppress populations of *M. javanica* and *M. Incognita* [47-49]. Results in our study agree with the earlier data by Yamamoto and Powell [50] and Fernandes *et al*. [51]. However, their *Bacillus* spp. isolates had no potential as bionematicides for controlling of *M. incognita* in common bean.

4. Conclusions

Both NPV and Btm have considerable potential in managing *S. littoralis* populations. The combination provides a small incremental increase, but the economic implications remain to be better defined. According to the data in our study, Btm could also provide an excellent tool for management of root-knot nematodes. A serious problem for efficacy of NPV or bacteria against foliage feeding pests is maintaining sufficient persistence under the harsh, sunny conditions. This problem is alleviated by a new formulation modified for use in the present study. Synergism between Btm and NPV in our new formulation seemed to have good efficacy in the field. With lepidoptera only, the application of viral-insecticide is preferable because of the rapid effect of NPV on lepidopteran insect pests, especially Egyptian cotton leafworm, beet armyworm, and fall armyworm, which are new invasive pests in Africa and Asia.

5. Acknowledgements

We are deeply grateful to Prof. Stefan Jaronski for his beneficial comments and advice on an early draft.

References

[1] Hosny, M.M. Topper, C.P., Moawad, G.M. and El-Saadany, G.B., 1986. Economic damage threshold of *Spodoptera littoralis* (Boisd.) (Lepidoptera: Noctuidae) on cotton in Egypt. *Crop Protection*, 5(2), 100-104.

[2] Hafez, M. and Hassan, S.M., 1969. On the correct identity of the Egyptian cotton leafworm (Lepidoptera: Noctuidae). *Bulletin de la Société Entomologique d'Égypte*, 53, 63-68.

[3] Brown, E.S. and Dewhurst, C.F., 1975. The genus *Spodoptera* (Lepidoptera, Noctuidae) in Africa and the Near East. *Bulletin of Entomological Research*, 65, 221-265.

[4] Hegazi, E.M. and Schopf, A., 1984. The influence of temperature on consumption and utilization of artificial diet by *Spodoptera littoralis* (Boisd.) (Lepidoptera., Noctuidae). *Journal of Applied Entomology*, 97, 321-326.

[5] Temerak, S.A., 2002. Historical records of cotton leafworm (*Spodoptera littoralis*) resistance to conventional insecticides in the field as influenced by the resistance programs in Egypt from 1950-2002. *Resistant Pest Management Newsletter*, 12(1), 7-10.

[6] El-Sheikh, T.A.A., 2012. Biological, biochemical and histological effects of spinosad, *Bacillus thuringiensis* var. *kurstaki* and cypermethrin on the cotton leaf worm, *Spodoptera littoralis* (Boisd.). *Egyptian Academic Journal of Biological Sciences*, 4, 113-124.

[7] El-Geddawy, A.M.H., Ahmed, M.A.I. and Mohamed, S.H., 2014. Toxicological evaluation of selected biopesticides and one essential oil in comparison with Indoxacarb pesticide on cotton leaf worm, *Spodoptera littoralis* (Boisd.) (Lepidoptera: Noctuidae) under laboratory conditions. *American Eurasian Journal of Sustainable Agriculture*, 8(2), 58-64.

[8] Ahmed, M.A.I., Abdel-Galil, F.A., Temerak S.A.S. and Manna, S.H.M., 2015. Bio-residual activity of selected biopesticides in comparison with the conventional insecticide Dursban against cotton leaf worm, *Spodoptera littoralis* (Boisd.) (Lepidoptera: Noctuidae). *American-Eurasian Journal of Sustainable Agriculture*, 9(1), 9-13.

[9] Ahmed, M.A.I., Temerak, S.A.S., Abdel-Galil, F.A. and Manna, S.H.M., 2015. The effect of selected host plants on the efficacy of Spinosad pesticide on cotton leaf worm, *Spodoptera littoralis* (Boisd.) (Lepidoptera: Noctuidae) under laboratory conditions. *Advances in Environmental Biology*, 9, 372-375.

[10] Plowright, R. and Bridge, J., 1990. Effects of *Meloidogyne graminicola* (Nematoda) on the establishment; growth and yield of rice cv IR36. *Nematologica*, 36, 81-89.

[11] Karssen, G., Wesemael, W.M.L. and Moens, M., 2013. Root-knot nematodes. In: R.N. Perry and M. Moens, eds. *Plant Nematology*. Wallingford: CABI, pp.73-108.

[12] Castillo, P., Vovlas, N., Subbotin, S. and Troccoli, A., 2003. A new root-knot nematode, *Meloidogyne baetican*. sp (Nematoda: Heteroderidae), parasitizing wild olive in Southern Spain. *Phytopathology*, 93(9), 1093-1102.

[13] Mukhtar, T. and Kayani, M.Z., 2019. Growth and yield responses of fifteen cucumber cultivars to root-knot nematode (*Meloidogyne incognita*). *Acta Scientiarum Pollonorum Hortorum Cultus*, 18(3), 45-52.

[14] Bridge, J., Luc, M. and Plowright, R.A., 1990. Nematode parasites of rice. In: M. Lue, R.A. Sikora and J. Bridge, eds. *Plant Parasitic Nematodes in Subtropical and Tropical Agriculture*. Wallington: CABI, pp. 69-108.

[15] Brader, L., 1979. Integrated pest control in the developing world. *Annual Review of Entomology*, 24, 225-254.

[16] Ahmed, M.A.I, 2014. Evaluation of novel neonicotinoid pesticides against cotton leaf worm, *Spodoptera littoralis* (Boisd.) (Lepidoptera: Noctuidae) under laboratory conditions. *Advances in Environmental Biology*, 8, 1002-1007.

[17] Marrone, P.G., 2019. Pesticidal natural products-status and future potential. *Pest Management Science*, *75*(9), 2325-2340.

[18] Gómez, I., Rodríguez-Chamorro, D.E., Flores-Ramírez, G., Grande, R., Zúñiga, F., Portugal, F.J., Sánchez, J., Pacheco, S., Bravo, A. and Soberón, M., 2018. *Spodoptera frugiperda* (J.E. Smith) aminopeptidase N1 is a functional receptor of the *Bacillus thuringiensis* Cry1Ca toxin. *Applied and Environmental Microbiology*, 84(17), e01089-18, https://doi.org/10.1128/AEM.01089-184

[19] Branscome, D.D., Storey, R.D., Eldridge, J.R., Brazil, E.E. and Valent BioSciences LLC, 2018. *Synergistic Bacillus thuringiensis* subsp*. aizawai*, *Bacillus thuringiensis* subsp*. kurstaki and Cyantraniliprole Mixtures for Diamondback Moth, Beet Armyworm, Southwestern Corn Borer, and Corn Earworm*. U.S. Pat. 9, 968, 098.

[20] Branscome, D.D., Storey, R.D., Eldridge, J.R., Brazil, E.E. and Valent BioSciences LLC, 2019. *Synergistic Bacillus thuringiensis subsp. kurstaki and Cyantraniliprole Mixtures for Diamondback Moth, Beet Armyworm, Sugarcane Borer, and Soybean Looper Control.* U.S. Pat. 10, 278, 396.

[21] Yang, F., González, J.C.S., Williams, J., Cook, D.C. Gilreath, R.T. and Kerns, D., 2019. Occurrence and ear damage of *Helicoverpa zea* on transgenic *Bacillus thuringiensis* maize in the field in Texas, US and its susceptibility to Vip3A protein. *Toxins*, 11(2), 102, https://doi: 10.3390/toxins11020102

[22] Racke, J. and Sikora, R.A., 1992. Influence of the plant health-promoting rhizobacteria Agrobacterium radiobacter and *Bacillus sphaericus* on *Globodera pallida* root infection of potato and subsequent plant growth. *Journal of Phytopathology*, 134(3), 198-208.

[23] Devidas, P. and Rehberger, L.A., 1992. The effects of exotoxin (thuringiensin) from *Bacillus thuringiensis* on *Meloidogyne incognita* and *Caenorhabditis elegans*. *Plant and Soil*, 145(1), 115-120.
[24] Ravari, S.B. and Moghaddam, E.M., 2015. Efficacy of *Bacillus thuringiensis* Cry14 toxin against root knot nematode, *Meloidogyne javanica*. *Plant Protection Science*, 51(1), 46-51.
[25] Rohrmann, G.F., 2013. *Baculovirus Molecular Biology*. Bethesda: National Center for Biotechnology Information.
[26] El-Salamouny, S., Lange, M., Jutzi, M., Huber, J. and Jehle, J.A., 2003. Comparative study on the susceptibility of cutworms (Lepidoptera: Noctuidae) to *Agrotis segetum* nucleopolyhedrovirus and *Agrotis ipsilon* nucleopolyhedrovirus. *Journal of Invertebrate Pathology*, 84(2), 75-82.
[27] Alfy, H. 2014. *Microbial Control of Certain Insect Pests of Field Crops*. Ph.D. University of Alexandria.
[28] Senthil-Nathan, S., 2015. A review of biopesticides and their mode of action against insect pests. In: P. Thangavel and G. Sridevi, eds. *Environmental Sustainability*. New Delhi: Springer, pp. 49-63.
[29] Alfazairy, A.A., El-Ahwany, A.M., Mohamed, E.A., Zaghloul, H.A. and El-Helow, E.R., 2013. Microbial control of the cotton leafworm *Spodoptera littoralis* (Boisd.) by Egyptian *Bacillus thuringiensis* isolates. *Folia Microbiologica*, 58(2), 155-162.
[30] Okuno, S., Takatsuka, J., Nakai, M., Ototake, S., Masui, A., Kunimi, Y. 2003. Viral-enhancing activity of various stilbene-derived brighteners for a *Spodoptera litura* (Lepidoptera: Noctuidae) nucleopoly hedrovirus. *Biological Control*, 26, 146-152.
[31] de Moraes, R.R. and Maruniak, J.E., 1997. Detection and identification of multiple baculoviruses using the polymerase chain reaction (PCR) and restriction endonuclease analysis. *Journal of Virological Methods*, 63(1-2), 209-217.
[32] Abbott, W.S., 1925. A method of computing the effectiveness of an insecticide. *Journal of Economic Entomology*, 18(2), 265-267.
[33] Hussey, R.S., 1973. A comparison of methods of collecting inocula of Meloidogyne spp., including a new technique. *Plant Disease Report*, 57, 1025-1028.
[34] Ayoub, S.M., 1980. *Plant Nematology: An Agricultural Training Aid. (Revised).* California: NemaAid Publication.
[35] Çakici, F.Ö., Sevim, A., Demirbag, Z. and Demir, I., 2014. Investigating internal bacteria of Spodoptera littoralis (Boisd.) (Lepidoptera: Noctuidae) larvae and some *Bacillus* strains as biocontrol agents. *Turkish Journal of Agriculture and Forestry*, 38(1), 99-110.
[36] Da Silva, K.F., Spencer, T.A., Crespo, A.L.B. and Siegfried, B.D., 2016. Susceptibility of *Spodoptera frugiperda* (Lepidoptera: Noctuidae) field populations to the Cry1F *Bacillus thuringiensis* insecticidal protein. *Florida Entomologist*, 99(4), 629-633.
[37] Nathan, S.S., Kalaivani, K. and Murugan, K., 2006. Behavioural responses and changes in biology of rice leaffolder following treatment with a combination of bacterial toxin and botanical pesticides. *Chemosphere*, 64(10), 1650-1658.
[38] Sarker, N. and Mahbub, K.R., 2012. *Bacillus thuringiensis*: An environment friendly microbial control agent. *Microbiology Journal*, 2(2), 36-51.
[39] Konecka, E., Kaznowski, A., Stachowiak, M. and Maciąg, M., 2018. Activity of spore-crystal mixtures of new *Bacillus thuringiensis* strains against *Dendrolimus pini* (Lepidoptera: Lasiocampidae) and *Spodoptera exigua* (Lepidoptera: Noctuidae). *Folia Forestalia Polonica*, 60(2), 91-98.
[40] Abad, A.R., Dong, H., Lo, S.B., Shi, X. and Wolfe, T.C., Pioneer Hi-Bred International Inc, 2018. *Bacillus thuringiensis gene with lepidopteran activity*. U.S. Pat. 10/000, 769.

[41] Eroglu, G.B., Demir, I. and Demirbag, Z., 2018. A novel alphabaculovirus isolated from the cotton bollworm, *Helicoverpa armigera* (Hubner) (Lepidoptera: Noctuidae): characterization and pathogenicity. *Biologia*, 73(5), 545-551.
[42] Raghunandan, B.L., Patel, N.M., Dave, H.J. and Mehta, D.M., 2019. Natural occurrence of nucleopolyhedrovirus infecting fall armyworm, *Spodoptera frugiperda* (JE Smith) (Lepidoptera: Noctuidae) in Gujarat, India. *Journal of Entomology and Zoology Studies*, 7(2), 1040-1043.
[43] Luna-Espino, J.C., Castrejón-Gómez, V.R., Pineda, S., Figueroa, J.I. and Martínez, A.M., 2018. Effect of four multiple nucleopolyhedrovirus isolates on the larval mortality and development of *Spodoptera exigua* (Lepidoptera: Noctuidae): determination of virus production and mean time to death. *Florida Entomologist*, 101(2), 153-159.
[44] Mohammed, S.H., El Saedy, M.A., Enan, M.R., Ibrahim, N.E., Ghareeb, A. and Moustafa, S.A., 2008. Biocontrol efficiency of *Bacillus thuringiensis* toxins against root-knot nematode, *Meloidogyne incognita. Journal of Cell and Molecular Biology*, *7*(1), 57-66.
[45] Ashoub, A.H. and Amara, M.T., 2010. Biocontrol activity of some bacterial genera against root-knot nematode, *Meloidogyne incognita*. *Journal of American Science*, 6(10), 321-328.
[46] Ismail, A.E. and Fadel, M., 1999. Field application of three local isolates of *Bacillus thuringiensis* for controlling the citrus nematode, *Tylenchus semipenetrans*. *Egyptian Journal of Biological Pest Control*, 9, 21-27.
[47] Dhawan, S.C., Kaur, S. and Singh, A., 2004. Effect of *Bacillus thuringiensis* on the mortality of root-knot nematode, *Meloidogyne incognita*. *Indian Journal of Nematology*, 34(1), 98-99.
[48] Chahal, P.P.K. and Chahal, V.P.S., 1993. Effect of thuricide on the hatching of eggs root-knot nematode, *Meloidogyne incognita. Current Nematology*, 4, 247.
[49] Zuckerman, B.M., Dicklow, M.B. and Acosta, N., 1993. A strain of *Bacillus thuringiensis* for the control of plant-parasitic nematodes. *Biocontrol Science and Technology*, 3(1), 41-46.
[50] Yamamoto, T. and Powell, G., 1993. *Bacillus thuringiensis* crystal proteins: recent advances in understanding its insecticidal activity. In: L. Kim, ed. *Advanced Engineered Pesticides*. New York: Dekker, pp. 3-42.
[51] Fernandes, R.H., Lopes, E.A., Bontempo, A.F., Fuga, C.A.G. and Vieira, B.S., 2018. *Bacillus* spp. isolates for the control of *Meloidogyne incognita* in common bean. *Científica*, 46(3), 235-240.

Effect of Different Application Methods for Pendimethalin Herbicide on Growth and Productivity of Green Pea Plant (*Pisumsativum* L.)

Nahla Salim Hammok* and Fathi Abdullah Al-mandeel

Environmental Researches Center, University of Mosul, Mosul, Iraq

Received: 28 March 2020, Revised: 14 May 2020, Accepted: 25 June 2020

Abstract

The application of the right herbicides and the avoidance of their use at high levels can protect crops from weeds whilst reducing environmental dangers associated with their overuse. Effects of the use of the herbicide pendimethalin, henceforth referred to as PM, on green pea plants at pre-emergence and post-emergence were studied. Different concentrations of the herbicide were applied at 0.0, 1.4, 2.8 and 4.1ml/l, levels which were equal to doses in the field of 0.5, 1, 1.5 l/Donum. Post-emergent plants showed a significant decrease in plant height (cm), pod number/plant, pod weight (g), pod length (cm), fresh weight of plant (g) and weight of 1000 seeds (g). However, the decrease was not significant in the dry weight of plant (g) and the number of seeds/pod. Also, all studied traits decreased significantly when different concentrations of PM overlapped with the application methods, except in the case of the weight of 1000 seeds. These results showed that the effects of PM reps are apparent from low concentrations of the herbicide, and also that treatment at post-emergence reduces environmental pollution and protects the crop, and especially the parts of the plants that are consumed, from pesticide pollution.

Keywords: chemical pollution, pendimethalin, pea, pre-emergence, productivity
DOI 10.14456/cast.2020.35

1. Introduction

The risks of herbicide are associated with their toxic and mutagenic effects on the environment and human health [1]. Pendimethalin (PM) is an optional herbicide that belongs to the dinitroaniline group and is widely applied to control annual grasses and broad-leaved bushes when growing vegetables (such as green peas, tomatoes, peppers, onions and cabbage) and in corn, soy and wheat fields. PM can be found as a preparation known as Stomp E330, or mixed with other herbicides. Its chemical formula is N - (1-ethylpropyl) - 2, 6 - dinitro - 3 - 4 xylidine (Figure 1) [2-4]. Pendimethalin is predominantly applied to soil as a preplant, pre-emergence agent, but it is sometimes used as a post-emergence herbicide [5].

*Corresponding author: Tel: (+964) 7724555215
E-mail: Nahlahammok@yahoo.com

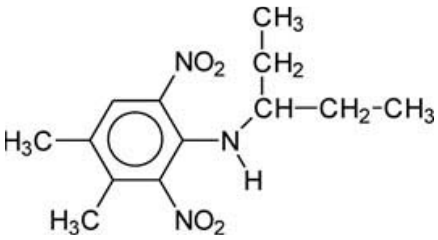

Figure 1. Structure of pendimethalin (PM) [4]

The herbicide PM's primary mode of action is to inhibit cell division. It does so by blocking filamentous division in the cells of the roots and targets the important microtubules that form the cell wall, spindle filaments and chromosomal separations [1, 5].The US Environmental Protection Agency (EPA) has classified PM as a herbicide with a cumulative toxic effect [6]. PM can cause negative effects on food crops, which is an unintended effect of its use. Moreover, these negative effects are of a genotoxic and morphological nature. The use of PM with imazethapyr to control weeds in lentil and pea fields that were cultivated for winter wheat yield was found to decrease the wheat biomass by 35-51% and the grain yield by 11-17% following treatment concentrations of 2.40 g/h of the herbicide [7]. It was also found that spraying PM (as Stomp) and oxiflorine (Joule) on seedlings of cotton (*Gossypium hirsutum*) and maize (*Zea mays* L.), at concentrations of 5 and 10 ppm, had a clear negative impact on both plants. Cotton seed and maize germination were negatively affected by both herbicides at 10 ppm. The levels of chlorophylls a and b decreased in the leaves of the cotton and maize plants when each pesticide was applied at the concentrations of 5 and 10 ppm, and the 10ppm concentration had a greater effect on the level of chlorophyll [8]. PM also causes DNA oxidation as a result of the formation of reactive oxygen species (ROS) responsible for the formation of mutations in cells. The damage occurs in the concentrations of 1-10000 µM [9].

Green peas (*Pisum sativum* L.) is an important vegetable crop that is used as fresh and dried vegetables and is a rich source of protein, calcium, phosphorus, iron, and vitamins. The pea crop is very useful for soil fertility as it provides the soil with nitrogen [10].

In consideration of the negative effects of herbicides, the present study aims to detect the optimal method and the appropriate concentration when applying the PM herbicide to avoid environmental pollution and promote crop conservation.

2. Material and Methods

2.1 Raw materials

The study was carried out in the facilities of the Life Science Department, Faculty of Education, during the winter season of 2018-2019.The seeds of green pea (*Pisum sativum* L.) used in this study were obtained from local markets, and the pendimethalin (PM) used was supplied by the Agrichem Company, Australia.

2.2 Study design and implementation

The experiment was designed according to the International Experimentation System (2x4) and utilized a Randomized Complete Block Design (RCBD) with six replicates. This study included two

parts: the first was a study of PM application on pea plant at pre-emergence and post-emergence. The second part included the testing of PM at the concentration of control, 1.4, 2.8, and 4.1ml/l, which were equivalent to doses in the field of 0.5,1, 1.5 l/Donum. Distilled water was used as the control. Homogenous seeds were selected and sown. The land was prepared and plowed twice (mid-December and the end of January) by deep plowing, softened, settled by hand, and then divided into six equal sections (2.2 x 3 m) per replication [11, 12].

The grains were planted in a light mixed soil (sand 38.12%, silt 41.13%, clay 20.15%, organic matter 0.98 %, and pH = 8.25) on 15/2/2019. Planting was linear, and each line was treated. The distance between the lines was 20 cm and the distance between grains in the same line was 7.5 cm ± 1 cm. Fifteen seeds were planted for each treatment before seed germination (pre-emergence) and the soil was sprayed with different concentrations of PM using a plastic sprayer that sprayed in lines, each line representing a specific concentration. After seed germination (post-emergence) and reaching of seedling stage which occurred at age 3 to 4 weeks, the seedlings were also sprayed.

The lines were separated by wooden barriers and three replicates were used for each method (pre- and post-emergence).

2.3 Harvest and analysis

When the pod maturated, it was directly harvested. Plants were eradicated from the roots and each plant was covered and separated by a sheet of paper. Each group of plants for each treated concentration (10 plants per concentration) and each replicate was bundled and transferred to the lab for further analysis. The analysis included: plant height (cm), pod number/plant, pod length (cm), pod weight (g), seeds number/pod, the total weight for each 1000 grain (g), dry weight of plant (g), and fresh weight of plant (g) [13].

2.4 Statistical analysis

Data analysis was performed according to the global experience system by designing the complete random sectors [11]. Moreover, Duncan test was used to compare averages at P-value < 0.05 [14]. The analysis was conducted according to the statistical program SAS [15].

3. Results and Discussion

The addition of PM to post-emergence peas resulted in a significant decrease in plant height (cm), number of pods/plant, pod weight and length, and fresh weight of plant except for the case of weight of 1000 seeds, when compared to the pre-emergence addition method. However, the effect of PM application methods was not significant on both the dry weight of plant and number of seeds/pod (Table 1).

The decrease of plant height, number of pods and length of the pod after spraying the post-emergence peas may be due to the contact of the herbicide with the apical meristem zoning regions. It seems likely that the inhibition of division and stopping of growth was observed [16]. Another explanation may be that the herbicide induced oxidative stress and thus damage to and oxidation of the DNA [9]. Furthermore, the herbicide may have affected the photosynthetic process and the amount of chlorophyll [8].

Table 1 recorded a decrease in the weight of pod (g). This decrease could be attributed to the effect of PM on pollens [16] and the low accumulation of dry matter could be due to the impact of photosynthesis as mentioned above. Besides, the fresh weight of the plant (g) decreased significantly after treatment with PM, and this was in line with previous studies of Karaye *et al*.

Table 1. The effect of PM application methods on green pea productivity

Application of PM	Plant height (cm)	Pod numbers/ Plant	Pod Weight (g)	Pod Length (cm)	Seed numbers/ Pod	Weight of 1000 seeds (g)	Dry weight of plant (g)	Fresh weight of plant (g)
Pre-emergence	57.90[a]	4.83[a]	2.78[a]	8.09[a]	3.37[a]	64.75[b]	5.05[a]	21.32[a]
Post-emergence	47.61[b]	3.92[b]	0.90[b]	6.96[b]	3.82[a]	88.25[a]	4.95[a]	12.79[b]

Note: Different letters mean significant differences at p 0.05 according to Duncan multiple range test at each characteristic.

[17], which highlighted the decrease in the fresh and dry weight of roots and vegetable seedlings of two types of chickpea. The increase in the weight of 1000 seeds in Table 1 is a positive point for the post-emergence method, and it may be attributed to the skillful application of the PM herbicide and its effectiveness in controlling weeds [10].

Table 2 shows the effect of the different concentrations of PM on the productivity characteristics at the probability level of 0.05. All the studied traits significantly decreased except for the dry weight of the whole plant (g), for which the decrease was insignificant. The decrease in plant height is due to the mechanism of action of PM, which is an inhibitor of mitosis affecting the division areas in the plant [3, 16].

The decrease in plant height is evident at low concentrations of PM and becomes more pronounced with increasing concentration. This result is consistent with Verma and Srivastava [18] and Ansari *et al.* [2], who concluded that PM inhibits the normal rate of cell division, increases the number of abnormal cells and chromosomal distributions in divided and non-dividing cells, and inhibits the root and vegetative systems of onion plants even at low concentrations. Table 2 records a significant decrease in the number of plant pods and the length of the pod. The effect on dividing zones may be the cause of the decrease in the number of pods/plants, the significant decrease in the weight of the pod (g), the number of seeds/pod, and the weight of 1000 seeds after treatment with PM may be due to the effect of herbicide concentrations on pollen. Silva *et al*. [19] observed small nuclei and reduction in fertile pollen in *Oleifera moringa* after treatment with PM. Dry matter affected by the deterioration of photosynthesis was also noticed. Furthermore, Shabana *et al.* [20] found a decrease in efficacy of photosynthesis, growth, cell numbers, level of chlorophyll a, and dry weight in green algae (*Protosiphon botryoides*) with increased concentration of PM.

The application of PM with trifluralin significantly decreased pea pods in comparison with other treatments [10]. Another effect of PM on the fresh weight (g) was to decrease the fresh weight of the whole plant significantly with increasing concentration, and importantly the decrease appeared from the low concentration of 1.4 ml/l. The decrease in fresh weight may have been due to the oxidative stress caused by the herbicide, which in turn affects the efficiency of photosynthesis, respiration and the water intake in the plant [8, 9]. These results are consistent with those of Karaye *et al*. [17], who pointed to the reduction of the fresh and dry weights of the roots and vegetative groups in two species of cowpea after treatment with PM. Wagner and Nadasy [12] studied the fresh and dry weight reductions of the total vegetative groups and roots of peas when treated at high concentrations of PM.

Table 2. The effect of different concentrations of PM on green pea productivity

Concentrations of PM (ml/l)	Plant height (cm)	Pod numbers/plant	Pod weight (g)	Pod length (cm)	Seed numbers /pod	Weight of 1000 seeds (g)	Dry weight of plant (g)	Fresh weight of plant (g)
control	66.71[a]	6.30[a]	2.33a	8.62[a]	5.27[a]	87.33[a]	6.26[a]	23.54[a]
1.4	54.20[b]	4.62[b]	2.19[ab]	7.97[b]	4.08[b]	87.33[a]	5.68[a]	19.01[b]
2.4	50.53[b]	4.16[b]	1.64[bc]	7.60[b]	3.15[c]	71.50[ab]	5.19a	15.85[c]
4.1	39.58[c]	2.42[c]	1.18[c]	5.93[c]	1.87[d]	60.17[b]	2.86[b]	9.87[d]

Note: Different letters mean significant differences at p 0.05 according to Duncan multiple range test at each characteristic.

The data in Table 3 shows the significant interactions that took place between the different herbicide concentrations (PM) and the methods of adding the herbicide. All productivity characteristics decreased in the cases of both pre- and post-emergence, except for the weight of 1000 seeds in post-emergence, a result which was not significant and it may be the reason that PM was well applied and effective in controlling weeds [10]. The condition of post-emergence reduced the effect of PM herbicide on the weight of 1000 seeds.

High concentrations of herbicide (PM) had more effects on the studied characteristics in post-emergence plants. This may be because of the action of the herbicide and its direct contact with the areas of division, apical meristem, and its inhibition [5, 6]. It could also be due to the effect of the herbicide on the effectiveness of photosynthesis [20]. The impact of pollen was a major factor in reducing the yield as found by Silva *et al.* [19]. Furthermore, the impact on bacteria in breeding may be a reason for reducing plant growth, especially stabilization of nitrogen in the root nodes. Aboulila *et al*. [1] reported that the impact on bacteria in the soil was clear after the treatment of pea with PM herbicide and that the herbicide had reduced all the qualities that were measured for *Vicia faba* L. including plant height, root length, diameter of wood vessels, phloem tissue thickness and vascular bundles compared to control group, and had caused abnormal rise in the normal division rate of root end of pea. The concentration of PM used in the field is high and harmful for the final receptor in the food chain used in the experiment. Thus, the use of *Pseudomonas resinovorand* bacterium, could reduce the genetic toxicity of PM on pea plants.

4. Conclusions

It is obvious from our current study that the application of the PM herbicide in the post-emergence has a greater effect on the characteristics of the productivity of pea crop (except for the weight of 1000 seeds) compared to its application in the pre-emergence, and despite its impact on the characteristics of productivity, it does not cause the killing of plants. However, the application of PM on post-emergence is considered as environmentally friendly due to reduction of soil pollution and reduction of the killing of other organisms when compared to its use pre-emergence. Finally, it was noted that effect of PM began from low concentrations.

5. Acknowledgements

The research was supported by the Environmental Researches Center, University of Mosul.

Table 3. The effect of interaction between of PM application methods and PM concentrations on green pea productivity

Application of (PM)	Concentrations of (PM) (ml/l)	Plant height (cm)	Pod numbers/plant	Pod weight (g)	Pod length (cm)	Seed numbers /pod	Weight of 1000 seeds (g)	Dry weight of plant (g)	Fresh weight of plant (g)
(1) pre-emergence	control	67.28^{a}	6.36^{a}	3.67^{a}	8.98^{a}	5.13^{ab}	87.67^{a}	6.66^{a}	25.37^{a}
	1.4	62.75^{a}	5.34^{ab}	3.41^{a}	8.37^{ab}	4.07^{bc}	77.67^{ab}	6.18^{ab}	25.30^{a}
	2.4	57.67^{ab}	4.72^{bc}	2.20^{b}	8.13^{b}	2.70^{de}	53.67^{bc}	4.43^{bc}	21.88^{a}
	4.1	43.92^{bc}	2.90^{de}	1.81^{bc}	6.88^{c}	1.57^{e}	40.00^{c}	2.91^{c}	12.79^{b}
(2) post-emergence	control	66.15^{a}	6.23^{a}	0.97^{cd}	8.25^{ab}	5.40^{a}	87.00^{a}	5.85^{ab}	21.70^{a}
	1.4	45.65^{bc}	3.90^{cd}	0.98^{cd}	7.57^{bc}	4.10^{bc}	96.33^{a}	5.17^{ab}	12.72^{b}
	2.4	43.40^{bc}	3.60^{d}	1.07^{cd}	7.07^{c}	3.60^{de}	89.33^{a}	5.95^{ab}	9.81^{bc}
	4.1	35.26^{c}	1.93^{e}	0.56^{d}	4.97^{d}	2.17^{e}	80.30^{ab}	2.81^{c}	6.94^{c}

Note: Different letters mean significant differences at p 0.05 according to Duncan multiple range test at each characteristic.

References

[1] Aboulila, A.A., Belal, E.B., Metwaly, M.M. and El-Ramady, H.R., 2016. Degenotoxicity of pendimethalin contaminated clay soil by *Pseudomonas resinovorans* using anatomical, cytogenetic and biochemical analysis in *Vicia faba* plants. *International Journal of Current Research in Biosciences and Plant Biology,* 3(2), 38-53.

[2] Ansari, S.M., Saquib, Q., Attia, S.M., Abdel-Salam, E.M., Alwathnani, H.A., Faisal, M., Alatar, A.A., Al-Khedhairy, A.A. and Musarrat, J., 2018. Pendimethalin induces oxidative stress DNA damage, and mitochondrial dysfunction to trigger apoptosis in human lymphocytes and rat bone-narrow cells. *Histochemistry and Cell Biology,*149(2), 127-141.

[3] Alshallash, K.S., 2014. Effect of pendimethalin, trifluralin and terbutryn on *Lolium multiflorum* growing with barley during pre-emergence stage. *Annals of Agricultural Science,* 59(2), 239-242.

[4] Mohamed, A.A., 2019. *Evaluation of the Effectiveness of Some Herbicides in the Growth and Yield of Maize (Zea mays L.) and Associated Weed*. Ph.D. Mosul University.

[5] Vighi, M., Matthies, M. and Solomon, K.R., 2017. Critical assessment of pendimethalin in terms of persistence, bioaccumulation, toxicity and potential for long-range transport. *Journal of Toxicology and environmental Health, Part B,* 20 (1), 1-21.

[6] El-Nady, M.F. and Belal, E.B., 2013. Effect of phytotoxicity of pendimethalin residues and its bioremediation on growth and anatomical characteristics of *Cucumis sativus* and *Echinochloa crus-galli* plants. *Asian Journal of Crop Science,* 5(3), 222-237.

[7] Hanson, B.D. and Thill, D.C., 2001. Effect of imazethapyr and pendimethalin on lentil (*Lens culinaris*), pea (*Pisum sativum*) and subsequent winter wheat (*Triticum aestivum*) crop. *Weed Technology,*15(1), 190-194.

[8] Samia, M.A.O., 2015. *Effect of Oxyfluorfen and Pendimethalin on Germination and Some Carbohydrate Parameters in Gossypium hirsutum L. and Zea mays L.* Ph.D. Khartoum University.

[9] Demir, N., Aydin, S. and Bucurgat, U., 2017. Assessment of genotoxic effects of pendimethalin in Chinese hamster over cells by single cell gel electrophoresis (comet) assay. *Turkish Journal of Pharmaceutical Sciences,*14(2), 185-190.

[10] Rana, S.C., Pandita, V.K., Chhokar, R.S. and Sanjai, S., 2015. Effect of pre and post emergence herbicides on weeds and seed yield of garden pea. *Legume Research*, 38 (4), 484-487.

[11] Dawod, K.M. and Zaki, A., 1990. *Statistical Procedures for Agricultural Research*. Mosul: Mosul University Press.

[12] Wagner, G. and Nadasy, E., 2006. Effect of pre- emergence herbicides on growth parameters of green pea. *Communication in Agricultural Applied Biological Sciences*, 71(3PtA), 809-813.

[13] Hammok, N.S., 2019. The response of two variety of Faba bean (at flowering stage) to different concentration of alpha cypermethrin insecticide. *Mesopotamia Journal of Agriculture*, 47(1), 70-79.

[14] Duncan, D.B., 1955. Multiple range and multiple F-test. *Biometrics*, 11, 1-42.

[15] Antar, S.H., 2010. *Statistical Analysis in Scientific Researches and (SAS) Program.* Mosul: Ibn Al Atheer Press House for Printing and Publishing.

[16] Singh, N. and Srivastava, A., 2014. Biomonitoring of genotoxic effect of glyphosate and pendimethalin in *Vigna mungo* populations. *Cytologia*, 79(2), 173-180.

[17] Karaye, I.U., Aliero, A.A. and Adili, I.S., 2014. Effects of butachlor and pendimethalin herbicides on seed germination and early seedling growth of species of cowpea. *Annals of Biological Sciences*, 2(4), 11-15.

[18] Verma, S. and Srivastava, A., 2018. Morphotoxicity and cytogenotoxicity of pendimethalin in the test plant *Allium cepa L*.-A biomarker based study. *Chemosphere,* 206, 248-254.

[19] Silva, N., Mendes-Bonato, A.B., Sales, J.G.C. and Pagliarini, M.S., 2011. Meiotic behavior and pollen viability in *Moringa oleifera* (Moringaceae) cultivated in Brazil. *Genetics and Molecular Research*, 10(3), 1728-1732.
[20] Shabana, E.F., Battah, M.G., Kobbia, I.A. and Eladel, H.M., 2001. Effect of pendimethalin on growth and photosynthetic activity of *Protosiphon botryoides* in different nutrient states. *Ecotoxicology and Environmental Safety*, 49(2), 106-110.

Instructions for Authors

Current Applied Science and Technology journal contains research reports, articles concerning development work, reviews of the literature and research activities. The objectives are to publish and promote research contributions and innovative work in fields associated with applied science and technology. An electronic journal is provided on the website (https://www.tci-thaijo.org/index.php/cast/index). The editors reserve the right to require revision of the submitted manuscript as a condition for final acceptance.

The institute and the editorial board claim no responsibility for the contents or views expressed by the authors of individual articles. Copying is allowed provided that acknowledgement is made. All articles submitted for publication will be assessed by a group of distinguished.

Ethics:

The journal is committed to maintaining the high level of integrity in the content published and has a Conflict of Interest policy in place. The journal uses plagiarism detection software to screen the submissions. If plagiarism is found, the COPE guidelines on plagiarism will be followed. For more details, please see https://www.tci-thaijo.org/index.php/cast/navigationMenu/view/Publication_Ethics.

Page Charge: Free

Submission of Manuscripts:

Manuscripts must be written in English and submitted online. Manuscripts are to be reviewed (double blinded) by at least 3 referees specializing in relevant fields. Revised manuscripts have to be sent online.

All manuscripts should be submitted to: https://www.tci-thaijo.org/index.php/cast/index

Contact:

Editor of Current Applied Science and Technology
King Mongkut's Institute of Technology Ladkrabang
1 Soi Chalongkrung 1, Ladkrabang District,
Bangkok 10520, Thailand
Tel: 662-329-8136
Fax: 662-329-8221
Email: cast@kmitl.ac.th

Manuscript Preparation Guide:

General: Manuscripts must be typewritten using *Microsoft Word for Windows*, single-spaced with margin set-up (in page set up menu) as follows (see also the document template):

Top Margin	1.5"	Bottom Margin	1.5"
Left Margin	1.5"	Right Margin	1.5"

Good quality printouts using A4 paper size are required. Format should be a single column. Times New Roman font type is required. Font sizes for various text functions are as follows:

Text functions	Size *	Typeface
Title	14 (CT)	Bold
Author and co-authors	11 (CT)	Normal
Address for correspondence	11 (CT)	Normal
Abstract and main text	10 (LJ)	Normal
Section heading and number including "Abstract", "Acknowledgement", "References"	12 (CT)	Bold
Subsection heading and number	11 (LJ)	Bold

* CT = Center Text, LJ = Left Justified.

The corresponding author should be noted (included a Fax number and E-mail address) and indicated with an asterisk. Full postal addresses must be given for all co-authors, keyed to names (if required) by superscripted Arabic numbers.

Paper Length: Should not normally exceed 10 pages including figures and tables
Spelling: American English
Abstract: Should not exceed 250 words
Keywords: Should not exceed 8 keywords
Text: Authors are requested to use the following order when typing:-

All research reports (Full Length or Short Reports): Title, Authors, Affiliations, Abstract, Keywords, Introduction (in reserch papers this must be confined to relevant matters, and must not be a general review of cognate literature), Materials and Methods, Results and Discussion, Conclusions, Acknowledgements, References.

Reviews and Discussion Papers will be considered in any format appropriate to the purposes of the authors, although adherence to the general guidelines described above is encouraged.

Line Art Figures: Figures can be drawn using several packages such as Win Draw®, Auto CAD®, Corel Draw®, VISIO® etc.

Photographs: Actual size photographs are acceptable. However, they can also be put into a text stream using a good-resolution scanner. All photographs must be clear when printed in monochrome.

Graphs: Several packages available today can produce attractive and professional graph presentation. Some also provide curve-fitting function, which can be useful. However, two-dimensional bar charts are preferred. All graphs must be clear in monochrome printing.
Equations and complex expressions: Math CAD®, Math Writer® and Equation Editor® (included in Microsoft Word®) are acceptable for presentation of this type of material.

Citations: Citations in the text should be denoted by numbers between square brackets (i.e. [1, 2], [1-3], [1, 3-8]…) *in the order of first appearance in the text.*

References: References should be numbered to correspond with the text citations. References must be arranged as follows:

Books

Authors, Initials., Year. *Title of Book.* Edition (only include this if not the first edition). Place: Publisher.

Example:

[1] Barker, R., Kirk, J. and Munday, R.J., 1988. *Narrative Analysis*. 3rd ed. Bloomington: Indiana University Press.

Chapters of edited books

Chapter authors' surname(s), initials., Year of book. Title of chapter. In**:** Book editor(s) initials. surnames, ed. or eds. *Title of Book*. Place of publication: Publisher. Chapter number or first and last page numbers.

Example:

[2] Samson, C., 1970. Problems of information studies in history. In: S. Stone, ed. *Humanities Information Research*. Sheffield: CRUS, pp. 44-68.

E-books

Author, Year, *Title of Book*. [e-book] Place of publication: Publisher. Available through: include e-book source/database, web address or URL.

Example:

[3] Carlsen, J. and Charters, S., eds. 2007. *Global Wine Tourism*.[e-book] Wallingford: CABI Pub. Available through: Anglia Ruskin University Library website <www.libweb.anglia.ac.uk>.

Journal articles

Author, Initials., Year. Title of article. *Full Title of Journal*, Volume number (Issue number), Page numbers.

Example:

[4] Ross, A.B., Junyapoon, S., Jones, J.M., Williams, A. and Bartle, K.D., 2005. A study of different soots using pyrolysis–GC–MS and comparison with solvent extractable material. *Journal of Analytical and Applied Pyrolysis*, 74(1-2), 494-501.

In case of online journal articles without page number:

Author, Initials., Year. Title of article. *Full Title of Journal*, Volume number (Issue number), DOI-based link.

Example:

[5] Mondal, N.K. and Basu, S., 2019. Potentiality of waste human hair towards removal of chromium (VI) from solution: kinetic and equilibrium studies. *Applied Water Science*, 9(49), https://doi.org/10.1007/s13201-019-0929-5

Proceedings

Author, Initials., Year. Title of article. *Full Title of Proceedings*, Place of Conference, Date, page.

Example:

[6] Thanaboripat, D., Ruangrattanametee, V. and Srikitkademwat, K., 2010. Control of growth and aflatoxin production of aflatoxin producing fungi in corn by salts. *Proceeding of the 8th International Symposium on Biocontrol and Biotechnology*, Pattaya, Thailand, October 4-6, 2010, 283-289.

Patent
Inventor name, Initial(s)., Assignee., Year. *Title*. Place. Patent number (status, if an application).
Example:
[7] Leonard, Y., Super Sports Limited., 2008. *Tin Can Manufacture and Method of Sealing*. Canada. Pat. 12,789, 675.

Dissertation
Author, Year of publication. *Title of Dissertation*. Level. Official name of University.
Example:
[8] Richmond, J., 2005. *Customer Expectations in the World of Electronic Banking: a Case Study of the Bank of Britain.* Ph.D. Anglia Ruskin University.

Websites
Authorship or Source, Year. *Title of Document*. [online] Available at: include web site address/URL (Uniform Resource Locator).
Example:
[9] NHS Evidence, 2003. *National Library of Guidelines*. [online] Available at: http://www.library.nhs.uk/guidelines

Acknowledgements: These should be as brief as possible.

Proofs:
Proofs will be sent to the corresponding author and *must* be returned as soon as possible. Corrections should be restricted to typesetting errors.

Copyright:

Page Numbering:
All pages must be sequentially numbered, preferably by using the automatic page numbering function on your computer.

Copyright Material:
It is the authors' responsibility to obtain written permission from the copyright holder (usually the book or journal publisher) to use copyright material, and to send a copy of this consent with the manuscript. This consent is not normally denied but it is an international legal requirement that it be obtained.

Note:

Please note that authors are urged to check their proofs carefully before returning, since the inclusion of late corrections cannot be guaranteed.

Author(s) are responsible for ensuring that the submitted manuscript fully meets the requirements specified in the above Instructions. Manuscripts which fail to do so will be returned unedited to the Author(s) for correction in accordance with the above requirements, before they can be submitted to the processes of Referee evaluation.

1.5 ”

TEMPLATE

Enter title here (14 PT type size, Title Case, Bold, Centered)

Author Information entered here:
Name (in full)

Affiliation
City
Country
(11 pt type size, upper and lower case, centered under the title)

How to Use This Document Template

Insert the information in your document in place of the text here. For the body of your document, use Times New Roman 10 pt. Font, upper and lower case, double-spaced. Allow an extra half space above a line containing superscripts and/or below a line containing subscripts. The whole text should be left-justified. The headings should be 12 pt size, uppercase, bold and centered.

1.5” 1.5”

Abstract (12pt)

Maximum 250 words here. (10 pt)
.....
.....
.....
.....
.....

Keywords: (10 pt)

Maximum of 8 words

1. Introduction (12 pt)

Clearly explain the nature of the problem, previous work, purpose, and contribution of the paper (10 pt).
.....
.....
.....
.....
.....

*Corresponding author: Tel.: ……..... Fax: …….
E-mail: ……

2. Materials and Methods (12 pt)

.....
.....
.....
.....

3. Results and Discussion (12 pt)

.....
.....…

4. Conclusions (12 pt)

Clearly indicate advantages, limitations and possible applications (10 pt).
.....
.....

5. Acknowledgements (12 pt)

A brief acknowledgement section may be included here (10 pt).
.....
.....

References (12 pt)

References must be numbered in the order cited in the manuscript and indicated in the text by a number in square brackets (e.g. [1, 2]) (10 pt).

Example of References must be arranged as follows:

[1] Barker, R. Kirk, J. and Munday, R.J., 1988. *Narrative Analysis*. 3rd ed. Bloomington: Indiana University Press.
[2] Samson, C., 1970. Problems of information studies in history. In: S. Stone, ed. *Humanities Information Research*. Sheffield: CRUS, pp. 44-68.
[3] Carlsen, J. and Charters, S., 2007. *Global Wine Tourism*. [e-book] Wallingford: CABI Pub. Available through: Anglia Ruskin University Library website <www.libweb.anglia.ac.uk>.
[4] Ross, A.B., Junyapoon, S., Jones, J.M., Williams, A. and Bartle, K.D., 2005. A study of different soots using pyrolysis-GC-MS and comparison with solvent extractable material. *Journal of Analytical and Applied Pyrolysis*, 74(1-2), 494-501.
[5] Thanaboripat, D., Ruangrattanametee, V. and Srikitkademwat, K., 2010. Control of growth and aflatoxin production of aflatoxin producing fungi in corn by salts. *Proceeding of the 8th International Symposium on Biocontrol and Biotechnology*, Pattaya, Thailand, October 4-6, 2010, 283-289.

[6] Leonard, Y., Super Sports Limited., 2008. *Tin Can Manufacture and Method of Sealing*. Canada. Pat. 12,789, 675.
[7] Richmond, J., 2005. *Customer Expectations in the World of Electronic Banking: a Case Study of the Bank of Britain.* Ph.D. Anglia Ruskin University.
[8] NHS Evidence, 2003. *National Library of Guidelines*. [online] Available at: http://www.library.nhs.uk/guidelines

Note:

Tables and Graphs: Minimum of 10 pt type size, all captions should be upper and lower case, centered. Each table and figure must be on a separate page (or pages if required), ***and must be embedded in the text.***

Illustrations and Photographs: Halftones, minimum of 10 pt type size, bold, captions should be in upper and lower case, centered. Images must be computer-designed with clearly visibility.

Contact

Editor of Current Applied Science and Technology
King Mongkut's Institute of Technology Ladkrabang
1 Soi Chalongkrung 1, Ladkrabang District
Bangkok 10520, Thailand
Tel: 662-329-8136 Fax: 662-329-8221
E-mail: cast@kmitl.ac.th
Website: https://www.tci-thaijo.org/index.php/cast/index

KING MONGKUT'S INSTITUTE OF TECHNOLOGY LADKRABANG
1 Soi Chalongkrung 1, Ladkrabang District Bangkok 10520, Thailand
Tel: 662-329-8136 Fax: 662-329-8221
E-mail: cast@kmitl.ac.th
Website: https://www.tci-thaijo.org/index.php/cast/index